# Electrostrictive Polymers for Advanced Sonar Transducers (EPAT)

February 1999 — May 2004

Final Program Report

VOLUME II

DARPA N00173-99-C-2003
Program Manager: Dr. L. Buckley

PI: Q. M. Zhang
Materials Research Laboratory
The Pennsylvania State University
University Park, PA 16802

Team Members:
Raytheon
University of Central Florida
NUWC
K-Tech
Rutgers University

# APPENDIX 10

# Characterization of electrostrictive P(VDF-TrFE) copolymers film for high frequency and high load applications

Z.-Y. Cheng, T.-B. Xu, V. Bharti, T. Mai and Q. M. Zhang

Materials Research Laboratory, The Pennsylvania State University, University Park, Pennsylvania 16802

T. Ramotowski

Naval Undersea Warfare Center, Newport, Rhode Island 02841, USA

R. Y. Ting

Department of Chemistry, University of Central Florida, Orlando, Florida 32816, USA

## ABSTRACT

In order to characterize the electromechanical properties of newly developed electrostrictive poly(vinylidene fluoride-trifluorethylene) copolymers for practical device applications, the following results are presented. 1). The driving field amplitude dependence of the material response. It was found that M(S=ME$^2$) exhibits the driving field amplitude dependence and that the apparent piezoelectric coefficient for the material under DC bias depends on both the driving field amplitude and DC field. 2). Load capability. The copolymer film has a high mechanical load capability. For example, the transverse strain remains 0.6% at 4 MV/m under a tensile load of 15 MPa. The load dependence of the material response prove that the electric field induced strain in the copolymer films mainly originates from the electric field induced phase transition in the crystal regions. 3). Frequency dependence of the material response. Although the strain response decreases with increasing frequency, it is found that the strain response at 1 kHz can reach more than 80% of the response at 1Hz.

**Keywords:** Electrostriction, P(VDF-TrFE), Electroactive Polymer, Unimorph, Load Effect, Phase Transition

## 1. INTRODUCTION

Recently, the research on electroactive polymers (EAP) is very active since the flexible polymer has many advantages over brittle ceramics for a lot of applications and the EAP can produce very high electric field induced strain [1] [2]. However, there are many concerns on EAP from the application point of view. For example, the material response for EAP under different load conditions, the change of material response with temperature and frequency, etc.

In this paper, many material properties related to the practice devices are characterized for a newly developed electrostrictive polymer, electron irradiated poly(vinylidene fluoride-trifluorethylene) (P(VDF-TrFE)) copolymer films [3-5]. For example, the mechanical load effect on the electric field induced strain response, the temperature and frequency dependences of the electric field induced strain response and dielectric behavior, the driving field amplitude dependence of the dielectric behavior and electrostrictive coefficient, and the apparent piezoelectric effect of the material under DC bias. Based on both the load and temperature dependences of the electric field induced strain, it is confirmed from the Devonshire theory that the electric induced strain response in the irradiated P(VDF-TrFE) copolymer is mainly from the electric field induced phase transition between nonpolar to polar phases in the crystalline area. In addition, a prototype device (unimorph) was made using the copolymer films. The performance, such as the tip displacement and blocking force, is also presented. It is found that the performance of the unimorph is very close to the estimated value from the material properties.

In *Smart Structures and Materials 2000: Electroactive Polymer Actuators and Devices (EAPAD)*, Yoseph Bar-Cohen, Editor, Proceedings of SPIE Vol. 3987 (2000) • 0277-786X/00/$15.00

## 2. EXPERIMENT

P(VDF-TrFE) copolymer powders were purchased from Solvay and Cie. Bruxelles, Belgium. The compositions used here are 50/50, 65/35 and 68/32 mol%. The copolymer films studied here were prepared using solution cast and melt press. In the melt press process, the copolymer powders were pressed between two pieces of aluminum foil at 215 to 240 °C. In solution cast process, the copolymer powders were dissolved in dimethyl formanide (DMF) and then the solution was cast on a flat glass plate and dried in an oven at 70 °C. Two types of films, the stretched and unstretched films, were studied in this work. In order to prepare the stretched films, the films made from solution cast or quenched from melt press were uniaxially stretched up to 5 times at a temperature between 25 to 50 °C. Both the unstretched and stretched films prepared above were annealed at 140 °C for a time period between 12 to 14 hrs to improve the crystallinity. During the annealing process, the two ends of the films were mechanically fixed. The crystallinity of the final films is about 75%. The thickness of the final films was in the range from 15 to 30 μm. The electron irradiation was carried out in a nitrogen atmosphere at different temperatures with an electron energy of 2.55 MeV, 1.2 MeV, and 1.0 MeV respectively.

Gold electrodes with a thickness of about 40 nm were sputtered on both surfaces of the film in order to characterize the material properties. The driving field amplitude dependence of the dielectric behavior was measured through measuring the first harmonic component of the polarization using a lock-in amplifier. For the strain response at frequency lower than couple hundreds Hz, the longitudinal response of the film under a stress free condition was characterized using a specially designed strain sensor based on the piezoelectric bimorph [6], while the transverse one of the films under different tensile conditions was characterized using a cantilever-based dilatometer that was newly developed for characterizing transverse strain response of polymeric film [7]. The longitudinal strain response at high frequency was characterized using a single beam interferometer. In these kinds of experiments, the sample was clamped on a glass substrate.

In order to make copolymer multilayers, a spurr low-viscosity embedding media from Polysciences Inc. PA, was used. The spurr was cured at room temperature for about 4 days. The spurr thickness after being cured is in the range from 0.5 μm to 3 μm depending on the process. For simple unimorph in which one active layer is used, the spurr thickness is usually smaller than 1μm. However, for the multilayer structure, the average thickness of the spurr layer is about 2 to 3 μm.

## 3. RESULTS AND DISCUSSION

The electric field induced strain responses of some irradiated copolymer films at room temperature are shown in Fig. 1. A sinusoidal electric field with a frequency of 1 Hz was applied and the strain was measured at 2 Hz using a lock-in amplifier since the material is electrostrictive. The longitudinal strain is a result of the thickness change of the film, while the transverse strain is related to the length change of the film perpendicular to the applied field direction. The transverse data reported here was measured along the stretch direction of the stretched samples. Clearly, the material exhibits a very high strain response.

It should be noticed that the longitudinal strain is always negative. For unstretched films, the transverse strain, which is about 1/3 of the absolute value of the longitudinal strain, is always positive. However, for the stretched sample, it is found that the transverse strain along the stretch direction, which is comparable with the strain level of the longitudinal strain, is positive, while the transverse strain along the direction perpendicular to the stretch direction, which is about or less than 1/3 of the longitudinal strain, is negative. That is, the volume strain of the irradiated copolymer is also very high [5]. It should also be mentioned that in many electroactive materials, such as polyurethane, silicone, and piezoelectric ceramics, the volume strain is very small [1], [8]. For EAP, the contribution to the strain response from Maxwell effect is an important concern [1] [2]. Anyhow, the volume strain of Maxwell effect is very small. The large volume strain response obtained here indicates that the contribution of Maxwell effect to the strain response of EAP studied here is small. The large volume strain generated by the irradiated copolymer indicates that the material also has a potential for hydrostatic applications.

Based on all the above discussion, one can assume that the electric field induced strain response in the electron irradiated P(VDF-TrFE) copolymer originates from the electric field induced phase transition. This will be further discussed below. Actually, this conclusion is proven by the recent X-ray experiments for the sample under a different electric field [9].

With regard to the composition, it is found that the longitudinal strain response of both stretched and unstretched 50/50, 65/35 and 68/32 films are almost the same. However, the transverse strain response along the stretching direction of both 65/35 and 68/32 film is much higher than that of the 50/50 film. Therefore, for the applications where the longitudinal strain is used, the unstretched films are more suitable than the stretched ones due to convenience of the process. For the applications where the transverse strain is used, the stretched 65/35 and 68/32 films are more suitable.

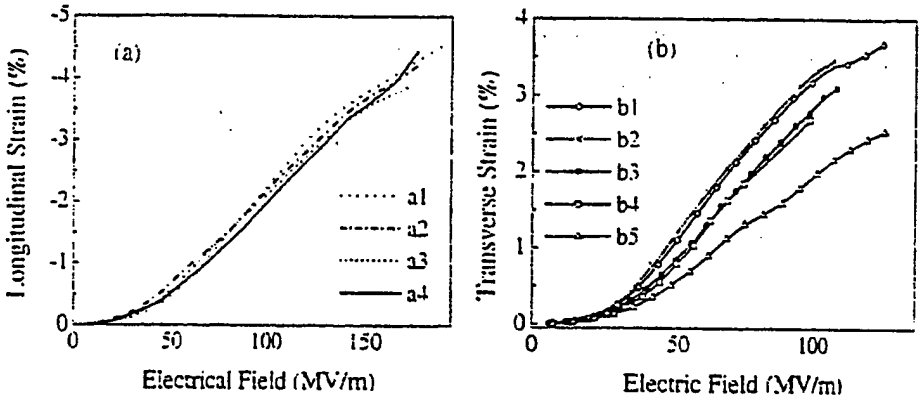


Fig. 1. Amplitude of the strain response vs. amplitude of the electric field.
(a). Longitudinal strain of samples irradiated with 2.55 MeV electrons. Curves a1, a2, a3 and a4 are the stretched 65/35 irradiated at 120 °C with 80 Mrad dose, unstretched 65/35 irradiated at RT with 100 Mrad dose, stretched 50/50 irradiated at 77 °C with 60Mrad dose, and unstretched 50/50 irradiated at RT with 100 Mrad dose.
(b). Transverse strain of stretched samples. Curves b1 and b2, are 68/32 film irradiated at 100 °C with 65 Mrad and 70 Mrad doses, respectively, using 1.2 MeV electrons. Curve b3 is 65/35 irradiated at 105 °C with 70 Mrad dose using 1.0 MeV electrons. Curves b4 and b5 are 65/35 irradiated at 95 °C with 60 Mrad dose and at [illegible] °C with 80 Mrad dose, respectively, using 2.55 MeV electrons.

For electrostrictive effect, it is well known that the electric field induced strain response (S) can be described as:

$$S = ME^2 \quad \text{or} \quad S = QP^2 \qquad (1)$$

where $E$ and $P$ are the electric field strength and polarization, respectively, while $M$ and $Q$ are charge related and electric field related electrostrictive coefficients, respectively. Using Eq. (1) and the strain data, the value of the effective electrostrictive coefficients, $M$ and $Q$, can be obtained. A set of typical results is shown in Fig. 2. As expected from the electrostrictive effect, the charge related electrostrictive coefficient, $Q$, is nearly independent of the polarization or electric field. In Fig. 2, $Q_{13}^0$ is the value of $Q_{13}$ at room temperature for the sample under low electric field. $Q_{13}$ and $M_{13}$ are the transverse electrostrictive coefficients. However, the electric field related electrostrictive coefficient, $M$, strongly depends on the electric field. This is what is not expected from the electrostrictive effect.

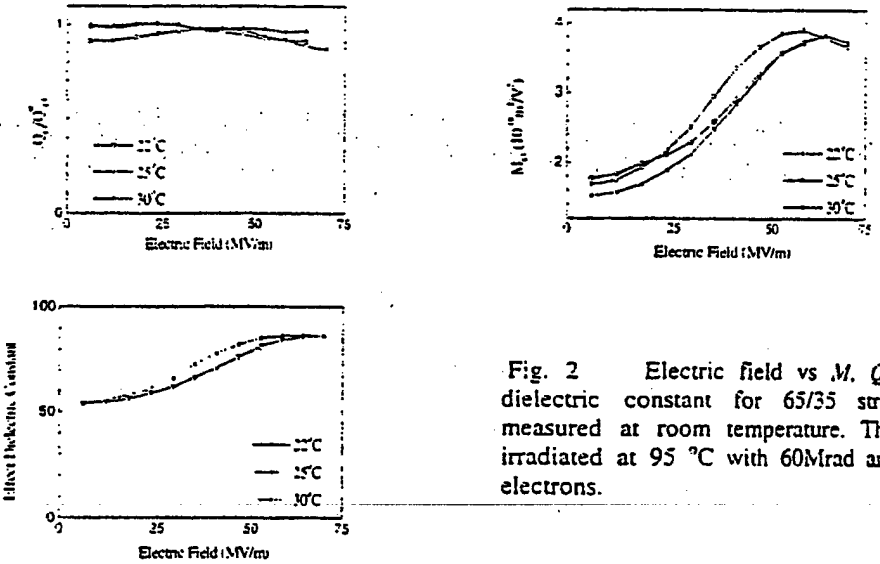


Fig. 2 Electric field vs $M$, $Q$ and effect dielectric constant for 65/35 stretched film measured at room temperature. The film was irradiated at 95 °C with 60Mrad and 2.55MeV electrons.

In order to understand the driving field dependence of $M$, the dielectric and polarization behaviors of the sample were investigated. Since the ferroelectric nature of the material, the relation between the electric field and polarization exhibits strongly nonlinear as shown in Fig. 3. Thus, it is expected that the dielectric properties of the material are strongly nonlinear. The effective dielectric constant for the material under different electric field is plotted in Fig. 2. Clearly, the effective dielectric constant is strongly dependent on the electric field. At beginning, the effective dielectric constant at the temperatures close to room temperature increases with increasing electric field. However, in high electric field range, the effective dielectric constant decreases with increasing electric field.

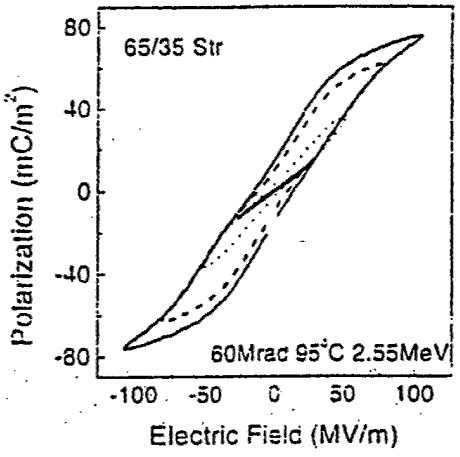


Fig. 3 Polarization vs. electric field of 1Hz for stretched 65/35 film under different electric field. The film was irradiated at 95 °C with 60Mrad and 2.55MeV electrons.

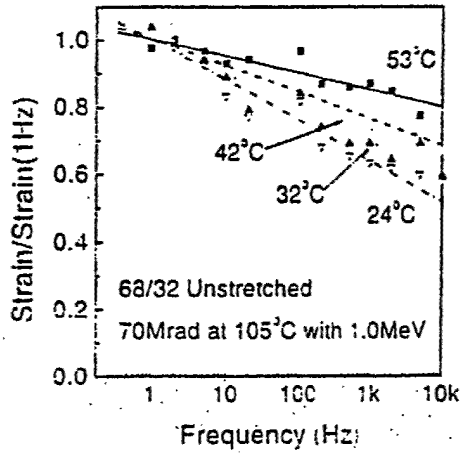


Fig. 4 Frequency dependence of strain response for unstretched 68/32 at a electric field of 20MV/m. The film was irradiated at 105 °C with 70Mrad and 1.0MeV electrons.

The strain response reported above was measured at low frequencies. However, the strain response of the material at relative high frequencies is very interesting for many applications. The frequency dependence of an electrostrictive film at 20 MV/m, unstretched 68/32 film irradiated at 105 °C with 70 Mrad dose and 1.0 MeV electrons, was presented in Fig. 4. The electric field used is limited due to the high voltage electric source. In these kinds of measurements, the film was completely clamped on a glass. From the data in Fig. 4, one can see that the electric field induced strain response does decrease with increasing frequency. However, the reduction is dependent on the temperature. In addition, as will be discussed in below, the temperature dependence can be modified a lot through changing the irradiation condition. For the film presented in Fig. 4, at room temperature the strain at 1 kHz can reach more than 60% of that at 1 Hz. At a temperature a little higher than room temperature, the strain at 1 kHz can reach more than 80% of that at 1 Hz. Considering the strain response at low frequency presented above and the frequency dependence of the strain response presented in Fig. 4, it is expected the strain response at high frequency for the material studied here at high electric field should be much higher than strain level of comment piezoelectric materials. The high strain at high frequency is highly expected for many applications.

For actuator applications, the electrostrictive effect is better than the piezoelectric effect in many cases. However, for the sensor and transducer applications, the piezoelectric effect is needed. For electrostrictive materials, an apparent piezoelectric effect can be observed for the material under a DC bias. It is well known that the apparent piezoelectric coefficient strongly depends on the DC bias. For the electrostrictive polymer studied here, one set of data is presented in Fig. 5. From the data, one can see that the piezoelectric coefficient depends on both the DC bias and the amplitude of AC driving field. That is, the piezoelectric coefficient of the electrostrictive polymer studied here can be turned in a broad range through the external electric field.

For a practice device, the load capability of the electroactive material is the other key parameter. In order to study the load capability of the electrostrictive polymer studied here, the transverse strain along the stretch direction for the material under different tensile loads along the stretch direction is measured. The results measured at room temperature for a stretched 65/35 copolymer film, irradiated at 95 °C with 60Mrad dose using 2.55 MeV electrons, are shown in Fig. 6. It was found that the film broke down after working at the tensile stress of 45 MPa for a while. That is, the elastic strength of the film is about 45 MPa which is comparable to that of commercial nylon, a typical structure polymer. Even at the tensile stress of 45 MPa, the film still exhibits a very large strain response. For example, for the films at an electric field of 47Mv/m, the electric induced strain under a mechanical load of 45 MPa is about 0.6%, which is nearly equal to the strain response of film under mechanical stress free conditions. These results indicate that the materials studied here have a high load capability. This is a great advantage of the irradiated copolymer over the other EAP [1] [2].

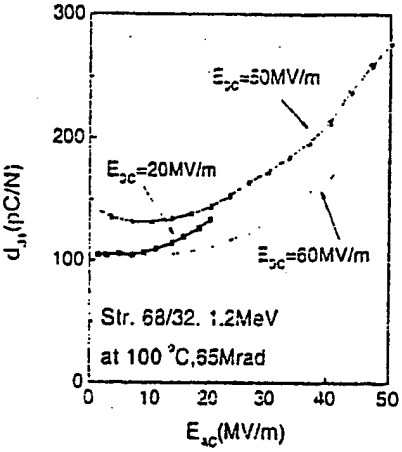


Fig. 5 Apparent piezoelectric coefficient ($d_{31}$) vs. the amplitude of AC driving field for the electrostrictive film under different DC bias. The film is stretched 68/32 irradiated at 105 Oc with 65 Mrad dose using the electrons of 1.2 MeV.

From the data in Fig. 6. one can find that the transverse strain response at room temperature increases with tensile stress at the beginning and then decreases with the stress. There is a tensile stress ($S_M$) at which the strain exhibits a maximum for the film under a constant electric field.

In order to understand the stress dependence of the electric field induced strain response and to determine the working temperature range for the material, the temperature dependence of the strain response was measured. For the material studied in Fig. 6, the temperature dependence of the strain response is shown in Fig. 7. The temperature used here was limited by the set-up.

From the data in Fig. 7, one can find that the strain response decreases with increasing temperature beginning at RT. When decreasing the temperature, the strain response increases at the beginning and then decreases. There is a temperature ($T_m$) at which the strain response exhibits a maximum for the film under a constant electric field.

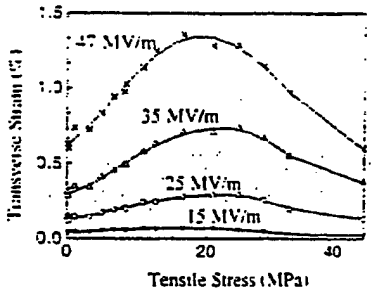


Fig. 6. Transverse strain amplitude vs. tensile for the film under different electric fields. The electric field is 1 Hz since wave.

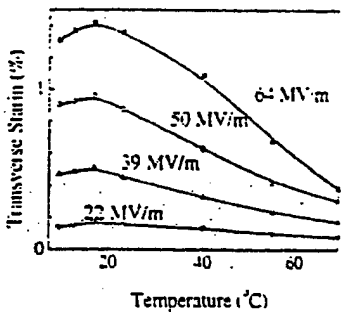


Fig. 7. Transverse strain response vs. temperature for a film under a constant electric field of 1Hz.

The temperature dependence of the electric field induced strain reported here can be easily understood by considering the fact that the irradiated copolymer is relaxor ferroelectrics [3], [10]–[12]. For relaxor ferroelectrics, the electric field induced strain is related to the electric field induced breathing of the polar regions [11], [12]. At high temperatures, the concentration of the polar region increases with decreasing temperature. The electric field induced strain, therefore, increases with decreasing temperature. At low temperatures, a freezing of the polar region happens. With decreasing temperature, an increased amount of the frozen polar regions results in the decrease of the electric field induced strain response. Therefore, the $T_m$ is related to the freezing process of the polar regions.

Before irradiation, the copolymers exhibit a phase transition between ferroelectric phase at low temperatures and paraelectric phase at high temperatures. After irradiation, the material is transferred from a normal ferroelectric to a relaxor ferroelectric. Although the relaxor ferroelectric does not have Curie temperature, there are polar regions whose behavior is very similar to ferroelectrics. Thus, we can discuss, approximately, the relaxor ferroelectric using the Devonshire phenomenological theory of the ferroelectric. For a normal ferroelectric, the Curie temperature changes with external stress as following [13]:

$$\Delta T = 2\varepsilon_0 C Q_{ij} X_i \qquad (2)$$

Where $\Delta T$ is the change of Curie temperature corresponding to the stress ($X_i$). Both $C$ and $Q_{ij}$ are the material properties, the Curie-Weiss constant and the electrostrictive coefficients. $\varepsilon_0$ is the vacuum permittivity. For the material studied here, it has been reported that $Q_{13}>0$ [5]. Thus, the Curie temperature increases with increase tensile.

Let us discus the data in Fig. 6 now with Eq. (2). With an increasing tensile stress, since the increase of $\Delta T$, the $T_m$ shifts toward RT, at first due to $T_m$ being lower than RT. This will result in the strain response of the material at RT increasing with tensile stress at the beginning. If the tensile stress increases further, the $T_m$ will be higher than RT. In this case, the increase of tensile stress will result in the $T_m$ deviating away from RT. Thus, the electric field induced strain response of the film at RT will decrease with increasing tensile stress. That is, the Devonshire theory can be used to explain the stress effect on the strain response of the irradiated copolymer films studied here. This confirms the above conclusion about the strain response of the material studied here originating from the electric field induced phase transition.

With regard to the temperature dependence of the electric field induced strain shown, it is found that the relation between the strain response and the temperature can be modified in a very broad range through different irradiation conditions. The temperature dependence of the longitudinal strain response for a copolymer film under a constant electric field is shown in Fig. 8. Clearly, for this material, 68/32 irradiated at 105 °C with 70 Mrad dos using 1.0MeV electrons, the strain response is only weekly dependent on the temperature.

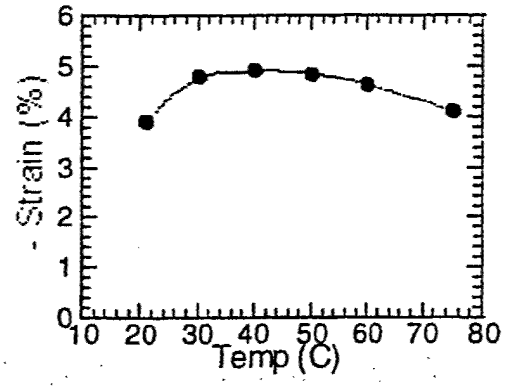


Fig. 8 The temperature dependence of the longitudinal strain response for 68/32 copolymer film at a constant electric field of 1Hz. The film was irradiated at 105 °C with 70 Mrad dose using 1.0MeV electrons.

In order to demonstrate the applications of the EAP studied here, a prototype device, a unimorph, was made using the copolymer films. For the unimorph having only one active layer, the performance is shown in Fig. 9. Clearly, the electric field can drive the material a lot, from straight to a circle. Clearly, the unimorph can supply very large displacement. The electrode area on the active layer is 10X20 mm$^2$. The thickness of the active layer about 22 μm, while thickness of the whole unimorph is about 45 μm. Around the electrode area, non-electrode edge with a width of 1 to 2 mm was applied.

The performance of the unimorph can be derived from the material properties of both the active layer and the substrate. For example, the tip displacement ($\delta$) and the tip blocking force ($F$) can be expressed as [14]:

$$\delta = \frac{3L^2}{2t}\frac{2AB(1+B)^2}{A^2B^4+2AB(2+3B+2B^2)+1}S_1 \qquad (3a)$$

$$F = \frac{3wt^2E_c}{8L}\frac{2AB}{(AB+1)(1+B)}S_1 \qquad (3b)$$

where $L$, $w$ and $t$ are the length, width and thickness of the unimorph, respectively. $S_1$ and $Ec$ are the transverse strain and the Young's modulus of the active layer respectively, the $A$ and $B$ are the Young's modulus ratio of substrate to active layer and the thickness ratio of substrate to active layer, respectively. It should be noticed that Eq. (3) was derived for very small displacement. Therefore, one can not use eq. (3a) to describe the performance of the unimorph presented in Fig. 9 with the material properties. However, the effect of the geometric parameters on the displacement and force can be discussed with eq. (3). From eq. (3), one can see that the displacement decreases with increasing the thickness of the unimorph. However, the blocking force increases with increasing thickness. Thus, one can make a thick unimorph using the material studied here to reduce the displacement and increase the blocking force. In this case, eq. (3) can be used to characterize the performance of the unimorph.

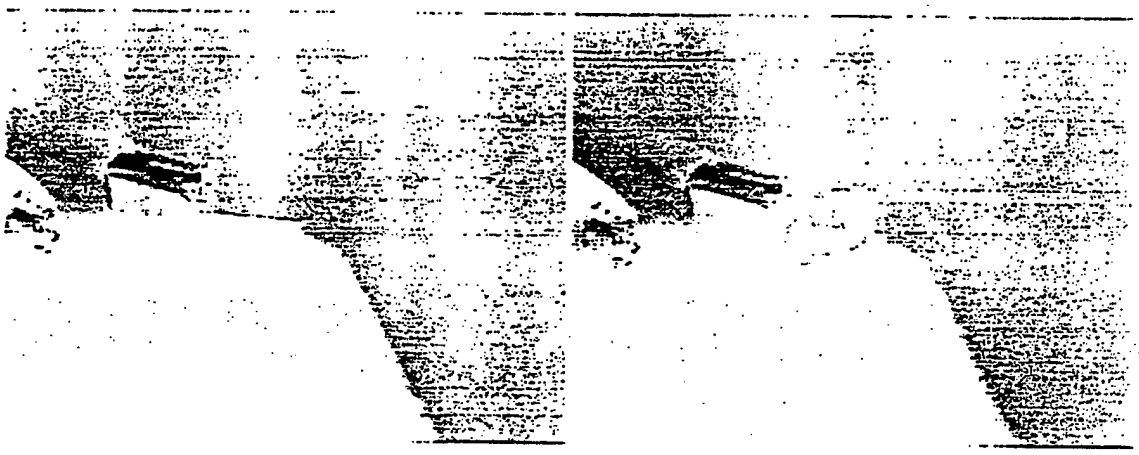

Fig. 9 The performance of a unimorph with one electrostrictive P(VDF-TrFE) copolymer layer of 22 μm. The picture in the left shows the unimorph without electric field. The picture in the right shows the unimorph for the active layer at an electric field of about 65 MV/m.

In order to make things easy and measure the blocking force, a multilayer kind of unimorph, which has eight active layers, was made. The length, width and thickness of the unimorph is 22 mm, 13 mm and 0.32 mm respectively. The electrode area on the active layer is 20X10 mm$^2$. The active layers were stretched 68/32 copolymer films irradiated at 100 °C with 75Mrad dose using the electrons of 1.2 MeV. The thickness of each active layer is about 18 to 20 μm. The Young's modulus of the active layer is about 1 GPa. The substrate used here was unirradiated copolymer film. When an AC electric field of 1 Hz was applied on the unimorph with amplitude of 550Vrms (that is, the amplitude of the electric field on the active layer is about 40 MV/m), the measured block force is 3.3 gram. For the free standing copolymer film, it is found that the transverse strain at an electric field of 40 MV/m is about 0.33%. Using eq. (3b) with A=3 and B=1, one can get the blocking force of 4.2 gram for this unimorph. Considering the following factors, the geometric parameters used in the calculation are the electrode area, the surface area of the unimorph is larger than the electrode area, and the glue effect, one can conclude that the estimated blocking force is very close to the measured value. This consistency indicates that the strain response of the polymer under free standing can be used to estimate the device behavior in which the polymer is used.

## 4. SUMMARY

High energy (MeV) electron irradiated P(VDF-TrFE) copolymer (50/50, 65/35, and 68/32 mol%) films have very large electric field induced strain response (about 5% longitudinal strain and more than 3% transverse strain). Compared to the other electroactive materials, a great advantage of the irradiated copolymers is that the material has a very high volume strain, which makes the material very well suitable for hydrostatic applications. The apparent piezoelectric coefficients can be turned in a broad range through the external electric field. In addition, the material also exhibits a high strain response at high frequency. The strain response of the material under different stress conditions shows that the irradiated copolymer films have

very high load capability. The temperature dependence of the strain response was presented. The relationship between the stress dependence and temperature dependence of the strain responses is discussed with the Devonshire phenomenological theory. The consistence between the Devonshire theory and experimental data indicates that the strain response obtained in the irradiated copolymer originates from the electric field induced phase transition of the local polar regions.

## ACKNOWLEDGEMENTS

The work was supported by DARPA through Grant No. N00173-99-C-2003, ONR through Grant No. N00014-97-1-0900, and NSF through Grant No. ECS-9710459.

## REFERENCES

1. Y. Bar-Cohen, *Electroactive Polymer Actuators and Devices*, Proc. of SPIE, Vol.3669 (1999).
2. Q. M. Zhang, *Electroactive Polymers*, MRS Proc. Vol.600 (1999).
3. Q. M. Zhang, V. Bharti, and X. Zhao, "Giant Electrostriction and Relaxor Ferroelectric Behavior in Electron-Irradiated Poly(vinylidene fluoride-trifluoroethylene) Copolymer", *Science*, **280**, 2101 (1998).
4. X. Zhao, V. Bharti, Q.M. Zhang, T. Romotowski, F. Tito, and R. Ting, "Electromechanical Properties of Electrostrictive Poly(vinylidene fluoride-trifluoroethylene vinylidene fluoride-trifluoroethylene) Copolymer", *Appl. Phys. Lett.* **73**, 2054 (1998).
5. Z. -Y. Cheng, T. -B. Xu, V. Bharti, S. Wang, and Q. M. Zhang, "Transverse Strain Response in the Electrostrictive Poly(vinylidene fluoride-trifluoroethylene) Copolymer", *Appl. Phys. Lett.* **74**, 1901 (1999).
6. J. Su, P. Mouse, and Q.M. Zhang, "A Bimorph Based Dilatometer for Field Induced Strain Measurement in Soft and Thin Free Standing Polymer Films", *Rev. Sci. Instrum.* **69**, 2480 (1998).
7. Z.-Y. Cheng, V. Bharti, T.-B. Xu, S. Wang, and Q.M. Zhang, "Transverse Strain Response in the Electrostrictive Poly(vinylidene fluoride-trifluoroethylene) Copolymer and Development of a Dilatometer for the Measurement", *J. Appl. Phys.* **86**, 2208 (1999).
8. R. E. Pelrine, R. D. Kornbluh, and J. P. Joseph, "Electrostriction of Polymer Dielectrics with Compliant Electrodes as a Means of Actuators", *Sens. Actuators A*, **64**, 77 (1998).
9. Q. M. Zhang, Z.-Y. Cheng, and V. Bharti, "Relaxor Ferroelectric Behavior in High Energy Electron Irradiated Poly(vinylidene fluoride-trifluoroethylene) Copolymers", *Appl. Phys. A* (in press) (2000).
10. V. Bharti, X. Zhao, Q.M. Zhang, T. Ramotowski, F. Tito, and R. Ting, "Ultrahigh Electric Induced Strain and Polarization Response in Electron Irradiated Poly(vinylidene fluoride-trifluoroethylene) Copolymer", *Mater. Res. Innovat.* **2**, 57 (1998).
11. Q.M. Zhang and J. Zhao, "Polarization Response in Lead Magnesium Niobate Based Relaxor Ferroelectrics", *Appl. Phys. Lett.* **71**, 1649 (1997).
12. Z.-Y. Cheng, R.S. Katiyar, X. Yao, and A.S. Bhalla, "Temperature Dependence of the Dielectric Constant of Relaxor Ferroelectrics", *Phys. Rev. B* **57**, 8166 (1998).
13. M.E. Line and A. M. Glass, *Principles and Applications of Ferroelectrics and Related Materials* (Oxford University Press, New York, 1977).
14. Q.M. Wang, Ph.D Thesis, The Pennsylvania State University, 1998.

# APPENDIX 11

PROCEEDINGS
EUROPTO®
SERIES

*Fifth European Conference on*

# *Smart Structures and Materials*

**Pierre François Gobin**
**Clifford M. Friend**
*Chairs/Editors*

**22–24 May 2000**
**Glasgow, Scotland, United Kingdom**

*Sponsored by*
EOS—The European Optical Society
SPIE—The International Society for Optical Engineering
Scottish Enterprise (UK)
Greater Glasgow and Clyde Valley Tourist Board (UK)

*Cooperating Organizations*
IEE—Institute of Electrical Engineers
IMECHE—Institution of Mechanical Engineers (UK)

*Published by*
SPIE—The International Society for Optical Engineering


**Volume 4073**

# New electrostrictive PVDF copolymers for large-strain actuator application

Robert Y. Ting*a and Qiming Zhang b
a Department of Chemistry, University of Central Florida, Orlando, FL 32816-2366
b Materials Research Laboratory, The Pennsylvania State University, University Park, PA 16802

## Abstract

A new class of ferroelectric polymeric material was developed by using the copolymers of polyvinylidene fluoride and trifluoroethylene, P(VDF-TrFE). Copolymer samples were subjected to high-energy electron irradiation, and the material appeared to be converted into a relaxor ferroelectric. The polarization hysteresis loop near the dielectric peak temperature became nearly non-hysteric, but gradually broadened and evolved into a normal ferroelectric hysteresis loop as the temperature was reduced. The dielectric constant as a function of temperature showed a broad dispersive peak in frequency, with the dispersion obeying the Vogel-Fulcher law. The dielectric constant was greatly increased with electron bombardment and a massive electrostriction was observed. Accompanying these changes were the resulting large electrically induced strain and high elastic energy density. The cause of these changes is presently believed to be the breakup of the coherent macro-polar regions containing the all-trans molecular conformation into micro-polar regions with increasing amorphous-crystalline interface as the sample was exposed to electron irradiation.

**Keywords**: Strain, electostriction, actuator material, copolymer, PVDF, ferroelectrics

## 1. INTRODUCTION

In recent years, there is an increasing interest in the development of new active materials for actuator application in smart structure designs. The design goal usually requires a material that can deliver large strains under external stimuli of reasonable electric field and temperature range. High strain energy density is desirable for the generation of sufficient mechanical forces. Furthermore, the material should be low in hysteresis in order to minimize internal heating and to maximize device lifetime and reliability. Among the currently available materials, few can fully meet these requirements: PZT ceramics and their piezocomposites offer adequate response speed but their strain levels are too low. Shape-memory alloys such as terfenol-D generate high strain and large force but are often associated with large hysteresis and very low speed. Ferroelectric polymeric materials offer the advantage of being light weight, low cost and

In *Fifth European Conference on Smart Structures and Materials*, Pierre François Gobin, Clifford M. Friend, Editors, Proceedings of SPIE Vol. 4073 (2000) • 0277-786X/00/$15.00

ease of processing into large sheets that can be made conformable to the surfaces of complex shapes. However, for electromechanical applications their strain levels are just as low as the PZT piezoceramics and hysteresis as high, two factors greatly limiting their usefulness.

A well-known ferroelectric polymer is poly(vinylidene fluoride), PVDF. This semicrystalline polymer exhibits a morphology consisting of small crystallites surrounded by or connected with an amorphous phase of long and flexible polymer chains, such as depicted in Fig. 1. Mechanical stretching and annealing can usually induce the so-called "beta-phase" with the all-trans conformation along the main carbon backbone in the crystalline phase (1). Fig. 2 shows this conformation of PVDF molecules. Additional poling at elevated temperatures would subsequently produce a piezoelectric polymer with good usable qualities, though such processing is quite costly and tedious. As an alternative, PVDF random copolymers with trifluoroethylene (TrFE) have been developed (2). In such compositions a ferroelectric-paraelectric phase transition exists, which leads to large lattice strains, as observed in X-ray diffraction and thermal expansion coefficient measurements (3,4). However, the large strain in these copolymers has the disadvantage of being associated with the F-P phase transformation involving very large hysteresis.

The existence of hysteresis in ferroelectric materials is known to be related to the energy barrier of switching the polarization direction or inducing phase transformation from one to another. In the development of electrostrictive ceramics such as PMN or PZN, it was shown that the energy barrier can be significantly lowered or eliminated if the dimension of the coherent polarization regions can be reduced to near nanometer scales (5). The question is therefore asked whether in P(VDF-TrFE) copolymers the size of the all-trans conformation region can be effectively reduced by introducing defects along the polymer chain via a proper means such as high-energy irradiation.

Many investigators studied the effect of high energy electron and gamma irradiation on structural modification and property changes in P(VDF-TrFE) copolymers (6,7). It was found that the irradiation changes the molecular conformation of the all-trans crystalline structure by introducing crosslinking and therefore creating an apparent paraelectric phase. The dielectric peak associated with this transformation takes place at a lower temperature than the original F-P transition, and is also effectively broadened. It appeared that irradiation breaks up the coherent macro-polar crystalline regions of the all-trans conformation into micro-polar regions, which results in an increase in the amorphous-crystalline interface boundary in the polymer.

By following this line of approach, conventional P(VDF-TrFE) copolymers were subjected to high-energy electron irradiation. The effects of such irradiation on the ferroelectric and electromechanical properties of the modified polymers were investigated as a function of temperature and electric field. It will be shown that the large polarization hysteresis would effectively be eliminated, and a massive electrostriction achieved. The irradiated copolymers essentially behave like a ferroelectric relaxor, representing a new

class of ferroelectric polymers with large strain and high strain energy density, which can be used in actuator development for smart structure applications.

## 2. EXPERIMENTAL

Copolymer samples were prepared by melt-pressing polymer resin pellets at 225 C, followed by cooling slowly to room temperature. The resulting films had a thickness of the order of 25 micro-meters. The molar percentage of the VDF moiety ranged from 50, 65 to 68, giving a designated copolymer composition of 50/50, 65/35 or 68/32. Gold sputtered electrodes were applied to the films for electrical measurements. Dielectric constant and loss property were determined by using a Hewlett Packard multi-frequency LCR meter (HP4274A) equipped with a temperature chamber. The frequency coverage was from 50 Hz to 1 MHz over the temperature range of –65 to 125 C at the heating or cooling rate of 2 C/min. The polarization hysteresis loops were measured by using a Sawyer-Tower bridge (8) at temperatures from –25 to 50 C. The sample was allowed to equilibrate at each measurement temperature for fifteen minutes before the polarization hysteresis loop was measured. The electric field induced strain was characterized by using a bi-morph strain sensor originally designed by Su et al. (9). The frequency range for both the strain and the polarization measurement was from 1 to 10 Hz.

## 3. RESULTS AND DISCUSSION

### 3.1 Dielectric Properties

Fig. 3 shows the temperature dependence of the dielectric constant and loss of a 65/35 copolymer sample at different frequencies. In comparison with the properties of an unirradiated sample, the dielectric peak is considerably broadened. A strong frequency dispersion is observed, and the temperature where the dielectric peak appears (Tm) shifts to higher temperature with increasing frequency. These features resemble those of a ferroelectric relaxor of electrostrictive ceramics (5). Indeed, the frequency dispersion was found to obey the well-known Vogel-Fulcher law (10):

$$f = f_o \exp\{-U/k(T_m - T_f)\}$$

which is typically shown in Fig. 4 by fitting the dielectric data of a 50/50 sample irradiated with 40 Mrad at 120 C. Both the dielectric peak temperature and the freezing temperature, Tf, move to lower temperatures when the samples were irradiated. Since these temperatures are related to the activation energy, this shift suggests that the irradiation had the effect of breaking up the ferroelectric macro-polar regions, resulting in a significant reduction in the activation energy.

## 3.2 Polarization Hysteresis

For irradiated copolymer samples, the polarization hysteresis loop obtained as a function of applied electric field becomes significantly slimmer, as compared with that for an unirradiated sample. Fig. 5 gives an example of this result for a 65/35 sample. It can be seen that the broad hysteresis loop of the original copolymer sample was reduced when the sample was irradiated with 40, 60, 80 and 100 Mrad, respectively, at 120 C. The slim hysteresis loop suggests that the energy barrier for phase transformation is reduced or nearly eliminated by irradiation. This is an additional indication that the size of coherent polarization regions has been reduced in due process. At a given electric field, the polarization decreases with increasing radiation dosage, pointing to a smaller and smaller crystalline domain in the sample as a result of irradiation. As the measurement temperature was lowered to room temperature, a gradual appearance of polarization hysteresis was observed, shown here in Fig. 6 for a 50/50 sample irradiated with 100 Mrad at 120 C. The gradual appearance of remanent polarization at lower temperatures suggests that the sample remains ferroelectric but the defect structure created by irradiation is not restored at high electric field, an important factor for electromechanical applications. Furthermore, irradiation is proven in this case an effective way to remove the polarization hysteresis. Fig. 7 shows the remanent polarization as a function of temperature for both the original and the irradiated samples. At low temperatures the remanent polarization increases to a constant level, which is nevertheless considerably lower in the irradiated sample.

## 3.3 Electric Field Induced Strain

The electric field induced strain was measured as a function of field strength at 1 Hz. Fig. 8 shows the strain of a 50/50 sample irradiated with 40 Mrad at 120 C. At an electric field of 150 MV/m, the measured strain in the thickness direction exceeded 4% and the strain hysteresis was negligibly small. When fitted with the polarization data, the strain follows a linear relationship with the square of polarization. This provides the strongest support that the material is now electrostrictive (11).

Another interesting feature of the strain response in irradiated copolymer samples is the strain measured in the transverse direction in the plane of the film. For a sample that is not stretched, the amplitude of the longitudinal strain in the thickness direction is much higher than that of the transverse strain. However, if the film is stretched, the transverse strain amplitude in the stretched direction in the film is just as high as that of the longitudinal strain. Fig. 9 shows the measured result of strain amplitudes in a 65/35 sample irradiated with 140 Mrad at room temperature and with 60 Mrad at 120 C. In P(VDF-TrFE) copolymers a change in polarization is known to produce a strain along the polymer chain in opposite sign to that perpendicular to the chain. A uniaxial stretching of the copolymer film aligns the polymer chain along the drawing direction and will enhance the strain response in that direction. The observed large

transverse strain in the stretched direction is important in that it may offer new opportunities for actuator and transducer designs using this particular mode.

## 4. CONCLUDING REMARKS

It is clear that P(VDF-TrFE) copolymer films irradiated with high-energy electron radiation represents a new class of active material for electromechanical applications. Once irradiated, the copolymers exhibit high electrostrictive strain levels in both the longitudinal and the stretched transverse directions. The observed strain level is as high as 4% at a biased electric field of 150 MV/m measured at 1 Hz. Both the strain and the polarization hysteresis are negligibly small. With these attractive properties, these new copolymers should offer new possibilities in actuator, sensor and transducer applications. Table 1 shows a comparison of the new copolymer properties with those of some other known active materials, including the new PZN-PT single crystal (12). Since the polymer materials are usually very thin, strain energy density is also included in Table 1 for evaluation as an actuator material. It can be seen that the irradiated P(VDF-TrFE) copolymers are greatly favored in terms of their strain and strain energy density parameters. From a practical point of view, since thick films are more difficult to produce, methods for developing multi-layered copolymer stacks are currently being investigated. One particular design is presently being considered for use in an underwater acoustic projector at high frequencies. Fig. 10 shows the predicted transmitting voltage response (TVR) of this transducer array based on the measured electromechanical properties of a 68/32 irradiated copolymer material. The predictive model was validated in a standard copolymer transducer by comparing the theory with measured acoustical data. The predicted acoustical gain in TVR in this particular case in more than 30 dB for a 14x30 transducer array with the new copolymer. It is expected that such an improvement in device performance be demonstrated soon in a planned in-water acoustical test based on the new P(VDF-TrFE) copolymers as the active material of choice.

## ACKNOWLEDGEMENTS

This work is supported by the Office of Naval Research and the Defense Advanced Research Project Agency. The authors gratefully acknowledge the contribution of V. Bharti, Z.Y. Cheng, and X. Zhao of Penn State in sample characterization, and also of W. Pozzo of Raytheon for the transducer modeling work.

## REFERENCES

1. A. J. Lovinger, Science, **220**, 1115 (1983)
2. K. Toshiro, in *Ferroelectric Polymers*, ed. H. S. Nalwa, Dekker, New York, 1995, pp. 63-181.

3. T. Furukawa, Phase Transition, **18**, 143 (1989)
4. A. J. Lovinger, D. A. Davis, R. E. Cais and J. M. Kometani, Polymer, **28**, 617 (1987)
5. L. E. Cross, Ferroelectrics, **76**, 241 (1987)
6. B. Daudin, M. Dubus and J. F. Legrand, J. Appl. Phys. **62**, 994 (1987)
7. A. J. Lovinger, Macromolecules, **18**, 910 (1985)
8. J. K. Sinha, Rev. Sci. Instruments, **42**, 696 (1965)
9. J. Su, P. Moses and Q. M. Zhang, ibid **69**, 2480 (1998)
10. H. Vogel, Z. Phys. **22**, 645 (1921); G. S. Fulcher, J. Am. Ceramic Soc. **8**, 339 (1925)
11. V. Sundar and R. E. Newnham, Ferroelectrics, **135**, 431 (1992)
12. S. E. Park and T. Shrout, J. Appl. Phys. **82**, 1804 (1997)

*Correspondence: E-mail rting@pegasus.cc.ucf.edu; Telephone 407-823-6065; FAX 407-823-2252

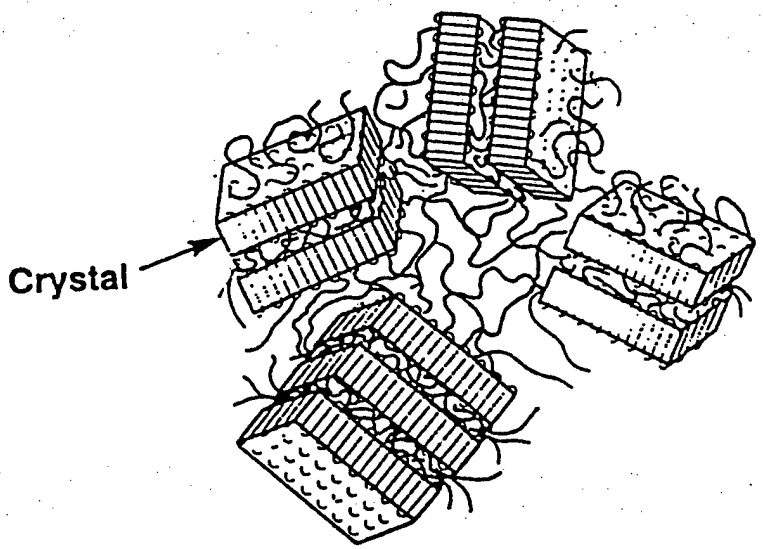


Fig. 1 A schematic showing the morphology of a semi-crystalline polymer with both crystallites and an amorphous phase.

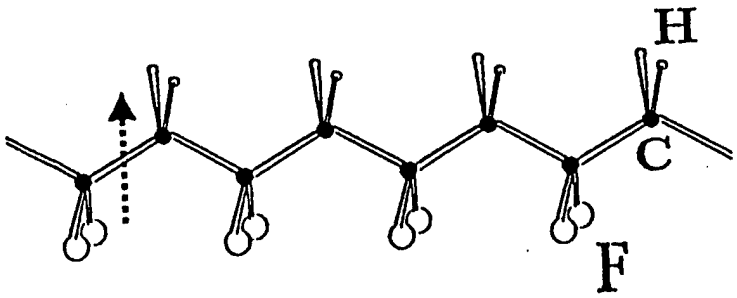


Fig. 2 A schematic showing the all-trans conformation of PVDF.

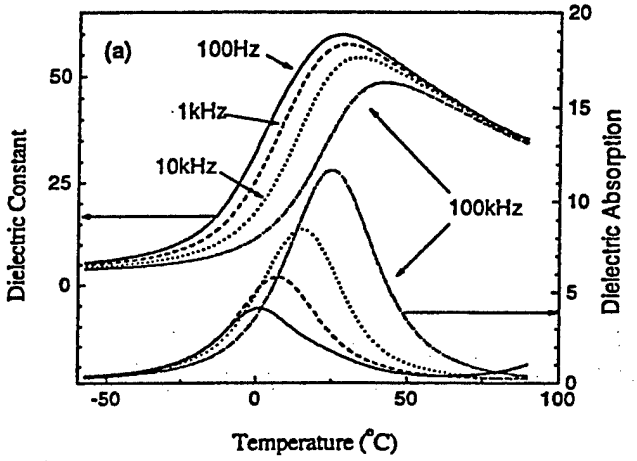


Fig. 3 Dielectric response of a 65/35 irradiated copolymer sample.

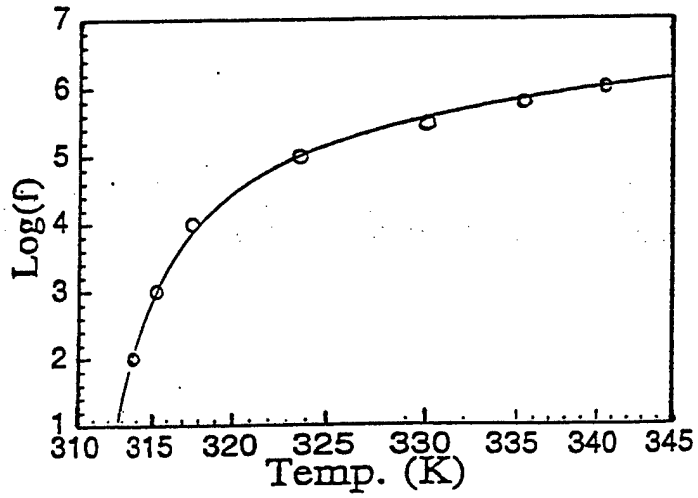


Fig. 4 Frequency dispersion of the dielectric response of a 50/50 irradiated copolymer sample obeying the Vogel-Fulcher law.

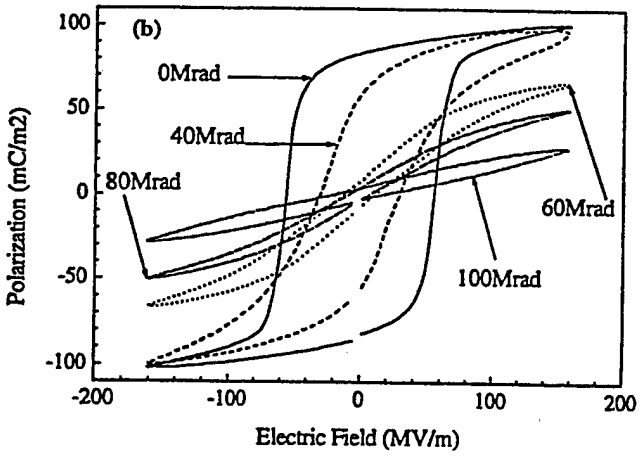


Fig. 5 Polarization hysteresis of a 65/35 copolymer sample, irradiated at 40, 60, 80 and 100 Mrad.

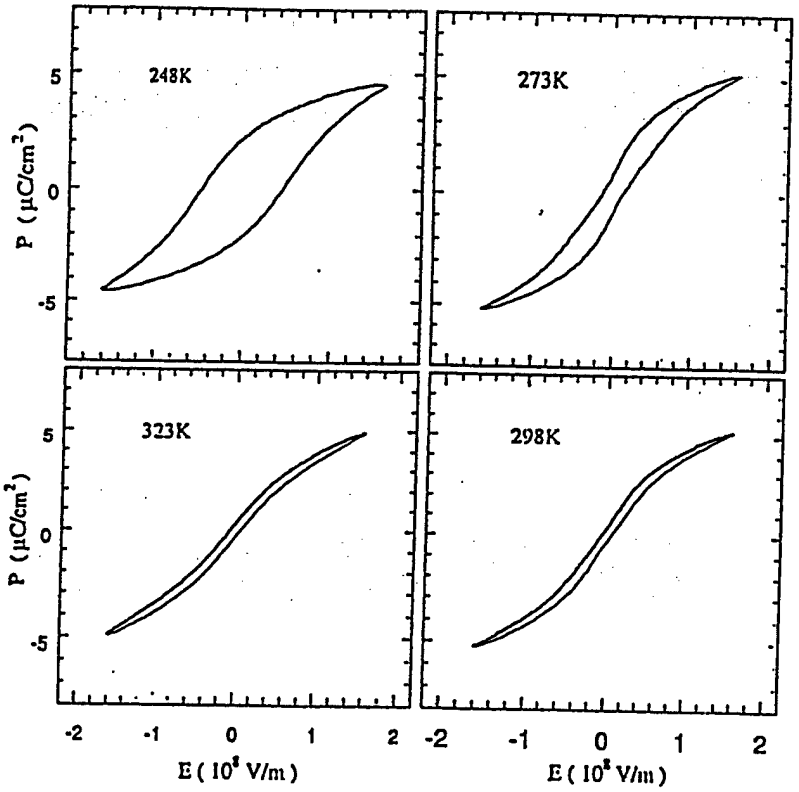


Fig. 6 Polarization hysteresis of a 50/50 irradiated copolymer sample at different temperatures.

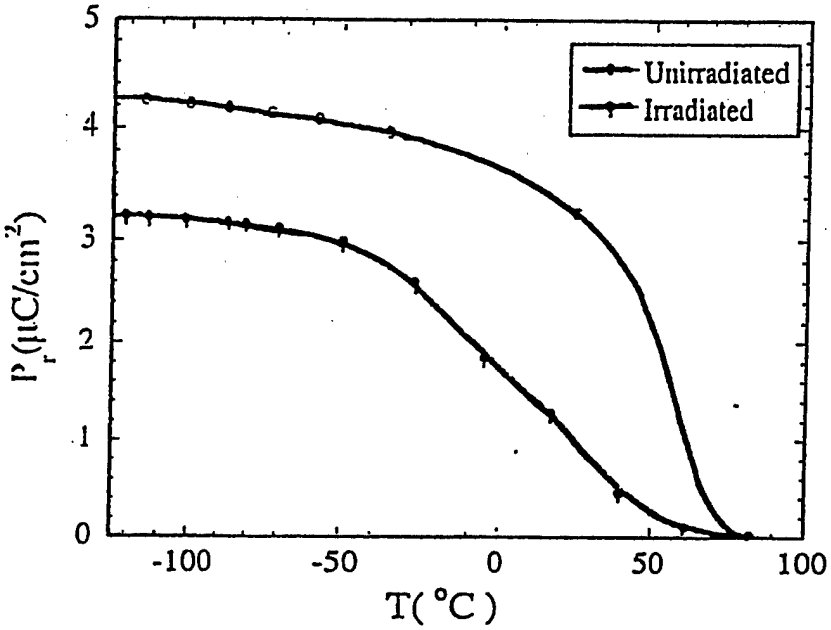


Fig. 7 Remanent polarization of a 50/50 irradiated copolymer sample as a function of temperature in comparison with the unirradiated original sample.

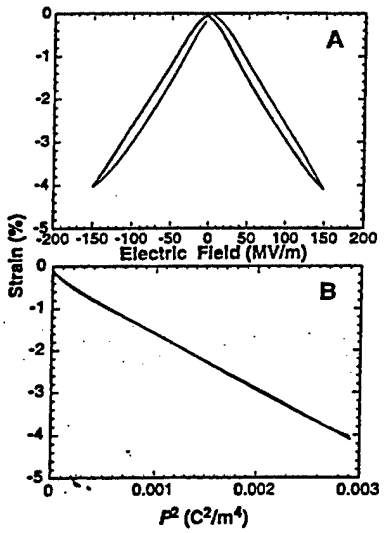


Fig. 8 Electric field induced strain of a 50/50 irradiated sample (A) as a function of field, (B) as a function of $P^2$.

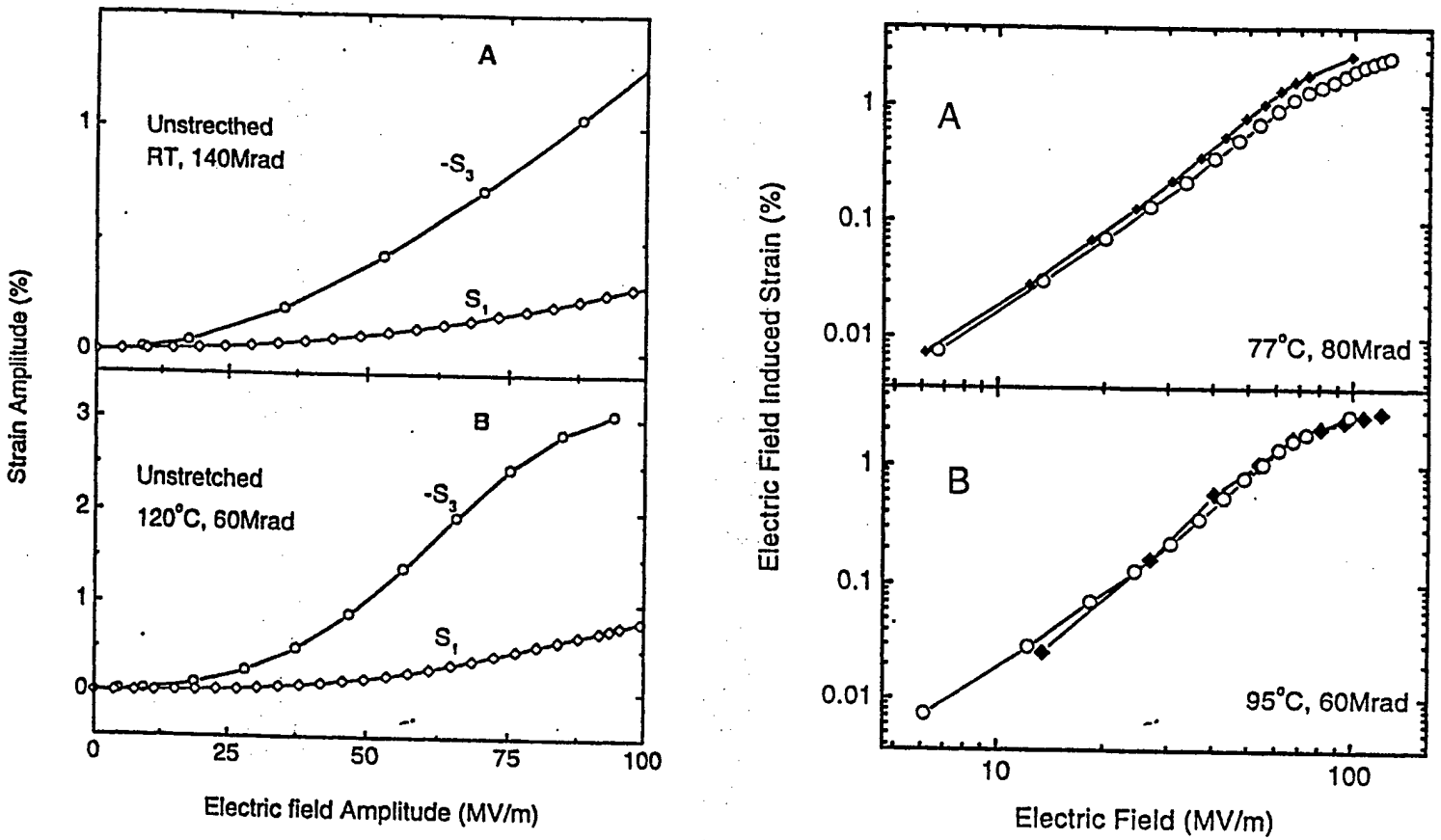


Fig. 9 Longitudinal and transverse strain amplitudes of a 65/35 irradiated copolymer sample as a function of electric field, (left) unstretched film, (right) stretched.

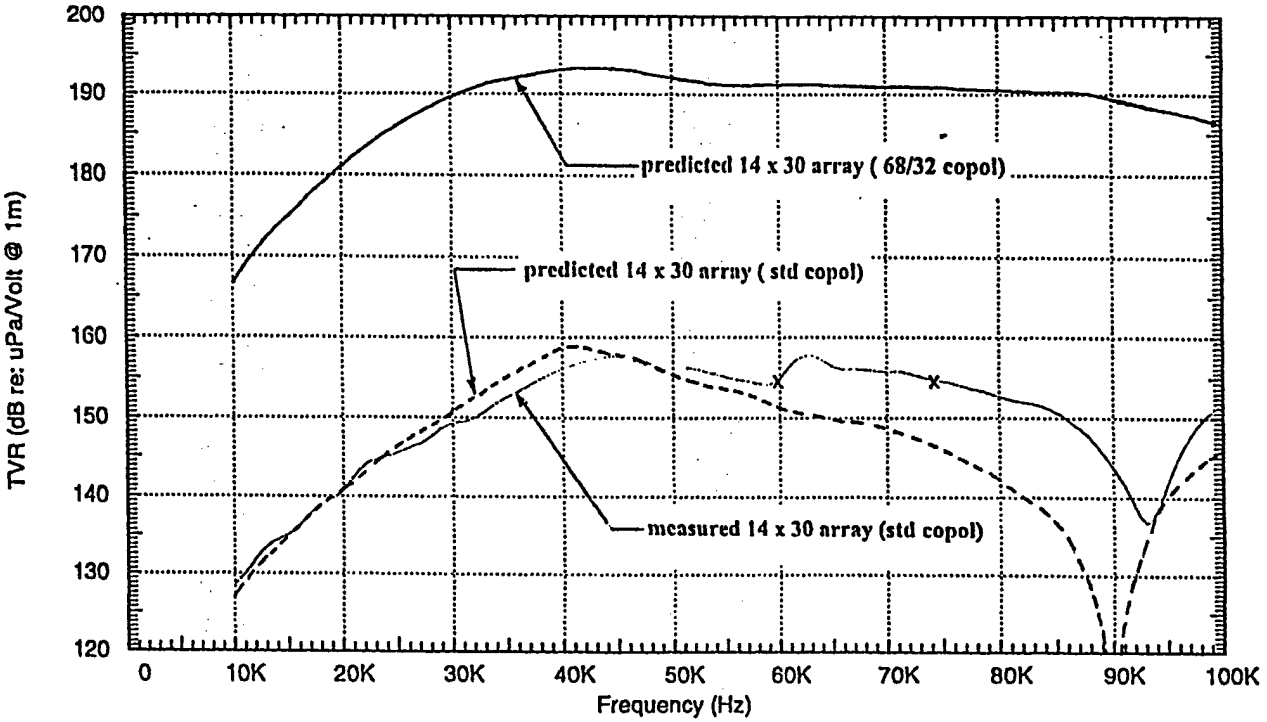


Fig. 10 Transmitting voltage response of a transducer array with an unirradiated copolymer and a 68/32 irradiated copolymer as the active material, showing higher TVR.

Table 1. Comparison of Strain and Strain Energy Density

| Materials | | Y (GPa) | $S_m$ (%) | $YS_m^2/2$(J/cm$^3$) | $YS_m^2/2\rho$ |
|---|---|---|---|---|---|
| P(VDF-TrFE) Electrostrictor | $S_L$ | 0.4 | 4.5 | 0.4 | 200 |
| | $S_T$ | 1.3 | 3.0 | 0.59 | 294 |
| Piezoceramic | | 64 | 0.2 | 0.13 | 17 |
| Magneto-strictor | | 100 | 0.2 | 0.2 | 21.6 |
| PZN-PT Single Crystal | | 7.7 | 1.7 | 1.0 | 131 |

Appendix 2

"Characterization of electrostrictive P(VDF-TrFE) copolymers film for high frequency and high load applications", Z.Y. Cheng, T.B. Xu, V. Bharti, T. Mai and Q.M. Zhang, T. Ramotowski and R. Y. Ting, in Smart Structures and Materials 2000: Electroactive Polymer Actuators and Devices, Y. Bar-Cohen, ed. Proc. SPIE Vol. 3987, p.73, (2000).

# APPENDIX 12

# SYNTHESIS AND ELECTRIC PROPERTY OF VDF/TrFE/HFP TERPOLYMERS

A. Petchsuk, T. C. Chung
Department of Material Science and Engineering, The Pennsylvania State University, University Park, PA 16802

## ABSTRACT

This paper focuses on the molecular structure-electric property relationships of VDF/TrFE/HFP terpolymers, containing vinylidene difluoride (VDF), trifluoroethylene (TrFE) and hexafluoropropene (HFP) units. Several terpolymers were synthesized and evaluated with the corresponding VDF/TrFE copolymers. In general, a small amount of bulky HFP units in the polymer chain prevents the long sequence of crystallization and results in smaller ferroelectric (polar) micro-domains, which show the improved electric properties. The resulting terpolymer possesses a interesting combined properties with good processibility, low Curie transition temperature and high dielectric constant, narrow polarization hysteresis loop, and high strain response (2.5%) at relatively low electric field (50 MV/m).

## INTRODUCTION

In the past decade, many research activities in ferroelectric fluorocarbon polymer have been focussing on VDF/TrFE copolymer with a general goal of reducing the energy barrier for ferroelectric-paraelectric (Curie) phase transition and generating large and fast electric-induced mechanical response at ambient temperature. Although VDF/TrFE copolymer exhibits a high piezoelectric and high pyroelectric constant [1], the response of the dipoles to the electric field is very slow at the ambient temperature, the polarization hysteresis loop of the copolymer is very large. The close connection between the crystalline structure and electric properties led to many attempts to alter copolymer morphology by mechanical deformation [2], electron-radiation [3], crystallization under high pressure [4], crystallization under high electric field [5], etc.

Zhang et al. [6] at Penn State University recently perfect the electron-radiation process with systematical study of the radiation conditions, such as dosage, temperature, inert atmosphere, stretching sample, etc. They revealed an exceptionally high electrostrictive response (> 4%) of the irradiated copolymer that behaves like a relaxor ferroelectric. The polarization hysteresis loop became very slim at room temperature, comparing with that of the sample before irradiation. However, the polarization was also significantly reduced and the sample became intractable because of the crosslinking. The increase of hardness of the copolymer sample was also revealed in its electric response, very high electric field was required (150 MV/m) for the irradiated sample to get a high strain response. It appears that the radiation process not only reduces the polar crystalline domain size but also involves some undesirable side reactions that increases the amorphous phase and diminishes the processibility of sample.

Another method of altering the morphology of VDF/TrFE copolymer is to introduce third (bulky) comonomer, such as hexafluoropropene (HFP), into the polymer chain. Freimuth et al. [7] studied VDF/TFE/HFP terpolymer. They concluded that the incorporation of HFP did not affect the crystalline structure, but strongly reduced the degree of crystallinity. The terpolymer exhibited thermal behavior similar to those observed in copolymer. Tajitsu et al. [8] reported the switching phenomena in VDF/TrFE/HFP terpolymers having a low HFP content (< 2.5 mol%).



Mat. Res. Soc. Symp. Proc. Vol. 600 © 2000 Materials Research Society

ıe increase of HFP content, both polarization and dielectric constant decreased at the emperature, and the switching time was very much independent on the HFP content. lthough there are experimental results on switching time, little information is available on ıcture and the piezoelectric and pyroelectric properties of the VDF/TrFE/HFP 'mers. It is very interesting to understand their structure-property relationship, especially ıple containing only a very small content of HFP termonomer (enough to reduce the size ır crystalline domains, but not the overall crystallinity). The interested terpolymers have )F/TrFE mole ratio between 50/50 and 70/30, that provide high polarization at low Curie 'ature (~ 60 °C). In this study, we will investigate their thermal and electrical properties, ; dielectric constant, polarization hysteresis loop, and electrostrictive response.

## LTS AND DISCUSSION

ıble 1 summarizes several VDF/TrFE/HFP terpolymers that were prepared by borane/$O_2$ ıloroacetyl peroxide initiators at low temperature. Two commercial copolymers with 'rFE mol% of 50/50, and 62/38 were also investigated for comparison.

Table 1 A Summary of VDF/TrFE/HFP Co- and Ter-polymers.

| un lo. | Polymer Comp.(%) | | | Tm (°C) | ΔHm (J/g) | Tc (°C) | ΔHc (J/g) | Mw ($x10^{-4}$) |
|---|---|---|---|---|---|---|---|---|
| | VDF | TrFE | HFP | | | | | |
| )/50 | 50 | 50 | - | 158.2 | 28.1 | 63.8 | 6.3 | 19.67 |
| ?/38 | 62 | 38 | - | 152.0 | 32.7 | 103.1 | 22.7 | 34.30 |
| 03 | 54.3 | 43.8 | 1.83 | 128.3 | 18.0 | 40.6 | 4.1 | 3.40 |
| 04 | 69.2 | 30.0 | 0.84 | 137.9 | 25.1 | 44.8 | 7.4 | 3.35 |
| 06 | 65.9 | 33.4 | 0.71 | 139.6 | 28.8 | 61.2 | 15.3 | 3.43 |
| 08 | 59.7 | 38.2 | 2.1 | 138.4 | 19.6 | 40.9 | 4.7 | 3.36 |
| 12 | 73.3 | 26.5 | 0.14 | 143.0 | 27.5 | 55.6 | 13.3 | 11.3 |
| 13 | 57.7 | 41.96 | 0.3 | 142.0 | 25.7 | 45.5 | 5.7 | 8.89 |
| 14 | 52.59 | 46.63 | 0.8 | 139.3 | 23.2 | 49.5 | 9.3 | 8.61 |
| 15 | 63.4 | 35.8 | 0.8 | 139.7 | 22.7 | 42.4 | 4.6 | 18.20 |
| 19 | 60.49 | 37.2 | 2.3 | 131.5 | 20.9 | 42.4 | 4.8 | 5.19 |
| 21 | 55.17 | 42.35 | 2.46 | 129.1 | 15.6 | 35.6 | 2.6 | 17.20 |

### ıal Properties

SC measurement was used to investigate the thermal behaviors of the terpolymers. Figure ɔares three terpolymers having VDF/(TrFE+HFP) mole ratio in the vicinity of 55/45 (run ł,103, 121) with the copolymer having VDF/TrFE 50/50 mole ratio. It is very clear that as P molar content increased the Curie and melting temperatures of the terpolymer

decreased. The Curie temperature decreased from 63 °C (commercial VDF/TrFE 50/50 copolymer) to 49.5, 40.6, 35.6°C (our VDF/TrFE/HFP terpolymers with 0.18, 1.8, 2.46 mol%HFP, respectively). The bulky HFP units clearly effect the crystalline domains. The smaller polar domains may result in the lower energy for the conformation transition, hen Curie transition temperature decreases. In addition, the bulky groups may also reduce the intermolecular interaction between the polymer chains.

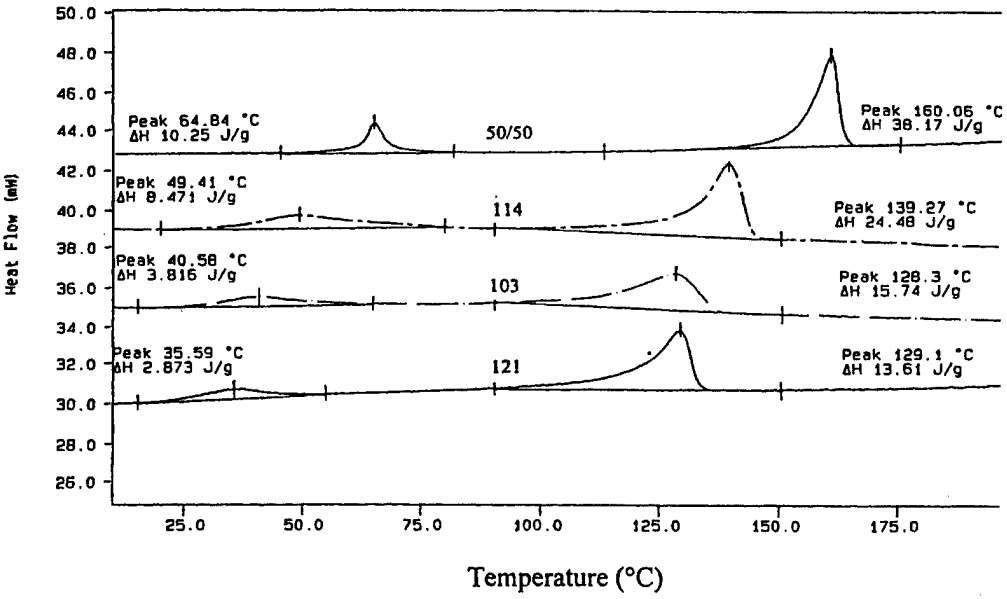


Figure 1. Comparison of DSC thermograms of VDF/TrFE/HFP terpolymer (run no. 114,103, 121) with the copolymer having VDF/TrFE 50/50 mole ratio.

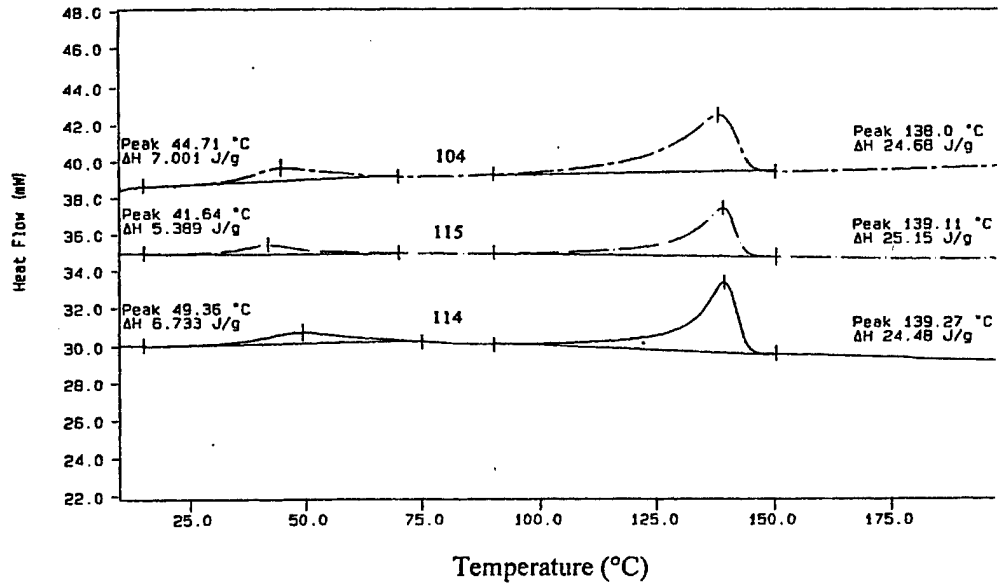


Figure 2. Comparison of DSC thermograms of VDF/TrFE/HFP terpolymers having abou mol% HFP and the TrFE content, 30 (104), 35.8(115), and 46.6 (114) mol%, respectively

igure 2 compares DSC curves of the terpolymers having about 0.8 mol% HFP and the content, 30, 35.8, 46.6 mol% respectively. Both Tm and Tc are not very sensitive to the contents. VDF and TrFE units in the terpolymer must co-crystallize well in the lattice, and ystal structure and polar domain size maintains invariable despite the change of the TrFE mole ratio. Comparing with the corresponding VDF/TrFE copolymers, it appears that ll amount (< 1 mol%) of bulky HFP in VDF/TrFE/HFP terpolymers may only reduce the domain size, but not overall crystallinity and the magnitude of the dipole.

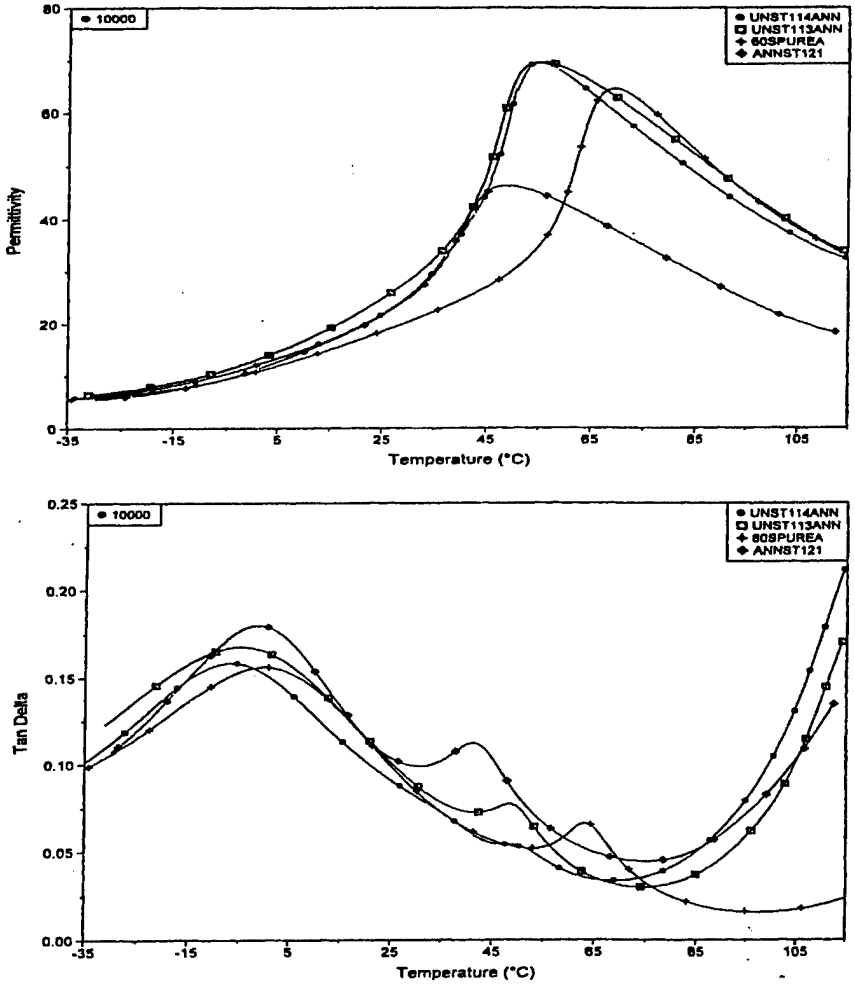


3. The comparison of dielectric constant (top) and dielectric loss (bottom) of three rmers with HFP content of, 0.3, 0.8, 2.46 mol%, designated as □, ●, ♦, respectively, and nmercial copolymer, P(VDF/TrFE) 55/45, ✧

## tric Properties

gures 3 compares permittivity and dielectric loss at 10,000 Hz, respectively, of three ched and annealed VDF/TrFE/HFP terpolymers containing 0.3, 0.8, 2.46 mol% HFP (run 3, 114, 121)and a VDF/TrFE copolymer. All polymers have a similar VDF/TrFE mol

'igure 2 compares DSC curves of the terpolymers having about 0.8 mol% HFP and the content, 30, 35.8, 46.6 mol% respectively. Both Tm and Tc are not very sensitive to the contents. VDF and TrFE units in the terpolymer must co-crystallize well in the lattice, and ystal structure and polar domain size maintains invariable despite the change of the TrFE mole ratio. Comparing with the corresponding VDF/TrFE copolymers, it appears that ll amount (< 1 mol%) of bulky HFP in VDF/TrFE/HFP terpolymers may only reduce the domain size, but not overall crystallinity and the magnitude of the dipole.

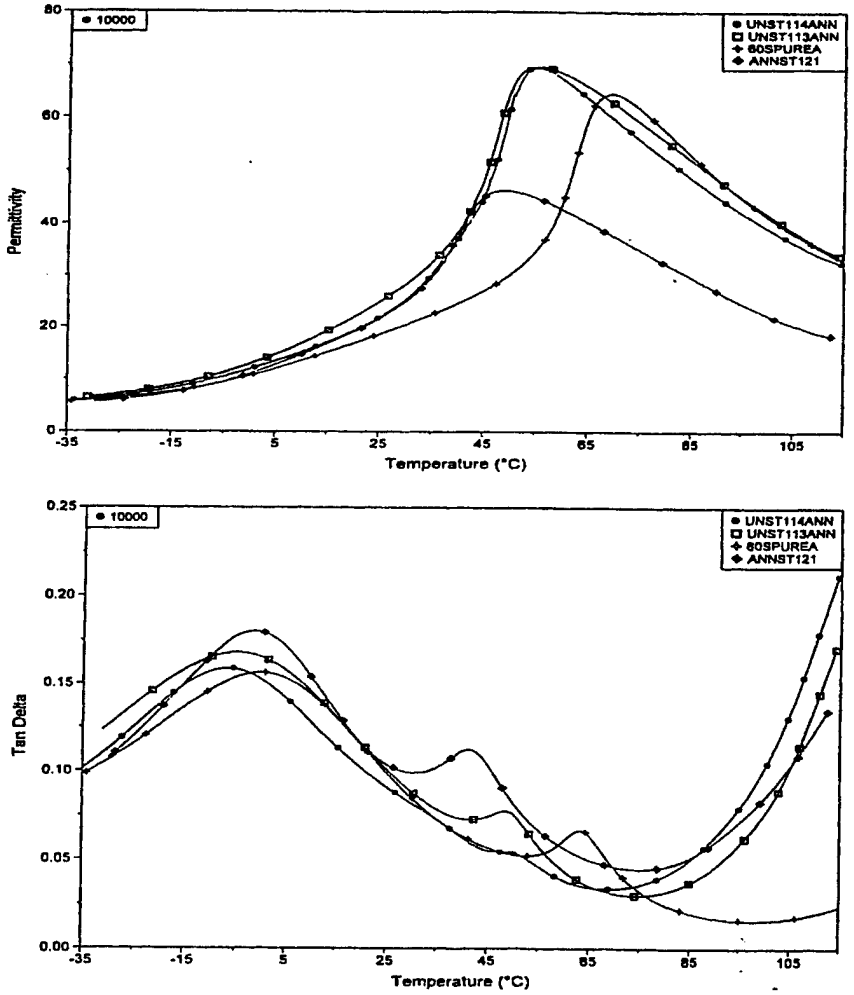


3. The comparison of dielectric constant (top) and dielectric loss (bottom) of three /mers with HFP content of, 0.3, 0.8, 2.46 mol%, designated as □, ●, ♦, respectively, and nmercial copolymer, P(VDF/TrFE) 55/45, ✧

## tric Properties

.gures 3 compares permittivity and dielectric loss at 10,000 Hz, respectively, of three :ched and annealed VDF/TrFE/HFP terpolymers containing 0.3, 0.8, 2.46 mol% HFP (run 3, 114, 121)and a VDF/TrFE copolymer. All polymers have a similar VDF/TrFE mol

ratio 55/45. The results clearly show a significant permittivity dependence on the HFP The correlated Tg (at γ relaxation) of the polymer, associated with the amorphous phas no change in dielectric loss with small amount of HFP units. However, small quantity units in the crystalline domains has a large impact to the crystallization process of the j domains. The Curie transition temperature shifts to the lower temperature as the HFP c increases. It is worth noting that the dielectric constant values of the terpolymers are a same as comparing with copolymer. This result indicates the fact that the introduction units into polymer do not alter the conformation of the polymer chain (polymer chains possess an all-trans ferroelectric conformation at the room temperature). Indeed, it fac rotation of the dipoles upon heating by presumably breaking up the large polar domain microdomains. The small ferroelectric domain only need a small amount of energy to polymer conformation from polar to non-polar.

## Ferroelectricity

Figure 4 compares the electric displacement vs. electric field of three terpolymers 115, 108, 119) with similar VDF/TrFE (~ 60/38) and different HFP content, 0.8, 2.1, 2 HFP, respectively. As HFP content increases, the coercive field decreases as well as th polarization. For the terpolymer, the coercive field (Ec) required to change the directic dipoles is much lower comparing with those of the commercial copolymer. Coercive f terpolymer is in the range of 20-30 MV/m while the coercive field of the commercial c is in the range of 50-60 MV/m. This is presumably due to HFP termonomer breaks lar domain size into smaller domain size, and allows reversal of the dipoles at lower field.

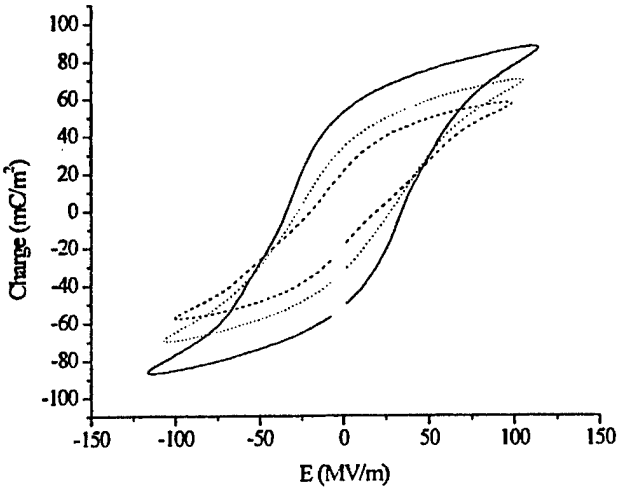


Figure 4. Comparison of electric displacement vs. electric field at 22°C of unstret VDF/HFP/TrFE terpolymers with various HFP contents, 0.8, 2.1, 2.3 m designated as —, ...., ----, respectively.

It is interesting to note that polarization of terpolymer is also dependent on the rel amounts of α- and β-phase. [12] For some terpolymers with relatively low TrFE conte

ant polarization of the stretched polymer film increases dramatically compared to that of etched film. Mechanical drawing clearly increases the relative amount of β-phase by asing the amount of oriented dipoles resulting in an increase in the remnant polarization.

Figure 5 compares the coercive field and the polarization of VDF/TrFE/HFP 7/42.35/2.46) terpolymer 121 under various temperatures. As the temperature increased 21°C to 42°C, the coercive filed reduce since the higher temperature facilitate the change of irection of the dipoles. As the temperature increased to 50°C, the coercive field slightly ased arising from space charge trapped in samples. As the temperature increases further nd the Curie transition temperature, the hysteresis loop obtained was very large with ıding" at the ends indicative of conduction losses. The ability of switching the direction of ipoles is reduced as the temperature goes beyond the phase transition temperature.

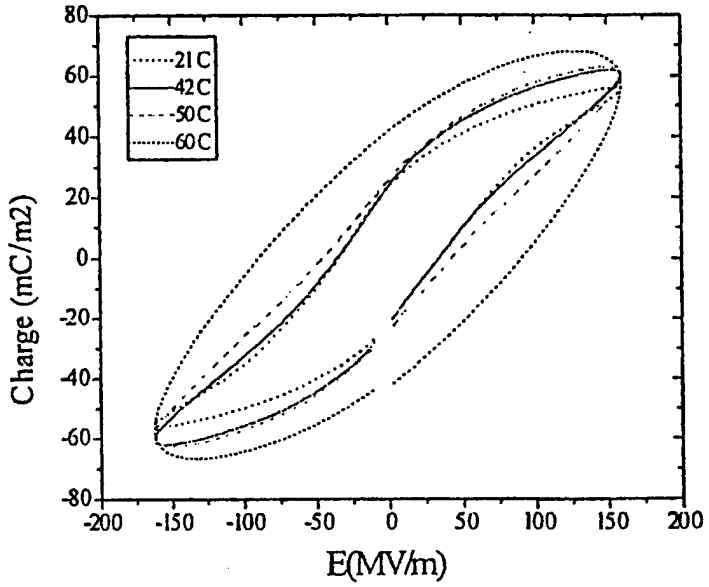


Figure 5. Comparison of polarization hysteresis loop of stretched VDF/TrFE/HFP (55.17/42.35/2.46) terpolymer 121 under various temperatures.

**electricity**

One of the most desirable properties of the eletroactive polymer is to possess large anical deformation at low external field. Figure 6 shows the deformation of the TrFE/HFP (55.17/42.35/2.46) terpolymer under electric field at various temperatures. The nation of the terpolymer has a highest value at 50°C, near the Curie temperature (40°C). e temperature increases further, the deformation drops at low field. After the temperature ıses beyond the Curie transition temperature, the polymer chains lose the piezoelectric rties. Consequently, the deformation drops.

It is very interesting to quantify the effect of HFP content to the strain. Figure 7 ares a deformation under electric field of stretched VDF/TrFE/HFP (55.17/42.35/2.46) ymer with that of the irradiated VDF/TrFE copolymer at Curie temperature. The nation of the terpolymer indeed is higher than that of the irradiated sample at low field. · before has the strain of almost 2.5% been achieved at 50 MV/m. It should be noted that

the high strain response of the terpolymer was obtained at 50°C because the Curie tem of the terpolymer is still above room temperature.

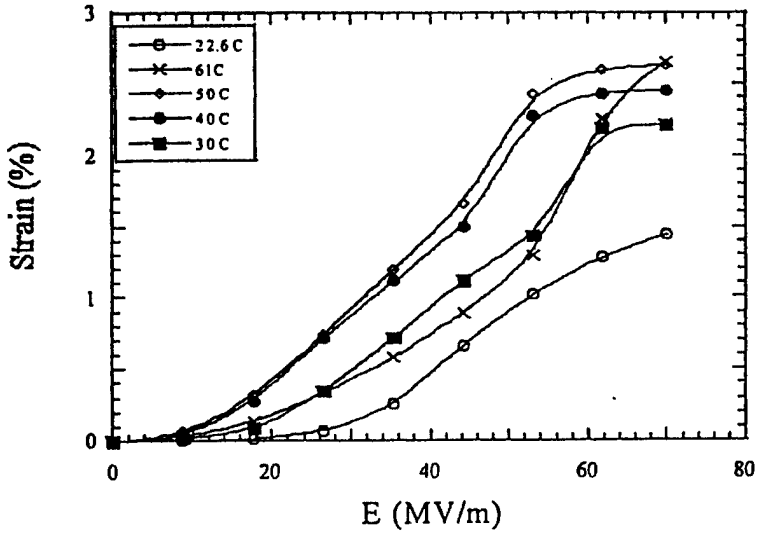


Figure 6. The dependence of the strain response of the stretched VDF/TrFE/HFP (55.17/42.35/2.46) terpolymer on the temperature.

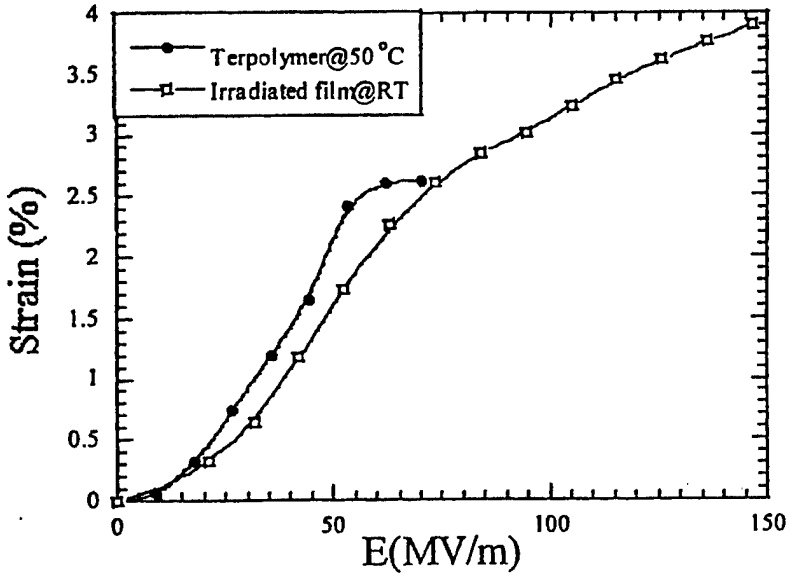


Figure 7. Comparison of the strains of stretched VDF/TrFE/HFP terpolymers m the Curie temperature with that of irradiated VDF/TrFE copolymer at temperature* (*data are reproduced from ref. 6).

## CONCLUSIONS

All the experimental results of VDF/TrFE/HFP terpolymers consistently show that a small amount of HFP units have a significant effect to the polymer morphology and electric properties. Few bulky groups effectively reduce the size of polar crystalline domains, but not the overall crystallinity and conformation of the polymer. The flexible dipoles in the smaller polar domains reflect in the piezoelectric property. A highest value of strain (about 2.5%) at very low field (50 MV/m) was observed in the terpolymer, which is significantly higher than that of the irradiated copolymer sample under the same conditions.

## ACKNOWLEDGMENTS

The authors would like to thank Professor Q. M. Zhang for his technical assistance in the electric property studies. We gratefully acknowledge the financial supports of DARPA and Office of Naval Research.

## REFERENCES

1. K. Koga, and H. Ohigashi, J. Appl. Phys., **59**, 2142 (1986).
2. K. Tashiro, S. Nishimura, and M. Kobayashi, Macromolecules, **21**, 2463 (1988), and **23**, 2802 (1990).
3. B. Daudin, and M. Dubus, J. Appl. Phys., **62**, 994 (1987).
4. T. Yuki, S. Ito, T. Koda, and S. Ikeda, Jpn. J. Appl. Phys., **37**, 5372 (1998).
5. S. Ikeda, H. Suzaki, and S. Nakami, Jpn. J. Appl. Phys., **31**, 1112 (1992).
6. Q. M. Zhang, V. Bharti, and X. Zhao, Science, **280**, 2102 (1998).
7. H. Freimuth, C. Sinn, and M. Dettenmaier, Polymer, **37**, 832 (1996).
8. Y. Tajitsu, A. Hirooka, A. Yamagish, and M. Date, Jpn. J. Appl. Phys., **36**, 6114 (1997).
9. T. C. Chung, and W. Janvikul, J. Organomet. Chem., **581**, 176 (1999).
10. J. E. Leffler, and H. H. Gibson, jr., J. Amer. Chem. Soc., **90**, 4117 (1968).
11. P. K. Isbester, J. L. Brandt, T. A. Kestner, and E. J. Munson, Macromolecules, 31, 8192 (1998).
12. B. A. Newman, C. H. Yoon, K. D. Pae, And J. I. Scheinbeim, J. Appl. Phys, **50**, 6095 (1979).

# APPENDIX 13

# Giant Electrostrictive Response in Poly(vinylidene-fluoride hexafluoropropylene) copolymer

**Xiaoyan Lu, Adriana Schirokauer and Jerry Scheinbeim**
**Dept. of Chemical and Biochemical Engineering,**
**Rutgers University, Piscataway, NJ 08855**

## ABSTRACT

In the present study, the strain response of a new class of copolymers of $PVF_2$ is investigated. Electrostrictive strains were measured in poly(vinylidene-fluoride hexafluoropropylene), P($VF_2$-HFP), using a capacitance method (air-gap capacitor), as a function of electric field. Three different thermal treatments (ice water quenched, air quenched and slow cooled) were given to samples of composition 5% and 15% HFP. Strains greater than 4 % were observed in the 5% HFP ice water quenched P($VF_2$-HFP) copolymer. Values of elastic modulus were lower for the quenched 5 % films than for the slow cooled ones, and in both cases they were higher than previously studied polyurethane elastomers and poly(vinylidene-fluoride trifluoroethylene) copolymers.
Key words: Electrostrictive Polymer, Poly(vinylidene-fluoride hexafluoropropylene) copolymer, Ferroelectic, X-ray, DSC.

## INTRODUCTION

Field-induced electrostrictive strains can be observed in a material upon application of an electric field. These strains are known to be proportional to the square of the applied field. If the strains are high enough, materials having this property offer great promise in applications such as sensors, actuators, artificial muscle, robotics and MEMS.
Giant electrostrictive strains were first observed in a polyurethane elastomer [1]. The polyurethane exhibited strains greater than 3% under electric fields of up to 40 MV/m and an elastic modulus on the order of 0.01 GPa. Recently, strains up to 4% were observed in a copolymer of $PVF_2$, Poly(vinylidene fluoride/ trifluoroethylene), [P($VF_2$/TrFE)] upon application of electric fileds up to 150 MV/m. These films were subjected to a two step process in which the materials were first melt-pressed and slow cooled and then irradiated with a high energy electron beam [2]. The irradiated P($VF_2$/TrFE) films were observed to have an elastic modulus of approximately 0.4 GPa.
In the present study, the electrostrictive strains were measured in poly(vinylidenefluoride/hexafluoropropylene), P($VF_2$/HFP), random copolymers under electric fields up to 60 MV/m. The strain response of ice water quenched, air quenched and slow cooled samples was compared for 5% and 15% HFP copolymer compositions. The thickness strain constant, $d_t$, was then calculated from the strain vs. electric field curve. Dielectric constant of the materials, elastic modulus, $d_{31}$ and $e_{31}$ were studied, as well as the material's melting behavior and crystallinity observed from DSC and X-Ray Diffraction data.



Mat. Res. Soc. Symp. Proc. Vol. 600 © 2000 Materials Research Society

## :XPERIMENTAL

Films of the 5% and 15% mol % HFP copolymers of $PVF_2$/HFP were prepared in a :arver Laboratory Press®. The copolymers were obtained in pellets from Soltex, and onverted then into powder in a Freezer Mill. The powder was melted at 190 °C and ressed at 4,000 psi. For each composition, three different thermal treatments were used: :e water quench, air quench and slow cool. All samples were 50 to 60 μm in thickness ıd were cut into strips of 3 x 2 cm. Two strips of the same film were cut for each kind of ımple. Gold electrodes 30 nm in thickness were deposited on the two sides of the films sing a Sputter Coater EMS 650. The electrode area was 2.5 x 1.5 cm. The two films ere placed on the sides of an air-gap capacitor, sandwiched between the capacitor plates ig.1). One electrode of each film was connected to the high voltage supply and the her electrode was grounded. Electrostrictive strains were measured as a function of dc ectric field up to 60 MV/m using the air-gap capacitor.

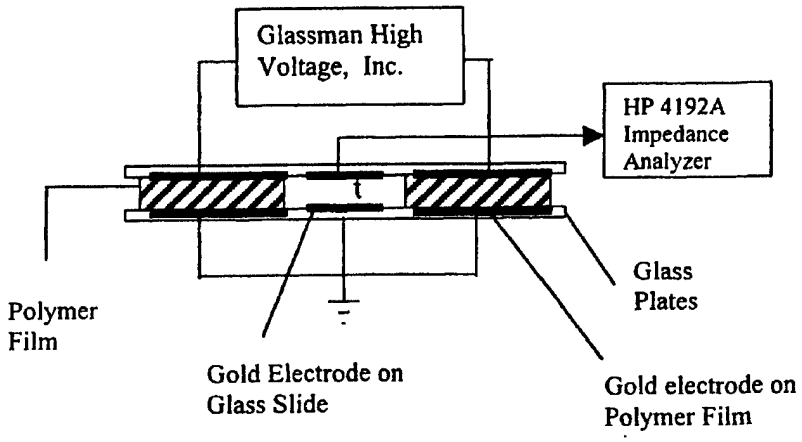


g. 1- Schematic of the air-gap capacitance system. Air-gap electrode area is 4.0 $cm^2$.

ıe capacitance of the air-gap, measured using an HP 4192A Impedance Analyzer, was en related to the strain change in the film. The measured capacitance is related to the :-gap thickness through equation 1.

$$t = \varepsilon_o \cdot A/C \qquad [1]$$

ıere $\varepsilon_o$ is the permittivity of air, A is the air-gap electrode area and C is the measured pacitance. Given the arrangement of the polymer films sandwiched between the pacitor plates, the air-gap thickness is approximated to the film thickness, t. The rcent strain of the film is then approximated to the percent change of the air-gap. ılibration of the system was first performed using a 1.00 pF standard capacitor. The

precision of the measurement was 2%. The accuracy of the capacitance system w confirmed using the previously tested polyurethane films. The results obtained w system matched the ones previously obtained [1]. For a given composition, the re of ice water quenched, air quenched and slow cooled samples were compared. modulus and relative dielectric constant were measured at 100 Hz and room tempe as well as a function of frequency (ranging from 0.01 to 10,000 Hz) and temp (ranging from -80°C to 100°C) using a Rheolograph Solid® Toyoseiki, Japan.

X-Ray Diffraction patterns were obtained using a Diffraktometer Kristall Siemens. The melting behavior of the material was studied using a Differential Sc Calorimeter (DSC), TA Instruments®. Values of remanent polarization and c field were obtained by poling the films using a high voltage source Trek® Mode and Keithley® 617 electrometer and 195A digital multimeter, and the aid of co software.

## RESULTS AND DISCUSSION

Both P($VF_2$-HFP) copolymers of 5 % and 15 % mol % HFP content exhibited th behavior with respect to thermal treatment; slow cooled and air quenched s showed the smallest response (strains ≈ 1 %), whereas the ice water quenched s exhibited the largest response in both, the 5 % and the 15% HFP compositions ( Strains greater than 4 % were observed in the 5% HFP ice water quenched P(VF copolymer, the largest response observed among all of the samples. Following th behavior, 15 % HFP ice water quenched films showed the largest strains (≈ 3%) the samples of the same composition. All curves were proportional to the square electric field until saturation. The ice water quenched 5% HFP copolymer also sh highest thickness strain coefficient, $d_t$, among all of the samples (Fig. 3). The th strain coefficient increased linearly with increasing electric field up to the begin saturation indicating electrostrictive response. The $d_t$ value for the 5% HFP ic quenched copolymer was approximately 16.5 Å/V. The value of the electros constant, $M_{33}$, was $5.5 \times 10^{-17}$ $m^2/V^2$. Both values are larger than the ones obse previously studied polyurethane elastomers and P($VF_2$-TrFE) copolymer.

To gain an understanding of the structure of these copolymers and the diff between them that can be accounted for in terms of their strain responses, ch dielectric constant with temperature and frequency, DSC scans and X-Ray dif were performed. Figure 4 shows the change in dielectric constant with temperatur 5% and 15% HFP ice water quenched copolymers showed an increase in di constant with increasing temperature with a pattern similar to that of $PVF_2$ homop The dielectric loss curves showed the glass transition temperature peak at around for the 5% HFP ice water quenched copolymer. This peak shifts to higher tempera the HFP content is increased as shown in the curve for the 15% HFP ice water qu copolymer with glass transition temperature at around -20°C. The dielectric c frequency scans showed a decrease in dielectric constant with frequency. The ch dielectric constant with frequency is also similar to that of $PVF_2$ homopolym Curie transition temperature is observed on the dielectric constant-temperature sca

The X-Ray diffraction patterns of the 5% and 15% ice water quenched samp not lead to a characterization of the crystal structure of these copolymers. It was

from previous work [3] that $PVF_2$ homopolymers exhibit two phases, phase I, a non-polar phase and phase II which is a polar ferroelectric phase. To gain more information on

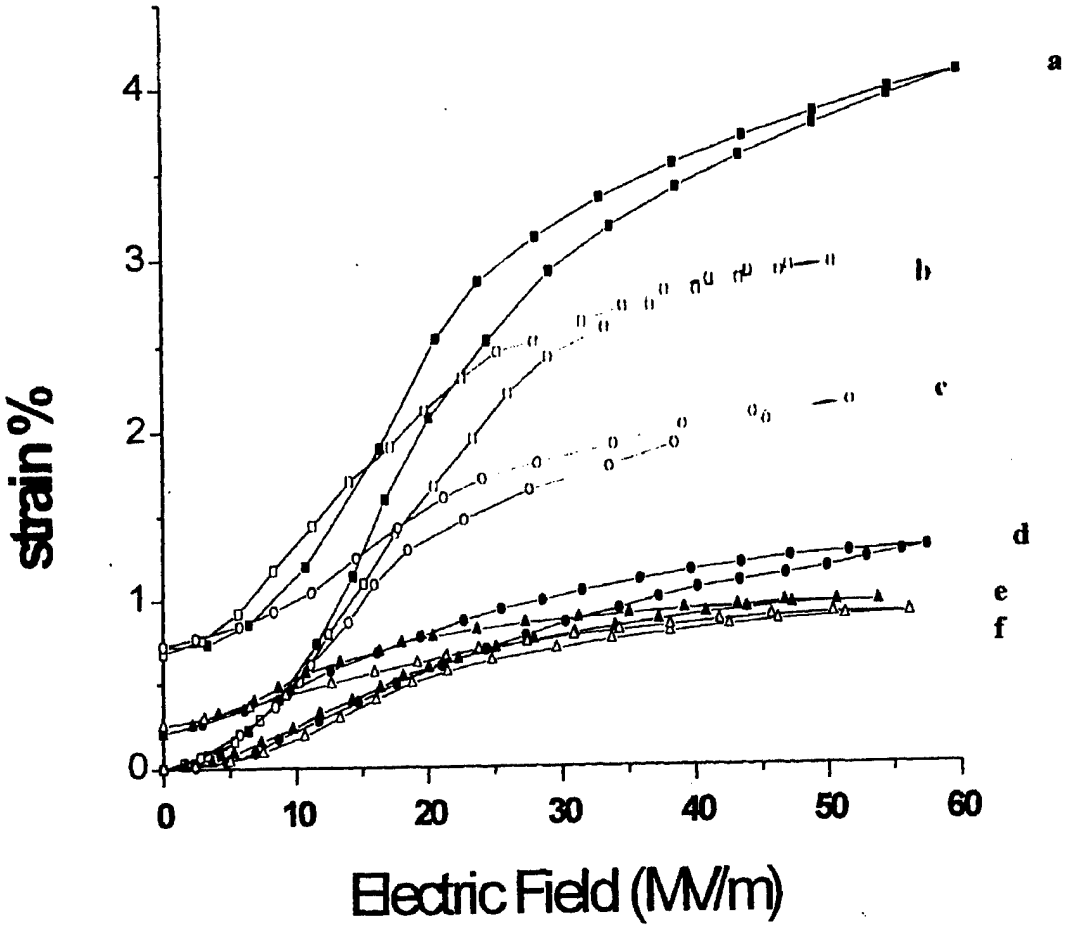


. 2- Strain response of PVF2/HFP copolymers with applied electric field. a) ice water quenched $PVF_2$/HFP 5%, b) ice water quenched $PVF_2$/HFP15%, c) air quenched $PVF_2$/HFP 15%, d) air quenched $PVF_2$/HFP 5%, e) slow cooled $PVF_2$/HFP 5% and f) slow cooled $PVF_2$/HFP15%.

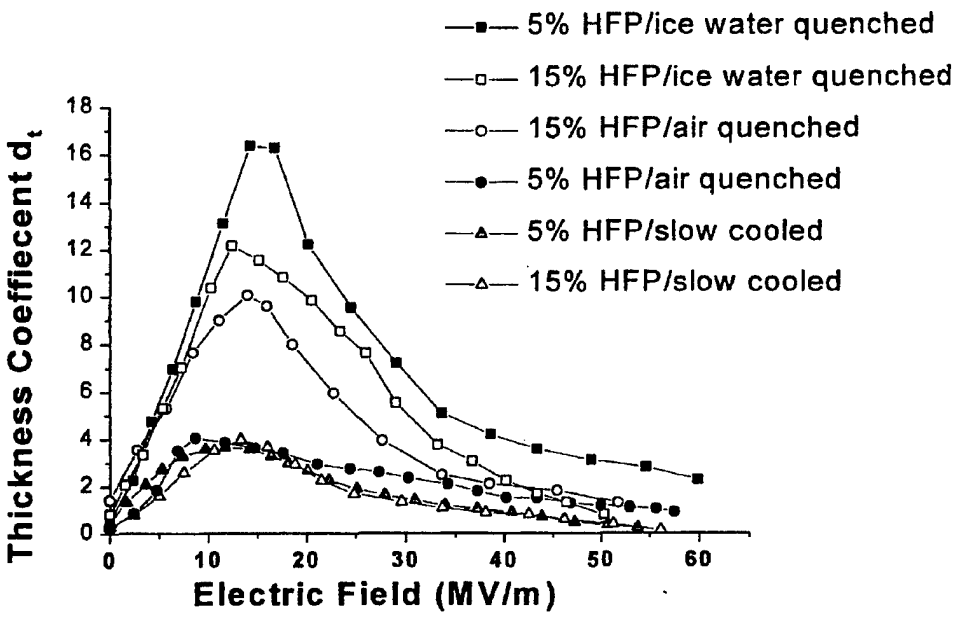


Fig. 3- Thickness strain constant, $d_t$, as a function of electric field.

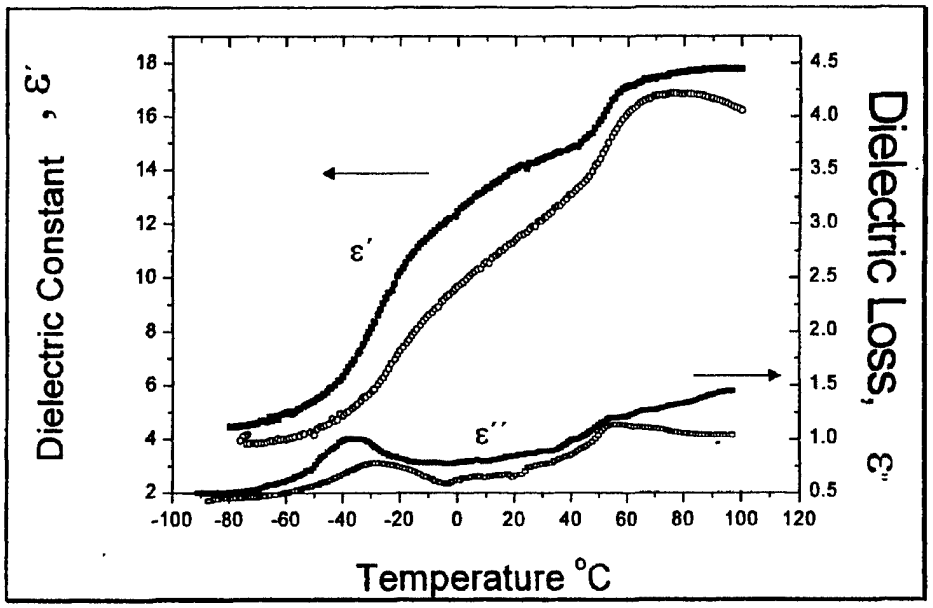


Fig. 4- Dielectric constant vs. temperature for ice water quenched samples, 5% HFP (•) and 15% HFP (o). The frequency of measurement is 104 Hz.

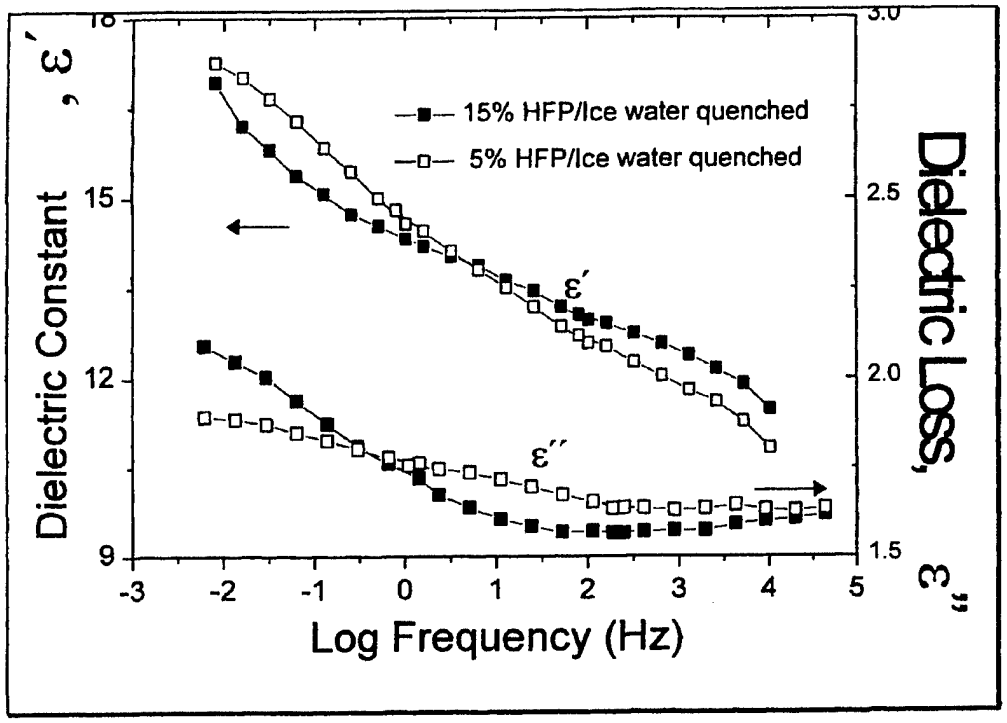


Fig. 5- Dielectric constant vs. frequency for ice water quenched samples measured at room temperature.

oelectric behavior of the 5% and 15% HFP ice water quenched copolymer a poling eriment was performed in the range of -150 MV/m to 150 MV/m. At the higher tric fields, the 5% and 15% HFP copolymers showed ferroelectric behavior. The oelectric switching occurred at electric fields that are higher than the range used for in measurements (electrostrictive strains were measured up to 60 MV/m). Figure 6 ws the electric displacement, D, vs. electric field curves for the ice water quenched and 15% HFP copolymers. The remanent polarization, Pr, decreased about 20% from 5% HFP copolymer ($\approx$ 60 mC/m$^2$) to the 15% HFP copolymer ($\approx$ 48 mC/m$^2$) due to decrease in crystallinity when adding more HFP. For all other samples the remanent arization was negligible.The previous result suggests that the material exhibits oelectric behavior at higher electric fields, however no conclusion can be drawn as to ather or not this property plays a role in the mechanism of electrostriction.

The crystallinity of the material was studied using Differential Scanning Calorimeter SC) to analyze the melting behavior and X-Ray Diffraction (WAXD) to find out nges in crystal structure. Fig 7 shows the increase in crystallinity as well as the crystal m from before and after the application of high field ($\approx$ 50 MV/m). Also as suggested the enthalpy values, crystallinty decreases with increasing HFP content in the olymer, which is due to the bulky size of the $CH_3$ groups.

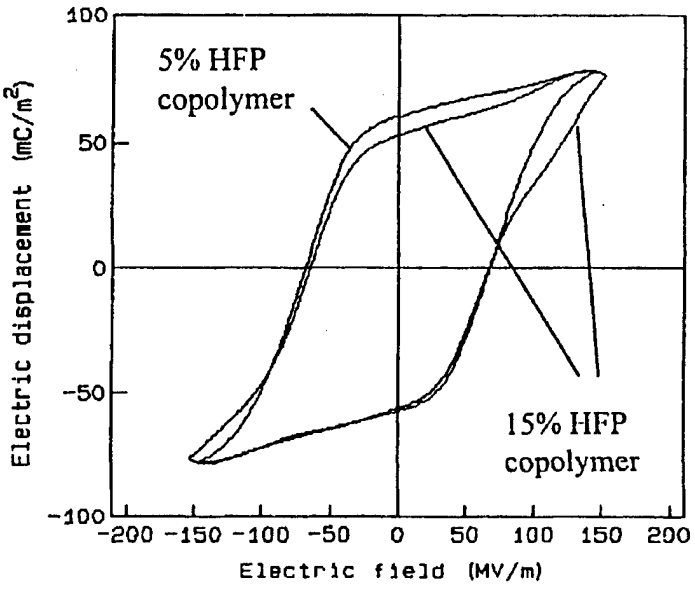


Fig. 6- Electric Displacement vs. Electric Field for ice water quenched 5% and 15% % HFP copolymers.

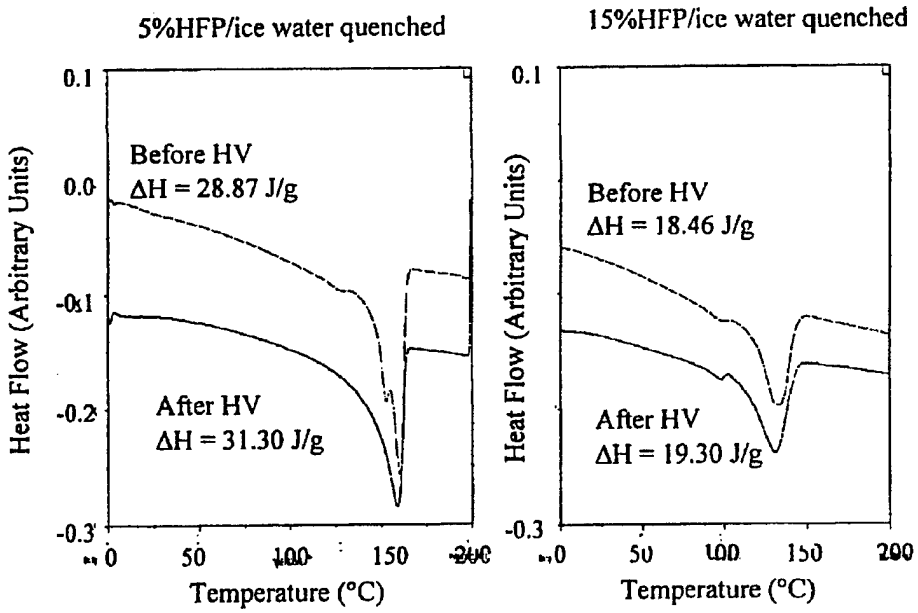


Fig. 7- DSC Thermograms of ice water quenched 5% and 15% HFP, P(VDF-HFP) samples before and after application of high voltage (HV).

This observation was confirmed by the X-Ray diffraction patterns (WAXD) of the ıples. (Figure 8). For 5% HFP/ice water quenched sample, both curves before and r application of field can be matched to the pattern of $PVF_2$ polar phase II [3], wing the (010) peak at around $2\theta = 19$ and (110) peak at around $2\theta = 20$. For 15% ?/ice water quenched sample, the diffraction pattern is unsolved. Further racterization of these crystal structures will be performed using IR spectroscopy.
Values of elastic modulus and dielectric constants for both samples before and after lication of field were measured and tabulated in tables 1 and 2. Values of elastic lulus for both 5% and 15% HFP ice water quenched samples were higher than the viously studied polyurethane elastomers (elastic modulus = 0.068 GPa), [1], and (vinylidene-fluoride trifluoroethylene) copolymers (0.38 GPa), [2]. The energy isty of 5% HFP ice water quenched sample is also much higher compared to viously studied polyurethane elastomers and high energy electron irradiated trostrictive poly(vinylidene-fluoride trifluoroethylene) copolymers .

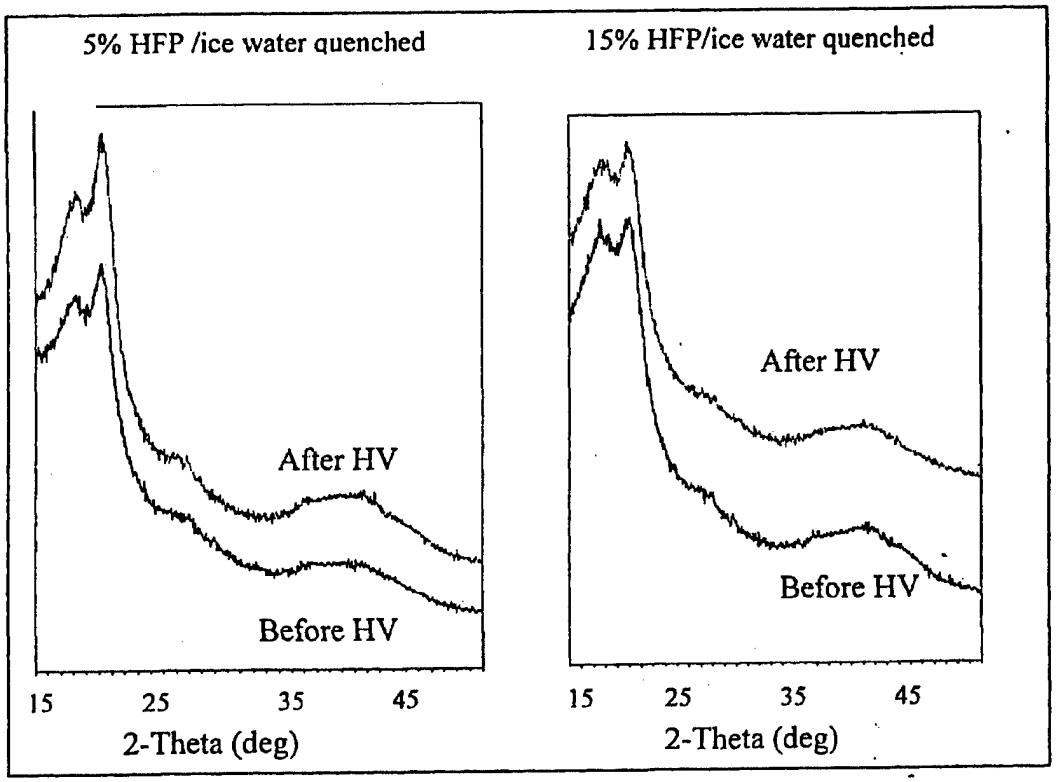


Fig. 8- X- Ray diffraction patterns of ice water quenched samples before and after application of high voltage.

| Material P(VDF-HFP) | Y (GPa) | $\varepsilon_r$ | $YS^2/2$ ($J/cm^3$) |
|---|---|---|---|
| 5% HFP/Ice Water Quenched | 0.88 | 13.5 | 0.7 |
| 15% HFP/Ice Water Quenched | 0.55 | 12.7 | 0.25 |

Table 1. Elastic modulus ,dielectric constant and energy density for ice water quenched P(VDF-HFP) copolymer with 5 and 15% HFP before polir

| Material P(VDF-HFP) | Y (GPa) | $\varepsilon_r$ | $YS^2/2$ ($J/cm^3$) |
|---|---|---|---|
| 5% HFP/Ice Water Quenched | 1.10 | 13.3 | 0.88 |
| 15% HFP/Ice Water Quenched | 0.50 | 13.3 | 0.23 |

Table 2. Elastic modulus , dielectric constant and energy density for ice wate quenched P(VDF-HFP) copolymer with 5 and 15% HFP after poling

Further research will investigate other structure property relationships in copolymers and will be directed towards gaining an understanding of the mole mechanisms responsible for the observed electrostrictive response.

## REFERENCES


[1] Ma, Z, J. Scheinbeim, J. Lee and B. Newman. High Field Electrostrictive Respon Polymers, Journal of Polymer Science: Part B: Polymer Physics, **32**, 2721 (1994)

[2] Zhang, Q. M, V. Bharti and X. Zhao. Giant Electrostriction and Relaxor Ferroelec Behavior in Electron-Irradiated Poly(vinylidene fluoride-trifluoroethylene) Copolymer, Science, **280**, 2101 (1998).

[3] B. A. Newman and J. Scheinbeim. Polarization Mechanism in phase II Poly(vinylidene fluoride) films, Macromolecules, **16**, 60 (1983).

# APPENDIX 14

# ELECTRO-MECHANICAL PROPERTIES OF ELECTRON IRRADIATED P(VDF-TrFE) COPOLYMERS UNDER DIFFERENT MECHANICAL STRESSES

Z.–Y. Cheng,* S.J. Gross, V. Bharti, T.–B. Xu, T. Mai and Q. M. Zhang
Materials Research Laboratory, The Pennsylvania State University
University Park, PA 16802 (*E-mail: zxc7@psu.edu)

## ABSTRACT

The electro-mechanical properties of high energy electron irradiated poly(vineylidene fluoride-trifluorethylene) (P(VF-TrFE)) copolymers under different mechanical stress conditions are reported. In stress free condition, the electric field induced longitudinal and transverse strains of the irradiated P(VDF-TrFE) copolymer films at room temperature (RT) can reach about 5% and more than 3% respectively. The longitudinal strain response of the material under hydrostatic a pressure up to 83 atmospheses was studied at RT. The transverse strain response of the material at RT was studied under uniaxial tensile stress. It was found that the material has a high load capability and for stretched films along the stretching direction the induced strain remains high, even at about 45 MPa. The temperature dependence of the strain re ponse is also characterized. Both the temperature and stress dependence of the strain response indicate that the electric field induced strain response originates from the electric field induced local phase transition.

## INTRODUCTION

Electroactive materials have been used in numerous applications, such as robotics, active damping, vibration control and isolation, manipulation, ultrasonic transducers for medical diagnosis and sonar. However, most of the activities in the area of electroactive materials was focused on inorganic ceramics/crystals [1]. Not much attention was paid to electroactive polymer (EAP) due to the small number of available materials, as well as their limited actuation capability.

For electro-mechanical applications, a material exhibiting a high electric field induced strain response is always highly desirable. Recently, a very high electric field induced strain response was observed in many EAP systems [2], such as heavily plasticized poly(vineylidene fluoride-trifluorethylene [P(VDF-TrFE)] [3], polyurethane and silicone [3], [4]. Very recently, we reported that high energy electron irradiated P(VDF-TrFE) copolymer film exhibits a very large electric field induced strain response [5], [6]. The irradiated P(VF-TrFE) copolymers possesses a very high elastic energy density besides the high strain response since the material is of relative high elastic modulus compared to other EAP [5], [6]. In addition, these polymers have many advantages over ceramics/crystals, such as low cost, flexible, easy to process and shape. All these make the electroactive polymer (EAP) very attractive for a broad range of electromechanical applications [2].

In most electromechanical applications, the material is under some mechanical load condition. Thus, for a soft polymeric material, the electromechanical properties of the material under different stresses conditions or the load capability of the material is always an important concern. In this paper, the studies of the electric field induced strain response of irradiated P(VDF-TrFE) copolymer under different mechanical boundary conditions are reported. The results show that the material has high load capability.



Mat. Res. Soc. Symp. Proc. Vol. 600 © 2000 Materials Research Society

## ERIMENT

(VDF-TrFE) copolymer powders were purchased from Solvay and Cie, Bruxelles, Belgium. compositions used here are 50/50, 65/35, and 68/32 mol%. The copolymer films studied were prepared using two approaches: melt press and solution cast. In the melt press process, opolymer powders were pressed between two pieces of aluminum foil at 215 to 240 °C. In olution cast method, the copolymer powders were dissolved in dimethyl formanide (DMF) hen the solution was cast on a flat glass plate and dried in an oven at 70 °C. Two types of , the stretched and unstretched films, were studied in this work. For the unstretched films, ilms prepared above were annealed at 140 °C for a time period between 12 to 14 hrs to ɔve the crystallinity. In order to prepare the stretched films, the films made from solution or quenched from melt press were uniaxially stretched up to 5 times at a temperature ɛen 25 to 50 °C. The stretched films were then annealed at 140 °C for 12 to 14 hrs to ase the crystallinity. During the annealing process, the two ends of the stretched films were ıanically fixed. The crystallinity of the final films is about 75%. The thickness of the films in the range from 15 to 30 μm. The electron irradiation was carried out in nitrogen sphere at different temperatures with an electron energy of 2.55 MeV, 1.2 MeV, and 1.0

ı order to characterize the electric filed induced strain response, gold electrodes of a ness of about 40 nm were sputtered on both surfaces. The longitudinal strain response of the under a stress free condition was characterized using a specially designed strain sensor based e piezoelectric bimorph [7]. The longitudinal strain response of the films under hydrostatic ure was characterized using a specially designed set-up [8]. The transverse strain of the under different tensile conditions was characterized using a cantilever-based dilatometer was newly developed for characterizing transverse strain response of polymeric film [9].

## ULTS AND DISCUSSION

### in Response of Films under Stress Free Condition

'he electric field induced strain responses of some irradiated copolymer films at RT are 'n in Fig. 1. A sinusoidal electric field with a frequency of 1 Hz was applied and the strain measured at 2 Hz using a lock-in amplifier since the material is electrostrictive. The tudinal strain is a result of the thickness change of the film, while the transverse strain is ɛd to the length change of the film perpendicular to the applied field direction. The verse data reported here was measured along the stretch direction of the stretched samples. rly, the material exhibits a very high strain response. It should be noticed that the tudinal strain is always negative. For unstretched films, the transverse strain, which is about ›f the absolute value of the longitudinal strain, is always positive. However, for the stretched ›le, it is found that the transverse strain along the stretch direction, which is comparable with ɜtrain level of the longitudinal strain, is positive, while the transverse strain along the :tion perpendicular to the stretch direction, which is about or less than 1/3 of the longitudinal ı and is negative. That is, the volume strain of the irradiated copolymer is also very high [6]. ould also be mentioned that in many electroactive materials, such as polyurethane, silicone, piezoelectric ceramics, the volume strain is very small [1], [4]. The large volume strain rated by the irradiated copolymer indicates that the material also has a potential for ostatic applications.

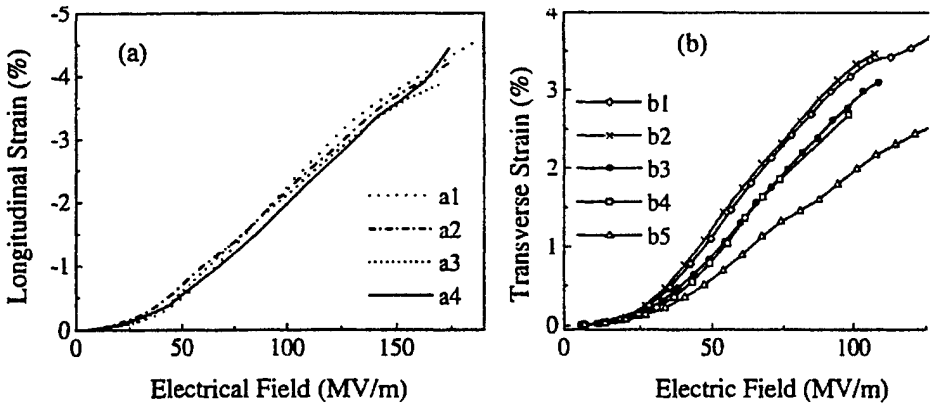


Fig. 1. Amplitude of the strain response vs. amplitude of the electric field.
(a). Longitudinal strain of samples irradiated with 2.55 MeV electrons. Curve: a3 and a4 are the stretched 65/35 irradiated at 120 °C with 80 Mrad dose, uns 65/35 irradiated at RT with 100 Mrad dose, stretched 50/50 irradiated at 77 60Mrad dose, and unstretched 50/50 irradiated at RT with 100 Mrad dose.
(b). Transverse strain of stretched samples. Curves b1 and b2, are 68/32 film ir at 100 °C with 65 Mrad and 70 Mrad doses respectively using 1.2 MeV e. Curve b3 is 65/35 irradiated at 105 °C with 70 Mrad dose using 1.0 MeV e. Curves b4 and b5 are 65/35 irradiated at 95 °C with 60 Mrad dose and at 77 °C Mrad dose respectively using 2.55 MeV electrons.

## Longitudinal Strain of Material under Hydrostatic Pressure

The hydrostatic pressure dependence of the longitudinal strain of an unstretcl copolymer film, irradiated at 95 °C with 60 Mrad dose using 2.55 MeV electrons, is Fig. 2. The pressure range applied here is limited by the experimental set-up. Eve pressure, the material can still produce the high strain response. With regard to th between the strain response and pressure, it is found that the strain does not change r the pressure at low driving electric field and that the strain response shows an increas pressure at high electric field.

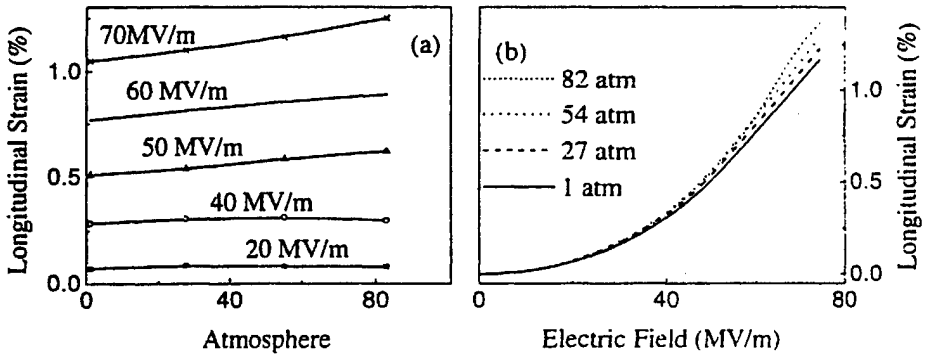


Fig. 2. (a). Longitudinal strain vs. electric field of film under different hydrost pressures. (b). Longitudinal strain vs. hydrostatic pressure for the material un different electric fields. The electric field was 1 Hz sine wave.

## iverse Strain of Stretched Film under Uniaxial Tensile

ıe transverse strain along stretch direction of a stretched 65/35 copolymer film, irradiated at with 60Mrad dose using 2.55 MeV electrons, under different tensile loads along the stretch on is shown in Fig. 3. It was found that the film broke down after working at the tensile of 45 MPa for a while. That is, the elastic strength of the film is about 45 MPa which is ırable to that of commercial nylon. Even at the tensile stress of 45 MPa, the film still ts a very large strain response. These results indicate that the materials studied here have a ɔad capability. This is a great advantage of the irradiated copolymer over the other EAP. ıta in Fig. 3 clearly shows that the transverse strain response increases with tensile stress at ginning and then decreases with the stress. There is a tensile stress ($S_M$) at which the strain ts a maximum for the film under a constant electric field. This tensile stress, $S_M$, is strongly lent on the electric field. The higher the electric field, the lower $S_M$.

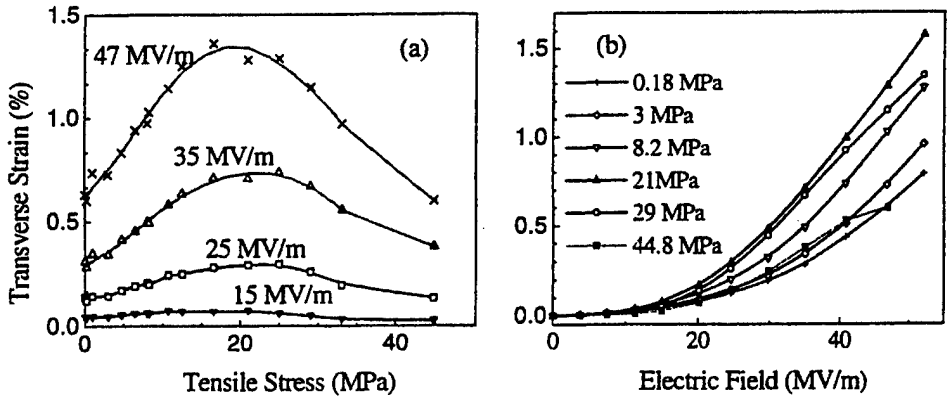


Fig. 3. (a). Transverse strain amplitude vs. tensile for the film under different electric fields. (b). Transverse strain amplitude vs. electric field amplitude for the film under different tensile. The electric field is 1 Hz since wave.

## rature Dependence of Strain Response

ɔrder to understand the stress dependence of the electric field induced strain response and rmine the working temperature range for the material, the temperature dependence of the esponse was measured. Two typical results are shown in Fig. 4. In both longitudinal and rse strain measurements, the temperature range used in this investigation was limited by up.

m the data in Fig. 4(b) one can see that the strain response decreases with increasing ature beginning at RT. When decreasing the temperature, the strain response increases at ginning and then decreases. There is a temperature ($T_m$) at which the strain response s a maximum for the film under a constant electric field. It seems that the $T_m$ increases with the electric field. The data in Fig. 4(a) show a similar behavior. However, since the at temperatures lower than RT can't be measured, the Tm can't be determined here. er, the trend is similar to that in Fig. 4(b).

: temperature dependence of the electric field induced strain reported here can be easily ood by considering the fact that the irradiated copolymer is relaxor ferroelectrics [5], [9], or relaxor ferroelectrics, the electric field induced strain is related to the electric field l breathing of the polar regions [11], [12]. At high temperatures, the concentration of the egion increases with decreasing temperature. The electric field induced strain therefore

increases with decreasing temperature. At low temperatures, a freezing of the pola happens. With decreasing temperature, an increased amount of the frozen polar regions i the decrease of the electric field induced strain response. Therefore, the $T_m$ is relate freezing process of the polar regions. However, the electric field has some influenc freezing process of the polar region. That is why the strain maximum temperature slightly with the driving electric field.

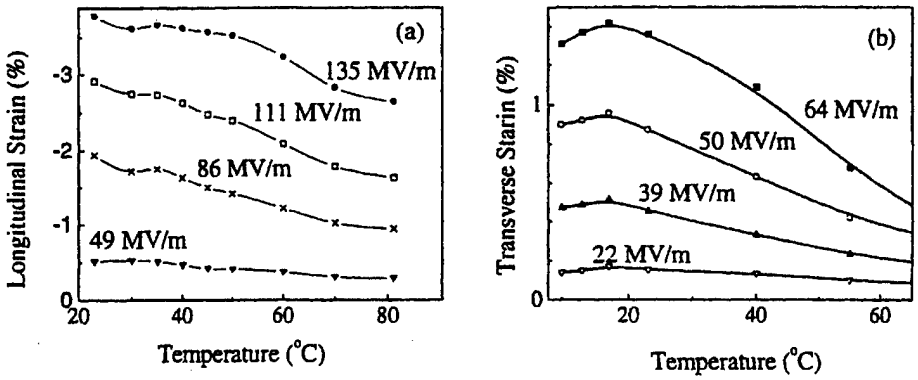


Fig. 4. Temperature dependence of the strain response for the films under constant electric field. (a). Longitudinal strain of the film characterized in Fig. 2 (b) Transverse strain of the film studied in Fig. 3.

## Relationship Between Stress Effect and Temperature Effect

For unirradiated copolymers, there is a Curie temperature, at temperatures below w material is the ferroelectric phase. After irradiation, the material is transferred from a ferroelectric to a relaxor ferroelectric. Although the relaxor ferroelectric does not hav temperature, there are polar regions whose behavior is very similar to ferroelectrics. Thus discuss approximately the relaxor ferroelectric using the Devonshire phenomenological t the ferroelectric. For a normal ferroelectric, the Curie temperature changes with external following [9], [13]:

$$\Delta T = 2\varepsilon_0 C Q_{i3} X_i \qquad (1)$$

Where $\Delta T$ is the change of Curie temperature corresponding to the stress ($X_i$). Both $C$ anc the material properties, the Curie-Weiss constant and the electrostrictive coefficients. $\varepsilon$ vacuum permittivity. For the material under a hydrostatic pressure (negative stress), th and $Q$ in Eq. (1) are the pressure and $Q_h(=Q_{33}+Q_{13}+Q_{23})$ respectively. For the ir copolymer studied here, it has been reported that $Q_{13}>0$, $Q_{33}<0$, and $Q_h= <0$ [6]. Thus, the hydrostatic pressure and the uniaxial tensile stress (positive stress), the Curie tem increase with increase pressure or tensile.

Now we discuss the stress effect on the strain for the material shown in Fig. 3 at a electric field. With an increasing tensile stress, the $T_m$ shifts toward RT, at first due to $T$ lower than RT. This will result in the strain response of the material at RT increasing wit stress at the beginning. If the tensile stress increases further, the $T_m$ will be higher than RT case, the increase of tensile stress will result in the $T_m$ deviating away from RT. Thus, the field induced strain response of the film at RT will decrease with increasing tensile stres observations are consistent with the experimental data shown in Fig. 3(a).

When the electric field changes, as shown in Fig. 4, the $T_m$ increases with increasing tensile stress. In a stress free condition, the higher the electric filed, the closer the $T_m$ is to RT. Therefore, the higher the electric field, the lower the stress needed to shift the $T_m$ to RT. That is, the higher the electric field, the smaller the $S_M$. This is consistent with the data shown in Fig. 3(a).

All the above discussions indicate that the Devonshire theory can be used to explain the stress effect on the strain response of the irradiated copolymer films studied here. The consistence of these results confirms again that: 1) the ferroelectric nature of the irradiated copolymer studied here; 2) the strain response is mainly from the electric field induced phase transition of the local polar region.

## SUMMARY

In summary, high energy (MeV) electron irradiated P(VDF-TrFE) copolymer films have very large electric field induced strain response (about 5% longitudinal strain and more than 3% transverse strain). Compared to the other electroactive materials, a great advantage of the irradiated copolymers is that the material has a very high volume strain, which makes the material very well suitable for hydrostatic applications. The strain response of the material under different stress conditions shows that the irradiated copolymer films have very high load capability. The temperature dependence of the strain response was presented. The relationship between the stress dependence and temperature dependence of the strain responses is discussed with the Devonshire phenomenological theory. The consistence between the Devonshire theory and experimental data indicates that the strain response obtained in the irradiated copolymer originates from the electric field induced phase transition of the local polar regions.

## ACKNOWLEDGEMENTS

The work was supported by ONR through Grant No. N00014-97-1-0900, NSF through Grant No. ECS-9710459, and DARPA through Grant No. N00173-99-C-2003.

## REFERENCES

1. L. E. Cross, Ceramic Trans. **68**, 15(1996).
2. Y. Bar-Cohen, *Elelctroactive Polymer Actuators and Devices*, Proc. of SPIE, Vol.3669(1999).
3. Z. Ma, J. I. Scheinbein and B. A. Newman, J. Polym. Sci. B, Polym. Phys. **32**. 2721 (1994).
4. R. E. Pelrine, R. D. Kornbluh and J. P. Joseph, Sens. Actuators A, **64**, 77(1998).
5. Q. M. Zhang, V. Bharti and X. Zhao, Science **280**, 2101 (1998).
6. Z. -Y. Cheng, T. -B. Xu, V. Bharti, S. Wang and Q. M. Zhang, Appl. Phys. Lett. **74**, 1901(1999).
7. J. Su, P. Mouse and Q.M. Zhang, Rev. Sci. Instrum. **69**, 2480 (1998).
8. S. Gross, M.S. thesis, The Pennsylvania State University, 1999.
9. Z.-Y. Cheng, V. Bharti, T.-B. Xu, S. Wang and Q.M. Zhang, J. Appl. Phys. **86**, 2208 (1999).
10. V. Bharti, X. Zhao, Q.M. Zhang, T. Ramotowski, F. Tito and R. Ting, Mater. Res. Innovat. **2**, 57 (1998).
11. Q.M. Zhang and J. Zhao, Appl. Phys. Lett. **71**, 1649 (1997).
12. Z.-Y. Cheng, R.S. Katiyar, X. Yao and A.S. Bhalla, Phys. Rev. **B 57**, 8166 (1998).
13. M.E. Line and A. M. Glass, *Principles and Applications of Ferroelectrics and Related Materials* (Oxford University Press, New York, 1977).

# APPENDIX 15

PROCEEDINGS OF SPIE
SPIE—The International Society for Optical Engineering

*Smart Structures and Materials 2001*

# *Electroactive Polymer Actuators and Devices*

**Yoseph Bar-Cohen**
*Chair/Editor*

**5–8 March 2001**
**Newport Beach, USA**

*Sponsored and Published by*
SPIE—The International Society for Optical Engineering

*Cosponsored by*
ASME—American Society for Mechanical Engineers
SEM—Society for Experimental Mechanics
The Boeing Company (USA)

*Cooperating Organizations*
Air Force Research Laboratory (USA)
DARPA—Defense Advanced Research Projects Agency (USA)
The Ceramic Society of Japan
Intelligent Materials Forum (Japan)
U.S. Army Research Office
Jet Propulsion Laboratory (USA)

SPIE
P
PROCEEDINGS SERIES

**Volume 4329**

# P(VDF-TrFE)–based Electrostrictive Co/Ter-polymers and its Device Performance

Z.-Y Cheng*[a], H.S. Xu[a], T. Mai[a], M. Chung[b], Q.M. Zhang*[a]
[a]Mterials Research Laboratory, [b]Department of Material Science and Engineering
The Pennsylvania State University, University Park, PA16802, USA

R. Y. Ting
Department of Chemistry, University of Central Florida, Orlando, Florida 32816, USA

## ABSTRACT

In our earlier work, we have demonstrated that the high-energy electron irradiation modifies (VDF-TrFE) copolymers from a normal ferroelectric to a relaxor ferroelectric with high electromechanical response. Here, we present two approaches we are taking recently. One is to explore the non-irradiation approach to modify the PVDF-based material to achieve high electromechanical response. A ter-monomer (HFP and CTFE are used here) with a relative large size is added to the copolymer to act as modifiers. The electromechanical and dielectric properties in the terpolymers seem to be similar to those in irradiated copolymers. The other approach addresses the fundamental issue of the low dielectric constant in the currently available electroactive polymers. By making use of composite approach and ultra-high dielectric constant in CuPc, a polymeric composite with very high dielectric constant but the elastic modulus similar to polymer has been demonstrated. The preliminary results indicate that the polymer composite has the potential to generate high strain under much lower field. In parallel to the material development, we investigated device performance based on the irradiated copolymers. The performance of irradiated copolymer multilayers with a thickness up to 1 mm was characterized. The design and device performance of a flextensional actuator fabricated from the irradiated copolymer multiplayer are presented. The flextensional actuator, whose resonance frequency is at a frequency of a few kHz to more than 10 kHz, exhibits more than 1 mm displacement and high force output, which are attractive for many applications.

**Keywords:** P(VDF-TrFE), PVDF-based Terpolymer, Composite, Electroactive Polymer, Actuator, Electrostriction, Maxwell Stress

## 1. INTRODUCTION

The research on various ElectroActive Polymers (EAP) is very active recently since recent results show that the EAP is a very promise material for many applications [1~3]. Compared to ceramics, EAP exhibits high electric induced strain and high elastic energy. In addition, flexible EAP has many advantages over brittle ceramics for many applications. In an effort to develop high performance EAP, we discovered a few years ago that high-energy electron irradiation transforms P(VDF-TrFE) copolymer from a normal ferroelectric to relaxor ferroelectrics and that the irradiated copolymer exhibits massive strain response and high elastic energy density [4~6]. In the following years, we carried out the characterization of various properties in the irradiated copolymers, which shows the irradiated copolymers possess high load capability, high strain response at high frequency up to 100 kHz, high electromechanical coupling factor, *et al* [4~13]. In this paper, we will first briefly summarize the results obtained in the irradiated copolymer. From the structure studies, it has been shown that the irradiation introduces defects structures which disrupt the polarization coherence, alter the energy balance among different molecular conformations, and as a result, lead to the significant modification of the phase transformation behavior between the polar phase and non-polar phase. Hence, it is reasonable to ask whether there is non-irradiation approach to introduce the similar defects in copolymer and to achieve high electromechanical performance. In this paper, we will present the

*Corresponding author: Fax: (814)-863-7846, E-mail: zxc7@psu.edu, qxz1@psu.edu.


Smart Structures and Materials 2001: Electroactive Polymer Actuators and Devices, Yoseph Bar-Cohen, Editor, Proceedings of SPIE Vol. 4329 (2001) © 2001 SPIE · 0277-786X/01/$15.00

preliminary results obtained in terpolymers, such as P(VDF-TrFE-HFP) and P(VDF-TrFE-CTFE). The results show that, by means of introducing a ter-monomer with a relative bulky size into P(VDF-TrFE) copolymer, the terpolymer exhibits similar dielectric and electromechanical properties as those observed in the irradiated copolymers.

One of the challenges in developing new electroactive polymers is how to significantly reduce the driving electric field. From the energy conservation point of view, it is clear that to achieve that, one has to significantly raise the dielectric constant of the polymer system since the input electric energy density is equal to $K\varepsilon_0E^2/2$, where K is the dielectric constant, E is the applied field, and $\varepsilon_0$ is a constant ($8.85\times10^{-12}$ F/m), and the output mechanical energy density is less than and should be proportional to the input electric energy density. To address this fundamental issue, we investigated the polymer composite with high dielectric constant which is still flexible with the elastic modulus in the range of normal polymers. Some of the results will be presented in this paper.

From application point of view, it is interesting to know the material performance in actual device condition. In this paper, we will also address the electromechanical performance of the irradiated copolymers in actual device condition by using the irradiated copolymer multiplayer to fabricate a flextensional transducer. Multilayers with a thickness up to 1 mm were fabricated and characterized. The displacement and resonance behavior of the transducer are presented.

## 2. HIGH ENERGY ELECTRON IRRADIATED P(VDF-TrFE) COPOLYMERS

P(VDF-TrFE) copolymer powders were purchased from Solvay and Cie, Bruxelles, Belgium. The compositions used are 50/50, 65/35 and 68/32 mol%. Two kinds of films, stretched and unstretched films, were investigated. The electron irradiation was carried out in a nitrogen atmosphere at different temperatures with an electron energy of 2.55 MeV, 1.2 MeV, and 1.0 MeV respectively. Gold electrodes with a thickness of about 40 nm were sputtered on both surfaces of the film in order to characterize the material properties. The details about the film preparation and strain measurements can be found in our earlier publications [10]. The material properties of irradiated copolymer films are summarized in the following.

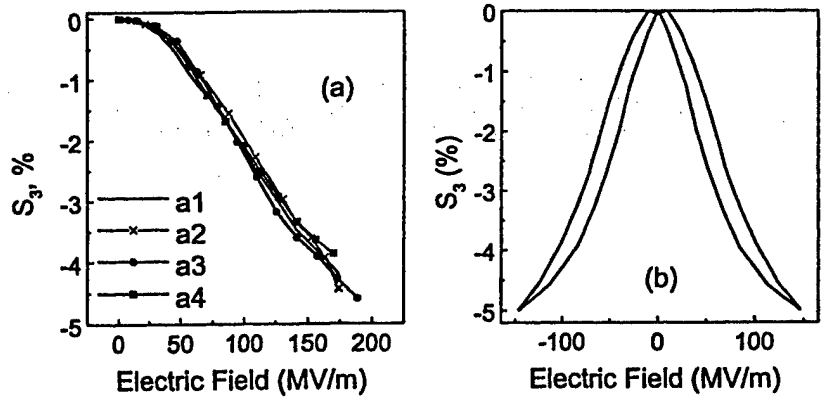


Fig. 1. (a) Amplitude of longitudinal strain response vs. amplitude of electric field at 1 Hz. All the films were irradiated using 2.55 MeV electrons. Curves a1 and a2 are unstretched 65/35 and 50/50 respectively, while curves a3 and a4 are stretched 65/35 and 50/50 respectively.
(b). Longitudinal strain response vs. electric field at 1Hz for unstretched 68/32 film. The films were irradiated using 1.0 MeV electrons.

The data shown in Fig. 1 are the electrostrictive strain along film thickness (Longitudinal strain, $S_3$) in both unstretched and stretched films. The electrostrictive strain in the plane of the film (Transverse strain) is shown in Fig. 2. Where, $S_1$ and $S_2$ are the strain along and perpendicular to the film stretched direction, respectively. Clearly, the material exhibits a large strain with small hysteresis. The longitudinal strain in both stretched and unstretched films is negative, while the transverse strain strongly depends on the stretching direction. For unstretched film, the transverse strain is positive and about one third of absolute value of longitudinal strain. For stretched film, $S_1$ is positive and $S_2$ is negative, and $|S_3|\approx|S_1|$ and $|S_3|\approx3|S_2|$. In both unstretched and stretched films, the volume strain calculated based on longitudinal and transverse strains can reach more than 1 %, which is much higher than other electroactive materials, such piezoceramics and dielectric elastomers.

The load capability of irradiated copolymer films was investigated in two conditions: film under hydrostatic pressure and uniaxial stress. In the former case, the longitudinal strain was studied. For the latter case, the transverse strain was studied, which are presented in Fig. 3(a). The results in both cases indicate the film possesses high load capability. Initially, the transverse strain response increases with tensile stress. The strain response in film under about 20 MPa tensile stress is almost double of the value obtained in film under stress free condition. The film under 40 MPa stress exhibits the same strain response as the film under stress free condition. The phenomenon is related to the ferroelectric nature in the material.

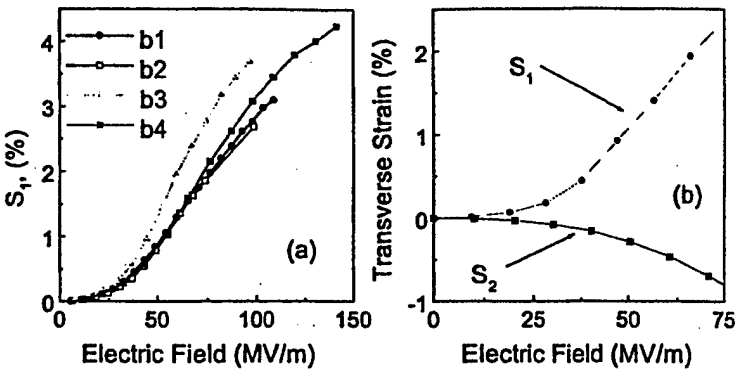


Fig. 2. Amplitude of transverse strain vs. amplitude of electric field for stretched films. (a) Strain along stretching direction. Curves b1 and b2 are 65/35 films irradiated using 1.0 MeV and 2.55 MeV respectively. Curves b3 and b4 are 68/32 films irradiated using 1.2 MeV electrons. (b). Strain along stretching direction and strain perpendicular to stretching direction respectively.

The frequency dependence of the strain response was characterized. A set of data are shown in Fig. 3(b). Although the strain response decreases with frequency, the reduction is not significant. In addition, the higher the temperature is, the smaller the reduction is. The data clearly demonstrate that the irradiated copolymer films studied here also exhibit large strains at high frequencies.

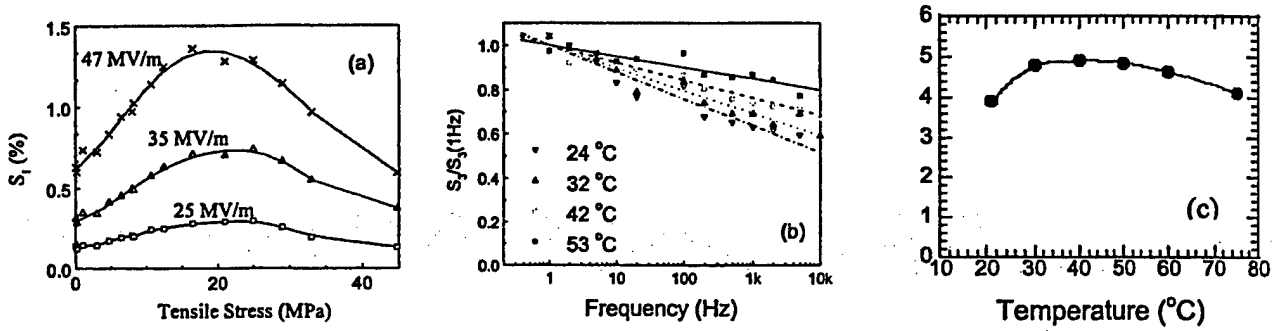


Fig. 3. (a). Transverse strain ($S_1$) amplitude vs. tensile stress for stretched 65/35 film under different electric field of 1 Hz. The film was irradiated with 2.55 MeV electrons. (b). Frequency dependence of longitudinal strain ($S_3$) for unstretched 68/32 film under an electric field of 20 MV/m. The film was irradiated with 1.0 MeV electrons. (c). Temperature dependence of longitudinal strain for 68/32 film under a constant electric field. The film was irradiated with 1.0MeV electrons.

The temperature dependence of strain response was studied and the results for longitudinal strain are presented in Fig. 3(c). The data indicate that the irradiated copolymer is capable of generating high strain over a relatively broad temperature range.

All these results demonstrate that the irradiated P(VDF-TrFE) copolymer is a promising EAP for various actuator and transducer applications. For these applications, the electromechanical coupling factor, which measures the efficiency of the material in converting energy between the electric and mechanical forms, is another important property. Both the longitudinal electromechanical coupling factor ($k_{33}$) and transverse electromechanical coupling factor ($k_{31}$) were examined at temperatures around room temperature. The results are shown in Fig. 4. The electromechanical coupling factors obtained here are higher than those achieved in piezoelectric P(VDF-TrFE) copolymers. More remarkably, $k_{31}$ of 0.45 is even higher than that in piezoelectric ceramics. Therefore, the irradiated P(VDF-TrFE) copolymers also possess high electromechanical coupling factors.

In an electrostrictive material, an effective piezoelectric state can be induced by means of applying a DC bias field [14]. The apparent piezoelectric constant was measured in both longitudinal and transverse directions for films under different DC bias fields. It is found that the irradiated copolymers exhibit a high effective piezoelectric constant. For example, the longitudinal piezoelectric constant $d_{33}$ can reach more than -380 pm/V, while the transverse piezoelectric constant $d_{31}$ can be higher than 300 pm/V. These values are much higher than these obtained in piezoelectric P(VDF-TrFE) copolymers ($d_{33}$=-30 pm/V and $d_{31}$=20 pm/V).

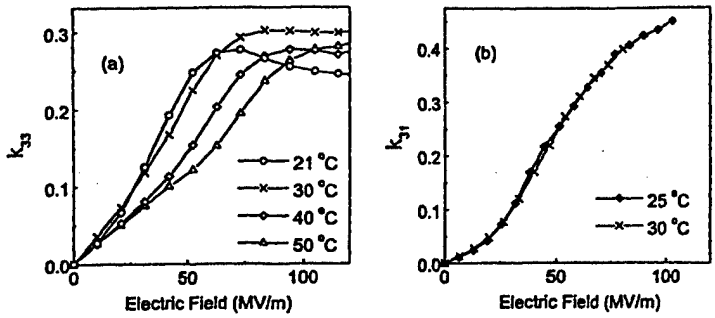


Fig.4. (a) Longitudinal electromechanical coupling factor $k_{33}$ vs. electric field at 1Hz for unstretched 68/32 film irradiated using 1.0MeV electrons.
(b). Transverse electromechanical coupling factor $k_{31}$ vs electric field at 1 Hz for stretched 68/32 film along stretching direction. The film was irradiated with 1.2 MeV electrons.

In the DC field biased effective piezoelectric state, one can make use of the resonance method to characterize the electromechanical coupling factors as recommended by IEEE. A typical resonance curve of irradiated copolymer film under DC bias is shown in Fig. 5(a). A clear electromechanical resonance peak can be observed at a frequency about 40 kHz. With increase the DC bias field, the electromechanical resonance becomes stronger as expected. Using the resonance data, the electromechanical coupling factor, which is shown in Fig. 5(b), was obtained. The comparison of the data in Fig. 5(b) which is taken at about 40 kHz and Fig. 4(b) which is at 1 or 10 Hz reveals that the electromechanical coupling factor in irradiated copolymer films studied here is almost independent of frequency. In other words, the film exhibits a high electromechanical coupling factor at high frequencies.

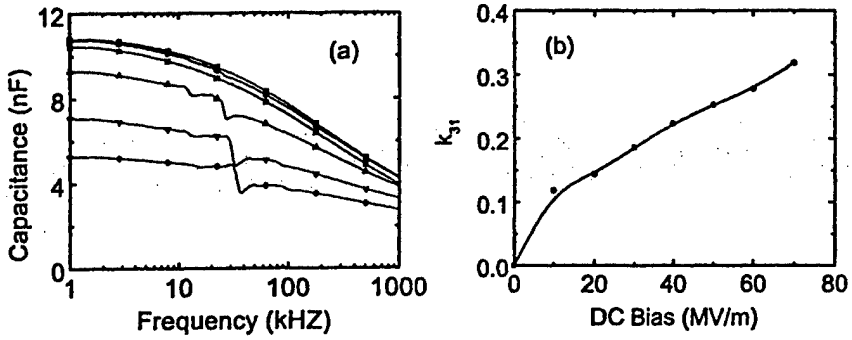


Fig. 5. (a). Capacitance vs. frequency for stretched 68/32 film under different DC biases. The DC bias corresponding top curve to bottom curve increases from 0 to 75 MV/m. The AC signal is 1Vrms. The film was irradiated using 1.2 MeV electrons
(b). Calculated electromechanical coupling factor k31 using resonance data vs. DC bias.

For electroactive materials, the elastic energy density is used quite often to compare different materials for electromechanical actuator application. Therefore, the strain energy density and other related parameters for this new class of EAP are shown in Table I, and as a comparison, the data for the conventional piezoelectric P(VDF-TrFE), the piezoceramic and magnetostrictive materials are also included. In the table, both the volumetric energy density, which is $YS_m^2/2$ and related to the device volume, and the gravimetric energy density, which is $YS_m^2/2\rho$ and related to the device weight, are listed. $S_m$ is the maximum strain level, $\rho$ is density, and $Y$ is the elastic modulus. In Table I, we also include another parameter, the blocking stress, which is the stress level generated under a given electric field when the strain of the sample is zero. For the data in the table, the maximum blocking stress has been approximated as $YS_m$ (neglect the possible non-linear effect).

The structural study on the irradiated P(VDF-TrFE) copolymer indicates that the irradiation introduces "defects" in crystalline regions and that the "defects" substantially modify the energy balance among different conformations and phase transformation behavior in the material. That is, the "defects" structure transforms the P(VDF-TrFE) copolymer from a ferroelectric phase to a non-polar phase at room temperature and causes a diffused phase transformation process between the polar and non-polar phase which occurs in a broad temperature range. The observed electrostrictive strain in the irradiated copolymers originates from the electric field induced diffused phase transformation which is reversible [9]. It is not difficult to recognize that the high-energy electron irradiation is not the only means to alter the energy balance among different molecular conformations and introduce defects structure to disrupt the polarization coherence in PVDF based ferroelectric polymers. There exist other non-irradiation approaches to achieve the similar effects. The non-irradiation approaches will be discussed in the following section.

Table I. Comparison of electromechanical properties in different actuator materials at room temperature

| Materials | | Y (GPa) | Typical $S_m$ | $YS_m^2/2$ ($J/cm^3$) | $YS_m^2/2\rho$ (J/kg) | Stress (MPa) | $d_{33}$ pm/V | $d_{31}$ Pm/V | $k_{33}$ | $K_{31}$ |
|---|---|---|---|---|---|---|---|---|---|---|
| Piezoceramic (PZT-5H) | | 64 | 0.2% | 0.13 | 17 | 128 | **593** | –274 | **0.75** | 0.39 |
| Magnetostrictor | | **100** | 0.2% | 0.2 | 21.6 | **200** | | | | |
| Piezo P(VDF-TrFE) | | 4 | 0.15% | 0.0045 | 2.5 | 6 | –30 | 10 | 0.23 | 0.1 |
| Electrostrictive P(VDF-TrFE) | $S_3$ | 0.4 | -5.0% | 0.5 | 267 | 20 | –380 | | 0.30 | |
| | $S_1$ | 1.0 | 4.3% | **0.92** | **492** | 43 | | **300** | | **0.45** |
| Maxwell stress Polyurethane | | 0.017 | 11% | 0.1 | 100 | 1.9 | | | | |
| *NewlyDeveloped terpolymesr* | | | | | | | | | | |
| P(VDF-TrFE-HFP) | | | -2% | | | | | | | |
| P(VDF-TrFE-CTFE), $S_3$ | | ~0.4 | -4% | 0.32 | 160 | 16 | | | | |
| | $S_1$ | | 3% | | | | | | | |

## 3. P(VDF-TrFE)-BASED TERPOLYMERS AND ITS ELECTROMECHANICAL RESPONSE

For P(VDF-TrFE), it is well known that the inter-chain spacing in the ferroelectric phase (β-phase with all-trans conformation) is smaller than that in the paraelectric phase which has a mixture of $TGT\overline{G}$ and $TTTGTTT\overline{G}$ conformations [15]. Therefore, by randomly introducing a bulkier monomer into the copolymer, one maybe able to achieve the similar effect, that is, to expand the inter-chain spacing to lower the energy of $TGT\overline{G}$ and $TTTGTTT\overline{G}$ conformations with respect to the TTTT conformation and to disrupt the polarization coherence to eliminate the polarization hysteresis. In addition, to maximize the effect, the bulkier monomer should also be able to co-crystallize with the VDF and TrFE. In Table II, several commercially available fluoromonomers are listed. Considering that the van der Waals (vdW) radii of the hydrogen, fluorine, and chlorine atoms is 1.2 Å, 1.35 Å, and 1.8 Å, respectively, HFP and CTFE were chosen for the study: P(VDF-TrFE-HFP) and P(VDF-TrFE-CTFE). The composition of the terpolymer is labeled as x/(1-x)/y for $VDF_x$-$TrFE_{1-x}$-$Q_y$, where the mole ratio of VDF/TrFE is x/1-x and the y is the mol% of Q (HFP or CTFE) in the terpolymers.

Table II. Commercially Available Fluoromonomers

| | Abbreviation | Monomer Structure |
|---|---|---|
| *Fluoromonomers* | | |
| Vinyl fluoride | VF | $CH_2$=CHF |
| Vinylidene fluoride | VDF | $CH_2$=$CF_2$ |
| Trifluoroethylene | TrFE | CHF=$CF_2$ |
| Tetrafluoroethylene | TFE | $CF_2$=$CF_2$ |
| Chlorotrifluoroethylene | CTFE | $CF_2$=CFCl |
| Hexafluoropropylene | HFP | $CF_2$=CF-$CF_3$ |
| Perfluoro(Methyl vinyl ether) | PMVE | $CF_2$=CF-O-$CF_3$ |

The polarization hysteresis loop of the terpolymers was characterized and the data from P(VDF-TrFE-CTFE) is shown in Fig. 6(a). In comparison, the data from 1.2 MeV electron irradiated P(VDF-TrFE) 68/32 copolymer is shown in Fig. 6(b). Clearly, two sets of data show very similar results. The slim polarization hysteresis loop indicates that the terpolymer is electrostrictive.

Although the data from the terpolymer P(VDF-TrFE-CTFE) shows promising results such as relatively high strain response and slim room temperature polarization hysteresis loop, the terpolymer based on HFP still exhibits relatively large room temperature hysteresis and the strain level is not very high (~2%). The reason behind this difference is that HFP seems not to be able to co-crystallize with VDF and TrFE and as a result, it can't impose effective influence on the molecular conformations and polar ordering in the crystalline phase. Hence, in the following, only the results from P(VDF-TrFE-CTFE) terpolymers will be presented.

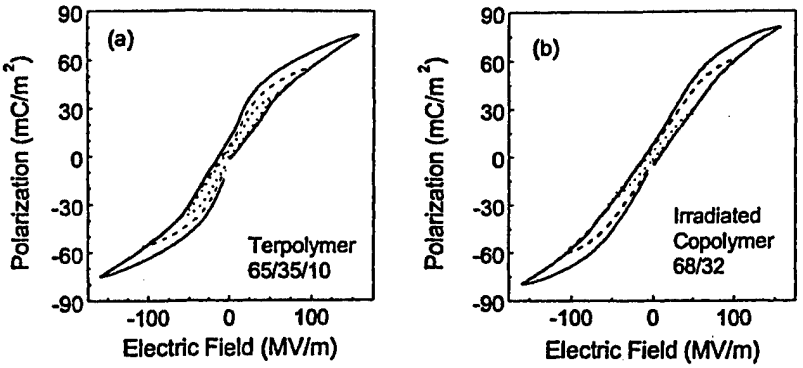


Fig. 6. Polarization hysteresis loop measured at room temperature using a triangle wave of 10 Hz with amplitude of 50 MV/m, 100 MV/m, and 150 MV/m respectively.
(a). Unstretched P(VDF-TrFE-CTFE) terpolymer with a composition of 65/35/10 mol%.
(b). Stretched P(VDF-TrFE) copolymer irradiated with 1.2 MeV electrons.

Presented in Fig. 7 is the longitudinal strain response from P(VDF-TrFE-CTFE) terpolymers. In analogy to the irradiated copolymer, the electrostrictive terpolymer exhibits a negatively longitudinal strain and the strain level can be compared with that observed in irradiated copolymers. The transverse strain response in the P(VDF-TrFE-CTFE) terpolymers was also characterized. The data shown in Fig. 8 is from the stretched P(VDF-TrFE-CTFE) at 70/30/10 composition. About 3% transverse strain can be achieved in this terpolymer under a field of 150 MV/m, which is smaller than that in the irradiated copolymers.

Since there are much more variables in chemical methods than the irradiation approach, it is quite possible to find a terpolymer with much better electromechanical properties than the irradiated copolymers. Clearly, this is an area which will be further investigated.

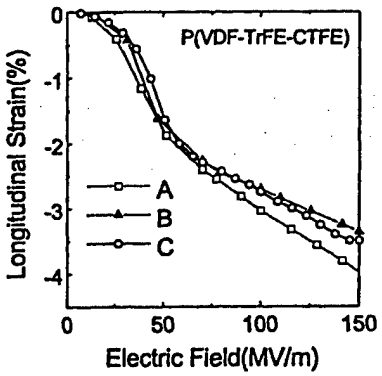


Fig. 7. Amplitude of longitudinal strain vs. amplitude of electric field at 1 Hz at room temperature for P(VDF-TrFE-CTFE) terpolymers. A: Unstretched 65/35/10, B: Unstretched 70/30/10, C: Stretched 70/30/10.

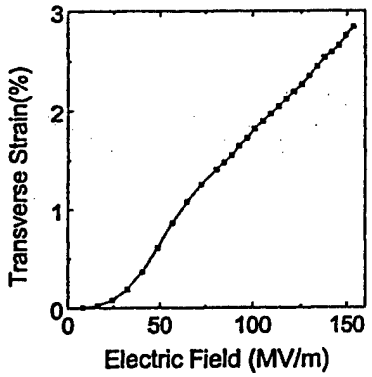


Fig. 8. Amplitude of transverse strain along stretching direction vs. amplitude of electric field at 1 Hz at room temperature for stretched P(VDF-TrFE-CTFE) 70/30/10 terpolymer.

One of the advantages of the irradiated copolymer is its high dielectric constant at temperatures near room temperature. The dielectric behavior of terpolymers was examined and the data taken from 65/30/10 terpolymer is shown in Fig. 9(a). For the comparison, the data from the irradiated 68/32 copolymers are shown in Fig. 9(b). Clearly, the terpolymer exhibits a similar dielectric behavior as irradiated P(VDF-TrFE) copolymer. We also find that the relation between frequency and dielectric maximum temperature in the terpolymer can be fitted well with Vogel-Fulcher relationship. The data in Fig. 9(a) combined with the data in Fig. 6(a) strongly suggest that the electrostrictive terpolymer studied here is a relaxor ferroelectric, an important kind of functional materials.

## 4. ELECTROACTIVE POLYMERIC COMPOSITES

Electrostatic force has been used for electromechanical actuation for many decades. However, only very recent, this force, the Maxwell stress, is made use of to generate large field induced strain in soft dielectric polymers. In the last several years, many dielectric elastomers have been examined by SRI and very large strain response has been observed in some of these elastomers [16]. However, in these elastomers the Young's modulus is quite low, a few MPa to a few tens MPa, which are not desirable for most of the device applications.

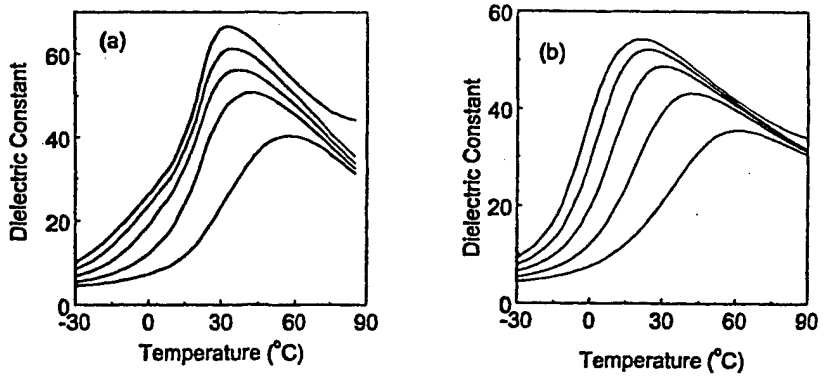


Fig. 9. Temperature dependence of dielectric constant at different frequencies. Curves from top to bottom correspond to 100Hz, 1kHz, 10kHz, 100 kHz, and 1 MHz respectively.
(a). P(VDF-TrFE-CTFE) 65/35/10
(b). P(VDF-TrFE) 68/32 irradiated using 1.2 MeV.

For a Maxwell stress induced strain response, it is well known that the strain response ($S_i$) is proportional to the ratio of the dielectric constant ($\varepsilon$) and Young's modulus (Y). That is,

$$S_i \propto \varepsilon / Y \qquad (1)$$

and the elastic energy density is proportional to the $\varepsilon^2/Y$. Thus, in order to increase the Young's modulus of the elastomer while keeping the high strain response, the dielectric constant must be increased. For example, if both dielectric constant and Young's modulus were increased by 1000 time, the material will maintain the strain level, while the elastic energy density can be increased by 1000 times. In other words, an important approach to improve the electromechanical performance in elastomers is to significantly increase the dielectric constant. Unfortunately, the dielectric constant in most of dielectric elastomers is quite low (<10).

In fact, this is a fundamental issue in electric field driven EPA to achieve high elastic energy density. Since the elastic energy density is limited by the input electric energy density, which is equal to $\varepsilon E^2/2$, a low dielectric constant in the electric field driven EAP means that to raise the input electric energy density, a high applied field E is required. For practical applications, it is highly desirable to have a low operation field. The irradiated P(VDF-TrFE) copolymers and the PVDF based terpolymers possess a room temperature dielectric constant >50, which is the highest among all known polymers, but is still substantially lower than those in inorganic electroactive materials.

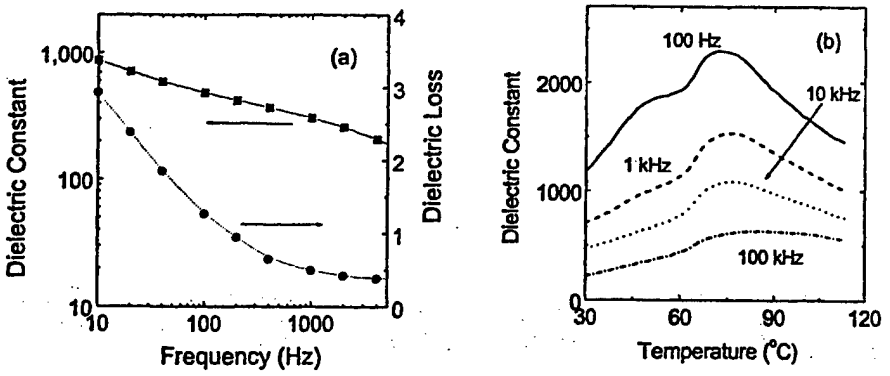


Fig. 10. Dielectric properties at weak electric field for a polymeric composite with 55 %wt CuPc.
(a). Frequency dependence at room temperature.
(b). Temperature dependence at 100 Hz, 1 kHz, 10 kHz, and 100 kHz, respectively.

In should be noted that some organic materials do possess high dielectric constant. For example, metallophthalocyanine oligomer, such as copper-phthalocyanine (CuPc), has a room temperature dielectric constant more than 1000 at 100 Hz. However, the dielectric loss in this material is also high. The challenge here is how to maintain the high dielectric constant with loss dielectric loss. In order to do so, a composite approach was investigated. The P(VDF-TrFE) 50/50 mol% copolymer was used as matrix while CuPC oligomer serves as active part.

The CuPc oligomer with a particle size about 1μm was synthesized by means of solution method [17]. The composite film was prepared by solution cast method. P(VDF-TrFE) copolymer was first dissolved in DMF and then CuPc powder was added into the solution. The solution was stirred for 12 hrs at room temperature before pouring onto glass plate. For a composite film with 55 wt% CuPc, the Young's modulus is 1.2 GPa and is quite flexible.

The composites with different concentration of CuPc were studied. It is found that the composite with 55% wt CuPc exhibits a high dielectric constant with a relative small dielectric loss as shown in Fig. 10.

The longitudinal strain response in the composite was examined at room temperature. It is found that the strain response is approximately equal to the square of the electric field. The film exhibits a longitudinal strain of -0.3% at an electric field of 1 MV/m at 1Hz, which is much higher than the strain level found in other field driven EAPs at the same field level. By extrapolation, one would expect a strain of –30% under a field of 10 MV/m which will be a very attractive EAP for a broad range of applications. We are currently working on the composites to raise the breakdown field of the composites.

## 5. DEVICE PERFROMANCE OF IRRADIATED P(VDF-TrFE) COPOLYMERS

From the results presented, it is clear that to make use of those electroactive polymers for practical device applications, a multilayer configuration is required to significantly reduce the driving voltage. For polymers, it is not difficult to produce films in the thickness range from 5 μm and up. For the devices investigated here, P(VDF-TrFE) copolymer films in the thickness range from 15 μm to 30 μm have been fabricated and multilayer stacks in the thickness up to several mm have been made out of those films. In those multilayer stacks, Spurr epoxy has been used as glue layer and the average glue layer thickness is at about 1 μm. In order to evaluate the electromechanical response of the multilayer stacks, the dielectric property, strain response, and electromechanical resonance at DC field biased state were characterized and the results indicate that the effect of the glue layers on the performance of multilayer stacks is very small. For example, the transverse strain along stretching direction of a 4-layer stack is shown in Fig. 11, which is very close to that of te single layer.

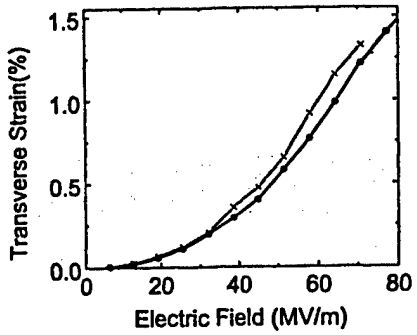


Fig.11. Amplitude of transverse strain along stretching direction in 4-layer multilayer stack vs. amplitude of electric field at room temperature. The stack was fabricated from stretched 68/32 copolymer films, which were irradiated using 1.2 MeV electrons. The thickness of each copolymer layer is about 20 μm. The electrode area on each polymer layer is 30 mm long along stretching direction and 10 mm wide in the other direction. There is a non-electrode area with a width of 1 mm on two sides.

In order to fully use the advantages of irradiated P(VDF-TrFE) copolymer films, a flextensional transducer is developed. The configuration of the transducer is shown in Fig. 12. The active part in this transducer is the active polymer multilayer made from the stretched electrostrictive P(VDF-TrFE) copolymer films. The passive element is two metal benders (flextensional element) on two sides of the polymeric multilayer stack. At static condition, the metal benders exert a tensile stress on the polymeric multilayer along the film stretched direction. When an electric field is applied onto the multilayer stack, the multilayer expands $\delta L$ along stretching direction. This expansion results in an amplified displacement ($\delta H$) at middle point of the bender.

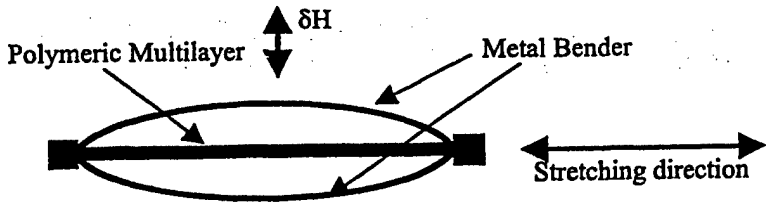


Fig. 12. Configuration of flextensional transducer.

Assuming the shape of the metal bender is an arc, we can obtain the relationship between δH and δL which depends on the length (L) of multiplayer stack along the film stretched direction and arc length (A) of the metal bender as following,

$$\frac{\delta H}{\delta L} = \frac{X}{2}\frac{2tg^{-1}X - X}{X + (X^2-1)tg^{-1}X} = \frac{X}{2}\frac{2Y - (X^2-1)}{(1+Y)(X^2+1) - 2Y} \quad (2)$$

where X=2h/L, Y=A/L, $h$ is the height of the arc (that is, the height of middle point in metal bender).

Using Eq. (2), the relation between $\delta H/\delta L$ and $A/L$ is plotted in Fig. 13, which indicates that the shorter the metal bender is, the large the amplifying ratio is. However, when the metal bender length becomes shorter, the displacement range $\delta H$ will also become smaller. Therefore, there is a balance between the amplification of the displacement and the displacement range, which depends on applications.

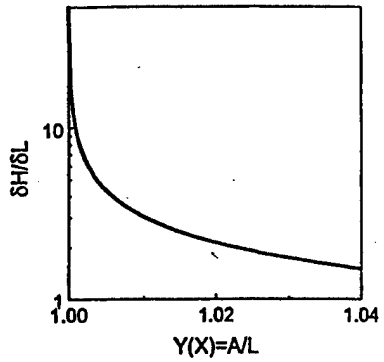


Fig. 13. Displacement ratio of δH to δL vs. ratio of metal bender length (A) to multilayer length (L). The curve is calculated using Eq. (2).

Flextensional transducers based on this design were fabricated. The typical EAP multilayer is a irradiated P(VDF-TrFE) copolymer stack with 1 mm thickness (fabricated from 30 layers of stretched and irradiated copolymer films. The thickness of each film is about 30 μm). The electrode area on both sides of each irradiated copolymer layer is 22x22 mm$^2$. The size of multilayer is 30 mm along the actuation direction and 25 mm width perpendicular to it.

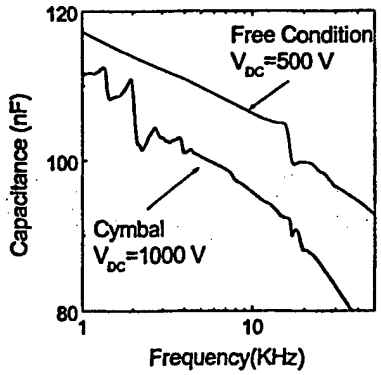


Fig. 14. Frequency dependence of capacitance for an irradiated copolymer multilayer with a thickness of 1mm under DC bias.

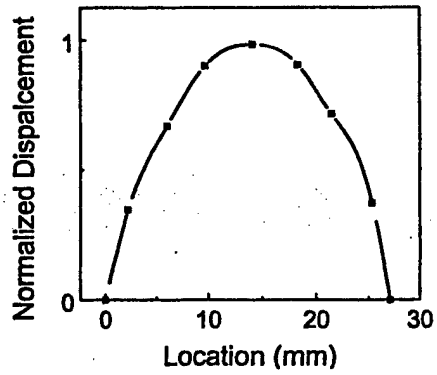


Fig. 15. Normalized displacement at different points on metal bender along stretching direction for the cymbal transducer under a constant electric field.

The electromechanical performance of the 1 mm thick multilayer stack was first characterized. As shown in Fig. 14, the curve labeled as "free condition $V_{DC}$=500 V", corresponds to the resonance curve of the multilayer stack under a DC bias voltage of 500 V (17 MV/m field on each layer). The AC single applied is 1 V. A clear resonance peak was observed at a frequency about 17 kHz, which corresponds to an acoustic velocity of 1000 m/s in the polymeric multilayer stack along the actuation direction (the film stretched direction). As has been discussed in Section 2, the electromechanical coupling factor in irradiated P(VDF-TrFE) copolymer films increases with DC electric bias field. With increased DC bias field, the resonance peak in Fig. 14 for the multilayer stack will become stronger.

The curve, "cymbal $V_{DC}$=1000V", in Fig. 14 corresponds to the resonance behavior of the flextensional transducer in which the metal benders are spring steel with a thickness of 0.127 mm and width of 26.5 mm. Clearly, there are two resonance peaks at lower frequency (~2 kHz) and a resonance peak at higher frequency (~18 kHz) close to the resonance frequency of free-standing multilayer stack. The resonance at higher frequency originates from the resonance of the multilayer stack itself. Two resonance peaks at lower frequency corresponds to the mechanical resonance of each metal bender due to a small difference between two metal benders. If two unidentifiable metal benders used here, these peaks will merge into one, which can be adjusted to different frequency position by using different metal bender (elastic constant and thickness) as well as varying the thickness of the multilayer stack.

The displacement profile of the metal bender was characterized and the data is shown in Fig. 15. The shape in Fig. 15 matches well with that predicted by the elastic model which was used to derive Eq. (2).

The electric field dependence of the displacement at middle point of metal bender was measured when electric field at 0.5 Hz was applied to the multilayer stack. The electric field dependence of the displacement is shown in Fig. 16.

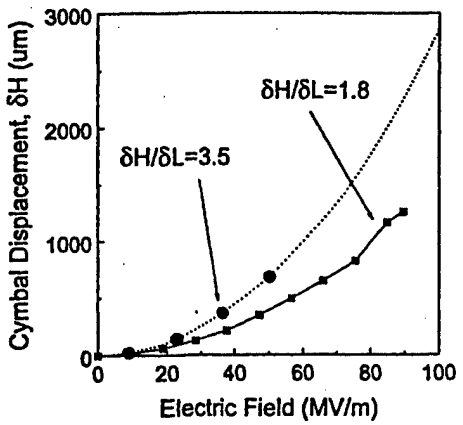


Fig. 16. Electric field dependence of cymbal displacement (displacement at middle point of metal bender). Two curves correspond to the cymbal with different metal benders.
The solid dots are the experimental data.
The solid line was draw by eye.
The dot line was extrapolated the experimental data using the electric field dependence of strain response in irradiated copolymer films.

The data in Fig. 16 demonstrate that the flextensional transducer fabricated from the irradiated copolymer films exhibits very large displacement. The load capability of the cymbal was also tested by means of applying a force up to 10 N at the middle point of the cymbal transducer. It is found that the displacement increases slightly with force in the stress range investigated. This indicates the high load capability of cymbal studied here.

## 6. SUMMARY

The electromechanical properties of high-energy electron irradiated P(VDF-TrFE) copolymer are summarized in the paper. It has been shown that the irradiated copolymer films possess large strain response, high load capability, relative flat frequency response, and relative broad working temperature range. These properties result in the high elastic energy density, high electromechanical coupling factor, and high effective piezoelectric constants of the irradiated copolymer. A pure synthetic approach, in which third monomers such as CTFE, with a relatively bulky size were added, is introduced to modify the copolymers. The preliminary results in terpolymers of P(VDF-TrFE-HFP) and P(VDF-TrFE-CTFE) indicate that the terpolymer approach can produce a polymer with a slim polarization hysteresis loop, large electric field induced strain, and high dielectric constant at near room temperature. In addition, in an effort to explore new EAPs, a composite approach is introduced to significantly enhance the Maxwell stress effect. A polymeric composite, P(VDF-TrFE) 50/50 mol% copolymer with copper-phthalocyanine (CuPc) oligomers, was developed. A dielectric constant more than 1000 with the elastic modulus at 1.2 GPa can be achieved in the composite which is very flexible. Large strain response can be observed at very low electric field in this composite.

To evaluate the performance of the irradiated copolymers for practical device applications, a flextensional transducer was designed and fabricated. In this design, multilayer stacks made from thin irradiated copolymer films were used as the driving element The experimental results show that multilayer exhibits electromechanical properties near those of the single layer. In addition, the flextensional transducer fabricated based on them exhibits a very large displacement with relative high load capability.

## ACKNOWLEDGEMENTS

The work was supported by DARPA under Contract No. N00173-99-C-2003 and ONR under Grant No. N00014-97-1-0900.

## REFERENCES

1. Y. Bar-Cohen, *Elelctroactive Polymer Actuators and Devices*. Proc. of SPIE, Vol.3669 (1999).
2. Q. M. Zhang, et al., *Electroactive Polymers*. MRS Proc. Vol.600 (1999).
3. Y. Bar-Cohen, *Elelctroactive Polymer Actuators and Devices*. Proc. of SPIE, Vol.3987 (2000).

4. Q. M. Zhang, V. Bharti, and X. Zhao. "Giant Electrostriction and Relaxor Ferroelectric Behavior in Electron-Irradiated Poly(vinylidene fluoride-trifluoroethylene) Copolymer", *Science*, **280**, 2101 (1998).
5. X. Zhao, V. Bharti, Q.M. Zhang, T. Romotowski, F. Tito, and R. Ting. "Electromechanical Properties of Electrostrictive Poly(vinylidene fluoride-trifluoroethylene vinylidene fluoride-trifluoroethylene) Copolymer", *Appl. Phys. Lett.* **73**, 2054 (1998).
6. Z. -Y. Cheng, T. -B. Xu, V. Bharti, S. Wang, and Q. M. Zhang. "Transverse Strain Response in the Electrostrictive Poly(vinylidene fluoride-trifluoroethylene) Copolymer", *Appl. Phys. Lett.* **74**, 1901(1999).
7. V. Bharti, Z.-Y. Cheng, S. Gross, T.B. Xu, and Q.M. Zhang, "Effect of mechanical Stress on Electrostrictive Strain of High-Energy Electron Irradiated Poly(vinylidene fluoride-trifluoroethylene)", *Appl. Phys. Lett.* **75**, 2653 (1999).
8. Z.-Y. Cheng, V. Bharti, T.-B. Xu, S. Wang, and Q.M. Zhang. "Transverse Strain Response in the Electrostrictive Poly(vinylidene fluoride-trifluoroethylene) Copolymer and Development of a Dilatometer for the Measurement", *J. Appl. Phys.* **86**, 2208 (1999).
9. Q. M. Zhang, Z.-Y. Cheng, and V. Bharti. "Relaxor Ferroelectric Behavior in High Energy Electron Irradiated Poly(vinylidene fluoride-trifluoroethylene) Copolymers", *Appl. Phys. A* **70**, 307 (2000).
10. Z.-Y. Cheng, V. Bharti, T. Mai, T.B. XU, Q.M. Zhang, T. Ramotowski, K.A. Wright, and R. Ting, "Effect of High Energy Electron Irradiation on the Electromechanical Properties of Poly(vinylidene fluoride-trifluoroethylene) 50/50 and 65/35 Copolymers", *IEEE Trans. Ultrason., Ferroelect., Freq. Contr.*, **47**, 1296 (2000).
11. V. Bharti, H.S. Xu, G. Shanthi, Q.M. Zhang, and K. Liang, "Polarization and Structural Properties of high energy electrons irradiated Poly(vinylidene fluoride-trifluoroethylene) Copolymer Films", *J. Appl. Phys.* **87**, 452 (2000).
12. H.S. Xu, G. Shanthi, V. Bharti, Q.M. Zhang, and T. Ramotowski, "Structural, Conformational, and Polarization Changes of Poly(vinylidene fluoride-trifluoroethylene) Copolymer Induced by High-Energy Electron Irradiation", *Macromolecules* **33**, 4125 (2000).
13. Z.-Y. Cheng, V. Bharti, T.-B. Xu, H. Xu, T. Mai, and Q.M. Zhang, "Electrostrictive Poly(vinylidene fluoride-Trifluoroethylene) Copolymers", *Sensors and Actuator A: Physical* **90**, 138 (2001).
14. Q.M. Zhang, Z.-Y. Cheng, V. Bharti, T.-B. Xu, H. Xu, T. Mai, and S.J. Gross, "Piezoelectric and electrostrictive polymeric actuator materials",*In Electroactive Polymer Actuators and Devices (EAPAD)*, edited by Y. Bar-Cohen, *Proceedings of SPIE.* Vol. **3987**, 34 (2000).
15. F. J. Balta, A. G. Arche, T. A. Ezquerra, C. S. Cruz, F. Batallan, B. Frick, and E. L. Cabarcos, "Structure and properties of ferroelectric copolymer poly(vinylidene fluoride)", *Prog. in Polym. Sci.* **18**, 1 (1993).
16. R. Pelrine, R. Kornbluh, Q. Pei, and J. Joseph, "High Speed Electrically Actuated Elastomers with Over 100% Strain", *Science*, **287**, 836 (2000).
17. H.S. Xu, Y. Bai, V. Bharti, and Z.-Y. Cheng, "High Dielectric Constant Composites Based on Metallophthalocyanine Oligomer and Poly(vinylidene fluoride-trifluoroethylene) Copolymer", *J. Appl. Polym. Sci.* (in press, 2000).

Appendix 9

"Characterization and development of P(VDF-TrFE) based high performance electroactive terpolymers", D. Olsen, H.S. Xu, H.F. Li, Z.Y. Cheng, Q.M. Zhang, R. Ting, G. Abdul-Sedar, K.D. Belfield, T. Ramotowski, R. Hughes and G. Kavarnos, presentation at the 2001 Fall Meeting, Materials Research Society, December 2001.

# APPENDIX 16

ELSEVIER

Sensors and Actuators A 90 (2001) 138–147

SENSORS AND ACTUATORS A PHYSICAL

www.elsevier.nl/locate/sna

# Electrostrictive poly(vinylidene fluoride-trifluoroethylene) copolymers

Z.-Y. Cheng*, V. Bharti, T.-B. Xu, Haisheng Xu, T. Mai, Q.M. Zhang

*Laboratory of Materials Research, Department of Electrical Engineering, The Pennsylvania State University, University Park, PA 16802, USA*

Received 9 June 2000; received in revised form 9 January 2001; accepted 16 January 2001

**Abstract**

High energy electron (1.0–2.55 MeV) irradiation was used to modify the phase transitional behavior of poly(vinylidene fluoride-trifluoroethylene) (P(VDF-TrFE)) copolymers in an attempt to significantly improve the electromechanical properties of the copolymers. It is found that the copolymers under a proper irradiation treatment exhibit very little room temperature polarization hysteresis and very large electrostrictive strain (the longitudinal strain of −5% can be achieved). Because of the large anisotropy in the strain responses along and perpendicular to the polymer chain, the transverse strain can be tuned over a broad range by varying the film stretching condition. For unstretched films, the magnitude of transverse strain is approximately about/less than 1/3 of that of the longitudinal strain, and for stretched films, the transverse strain along the stretching direction is comparable to the longitudinal strain. In addition to the high strain response, the irradiated copolymers also possess high elastic energy density and mechanical load capability as indicated by the relatively high elastic modulus of the copolymer and the high strain response of the transverse strain even under 40 MPa tensile stress. The high strain and high elastic modulus of the irradiated copolymer also result in an improved electromechanical coupling factor where the transverse coupling factor of 0.45 has been observed. The frequency dependence of the strain response was also characterized up to near 100 kHz and the results show that the high electromechanical response can be maintained to high frequencies. Several unimorph actuators were fabricated using the modified copolymer and the test results demonstrate high performance of the devices due to the high strain and high load capability of the material. © 2001 Published by Elsevier Science B.V.

*Keywords:* Actuator; Electrostriction; P(VDF-TrFE); Phase transformation; Irradiation

## 1. Introduction

Electroactive polymers (EAP), which change shape as an electric field is applied, can be used in many areas, such as artificial muscles and organs, smart materials for vibration and noise control, electromechanical actuators and sensors for robots, acoustic transducers used for underwater navigation and medical imaging, and fluid pumps and valves [1–10]. The function of the EAP in these applications is to perform energy conversion between the electrical and mechanical forms. Compared with piezoceramic and magnetostrictive actuator materials, polymers have many advantages, such as flexibility, easy processing, light weight, and low cost. Polymeric materials can also withstand a large dimensional change (strain) without fatigue and are quite robust. On the other hand, the traditional piezoelectric EAPs suffer low strain, low elastic energy density, and low electromechanical conversion efficiency, which limit their applications in comparison with the piezoelectric ceramics [1,2]. Hence, one of the challenges in the development and utilization of EAPs for a wide range of applications is how to significantly increase and improve the electromechanical responses so that to achieve high strain capability, high elastic power density, and high electromechanical conversion efficiency. In recent years, there has been a great deal of effort put forth to explore different new approaches to improve the performance of existing polymers and/or to develop high performance polymers [3,6,11–13]. The recent work on high energy electron irradiated poly(vinylidene fluoride-trifluoroethylene) (P(VDF-TrFE)) copolymer, which exhibits very high electrostrictive strain with high elastic modulus and high load capability [11,14–16], is one of the advances made in this field.

In order to provide understanding on the basic mechanism underlying the high electrostrictive responses in irradiated P(VDF-TrFE) copolymers, in this paper, we will first review briefly several unique features associated with ferroelectric–paraelectric (F–P) phase transition, which can be made use of in developing high performance EAPs. Then, the electromechanical responses of this newly developed polymer will

* Corresponding author. Tel.: +1-814-865-0146; fax: +1-814-863-7846.
*E-mail address*: zxc7@psu.edu (Z.-Y. Cheng).

0924-4247/01/$ – see front matter © 2001 Published by Elsevier Science B.V.
PII: S0924-4247(01)00496-4

be presented including the strain responses, electromechanical coupling factor, load capability, and frequency dependence behavior of the strain response. To demonstrate the performance of this class of material, several unimorph actuators were fabricated and test results will also be discussed.

## 2. Ferroelectric–paraelectric phase transformation in P(VDF-TrFE) copolymers

In this section, we will review several unique phenomena associated with F–P phase transformation, especially in P(VDF-TrFE) copolymers. In many polymeric materials, it is well known that there are large strain changes associated with transformation from one phase to another. For P(VDF-TrFE) copolymers, large lattice strains have been detected when the copolymer goes from the low-temperature (LT) ferroelectric phase to the high-temperature (HT) paraelectric phase. Presented in Fig. 1 is the X-ray data on the lattice strain along the polymer chain direction ((0 0 1) reflection) and perpendicular to the chain ((2 0 0, 1 1 0) reflections) for the copolymer of 65/35 mol% [17]. As revealed by the data, for this copolymer there is a lattice strain of −10 and 7% in the crystalline phase along and perpendicular to the polymer chain, respectively, as the copolymer goes through the phase transition. Therefore, for a highly aligned copolymer with a high crystallinity (>50% crystallinity), these strains can be translated to large macroscopic strains. Indeed, a thermal strain of more than 6% has been observed on a 65/35 copolymer when going through the phase transition [18]. In addition, for a ferroelectric polymer, the phase transformation can be controlled by an external field (both electric and mechanical), and hence, it is expected that a high field induced strain can be achieved in P(VDF-TrFE) copolymer by exploiting the lattice strain at F–P transformation.

Another interesting feature associated with the F–P transition is that there is a possibility of a very large electromechanical coupling factor ($k \sim 1$) being obtained near a first order F–P transition temperature. As shown by an earlier study based on phenomenological theory, in a ferroelectric single crystal at temperatures above the transition where a polar-state can be induced by external dc bias fields, the coupling factor can approach 1 (near 100% energy conversion efficiency) [19]. That result is presented in Fig. 2 where the parameters used for the phenomenological formula are those from the ferroelectric $BaTiO_3$ single crystal, a typical ferroelectric material. This is a general result for the first order F–P phase transformation in spite of the fact that the curves in Fig. 2 are from the parameters of $BaTiO_3$. For P(VDF-TrFE) copolymers, it has been shown that at compositions with VDF content >60%, the F–P transition is first order in nature [20]. The temperature range in which the electric field can induce the phase transition from non-polar to polar phases depends strongly on the material. For most of the inorganic ferroelectrics, this temperature range is relatively narrow. For instance, the range is about 8°C for $BaTiO_3$ (as approximately measured by the temperature range between F–P transition and critical temperature) [21]. For P(VDF-TrFE) copolymers, it has been found that this temperature range is relatively large as reported by a recent study on Langmuir–Blodgett film of P(VDF-TrFE) 70/30 mol%, where this temperature range is observed to be more than 50°C [22].

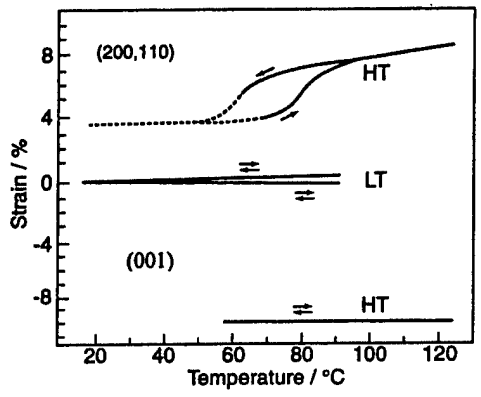


Fig. 1. Lattice strains along (0 0 1) and (2 0 0, 1 1 0), respectively, obtained from X-ray data for P(VDF-TrFE) 65/35 mol% copolymer.

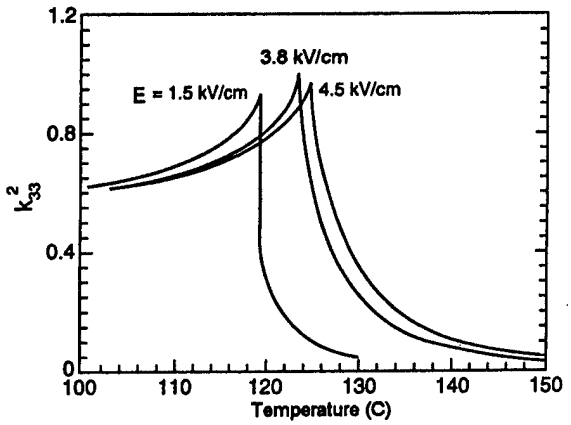


Fig. 2. Electromechanical coupling factor ($k_{33}$) as a function of temperature for a material with a first order F–P phase transition under different dc bias fields ($E$). The results are calculated based on Landau–Devonshire theory using the parameter obtained on $BaTiO_3$.

All these results indicate that one may be able to improve the electromechanical response of P(VDF-TrFE) copolymer significantly by operating the polymer near the F–P transition. However, there are several issues associated with the first order F–P transition in P(VDF-TrFE) copolymer that have to be addressed. As has been shown in the phase diagram (Fig. 3), F–P transition in all P(VDF-TrFE) compositions occurs at temperatures higher than room temperature and the transition is relatively sharp (over a relatively narrow temperature range). In addition, large hysteresis has been observed for the copolymers at the first order F–P transition, which is a basic feature for this type of transition. A large hysteresis is not desirable for practical applications.

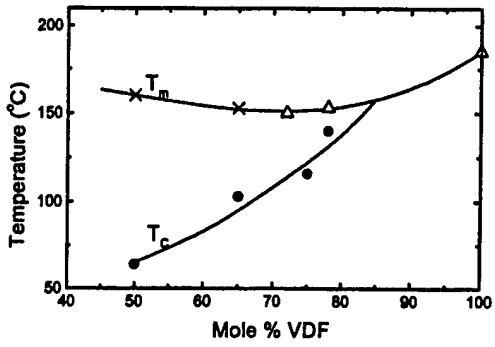


Fig. 3. Phase diagram of P(VDF-TrFE) copolymer. Where $T_m$ and $T_c$ are the melting temperature and F–P phase transition temperatures, respectively.

Therefore, to make use of the unique opportunities near the first order F–P transition in P(VDF-TrFE) copolymer systems, the copolymer should be modified as to broaden the phase transition region, move it to room temperature, and minimize the hysteresis.

## 3. Electromechanical properties of high energy electron irradiated P(VDF-TrFE) copolymer

In polymeric materials, high energy electron irradiation has been widely used to modify polymer properties. In P(VDF-TrFE) copolymers, Lovinger found that by using high energy electron irradiation, the ferroelectric phase at room temperature can be converted into a macroscopically paraelectric like phase [23]. Subsequent studies by Odajima et al. and Daudin et al. also found that a sharp dielectric constant peak from the F–P transition can be broadened markedly and moved to near room temperature [24,25]. Inspired by these early results, we carried out investigations on the electromechanical response of high energy electron irradiated P(VDF-TrFE) copolymers and the results show that indeed, the polarization hysteresis can be eliminated and copolymer with very high electrostrictive responses can be achieved.

### 3.1. Experimental

The P(VDF-TrFE) copolymer powders with a weight averaged mean molecular weight of 200,000 were purchased from Solvay and Cie, Bruxelles, Belgium. Two types of films are used in this investigation, stretched and unstretched films. In unstretched films, the films prepared were annealed at 140°C for a time period between 12–14 h to improve the crystallinity. In stretched films, films made from solution cast or quenched from melt press were uniaxially stretched up to five times at a temperature between 25 and 50°C. Afterwards, these films were also annealed at 140°C for 12–14 h to increase the crystallinity. The irradiation was carried out at nitrogen or argon atmosphere at different temperatures from room temperature to 120°C. Three electron energies were used in the irradiation: 1, 1.2, and 2.55 MeV. It was found that among the electron energies used, the irradiation with lower electron energy yields better electromechanical performance in the copolymers.

The elastic modulus of films was measured using a dynamic mechanical analyzer (TA Instrument, DMA model 2980). Gold electrodes with a thickness of about 40 nm were sputtered on both surfaces of the film for the electric and electromechanical characterizations. The field induced longitudinal strain was measured using a bimorph-based set-up [26]. The transverse strain was acquired using a newly developed set-up specially designed for flexible films [27]. An optical interferometer was applied to characterize the longitudinal strain response at high frequencies. An HP 4194A impedance analyzer was used to characterize the resonance behavior of the films under dc electric bias field.

Copolymers in the composition range with VDF content between 50 and 80 mol% were chosen for the investigation. In the experiment, it was found that there are two competing factors affecting the selection of the copolymers. On one hand, for copolymers in this composition range, the ferroelectricity becomes stronger with the VDF content as indicated by higher F–P transition temperature and increased coercive field for copolymers with higher VDF content. As a result, it becomes progressively more difficult to eliminate the polarization hysteresis and generate electrostrictive strain using the irradiation approach here for copolymers with high VDF content. In fact, for copolymers with VDF content higher than 70 mol%, it becomes very difficult to convert the copolymer into an electrostrictive material with small hysteresis at room temperature using the high energy electron irradiation [28]. On the other hand, the lattice strains associated F–P transition increase with the VDF content, implying a high induced strain response for copolymers with high VDF content [29]. As a compromise, therefore, in this paper, we focus on P(VDF-TrFE) copolymers with 65/35 and 68/32 mol% ratio.

Presented in Fig. 4 are polarization loops measured at room temperature at 10 Hz for 65/35 unstretched copolymer film before and after irradiation. For the unirradiated film, a typical polarization hysteresis loop was observed due to the high nucleation barrier when switching polarization from

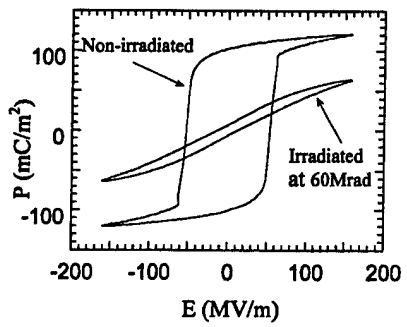


Fig. 4. Polarization loop for P(VDF-TrFE) 65/35 mol% film before and after irradiation.

the coherent macroscopic polar domains. After irradiation with 60 Mrad dose at 120°C, the polarization hysteresis is significantly reduced and the loop becomes quite slim due to the breaking up of macroscopic coherent polar domains to microscopic polar regions. The results indicate that the high energy irradiation is quite effective in eliminating the polarization hysteresis in these polymers.

### 3.2. Electrostrictive strains and electromechanical coupling factors at low frequency

Longitudinal strain ($S_3$), which is the thickness change of the film induced by applied electric fields, was characterized for films exhibiting slim polarization loops. Presented in Fig. 5(a) is the longitudinal strain measured for 65/35 mol% copolymers irradiated with 2.55 MeV electron at two irradiation temperatures and doses, where the external electric field is at 1 Hz while the strain was measured at 2 Hz because of electrostrictive nature of the strain response. In this paper, the frequency cited is that of the external electric field. The data indicate that there is no significant difference in $S_3$ between stretched and unstretched films. Shown in Fig. 5(b) is $S_3$ for unstretched 68/32 mol% copolymer film irradiated at 105°C with 70 Mrad dose of 1.0 MeV electrons. Apparently, a longitudinal strain $S_3 \approx -5\%$ can be induced by an electric field of 150 MV/m in the film. The temperature dependence of the strain response for 68/32 irradiated copolymer film (Fig. 5(b)) is summarized in Fig. 5(c), which shows that at a temperature range up to 80°C, the field induced strain can remain nearly constant.

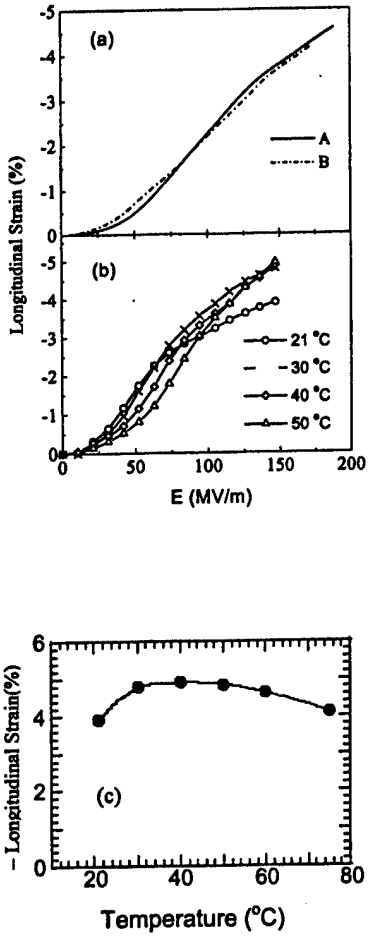


Fig. 5. Amplitude of the longitudinal strain as a function of the amplitude of the electric field at 1 Hz: (a) strain measured at room temperature for the 65/35 mol% copolymer films irradiated with 2.55 MeV electrons. Curves A and B correspond to the stretched film irradiated at 120°C with 80 Mrad dose and unstretched film irradiated at RT with 100 Mrad dose, respectively; (b) strain measured at different temperatures, which are indicated in figure, for unstretched 68/32 mol% copolymer film irradiated at 105°C with 70 Mrad dose of 1.0 MeV electrons; and (c) the temperature dependence of the longitudinal strain amplitude for the film shown in (b) under a constant electric field of 150 MV/m.

It should be mentioned that the doses used for the data in Fig. 5 are the optimum doses required to produce the slim polarization loop and high electrostrictive strain in these polymer films. Lowering the dosage will result in a large hysteresis and increasing the dosage will cause a significant reduction of the electrostrictive strain in the films.

In P(VDF-TrFE) copolymers, there exists large anisotropy in the strain responses along and perpendicular to the chain direction. Therefore, the transverse strain, which is associated with the length change of the film under an electric field, of the irradiated copolymers can be tuned over a large range by varying the film processing condition [15]. For unstretched films, the transverse strain is relatively small (approximately +1% level at ~100 MV/m) and in most of the films examined, the amplitude ratio between the transverse strain and longitudinal strain is less than 0.33. This feature is attractive for devices utilizing the longitudinal strain, such as ultrasonic transducers in the thickness mode, and actuators and sensors making use of the longitudinal electromechanical responses of the material. For example, a very weak transverse electromechanical response in comparison with the longitudinal one can significantly reduce the influence of the lateral modes on the thickness resonance and improve the performance of the thickness transducer.

On the other hand, for stretched films, a large transverse strain ($S_1$) along the stretching direction can be achieved as shown in Fig. 6, where the transverse strain about +3.5% is observed in the irradiated copolymer under an electric field of 110 MV/m. It is also found that for stretched films, the amplitude of the transverse strain along the stretching direction can be comparable with that of the longitudinal strain, while amplitude of the transverse strain in direction perpendicular to the stretching direction ($S_2$) is much small (approximately −1% at 100 MV/m).

It is interesting to note that for P(VDF-TrFE) copolymers, the strain along the thickness direction (parallel to the electric field) is always negative regardless the sample processing condition. That is, the thickness is reduced as the field or polarization is raised. In fact, this is a general feature for a system in which polarization response

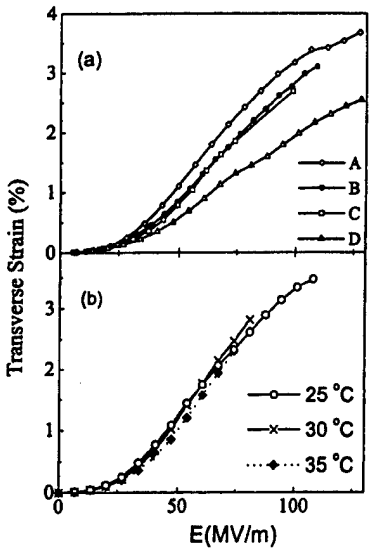


Fig. 6. Amplitude of the transverse strain along stretching direction as a function of amplitude of the electric field at 1 Hz for stretched samples: (a) curves A, B, C, and D correspond to the strain measured at room temperature for copolymer films under different irradiation conditions, A: 68/32 mol% film irradiated at 100°C with 65 Mrad doses of 1.2 MeV electrons, B: 65/35 mol% film irradiated at 105°C with 70 Mrad dose of 1.0 MeV electrons, C: 65/35 mol% film irradiated at 95°C with 60 Mrad dose of 2.55 MeV, and D: 65/35 mol% film irradiated at 77°C with 80 Mrad dose of 2.55 MeV; (b) strain measured at different temperatures, which are indicated in figure, for stretched 68/32 mol% copolymer film irradiated at 100°C with 70 Mrad dose of 1.2 MeV electrons.

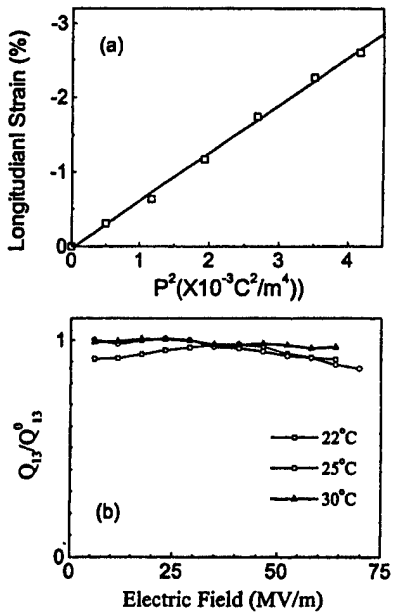


Fig. 7. (a) Longitudinal strain measured at room temperature vs. $P^2$ for unstretched 68/32 mol% copolymer film irradiated at 105°C with 70 Mrad dose of 1.0 MeV electrons, where $P$ is the polarization; (b) electrostrictive coefficient $Q_{13}$ vs. electrical field amplitude measured at 22, 25, and 30°C for stretched 65/35 film irradiated at 95°C with 60 Mrad dose of 2.5 MeV electrons, where $Q_{13}^0$ is the weak field $Q_{13}$ (measured at about 10 MV/m and 30°C).

originates from the dipolar interaction and, therefore, is true for all the polymeric piezoelectric and electrostrictive responses [30,31]. For the strains perpendicular to the applied field direction, the sign of the strain will depend on the sample processing conditions. For an anisotropic sample, such as stretched films examined here, the electric induced strain along the stretching direction, which is perpendicular to the applied field, is positive, while in the direction perpendicular to both stretching and applied field directions, the strain is negative. For unstretched samples which are isotropic in the plane perpendicular to the applied field, the strain component in the plane is an average of the strains along the chain (positive) and perpendicular to the chain (negative) and is in general positive.

From the data of the longitudinal and transverse strain responses, the volume strain can be determined, which is about 1/3 of the longitudinal strain. That is, the volume of the film decreases with applying electric fields and the volume strain can reach −1% under a field of 100 MV/m, which is relatively large compared with other electroactive materials, such as polyurethane, silicone, and piezoelectric ceramics. The large volume strain induced by external electric fields in the irradiated copolymer indicates that the copolymer should have a high response when used for hydrostatic applications. This large volume strain originates from the local electric field induced phase transformation, which is a unique feature of this class of material and has been confirmed directly in a recent X-ray experiment [32].

By plotting the field induced strain versus the square of induced polarization, it is found that the strain is almost linearly dependent on $P^2$ as shown in Fig. 7(a), confirming that the strain response is electrostrictive in nature. The charge related electrostrictive coefficients ($Q_{ij}$) can be obtained

$$S_3 = Q_{33}P^2 \text{ and } S_1 = Q_{13}P^2 \quad (1)$$

The $Q_{33}$ is found to be in the range from −4 to −12 $m^4/C^2$, depending on the irradiation condition. On the other hand, since the dielectric constant of the irradiated copolymer is strongly non-linear, the relationship between the strain and applied electric field $E_3$ is not well defined. Although the relationship of

$$S_3 = M_{33}E_3^2 \text{ and } S_1 = M_{13}E_3^2 \quad (2)$$

are often used in the literature to approximate the strain responses of ferroelectric-based electrostrictive materials, the field related electrostrictive coefficient $M_{ij}$ will change with the applied field amplitude.

We now discuss the electromechanical coupling factors for the irradiated copolymers, which are directly related to the energy conversion efficiency of the material, and hence, are important parameters for most of electromechanical applications. For electrostrictive materials, the

electromechanical coupling factor ($k_{ij}$) has been derived by Hom et al. based on the consideration of electric and mechanical energies generated in the material under external field [33]

$$k_{3i}^2 = \frac{kS_i^2}{s_{ii}^D[P_E \ln((P_S+P_E)/(P_S-P_E))+P_S \ln(1-(P_E/P_S)^2)]} \quad (3)$$

where $i = 1$ or 3, corresponding to the transverse or longitudinal direction (for example, $k_{31}$, is the transverse coupling factor) and $s_{ii}^D$ the elastic compliance under constant polarization, $S_i$ and $P_E$ are the strain and polarization responses, respectively, for the material under an electric field of $E$. The coupling factor depends on $E$, the electric field level. In Eq. (3), it is assumed that the polarization–field ($P$–$E$) relationship follows approximately [33]

$$|P_E| = P_S \tanh(k|E|) \quad (4)$$

where $P_S$ is the saturation polarization and $k$ a constant. It is found that Eq. (4) describes the $P$–$E$ relationship of the irradiated copolymers studied here quite well [14].

The elastic modulus for the films examined here are shown in Fig. 8. Using the data in Figs. 5b, 6b and 8, along with the polarization data, the coupling factors, $k_{33}$ for the unstretched sample and $k_{31}$ for the stretched sample along the drawing direction, are evaluated and presented in Fig. 9. At near room temperature and under 80 MV/m electric field, $k_{33}$ can reach more than 0.3, which is comparable to that obtained in single crystal P(VDF-TrFE) copolymer [13]. More importantly, the data also shows that a coupling factor $k_{31}$ of 0.45 can be obtained, which is much higher than those in unirradiated P(VDF-TrFE) copolymers and even higher than $k_{31}$ from most piezoceramics [34]. Since the energy conversion efficiency is proportional to the square of the coupling factor, this improvement is significant. In many applications, such as micro-electromechanical-systems (MEMS), electrical power generation from ocean waves, and artificial muscles, it is the transverse strain that is often used and a high transverse coupling factor, therefore, is highly desirable.

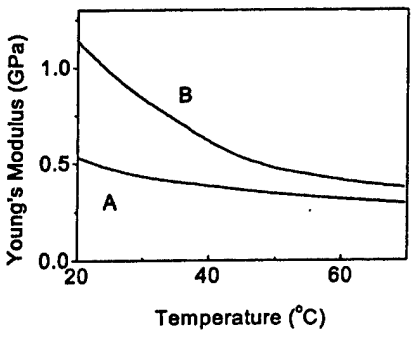


Fig. 8. Young's modulus at 1 Hz as a function of temperature for irradiated P(VDF-TrFE) copolymer films. Curve A is the modulus of unstretched 68/32 mol% irradiated at 105°C with 70 Mrad dose of 1.0 MeV electrons, and curve B is the modulus along stretching direction of stretched 68/32 mol% irradiated at 100°C with 70 Mrad dose of 1.2 MeV electrons.

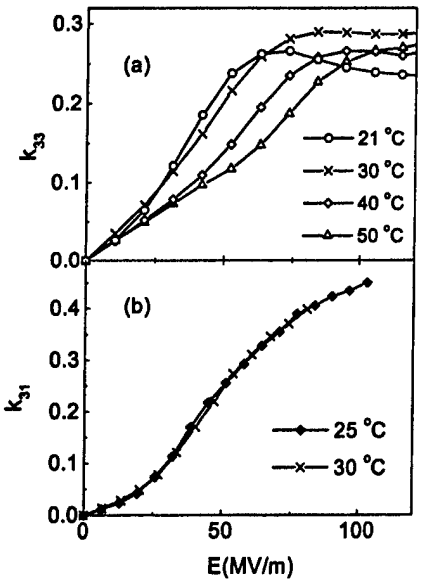


Fig. 9. Electromechanical coupling factor as a function of the electric field: (a) $k_{33}$ for unstretched P(VDF-TrFE) 68/32 mol% film irradiated at 105°C with 70 Mrad dose of 1.0 MeV electrons; (b) $k_{31}$ for stretched P(VDF-TrFE) 68/32 mol% film irradiated at 100°C with 70 Mrad dose of 1.2 MeV electrons.

### 3.3. High frequency strain response and electromechanical resonance behavior

The irradiated copolymer exhibits relaxor ferroelectric behavior which shows a strong dielectric dispersion at near room temperature [11]. Therefore, it is expected that there will also be frequency dispersion of the field induced strain since the electrostrictive strain is closely related to the polarization response in the material, i.e. Eqs. (1) and (2). To characterize the electromechanical responses at high frequencies, we carried out two experiments. One is to perform the field induced strain measurements directly to high frequencies. The other is to measure the electromechanical resonance, which occurs at frequencies higher than 30 kHz when the copolymers are under dc bias fields (for an electrostrictive copolymer, a dc bias field is required to induce an effective piezoelectric state) and from which the electromechanical coupling factor can be obtained.

The frequency dependence of the longitudinal strain (in reduced unit) for 68/32 unstretched film is shown in Fig. 10. The measuring field used here is limited to below 30 MV/m due to the limitation of the power supply. Although the strain response decreases with frequency as one would expect, this reduction is not severe. Over a four-decade frequency change, i.e. from 1 Hz to 10 kHz, the reduction of the strain at near room temperature is less than half and at higher temperatures, the strain level can remain nearly constant in this frequency range. The results demonstrate that the

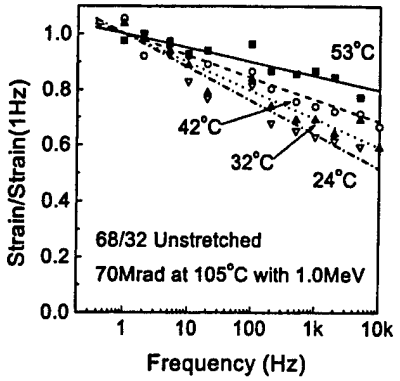


Fig. 10. Frequency dependence of longitudinal strain response for unstretched 68/32 mol% copolymer under 20 MV/m field. The film was irradiated at 105°C with 70 Mrad of 1.0 MeV electrons.

material studied here can produce high strain at high frequencies. The results here are also consistent with the dielectric data where at temperatures higher than the broad dielectric peak (>40°C), the dielectric dispersion becomes quite small. In fact, since the charge related electrostrictive coefficient $Q$ is nearly independent of frequency and weakly dependent on temperature, Eq. (1) indicates that the frequency dependence of high field polarization (and dielectric) response can be used to predict the frequency dependence of the strain response, which provides a more convenient means to estimate the strain response at high frequencies.

The electromechanical resonance behavior was characterized for copolymers under different dc bias fields and the results are presented in Fig. 11(a) where the ac signal used is 1 $V_{rms}$. In Fig. 11(a), the data were taken from stretched 68/32 film and the resonance occurred along the stretching direction. A very clear resonance (electromechanical behavior) was observed. For the data in Fig. 11(a), the elastic compliance ($s_{11}$) and related coupling factor ($k_{31}$) along the stretching direction can be derived from [35]

$$\frac{1}{s_{11}^{E}} = 4\rho f_s l \tag{5}$$

$$\frac{k_{31}^2}{1-k_{31}^2} = \frac{\pi f_p}{2 f_s} \tan\left(\frac{\pi}{2}\frac{\Delta f}{f_s}\right) \tag{6}$$

where, $s_{11}^{E}$ (Young's modulus $Y = 1/s_{11}^{E}$) is the elastic compliance along the stretching direction, $\rho$ the density, the $l$ the length along the resonance direction, $f_p$ and $f_s$ are the parallel and series resonance frequencies, and $\Delta f = f_p - f_s$. The Young's modulus along the stretching direction, thus, obtained is shown in Fig. 11(b). The comparison of the data here with that in Fig. 8 indicates that the Young's modulus increases significantly at high frequencies (3 GPa at 35 kHz as compared with 1 GPa at 1 Hz). The data also reveal that the modulus increases with dc bias field, which is associated with the reduced entropy in the copolymer under dc bias

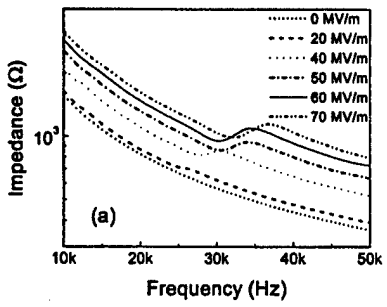


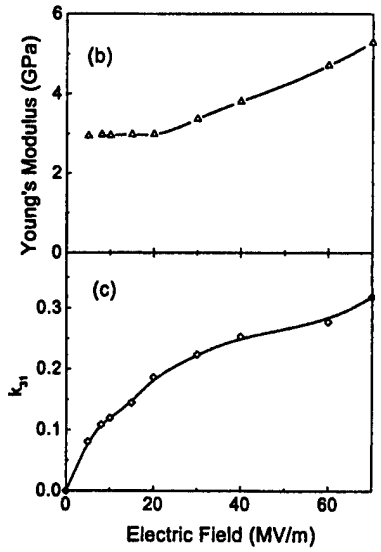


Fig. 11. (a) Frequency dependence of the impedance at room temperature for the stretched 68/32 mol% copolymer under different dc bias fields (from bottom to top, the dc bias is 0, 20, 40, 50, 60, 70 MV/m, respectively), the film was irradiated at 100°C with 70 Mrad of 1.2 MeV electrons; (b) and (c) are the Young's modulus and coupling factor $k_{31}$ deduced from the data in (a).

electric fields. In addition, the electromechanical coupling factor, $k_{31}$ shown in Fig. 11(c), determined from the resonance data is very close to and even higher than that obtained from Eq. (3) at near static limit, which again indicates that the copolymer can function well at high frequencies.

### 3.4. The mechanical load effect on the electrostrictive strains

Being a polymeric material, there is always a concern about the electromechanical response under high mechanical load, that is, whether the material can maintain the high strain level when subject to high external stresses. To address this concern, we carried out a series of measurement of the field induced strain under mechanical loads [16]. The data reported here are the transverse strain of stretched and irradiated 65/35 copolymer under tensile stress along the stretching direction and the longitudinal strain

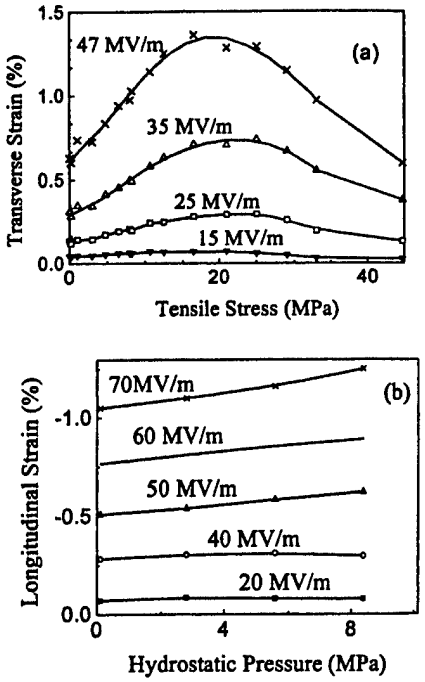


Fig. 12. (a) Transverse strain vs. tensile stress along the stretching direction for stretched 65/35 mol% copolymer film; (b) longitudinal strain vs. hydrostatic pressure for unstretched 65/35 mol% copolymer film. The strains were measured at room temperature. The films were irradiated at 95°C with 60 Mrad of 2.55 MeV electrons.

of unstretched and irradiated 65/35 copolymer under hydrostatic pressure [16,36].

The transverse strain at different tensile stresses along the stretching direction is presented in Fig. 12(a). As can be seen from the figure, under a constant electric field, the transverse strain increases with the load initially and reaches a maximum at the tensile stress of about 20 MPa. Upon further increase of the load, the field induced strain is reduced. One important feature revealed by the data is that even under a tensile stress of 45 MPa, the strain generated is still nearly the same as that without load, indicating that the material has a very high load capability.

The longitudinal strain for unstretched 65/35 films as a function of hydrostatic pressure was measured and the data is presented in Fig. 12(b). At low electric fields, the strain does not change much with pressure, while at high fields, it shows increase with pressure. Due to the limitation of the experimental set-up, we could not apply pressure higher than 8.2 MPa, which is the highest pressure level that the hydrostatic pressure system used can provide [36].

The results from both experiments demonstrate that the electrostrictive P(VDF-TrFE) copolymer has a high load capability and maintains its strain level even under very high load in contrast to many other EAPs. The observed change in the strain with load can be understood based on the consideration of the electrostrictive coupling in this relaxor ferroelectric material which has been analyzed in earlier publications [16,27].

### 3.5. *Performance of unimorph actuators fabricated from the electrostrictive P(VDF-TrFE) copolymers*

To demonstrate the device performance of the irradiated copolymers, several unimorph actuators were fabricated using the irradiated copolymer films. Shown in Fig. 13 is the field induced actuation of an unimorph made of an electrostrictive P(VDF-TrFE) 68/32 copolymer (active film) and an inactive polymeric substrate. The electrode area of the active film is 10 mm wide and 20 mm long. To prevent any possible edge discharge when operated under high voltage, there is ~1.5 mm wide unelectroded area at the edges of the active layer. The thickness of both the active and inactive films is 22 μm and the thickness of glue layer between two polymer films is about 1 μm. Fig. 13(a) shows the unimorph without electric field and Fig. 13(b) is under 65 MV/m field, where a transverse strain of about 1.7% was generated in the active film (68/32 copolymer, stretched and irradiated at 100°C with 65 Mrad dose of 1.2 MeV electrons). Clearly, there is a large actuation of the unimorph due to the high transverse strain.

For an unimorph, it has been derived that the tip displacement ($\delta$) and blocking force ($F$), which are dependent on the

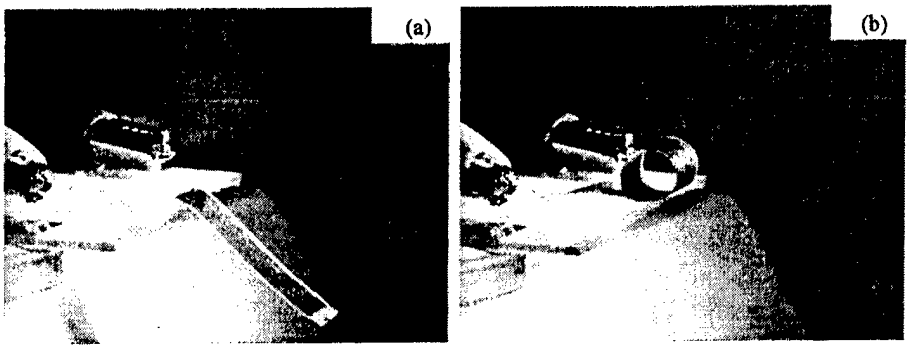


Fig. 13. The performance of an unimorph with one electrostrictive P(VDF-TrFE) copolymer layer of 22 μm bonded to an inactive polymer of the same thickness: (a) the picture shows the unimorph without electric field; (b) the picture shows the actuation of the unimorph under an electric field of 65 MV/m.

Table 1
Comparison of electromechanical properties

| Materials | | $Y$ (GPa) | Typical $S_m$ (%) | $YS_m^2/2$ (J/cm$^3$) | $YS_m^2/2\rho$ (J/kg) | Stress (MPa) |
|---|---|---|---|---|---|---|
| Piezoceramic | | 64 | 0.2 | 0.13 | 17 | 128 |
| Magnetostrictor | | 100 | 0.2 | 0.2 | 21.6 | 200 |
| Piezo P(VDF-TrFE) | | 4 | 0.15 | 0.0045 | 2.5 | 6 |
| Electrostrictive P(VDF-TrFE) | $S_3$ | 0.4 | 5.0 | 0.5 | 267 | 20 |
| | $S_1$ | 1.0 | 3.5 | 0.61 | 326 | 35 |

device geometric and material properties, can be expressed as [37]

$$\delta = \frac{3L^2}{2t}\frac{2AB(1+B)^2}{A^2B^4+2AB(2+3B+2B^2)+1}S_1 \quad (7)$$

$$F = \frac{2wt^2Y}{8L}\frac{2AB}{(AB+1)(1+B)}S_1 \quad (8)$$

where $L$, $w$ and $t$ are the length, width and thickness of the unimorph, $S_1$ and $Y$ are the transverse strain and the Young's modulus along the length direction of the active film, respectively. In the equations, $A$ and $B$ are the ratio of Young's modulus and the thickness ratio of the substrate to active film, respectively. Because the unimorph tip in Fig. 13 has travelled more than one circle, Eq. (7) cannot be used to make the comparison.

For an unimorph with small $t$, the blocking force is small as indicated by Eq. (8). By increasing the thickness $t$ of an unimorph, the blocking force can be increased. Here, in order to keep the driving voltage low, a multilayer configuration for the irradiated P(VDF-TrFE) copolymer is used [38]. The unimorph fabricated has eight active layers with each layer thickness of about 19 μm and bonded together by a polymer glue and the total thickness of the unimorph is 0.32 mm. The other dimensions and parameters are: $L = 22$ mm, $Y = 1$ GPa, $B = 3$ and $A = 1$. The actual unimorph width $w$ is 13 mm, but the width of the electroded area is 10 mm. The blocking force measured for the unimorph was 3.3 g when a field of 40 MV/m was applied which results in a transverse strain of 0.33%. By substituting all the parameters into Eq. (8), a blocking force of 4.2 g is predicted (here $w = 10$ mm is used since it is the electroded area which generates the force). Considering the fact that there is a dead area (unelectroded part of the unimorph) of about 25% of the total unimorph and the inactive glue layers, the agreement between the prediction of Eq. (8) and measured blocking force is quite good. The result indicates that the field induced strain $S_1$ can be used to estimate the blocking force of an unimorph actuator and the copolymer films do have high load capability.

## 4. Summary

As a summary, the field induced strain, the elastic energy density, which is another important parameter for electromechanical actuator materials, and other related parameters for this new class of EAP are compiled in Table 1 [39,40]. For the comparison, we include the data for the conventional piezoelectric P(VDF-TrFE) copolymer, the piezoceramic and magnetostrictive materials. In the table, both the volumetric energy density, which is $YS_m^2/2$ and related to the device volume, and the gravimetric energy density, which is $YS_m^2/2\rho$ and related to the device weight, are included. Here $S_m$ is the maximum strain level, $\rho$ the density, and $Y$ is the Young's modulus. In Table 1, we also include another parameter, the blocking stress, which is the stress level generated under a given electric field when the strain of the sample is zero. For the data in the table, the maximum blocking stress has been approximated as $YS_m$ (neglecting the possible non-linear effect). Apparently, the irradiated copolymers exhibit a high elastic energy density, which is consistent with the results of high load capability as presented in the paper.

The results presented here represent a significant improvement in the electromechanical properties of P(VDF-TrFE) copolymers and also points to a new approach for improving the electromechanical responses in other related ferroelectric polymers, i.e. making using of modified electric field controlled phase transition. Using high energy electron irradiation is only one means to modify the phase transition. There exist other non-irradiation approaches to modify the transition which are currently under investigation.

## Acknowledgements

This work was supported by DARPA (Contract no. N00173-99-C-2003) and ONR (Grant no. N00014-97-1-0667).

## References

[1] P.M. Galletti, D.E. De Rossi, A.S. De Reggi (Eds.), Medical Applications of Piezoelectric Polymers, Gordon and Breach Science Publishers, NY, 1988.
[2] T.T. Wang, J.M. Herbert, A.M. Glass (Eds.), The Application of the Ferroelectric Polymers, Blackie, Chapman & Hall, New York, 1988.
[3] R.H. Baughman, Synth. Metals 78 (1996) 339.
[4] S.G. Wax, R.R. Sands, Proc. SPIE Smart Structured Mater. 3669 (1999) 1.
[5] B.K. Kaneto, M. Kaneko, W. Takeshima, Syo Buturi 65 (1996) 803.

[6] R.E. Pelrine, R.D. Kornbluh, J.P. Joseph, Sens. Actuators A 64 (1998) 77.
[7] Y. Bar-Cohen, T. Xue, B. Joffe, S.S. Lih, P. Willis, J. Simpson, J. Smith, M. Shahinpoor, P. Willis, Proc. SPIE Smart Structured Mater. 3041 (1997) 697.
[8] E. Smela, O. Inganas, I. Lundstrom, Science 268 (1995) 1735.
[9] S. Guo, T. Nakamura, T. Fukuda, K. Oguro, in: Proceedings of the IEEE International Conference on Robotics and Automation, 1997, p. 266.
[10] S. Tadokoro, T. Muramura, S. Fuji, R. Kanno, M. Hattori, T. Takamori, in: Proceedings of the IEEE International Conference on Robotics and Automation, 1996, p. 205.
[11] Q.M. Zhang, V. Bharti, X. Zhao, Science 280 (1998) 2101.
[12] M. Zhenyi, J. Scheinbeim, J.W. Lee, B. Newman, J. Polym. Sci. B: Poly. Phys. 32 (1994) 2721.
[13] K. Omote, H. Ohigashi, K. Koga, J. Appl. Phys. 81 (1997) 2760.
[14] X. Zhao, V. Bharti, Q.M. Zhang, T. Romotowski, F. Tito, R. Ting, Appl. Phys. Lett. 73 (1998) 2054.
[15] Z.-Y. Cheng, T.-B. Xu, V. Bharti, S. Wang, Q.M. Zhang, Appl. Phys. Lett. 74 (1999) 1901.
[16] V. Bharti, Z.-Y. Cheng, S. Gross, T.B. Xu, Q.M. Zhang, Appl. Phys. Lett. 75 (1999) 2653.
[17] K. Tashiro, K. Takano, M. Kobayashi, Y. Chatani, H. Tadokoro, Ferroelectrics 57 (1984) 297.
[18] K. Tashiro, S. Nishimura, M. Kobayashi, Macromolecules 23 (1990) 2802.
[19] Q.M. Zhang, J. Zhao, T. Shrout, N. Kim, L.E. Cross, A. Amin, B.M. Kulwicki, J. Appl. Phys. 77 (1995) 2549.
[20] T. Furukawa, Phase Transitions 18 (1989) 143.
[21] F. Jona, G. Shirane, Ferroelectric Crystals, Dover Publications, New York, 1993, p. 138.
[22] S. Ducharme, A.V. Bune, L.M. Blinov, V.M. Fridkin, S.P. Palto, A.V. Sorokin, S.G. Yudin, Phys. Rev. B 57 (1999) 25.
[23] A. Lovinger, Macromolecules 18 (1985) 190.
[24] F. Macchi, B. Daudin, J.F. Legrand, Nucl. Instr. Meth. B 46 (1990) 324.
[25] A. Odajima, Y. Takasa, T. Ishibashi, Y. Yuasa, Jpn. J. Appl. Phys. 24 (1985) 881.
[26] J. Su, P. Moses, Q.M. Zhang, Rev. Sci. Instrum. 69 (1998) 2480.
[27] Z.-Y. Cheng, V. Bharti, T.B. Xu, S. Wang, Q.M. Zhang, T. Ramotowski, F. Tito, R. Ting, J. Appl. Phys. 86 (1999) 2208.
[28] Z.-Y. Cheng, V. Baarti, T. Mai, T.-B. Xu, Q.M. Zhang, T. Ramotowski, K.A. Wright, R. Ting, IEEE Trans. Ultrason. Ferro. Freq. Contr. 47 (2000) 1296.
[29] F.J. Balta, A.G. Arche, T.A. Ezquerra, C.S. Cruz, F. Batallan, B. Frick, Prog. Polym. Sci. 18 (1993) 1.
[30] W. Kinase, H. Takahashi, J. Phys. Soc. Jpn 10 (1955) 942.
[31] Y.M. Shkel, D.J. Klingenberg, J. Appl. Phys. 83 (1998) 415.
[32] Q.M. Zhang, Z.-Y. Cheng, V. Bharti, Appl. Phys. A 70 (2000) 307.
[33] C. Hom, S. Pilgrim, N. Shankar, K. Bridger, M. Massuda, S. Winzer, IEEE Trans. Ultrason. Ferro. Freq. Contr. 41 (1994) 542.
[34] K. Tashiro, in: H.S. Nalwa (Ed.), Ferroelectric Polymers, Marcel Dekker, NY, 1995, p. 63.
[35] IEEE Standard on Piezoelectricity, ANSI/IEEE Standard 176-1987, 1988.
[36] S.J. Gross, Z.-Y. Cheng, V. Bharti, Q.M. Zhang, Proc. IEEE 1999 Inter. Symp. Ultrsonics 2 (1999) 1019.
[37] Q.M. Wang, PhD Thesis, The Pennsylvania State University, 1998.
[38] M. Toda, S. Osaka, Trans. IECE Jpn. E 61 (1978) 507.
[39] L.E. Cross, Ceram. Trans. 68 (1996) 15.
[40] K.B. Hathaway, A.E. Clark, Mater. Res. Bull. 18 (1993) 34.

## Biographies

*Zhong-Yang Cheng* received his BS in physics, MS and PhD degrees in Electronic Materials and Engineering from Xian Jiaotong University, China in 1983, 1988 and 1995 respectively. His research interests are in characterization and fabrication of various functional materials (piezoelectric, ferroelectric, electroactive polymers, nonlinear optical polymers, single crystals, ceramics, thin films, et al.) and the application studies (actuators, sensors, transducers, MEMS, electro-optical modulation, et al.) of these materials. Dr. CHENG can be reached through e-mail: zxc7@psu.edu

*Dr. Vivek Bharti* received his BSc degree in science in 1989 from Meerut University, India, and masters in physics in 1992 and doctoral degree in polymer physics in 1997 from the University of Roorkee, Roorkee, India. His current research interests are in the area of characterization of structural and electromechanical properties of advanced materials for their applications as actuators, transducers, sensors, dielectrics and MEMS.

*Tian-Bing Xu* received the MSc degree in Electrical Engineering from the Pennsylvania State University in 1999. He is currently a candidate for the PhD degree in the Intercollege Graduate Program in Materials, The Penn State University. He is currently working on electroactive polymers and their application for actuators and transducers.

*Haisheng Xu* obtained his PhD degree in Department of Polymer Science and Engineering, Nanjing University, China. He is a faculty member of Nanjing University and became an associate professor since 1996. Currently, he works in Materials Research Laboratory, The Pennsylvania State University as a visiting scholar.

*Tian Mai* received the BS degree in Computer Science from the Shangdong University, China in 1988. He is currently working as a Visiting Research Assistant with the Material Research Laboratory, the Pennsylvania State University from Shangdong University. His research interest is the area of property characterization of electroactive materials.

*Qiming Zhang* is an associate professor of Electrical Engineering at the Materials Research Laboratory and Department of Electrical Engineering of Penn State University. He obtained his BS in 1981 from Nanjing University, China, and PhD degree in 1986 from Penn State University. He worked at the Brookhaven National Laboratory as a research scientist in the area of solid state thin films. He came back to Penn State University at 1991 as a faculty to conduct research in ferroelectric based materials and devices and electroactive polymer based materials and devices. The research activities in his research group include material development, modeling, and device development for transducers and actuators, dielectrics and capacitors, ferroelectric polymer thin film for memory devices, MEMS, photonic bandgap crystal, and electrooptic and acoustooptic materials and devices. He has delivered many invited presentations in those areas. There are 135 publications in those areas from his research group. He is a member of IEEE, Materials Research Society, and American Physical Society.

# APPENDIX 17

# Ferroelectric and electromechanical properties of poly(vinylidene-fluoride–trifluoroethylene–chlorotrifluoroethylene) terpolymer

Haisheng Xu, Z.-Y. Cheng, Dana Olson, T. Mai, and Q. M. Zhang[a)]
*Materials Research Laboratory, The Pennsylvania State University, University Park, Pennsylvania 16802*

G. Kavarnos
*EG&G, Inc., Groton, Connecticut 06340*

(Received 6 December 2000; accepted for publication 31 January 2001)

This letter reports the ferroelectric and electromechanical properties of a class of ferroelectric polymer, poly(vinylidene-fluoride–trifluoroethylene–chlorotrifluoroethylene) terpolymer, which exhibits a slim polarization hysteresis loop and a high electrostrictive strain at room temperature. The dielectric and polarization behaviors of this terpolymer are typical of the ferroelectric relaxor. The x-ray and Fourier transform infrared results reveal that the random incorporation of bulky chlorotrifluoroethylene (CTFE) ter-monomers into polymer chains causes disordering of the ferroelectric phase. Furthermore, CTFE also acts as random defect fields which randomize the inter- and intrachain polar coupling, resulting in the observed ferroelectric relaxor behavior. © *2001 American Institute of Physics.* [DOI: 10.1063/1.1358847]

Polymers with large electromechanical responses are attractive for a broad range of applications. Among them, the poly(vinylidene-fluoride–trifluoroethylene) [P(VDF–TrFE)] copolymers are especially interesting because of their relatively high piezoelectric response and thermal and chemical stability.[1–3] Recently, it has been observed that with a proper high-energy electron irradiation treatment, P(VDF–TrFE) copolymers at compositions near 65/35 mol % exhibit a high electrostrictive strain and improved electromechanical coupling factors (electromechanical conversion efficiency).[4–7] In addition, the modified copolymers possess a relatively high-room-temperature dielectric constant and exhibit many features typical of ferroelectric relaxors.[4–7] These results demonstrate that the properties of P(VDF–TrFE)-based polymers can be modified and improved markedly by the introduction of "defect" structures. In this letter, we report on the electromechanical and ferroelectric properties of another polymer based on the concept of the defect structure modification of the P(VDF–TrFE) polymer system, poly(vinylidene-fluoride–trifluoroethylene–chlorotrifluoroethylene) terpolymer [P(VDF–TrFE–CTFE)]. It will be shown that the introduction of "bulky" CTFE into the P(VDF–TrFE) copolymer converts the normal ferroelectric P(VDF–TrFE) into a ferroelectric relaxor with high electrostrictive strain.

P(VDF–TrFE–CTFE) terpolymer was synthesized using the bulk polymerization method. The VDF/TrFE ratio was evaluated from the $^{19}$F NMR spectrum; the CTFE mol % was determined by element analysis. To facilitate the discussion and comparison with the P(VDF–TrFE) copolymer, the composition of the terpolymer is labeled as $VDF_x$–$TrFE_{1-x}$–$CTFE_y$, where the mole ratio of VDF/TrFE is $x/1-x$ and the $y$ is the mol % of CTFE in the terpolymer. In this investigation, terpolymers in the composition range from $x=60\%$ to 80% and $y=4\%$ to 13% were synthesized and evaluated. Among them, the terpolymer of 65/35/10 exhibits the highest electrostrictive strain with very little polarization hysteresis at room temperature. Accordingly, the properties of the terpolymer 65/35/10 are chosen to be the subject of this letter.

The polymer films were prepared using the solution cast method by first dissolving P(VDF–TrFE–CTFE) terpolymer in dimethyl formamide (DMF). The films were subsequently annealed at a temperature between 100 and 120 °C for 6 h to improve the crystallinity. Gold electrodes were sputtered on the two surfaces of the films for the electric measurement and the typical film thickness is about 20 $\mu$m. The thickness of films used in the Fourier transform infrared (FTIR) study is below 5 $\mu$m. The strain along the thickness direction (longitudinal strain $S_3$) was measured using a piezobimorph-based sensor.[8] The Sawyer–Tower technique was used to characterize the polarization response in the films.

As the bulky and less polar termonomer CTFE is randomly introduced into P(VDF–TrFE) normal ferroelectric crystals, it is expected that the ferroelectric transition will be broadened, and that the ferroelectric–paraelectric (FP) transition temperature will be lowered. Indeed, as shown in Figs. 1(a) and 1(b), those features have been observed in the dielectric data for the terpolymer 65/35/10. There are three main features in the dielectric data of the polymer due to the addition of CTFE: (1) the original FP transition peak of the 65/35 copolymer is moved to room temperature; (2) the peak becomes much broader and its position shifts progressively with frequency towards higher temperature; (3) there is no thermal hysteresis in the dielectric data, i.e., the broad dielectric peak stays at the same temperature when measured in the heating and cooling cycles [Fig. 1(b)]. In contrast, the copolymer shows thermal hysteresis in the dielectric data. In addition, the relationship between the measuring frequency $f$ and the dielectric peak temperature $T_m$ follows quite well the Vogel–Folcher (VF) law, as shown in the inset of Fig. 1(a),[9]

$$f=f_0 \exp\left[\frac{-U}{k(T_m-T_f)}\right],$$

where $U$ is a constant and $k$ is the Boltzmann constant, $T_f$

a)Electronic mail: qxz1@psu.edu

 

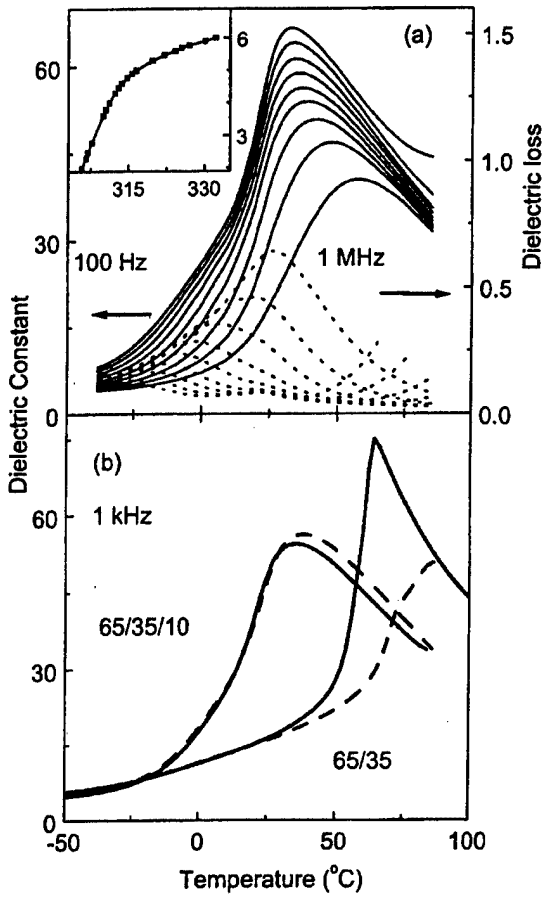


FIG. 1. Terpolymer P(VDF–TrFE–CTFE) 65/35/10. (a) Dielectric constant (solid curves) and dielectric loss (dashed curves) as a function of temperature at frequencies (from top to bottom for the dielectric constant and for the dielectric loss from bottom to top): 100, 300, 1, 3, 10, 30 kHz, 0.1, 0.3, and 1 MHz. (b) Dielectric constant at 1 kHz of the 65/35/10 terpolymer and 65/35 copolymer for both heating (dashed curves) and cooling (solid curves) cycles measured at room temperature.

can be regarded as the freezing temperature, corresponding to the peak temperature of the static dielectric constant (~0 Hz frequency), and the prefactor $f_0$ is the upper-frequency limit of the system, corresponding to the dipolar response when there is no coupling between the dipolar units in the system. The fitting yields $U=8.2$ meV, $f_0=15.4$ MHz, and $T_f=298.3$ K(25.15 °C). The results here are quite similar to those observed in the irradiated P(VDF–TrFE) copolymer.[4,6] It should also be noted that the terpolymer possesses a high-room-temperature dielectric constant (~60 at 1 kHz).

Figure 2(a) presents the polarization hysteresis loops measured at room temperature and −40 °C (233 K). Analogous to the irradiated copolymers, the terpolymer exhibits a slim polarization loop at room temperature, and as the temperature is lowered, both the remanent polarization and coercive field increase. All these features are remarkably reminiscent of ferroelectric relaxor behavior and the results suggest that the introduction of CTFE into P(VDF–TrFE) copolymers convert the normal ferroelectric P(VDF–TrFE) copolymer into a material closely resembling the ferroelectric relaxor.[10]

The terpolymer also exhibits a high-field-induced longitudinal strain $S$ (~4% under 150 MV/m), as shown in Fig.

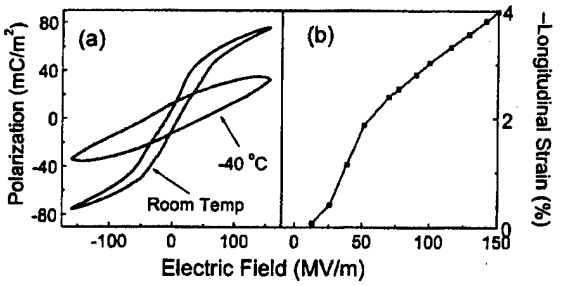


FIG. 2. Terpolymer P(VDF–TrFE–CTFE) 65/35/10. (a) Polarization hysteresis loops measured at room temperature (20 °C) and −40 °C and 10 Hz. (b) Longitudinal strain as a function of the driving field amplitude measured at room temperature and 10 Hz (dots are data and the solid line is drawn to guide the eyes).

2(b), which was measured at room temperature and 10 Hz. Combining the strain data with the measured elastic modulus $Y=0.4$ GPa yields a relatively high-elastic-energy density and the volumetric elastic-energy density $YS^2/2$ is 0.32 MJ/m$^3$.[4] For the copolymer, the corresponding strain is 0.15% and the volumetric elastic energy density is 0.0045 MJ/m$^3$.[5]

At this point, it is worthwhile to examine in more detail the effect of randomly introducing the termonomer CTFE or chlorine into the polymer chain and into the crystal. In comparison with the hydrogen and fluorine atoms, which have van der Waals (vdW) radii of 1.2 and 1.35 Å, respectively, chlorine has a much larger vdW radius of 1.8 Å. As a result, when considering the steric effects on the intrachain energies, the addition of chlorine to the polymer chain should favor the formation of transbond ($T$) rather than gauche ($G$) conformations. In the gauche conformation, substitution of chlorine in the polymer chain produces unfavorable 1, 4 steric repulsions between chlorine and fluorine atoms that can only be relieved by bond rotations to all-transconformations.[11] However, in order to accommodate the larger chlorine atom and relieve steric congestion, the interchain spacing in the crystalline phase in the terpolymers can expand and thereby favor energetically transgauche (TG) conformations in the neighboring chain segments. The delicate balance between those effects appears to leave room for incorporation of a certain number of gauche bonds. Indeed, computations on molecular models of terpolymers provide evidence of lattice expansion when CTFE termonomer units are substituted for TrFE monomers.[12] In addition, these calculations demonstrate that substitution of chlorine in the polymer chains raises the inter- and intrachain energies of $TGT\bar{G}$ forms to a greater extent than those of $T_3GT_3\bar{G}$ and all-trans forms because of steric repulsions. Consequently, the formation of the $T_3G$ conformation appears more likely in the terpolymer.[12] Those features are supported by the x-ray and FTIR studies described below. Furthermore, the random incorporation of CTFE into the VDF–TrFE chain would be expected to produce random fields to frustrate the ferroelectric (polar) coupling, both inter- and intrachain, which will destabilize the polar ordering, resulting in relaxor ferroelectric behavior.

In Fig. 3(a), we present the room-temperature x-ray data collected near the angular position of the (200, 110) reflection of the P(VDF–TrFE) copolymer. The change of the

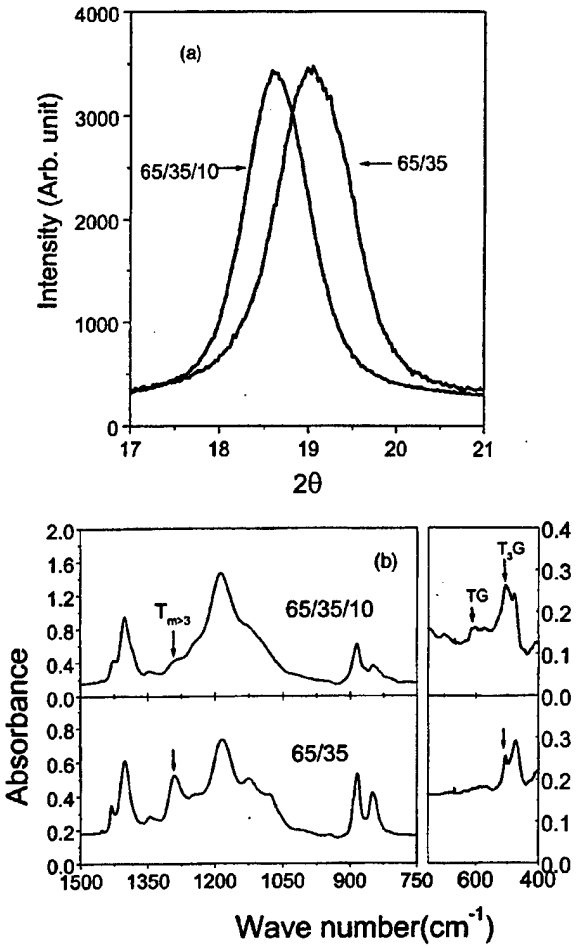


FIG. 3. (a) Comparison of the x-ray diffractions at $2\theta$ angle near the (200, 110) reflection, which shows the expansion of the interchain spacing due to the incorporation of CTFE into the crystalline phase (the x-ray wavelength is 1.54 Å). (b) Comparison of the FTIR data between the terpolymer and copolymer which shows the reduction of the absorbance for $T_{m>3}$ and increase of the absorbance for the $T_3G$ conformation in the terpolymer. Both x-ray and FTIR data were taken at room temperature.

crystallinity due to the introduction of CTFE can be estimated from the area of the crystalline diffraction peak and amorphous hola.[13] For the copolymer, the crystallinity is 75% while for the terpolymer here, it is reduced to 56%. For the 65/35 mol% copolymer, the interchain spacing from the (110, 200) reflection is 4.6 Å, while with 10 mol% CTFE, this spacing is increased to 4.8 Å, close to the interchain spacing of the paraelectric phase. Concomitantly with this shift in the x-ray peak position, the peak width is reduced, indicating an increase in the coherent x-ray diffraction length. This phenomenon is common to all the ferroelectric materials, where in the normal ferroelectric phase the x-ray peak width is limited by the ferroelectric domain size, which is normally much smaller than the crystallite size. The ferroelectric domains disappear in the nonferroelectric phase and the coherent x-ray diffraction length is mainly determined by the crystallite size.[14] This is consistent with the dielectric and polarization data presented in Figs. 1 and 2, indicating that there is no long-range polar ordering in the 65/35/10 terpolymer. However, unlike the paraelectric phase of copolymers, which is predominately all-transconformation,[15] the molecular conformation of 65/35/10 terpolymer is mainly $T_3GT_3\bar{G}$, as revealed by the FTIR data recorded at room temperature [Fig. 3(b)]. In this analysis, the method by Osaki and Ishida was used to calculate the fraction $F_i$ of each chain conformation:

$$F_i=\frac{A_i}{A_{\mathrm{I}}+A_{\mathrm{II}}+A_{\mathrm{III}}},$$

where $i$=I, II, and III, and $A_{\mathrm{I}}$, $A_{\mathrm{II}}$, and $A_{\mathrm{III}}$ are the absorbencies of the chain conformations with all-trans ($T_{m>3}$, absorbance peak at 1285 cm$^{-1}$), $T_3GT_3\bar{G}$ (peak at 510 cm$^{-1}$), and $TGT\bar{G}$ (peak at 610 cm$^{-1}$), respectively.[16,17] For the copolymer, the fraction of three conformations are 75% ($T_{m>3}$), 18% ($T_3GT_3\bar{G}$), and 7% ($TGT\bar{G}$), while for the terpolymer the values change to 34% ($T_{m>3}$), 61% ($T_3GT_3\bar{G}$), and 5% ($TGT\bar{G}$).

This work was supported by DARPA under Contract No. N00173-99-C-2003 and ONR under Grant No. N00014-00-1-0623.

[1] *The Applications of the Ferroelectric Polymers*, edited by T. T. Wang, J. M. Herbert, and A. M. Glass (Blackie, Chapman and Hall, New York, 1988).
[2] *Medical Applications of Piezoelectric Polymers*, edited by P. M. Galletti, D. E. De Rossi, and A. S. De Reggi (Gorden and Breach Science, New York, 1988).
[3] *Ferroelectric Polymers*, edited by H. S. Nalwa (Dekker, New York, 1995).
[4] Q. M. Zhang, V. Bharti, and X. Zhao, Science **280**, 2101 (1998).
[5] Q. M. Zhang, Z. Cheng, V. Bharti, T. Xu, H. S. Xu, T. Mai, and S. Gross, Proc. SPIE **3987**, 34 (2000).
[6] Q. M. Zhang, Z. Y. Cheng, and V. Bharti, Appl. Phys. A: Mater. Sci. Process. **70**, 307 (2000).
[7] V. Bharti and Q. M. Zhang, Phys. Rev. B (in press).
[8] J. Su, P. Moses, and Q. M. Zhang, Rev. Sci. Instrum. **69**, 2480 (1998).
[9] H. Vogel, Z. Phys. **22**, 645 (1921); G. S. Fulcher, J. Am. Ceram. Soc. **8**, 339 (1925).
[10] L. E. Cross, Ferroelectrics **151**, 305 (1994).
[11] G. J. Kavarnos and R. W. Holman, Polymer **35**, 5586 (1994); R. W. Holman and G. J. Kavarnos, *ibid.* **37**, 1697 (1996).
[12] G. J. Kavarnos (unpublished).
[13] V. Bharti, H. S. Xu, G. Shanthi, Q. M. Zhang, and K. Liang, J. Appl. Phys. **87**, 452 (2000).
[14] G. T. Davis, T. Furukawa, A. J. Lovinger, and M. Broadhurst, Macromolecules **15**, 329 (1982).
[15] K. Tashiro, K. Takano, M. Kobayashi, Y. Chatani, and H. Tadokoro, Ferroelectrics **57**, 297 (1984).
[16] S. Osaki and Y. Ishida, J. Polym. Sci., Polym. Phys. Ed. **13**, 1071 (1975).
[17] H. S. Xu, G. Shanthi, V. Bharti, and Q. M. Zhang, Macromolecules **33**, 4125 (2000).

# APPENDIX 18

Jpn. J. Appl. Phys. Vol. 40 (2001) pp. 672–675
Part 1, No. 2A, February 2001


# High Electromechanical Coupling Factor and Electrostrictive Strain over Broad Frequency Range in Electrostrictive Poly(vinylidene fluoride-trifluoroethylene) Copolymer Films

Vivek BHARTI, T.-B. XU, Z.-Y. CHENG, T. MAI, Q. M. ZHANG*, Tom RAMOTOWSKI[1] and K. A. WRIGHT[2]

*Materials Research Laboratory, The Pennsylvania State University, University Park, PA 16802, USA*
[1]*Naval Undersea Warfare Center, Newport, Rhode Island 02841, USA*
[2]*Laboratory of Electromagnetic and Electronic Systems, Massachusetts Institute of Technology, Cambridge, MA 02139, USA*

(Received July 27, 2000; accepted for publication November 8, 2000)

Electromechanical coupling factor is one of the most important parameters for measuring the performance of materials for electromechanical transduction applications. In this paper, we will show that a transverse electromechanical coupling factor $k_{31}$ of more than 0.45 can be achieved in poly(vinylidene fluoride-trifluoroethylene) [P(VDF-TrFE)] copolymer under certain electron irradiation treatment conditions. In addition, the effective piezoelectric coefficients of the irradiated copolymer have been found to increase markedly in comparison to non-irradiated copolymers. Experimental evidences also indicate that the improved electrostrictive strains in irradiated copolymer films can be maintained over a broad frequency and temperature range.

KEYWORDS: electrostriction, P(VDF-TrFE), piezoelectric, coupling coefficient

## 1. Introduction

As the best known electromechanical polymers, polyvinylidene fluoride (PVDF) and its copolymers with trifluoroethylene (TrFE) have been extensively investigated in the past thirty years for a wide range of applications such as artificial muscles, electromechanical transducers, and electric energy generation from ocean powers.[1–4] Although the P(VDF-TrFE) copolymers possess the highest piezoelectric coefficients and electromechanical coupling factors among all the known polymers, they are still far below those from the piezoceramics. For example, the longitudinal coupling factor $k_{33}$ for single crystal P(VDF-TrFE) 75/25 mol% copolymer is below 0.3, and other coupling factors have even lower values. The piezoelectric coefficients of these polymers at room temperature are also below 40 pm/V.[5–7] Therefore, continuous efforts are being made to improve the electromechanical properties of these copolymers by using different approaches.[8–12]

We have reported recently that by using high-energy electron irradiation, the electromechanical properties of P(VDF-TrFE) copolymers such as field-induced electrostrictive strains along both longitudinal and transverse directions can be improved significantly.[13,14] In the present study, we report that under a proper electron irradiation condition, an electromechanical coupling factor $k_{31} = 0.45$ (transverse coupling factor) can be reached in the irradiated copolymers, which is much higher than those in the non-irradiated copolymers ($k_{33} < 0.3$ and $k_{31} < 0.15$) and even higher than the $k_{31}$ value in most of the piezoceramics.[5–7,15] Since the energy conversion efficiency is proportional to the square of the coupling factor, this improvement is significant.[16] In addition, we will present the results showing that the irradiated copolymer can maintain their high strain level to higher frequencies and over a relative broad temperature range.

## 2. Experimental

The data reported in this article are taken from the P(VDF-TrFE) 68/32 mol% copolymer films, which exhibit the best electromechanical properties among the copolymers investigated.[13,14,17] The copolymer powder was purchased from Solvay and Cie, Belgium. The non-stretched and stretched (4.5×) films of thickness ~20–25 $\mu$m were prepared by extrusion and casting from $N,N$-dimethyl formamide (DMF) solvent, respectively. The non-stretched films were used to investigate the longitudinal strain response (the strain along the thickness direction). As has been shown earlier, in order to obtain a high transverse strain, a stretched copolymer film should be used.[17] In order to improve the crystallinity and also to remove the residual solvent from the solution cast films, the films were annealed at 140°C for 16 h before the irradiation. The electron irradiation was carried out using 1 MeV electrons at National Institute of Standards and Technology, and 1.2 MeV electrons at the Massachusetts Institute of Technology. In both the cases the irradiation was carried out in a nitrogen atmosphere at temperatures near 100°C for the irradiation doses ranging from 60 to 75 Mrad.

The strains along the thickness direction (longitudinal strain, $S_3$) and the stretching direction (transverse strain, $S_1$) were measured using a piezo-bimorph-based sensor and a cantilever-based dilatometer, respectively.[17,18] Both set-ups were designed and developed specifically for strain measurement in polymer thin films. In the piezo-bimorph set-up, the strain in the polymer films generates a deflection in the piezo-bimorph, which in turn, produces an electric signal output due to the piezoelectric effect. In the cantilever-based dilatometer set-up, one end of the polymer is fixed and the other end is attached to a plastic cantilever. The transverse strain in the films causes the deflection of the tip of the cantilever, which is measured by a photonic sensor. A laser interferometer set-up was used to measure the electrostrictive strain at higher frequencies (up to 5 kHz which was the limit of the voltage amplifier used).[19] The Sawyer-Tower technique was used to measure the polarization response in the films at 10 Hz frequency.

## 3. Results and Discussion

Figure 1(a) presents the amplitude of electric field-induced transverse strain at 1 Hz near room temperature obtained from the stretched copolymer films irradiated at 100°C using 1.2 MeV electrons with 70 Mrad dose. The transverse strain $S_1 \sim 3.3\%$ under the electric field of 105 MV/m is observed,

*E-mail address: qxz1@psu.edu

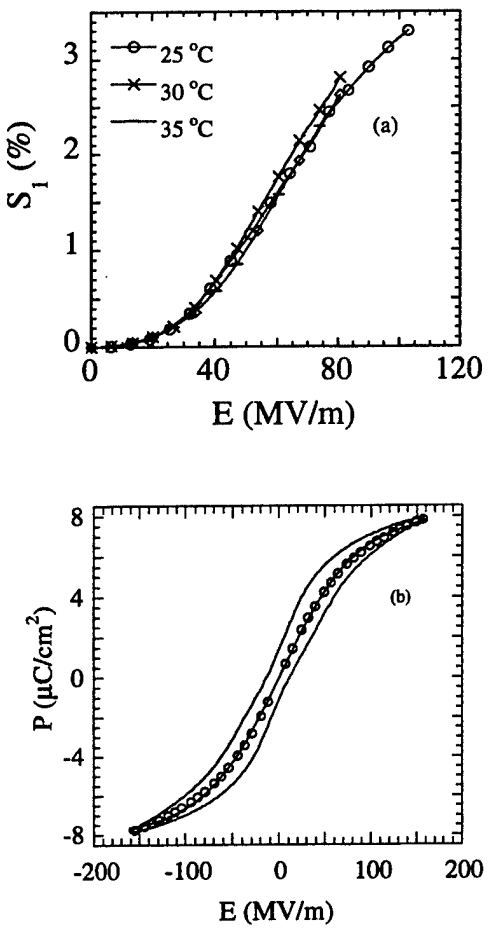


Fig. 1. (a) The dependence of electric field induced transverse strain ($S_1$) on electric field strengths at different temperatures, the solid curves are drawn to guide eyes; (b) the polarization hysteresis loop (solid curve) measured at 30°C, where the circles (O) are the average polarization of the observed polarization loop, while the solid line passes the circles is the fitted result using eq. (2). The material is stretched 68/32 mol% P(VDF-TrFE) copolymer films irradiated at 100°C with 1.2 MeV electrons for 70 Mrad dose.

which is higher than the transverse strain obtained at a similar field for copolymers irradiated with 2.55 MeV electrons, as reported earlier.[14,17]

The quasi-static electromechanical coupling factor for electrostrictive materials has been derived by Hom *et al.*,[20] where the coupling factor depends on the induced polarization level $P_B$ and strain $S_i$ under a given electrical field, i.e.,

$$k_{3i}^2 = \frac{kS_i^2}{s_{ii}^P \left[ P_B \ln\left(\frac{P_S + P_B}{P_S - P_B}\right) + P_S \ln\left(1 - \left(\frac{|P_B|}{P_S}\right)^2\right)\right]} \quad (1)$$

where $i = 1$ or 3, corresponding to the transverse or longitudinal direction (for example, $k_{31}$, is the transverse coupling factor) and $s_{ii}^P$ is the elastic compliance under constant polarization. The polarization–field ($P$–$E$) relation is assumed to be

$$|P_B| = P_S \tanh(k|E|) \quad (2)$$

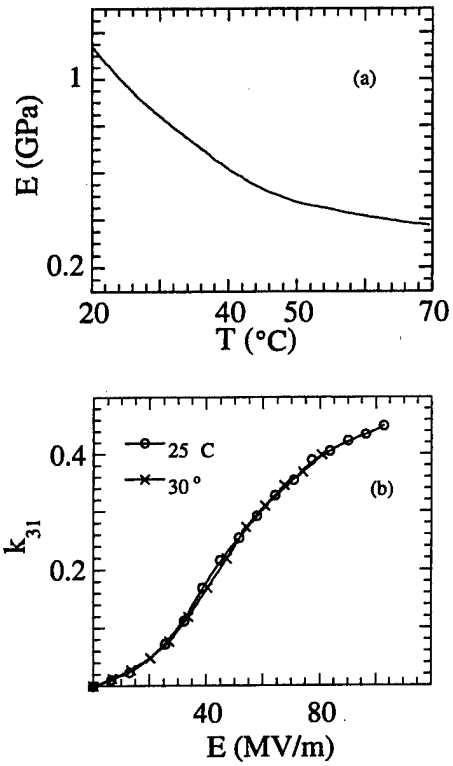


Fig. 2. The change in the (a) elastic modulus with temperature; (b) electromechanical coupling factor ($k_{31}$) with applied electric field at different temperatures (here the solid curves are drawn to guide eyes); measured for stretched 68/32 mol% P(VDF-TrFE) copolymer films irradiated at 100°C with 1.2 MeV electrons for 70 Mrad dose.

where $P_S$ is the saturation polarization and $k$ is a constant. As can be seen from Fig. 1(b), the averaged polarization loop can be quite well fitted by eq. (2). Using these data along with the elastic modulus shown in Fig. 2(a), the quasi-static transverse coupling factor $k_{31}$ is calculated and presented in Fig. 2(b). As can be seen, at near room temperature, $k_{31}$ is more than 0.45, which is much higher than that of non-irradiated P(VDF-TrFE) copolymers and even higher than $k_{31}$

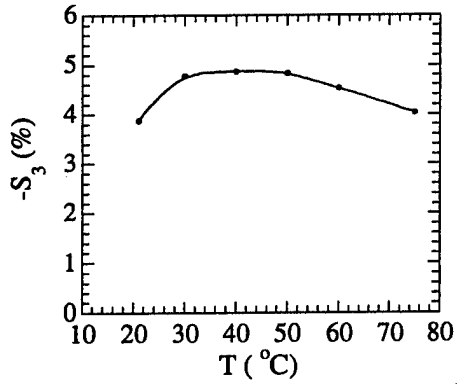


Fig. 3. The longitudinal strain ($S_3$) as a function of temperature measured under 147 MV/m and 1 Hz driving electric field for unstretched 68/32 mol% P(VDF-TrFE) copolymer films irradiated at 100°C with 1.0 MeV electrons for 70 Mrad dose. Data points are shown and the solid curve is drawn to guide eyes.

from most of the piezoceramics.[15] Since in many applications such as mico-electro-mechanical-systems (MEMS), electrical power generation from ocean waves, and artificial muscles, it is the transverse strain that is often used, a high transverse coupling factor, therefore, is highly desirable.[4,21–23]

The variation in longitudinal strain ($S_3$) at 1 Hz with temperature is presented in Fig. 3, where $S_3$ of near $-5\%$ can be induced by an electric field of 147 MV/m for unstretched copolymer films irradiated at 105°C with 70 Mrad dose of 1 MeV electrons. As can be observed that the induced strain is almost constant up to 80°C. Furthermore, the frequency effect on the field-induced strain, which is important for many actuator and transducer applications, was also characterized at near room temperature. The bimorph based set-up was used to measure the strain response in the frequency range from 1 Hz to near 100 Hz and a laser interferometer was utilized to measure strain at higher frequencies (up to 5 kHz). The $S_3$ data obtained from both set-ups are presented in Figs. 4(a) and 4(b). At lower frequencies (<50 Hz), the laser interferometer has relatively large error in the strain measurement due to the environment noise. In the overlapped frequency range, the data measured from the bimorph sensor and from the laser interferometer is consistent with each other within the error bar. The result shows that the electrostrictive strain extrapolated to 10 kHz remains to be more than 50% of the value at 1 Hz (over 4 frequency decades). For the comparison, the polarization level was also measured in the same frequency range using the Sawyer-Tower circuit. Since the electrostrictive strain $S$ is proportional to the square of the polarization $P$ ($S = QP^2$, where $Q$ is the electrostrctive coefficient), the change in the square of the polarization with frequency is also presented in Fig. 4. Apparently, the dispersion of the square of the polarization is smaller than that of the strain. Making use of the strain and polarization data, the electrostrctive coefficient $Q$ is determined and is shown in Fig. 4(c). As indicated by the data, there is a small decrease of $Q$ with frequency which suggests that there is a change of the polarization response with frequency and the low frequency component of the polarization is more effective in generating the strain response. This behavior is analogous to the one observed in the relaxor ferroelectric ceramic, $PbMg_{1/3}Nb_{2/3}O_3$, where due to the change in the polarization response with temperature, $Q$ exhibits a large variation.[24] In the irradiated copolymer, the polarization response can be from several different sources such as the rotation of dipoles and the local phase transformation due

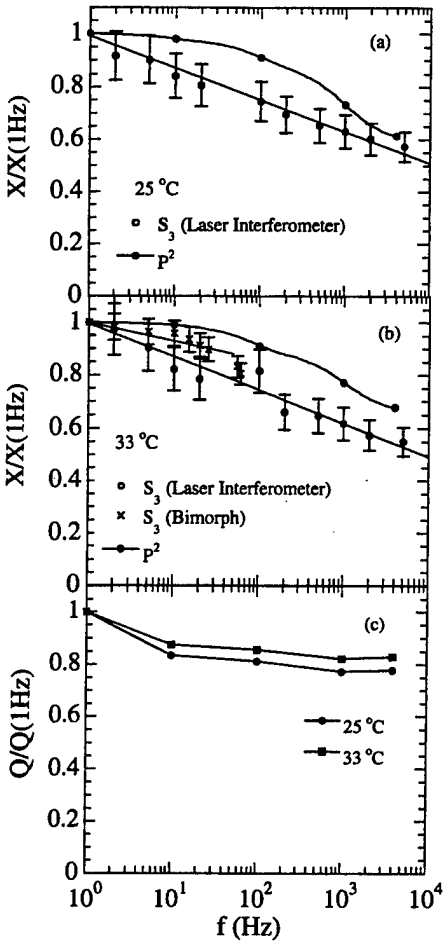


Fig. 4. The ratio of longitudinal strain ($S_3$) at higher frequencies to the strain at 1 Hz (open circles) as a function of frequency measured using laser interferometer at temperatures of (a) 25°C, and (b) 33°C; for unstretched 68/32 mol% P(VDF-TrFE) copolymer films irradiated at 105°C with 1.0 MeV electrons for 70 Mrad dose. For the comparison, the change in the square of the ratio of the polarization at higher frequencies to polarization at 1 Hz as a function of frequency is also shown (solid dots). The strain data (cross dots) measured using the bimorph based sensor is also presented. (c) The normalized electrostrictive coefficient $Q_{11}$ ($Q = S/P^2$) as a function of frequency for the two temperatures measured. The symbols here are the data points and the curves are drawn to guide eyes.

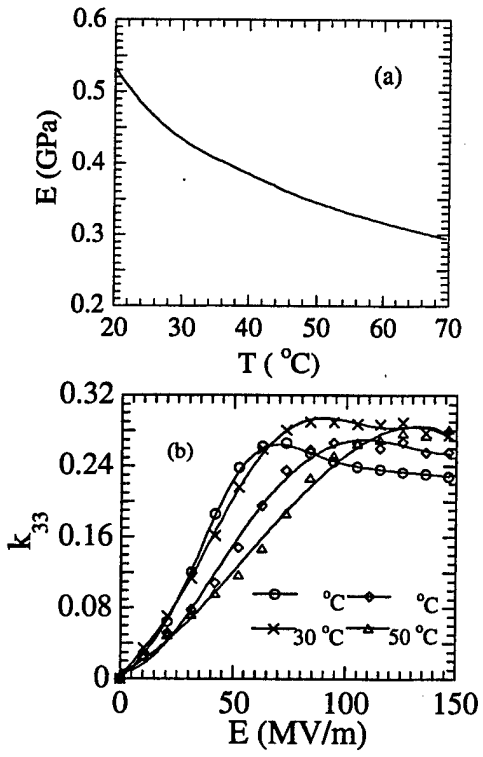


Fig. 5. (a) The elastic modulus as a function of temperature; (b) the electromechanical coupling factor ($k_{33}$) as a function of driving electric field at different temperatures (data points are presented and solid curves are drawn to guide eyes); for unstretched 68/32 mol% P(VDF-TrFE) copolymer films irradiated at 105°C with 1.0 MeV electrons for 70 Mrad dose.

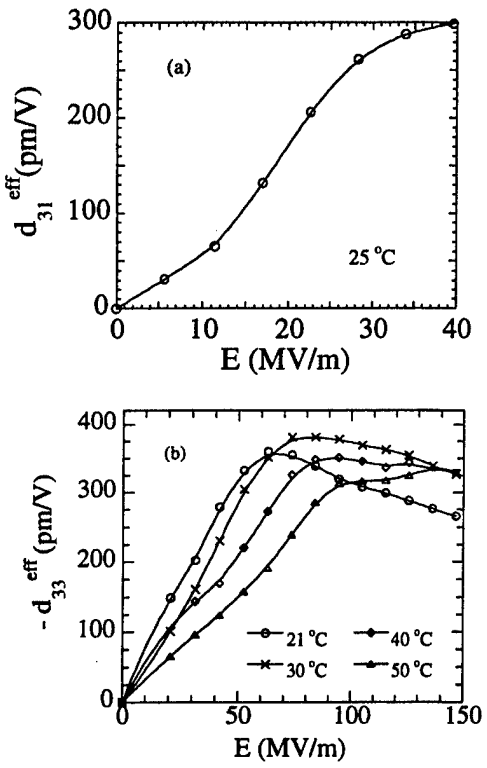


Fig. 6. Effective piezoelectric coefficients; (a) $d_{31}^{eff}$ measured for stretched P(VDF-TrFE) copolymer films irradiated at 100°C with 70 Mrad using the 1.2 MeV electrons, and (b) $d_{33}^{eff}$ measured for unstretched P(VDF-TrFE) copolymer films irradiated at 100°C with 70 Mrad using the 1.0 MeV electrons. The symbols here are the data points and the curves are drawn to guide eyes.

to the expansion and contraction of the local polar-regions.

Making use of eq. (1) with the elastic modulus [Fig. 5(a)] and polarization data, the longitudinal coupling factor ($k_{33}$) at 1 Hz is determined and presented in Fig. 5(b). At near room temperature and under 80 MV/m electric field, $k_{33}$ of more than 0.3 is achieved.

Although after irradiation at temperatures near and above room temperature the copolymer behaves as an electrostrictive material, to compare it with other electromechanical actuator materials, an effective piezoelectric coefficient is defined here as the ratio of the induced strain versus applied unipolar ac electric field [$S_i/E_3$, where $i = 1$ is for the effective transverse piezoelectric coefficient ($d_{31}^{eff}$) and $i = 3$ for the effective longitudinal coefficient ($d_{31}^{eff}$)].[17] As seen in Fig. 6, relatively large effective piezoelectric coefficients are obtained, and $d_{31}^{eff} = 300$ pm/V and $d_{33}^{eff} = -383$ pm/V are observed under 40 MV/m and 75 MV/m field for irradiated stretched and unstretched films, respectively. These values are comparable to the piezoelectric coefficient of conventional piezoceramic materials, for example PZT-5H ($d_{31} \sim -274$ pm/V and $d_{33} \sim 593$ pm/V).[15] It should be pointed out here that in many soft polymer elastomers, a high ratio of strain/applied field can be achieved due to the electrostatic force.[17,25,26] But because of the low elastic modulus of these polymer elastomers, the strain energy density, which is an important parameter for choosing a material as an actuator, is lower than irradiated copolymer films.[13,14,25,26]

## Acknowledgements

This work was supported by DARPA (grant no. N00173-99-C-2003), NSF (grant no. ECS-9710459), and ONR (grant no. N00014-97-1-0667). The authors also wish to thank A. Glazonov for stimulating discussions and assisting in the experiments.

1) T. T. Wang, J. M. Herbert and A. M. Glass: *The Application of the Ferroelectric Polymers* (Blackie, Chapman and Hall, New York, 1988).
2) M. A. Marcus: Ferroelectrics **40** (1982) 29.
3) J. A. Chilton and M. T. Goosey: *Special Polymers for Electronics and Optoelectronics* (Chapman & Hall, New York, 1995) Chap. 5.
4) I. Amato: Sci. News **136** (1989) 305.
5) K. Omote, H. Ohigashi and K. Koga: J. Appl. Phys. **81** (1997) 2760.
6) K. Omote and H. Ohigashi: Appl. Phys. Lett. **66** (1995) 2215.
7) H. Wang, Q. M. Zhang, L. E. Cross and A. O. Sykes: J. Appl. Phys. **74** (1993) 3394.
8) A. J. Lovinger: Science **220** (1983) 1115.
9) H. Ohigashi and T. Hattori: Ferroelectrics **171** (1995) 11.
10) V. Bharti, T. Kaura and R. Nath: IEEE Dielectr. Electr. Insul. **2** (1995) 1106.
11) J. Su, Y. Ma, J. Scheinbeim and B. A. Newman: J. Polym. Sci. B **33** (1995) 85.
12) G. M. Sessler and J. Hillenbrand: Appl. Phys. Lett. **75** (1999) 3405.
13) Q. M. Zhang, V. Bharti and X. Zhao: Science **280** (1998) 2101.
14) Z.-Y. Cheng, T.-B. Xu, V. Bharti, S. Wang and Q. M. Zhang: Appl. Phys. Lett. **74** (1999) 1901.
15) B. Jaffe, W. R. Cook and H. Jaffe, Jr.: *Piezoelectric Ceramics* (Academic Press, London, 1971).
16) IEEE Standard on Piezoelectricity, ANSI/IEEE Std 176–1987 (IEEE, New York, 1987).
17) Z.-Y. Cheng, V. Bharti, T. Mai, T.-B. Xu, Q. M. Zhang, T. Ramotowski, K. A. Wright and R. Ting: IEEE Trans. Ultrason. Ferroelectr. Freq. Control. **47** (2000) 1296.
18) J. Su, P. Moses and Q. M. Zhang: Rev. Sci. Instrum. **69** (1998) 2480.
19) Q. M. Zhang, W. Y. Pan and L. E. Cross: J. Appl. Phys. **63** (1988) 2492.
20) C. Hom, S. Pilgrim, N. Shankar, K. Bridger, M. Massuda and S. Winzer: IEEE Trans. Ultrason. Ferroelectr. Freq. Control. **41** (1994) 542.
21) D. L. Polla and L. F. Francis: MRS Bull (1996) July, 59.
22) L. E. Cross: Jpn. J. Appl. Phys. **34** (1995) 2525.
23) R. H. Baughman, C. X. Cui, A. A. Zakhidov, Z. Iqbal, J. N. Barisci, G. M. Spinks, G. G. Wallace, A. Mazzoldi, D. De Rossi, A. G. Rinzler, O. Jaschinski, S. Roth and M. Kertesz: Science **284** (1999) 1340.
24) A. E. Glazonov, J. Zhao and Q. M. Zhang: *Fifth Williamsburg Workshop: First-Principles Calculations for Ferroelectrics*, AIP Conf. Proc. **436** (1998) 118.
25) R. Kornbluh, R. Pelrine, J. Joseph, R. Heydt, Q. Pei and S. Chiba: Proc. SPIE **3669** (1999) 149.
26) M. Zhenyi, J. I. Scheinbeim, J. W. Lee and B. A. Newman: J. Polym. Sci. B **32** (1994) 2721.

# APPENDIX 19

# Structural Changes and Transitional Behavior Studied from Both Micro- and Macroscale in the High-Energy Electron-Irradiated Poly(vinylidene fluoride−trifluoroethylene) Copolymer

**Z.-Y. Cheng,* Dana Olson, Haisheng Xu, Feng Xia, J. S. Hundal, and Q. M. Zhang**

*Materials Research Laboratory, The Pennsylvania State University, University Park, Pennsylvania 16802*

**Fred B. Bateman**

*Radiation Interactions and Dosimetry, National Institute of Standards and Technology, Gaithersburg, Maryland 20899*

**G. J. Kavarnos**

*Department of Chemistry, University of Rhode Island, Kingston, Rhode Island 02881*

**T. Ramotowski**

*Naval Undersea Warfare Center, Newport, Rhode Island 02841*

*Received July 13, 2001; Revised Manuscript Received November 2, 2001*

ABSTRACT: The microstructural changes in high-energy electron-irradiated poly(vinylidene fluoride−trifluoroethylene) 68/32 mol % copolymer have been studied by X-ray diffraction, FTIR spectroscopy, and differential scanning calorimetry. The macroscopic polarization response in these materials was investigated by examining the dielectric and polarization behavior in a broad temperature and frequency range. It was found that besides reducing crystallinity in the copolymer film, irradiation produces significant changes in the ferroelectric-to-paraelectric phase transition behavior. The irradiation leads to a reduction in the polar domain size to below a critical size (a few nanometers), resulting in the instability of the macroscopic ferroelectric state and transforming the structure of the crystalline region in the copolymer from a polar all-trans ferroelectric to a nonpolar state represented by a trans−gauche conformation. However, a reentrant polarization hysteresis was observed in the copolymers irradiated with higher doses (>75 Mrad). Therefore, there is an optimized dose that generates a copolymer with a nonpolar structure but relatively high crystallinity whose electromechanical performance is the best. In the copolymers in this optimum dose range, FT-IR data revealed that there is not much change in the molecular conformation with temperature, even as the temperature passes through the dielectric peak, indicating that there is no symmetry breaking in both the macroscale and local level. Although the lattice spacing of the crystalline region along the molecular chain direction discontinuously changes between two special cases, the interchain spacing continuously changes with the irradiation dose, reflecting a strong intrachain coupling between the nonpolar and polar regions. On the other hand, the X-ray data reveal that the crystalline size perpendicular to the polymer chain does not change with irradiation until at doses exceeding 85 Mrad.

## I. Introduction

High-energy irradiation has been practiced widely to modify the properties of polymeric materials.[1,2] The effect of high-energy irradiation on the piezoelectric properties, crystal structures, and polymer morphology of poly(vinylidene fluoride−trifluoroethylene) (P(VDF−TrFE)) copolymers has been investigated quite extensively.[2] For instance, Lovinger observed the polymorphic transformation in P(VDF−TrFE) copolymers under high-energy electron irradiation, where the ferroelectric $\beta$-phase is converted to a paraelectric-like structure.[3] In addition, he found that the dosage required for this transformation increases with the VDF content in the copolymer, which was interpreted as arising from the increased close packing between the polymer chains in the copolymers with increased VDF content. In addition to the polymorphic transformation, irradiation also causes the conversion from the crystalline to amorphous phase due to cross-linking. At very high doses, the copolymer becomes totally amorphous. Macchi et al. also observed the disappearance of the ferroelectric phase in the copolymer due to irradiation and the transformation of the dielectric behavior from a strong first-order ferroelectric−paraelectric (F−P) transition peak to a broad dielectric peak at ambient temperatures much below the original F−P transition temperature in unirradiated copolymers.[4,5] The observed broad dielectric behavior in the irradiated copolymers was suggested to be an indication of a ferroelectric spin glass state.[6]

More recently, we reported that P(VDF−TrFE) copolymers with VDF contents below 70 mol % exhibit a slim polarization hysteresis loop at room temperature, following high-energy electron irradiation. Furthermore, because of the large magnitudes of conformational motions accompanying the interconversion between the all-trans (polar-phase) and trans−gauche (nonpolar phase) states, the electric-field-induced reversible polarization change results in a very high electrostrictive strain (~5%, Figure 1a) and a high strain energy density, as well as a much improved electromechanical efficiency.[7−9]

* Corresponding author. E-mail: zxc7@psu.edu.

10.1021/ma0112265 CCC: $22.00 
Published on Web 12/20/2001

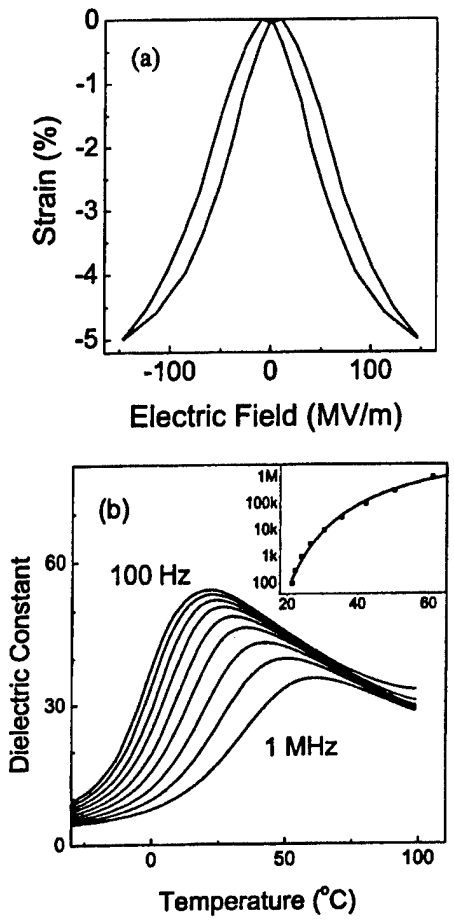


**Figure 1.** (a) Longitudinal strain response vs electric field (1 Hz) observed in electron-irradiated 68/32 copolymer films at room temperature. (b) Temperature dependence of the dielectric constant at frequencies of 100, 300, 1K, 3K, 10K, 30K, 100K, 300K, and 1 MHz for stretched 68/32 film irradiated at 100 °C with 75 Mrad dose. Inset is the measured relationship (square) between the frequency and dielectric constant peak temperature and the fitting results (solid line) using the Vogel−Fulcher relationship.

In addition, in a detailed study of dielectric and polarization behavior, it was shown that the irradiated copolymer exhibits a Vogel−Fulcher type dielectric relaxation as shown in Figure 1b,

$$f = f_0 \exp\left[\frac{-T_0}{T_m(f) - T_f}\right]$$

where $f$ is the measuring frequency, $T_m(f)$ is the corresponding dielectric peak temperature, $T_0$ and $f_0$ are constants, and $T_f$ is often regarded as the freezing temperature of a dipolar system (if the system is a dipolar glass). At temperatures below $T_f$, a ferroelectric state can be induced by a high electric field, while the remanent polarization increases gradually as the temperature is lowered. These features are very similar to those observed in inorganic relaxor ferroelectrics, and hence, the irradiated copolymer can be regarded as a polymeric relaxor ferroelectric, a "polar glass" system.[7,10,11]

In this paper, we will discuss in detail the microstructural changes occurring in this class of materials and the effects of irradiation-induced defects on the polar domains and crystallite sizes. As reported recently, the copolymer with a VDF/TrFE ratio of 68/32 mol % exhibits the best electromechanical performance at room temperature after irradiation.[8,9] Thus, we devote the current paper to a discussion of the macroscopic polarization responses and thermodynamic behavior of this composition in light of our analysis of its polarization, dielectric properties, and DSC data. It must be pointed out that although the macroscopic properties of the irradiated 68/32 copolymer were observed to exhibit similar trends to those of the 50/50 copolymer studied earlier, a detailed study the 68/32 mol % composition was considered desirable to compare the material and microstructural properties of these two compositions and to provide a conceptually improved picture of relaxor behavior in polymers.

With regard to the structural characterization, in an X-ray diffraction study to be described in this paper, a (110, 200) peak was observed at room temperature and at a temperature exceeding the Curie temperature. (Previously in the irradiated 50/50 copolymer this peak was recorded only at room temperature.[13]) These data lead to (1) a clearer picture of the microchanges in crystalline sizes and lattice spacings perpendicular to the chain direction and to (2) an improved understanding of the effects of irradiation-induced defects. More importantly, an X-ray diffraction (001) peak in the present study was analyzed to delineate the irradiation effect on the crystal size along the molecular chain direction and on the molecular conformations. The conformational changes were further confirmed by means of a Fourier transform infrared spectroscopic (FT-IR) study. When the results of the structural analysis are considered along with the macroscopic properties, a more refined picture emerges that describes the nature and role of the irradiation-induced defects.

## II. Experimental Section

P(VDF−TrFE) copolymer at the composition 68/32 mol % was chosen for this investigation. Among all the compositions investigated, this composition exhibits the highest room temperature electrostrictive responses. This is a result of the competition between the strain achievable in the copolymer due to conformational changes, which become large with VDF content, and the electron dose required to convert the copolymer into an electrostrictive material, which also increases with VDF content.[12] Increased electron dose will cause a large reduction in the crystallinity and as well as an increase in cross-linking density. These structural changes are detrimental to the electrostrictive strain.

The copolymer films used in this investigation were fabricated by solution casting and then uniaxially stretched at room temperature to 5 times of the original length. The thickness of films was in the range between 15 and 30 $\mu$m. The films were annealed before irradiation to improve the crystallinity. The irradiation was carried out in a nitrogen atmosphere at 100 °C with an electron energy of 1.2 MeV. It was found that irradiation at a temperature higher than the F−P transition reduces the doses needed to eliminate the room temperature polarization hysteresis and to achieve high electrostrictive strain. This could be due to increased chain mobility in the paraelectric phase, facilitating the polymorphic transformations. The irradiation was carried out in a dose range from 0 to $1.75 \times 10^6$ Gy. To stay consistent with our previous publications, the unit of dose used here is rad and Mrad (1 Mrad = $10^6$ rad and 1 Gy = 100 rad).

The X-ray experiments were performed at the National Synchrotron Light Source beam line X18A of the Brookhaven National Laboratory (the X-ray wavelength was 1.2399 Å). The (200, 110) peak reported here was obtained using the reflection

scan, while the (00*l*) peak was obtained using the transmission scan. The FT-IR spectra at room temperature were obtained using a BIO-RAD WIN Fourier transform IR spectrophotometer in the spectral region 4000–400 $cm^{-1}$. The high-temperature FT-IR spectra were measured using a high-temperature optical cell. The DSC data were taken with a scan rate of 10 or 20 °C/min using (TA Instruments, DSC2920). Gold-sputtered electrodes were used on films used for the characterization of the polarization responses. The dielectric properties as a function of the temperature of the films were measured with a LCR meter (HP 4284A) equipped with a temperature chamber with a scan rate of 2 °C/min. The polarization hysteresis loops were acquired by a computer-controlled automatic system based on the Sawyer–Tower circuit.

## III. Results and Discussion

**3.1. Polarization Responses and Transitional Behavior in Copolymers with Different Doses.** The polarization hysteresis loops measured at room temperature at 1 Hz for the copolymer films treated with different doses are presented in Figure 2a. The maximum induced polarization under 150 MV/m field $P_s$, the remanent polarization $P_r$, and coercive field $E_c$ extracted from the polarization loops are summarized in Figure 2b. The data show a slow and continuous decrease of $P_s$ with irradiation dose, a trend related to the conversion of the normal ferroelectric state into a nonpolar state and the reduction of the crystallinity in the polymer, as has been discussed in an earlier publication.[8] In contrast, a large drop in both $E_c$ and $P_r$ with dose is prominent, especially in the dose range between 35 and 70 Mrads. As a result, the sample irradiated with 75 Mrad exhibits the highest electrostrictive strain yet it displays only minor hysteresis. Interestingly, beyond 75 Mrad, there is an increased polarization hysteresis (reentrant hysteresis). In some of the samples irradiated with 100 Mrad dose, this reentrant hysteresis can be quite large as illustrated in Figure 2c. One possible cause for the observed reentrant hysteresis (ferroelectricity) is the high cross-linking density in the polymer irradiated with high doses.[13–15] Two cross-linking points located in close positions along the chains force a closer packing of the polymer chains in between, favoring the all-trans conformation and formation of small polar pockets. This reentrant behavior is also observed in X-ray data presented below.

The evolution of the dielectric behavior with irradiation dose is shown in Figure 3, which exhibits trends similar to those observed in Figure 2. For instance, the peak temperature associated with the original F–P transition decreases with dose, indicating the weakening of the F–P transition; above 75 Mrad, it moves up slightly. For doses below 35 Mrad, the transition peak is still relatively sharp and exhibits thermal hysteresis. That is, the peak position measured during a heating scan is different from that during a cooling scan, an indication of a first-order transition. For samples irradiated with doses above 35 Mrad, the dielectric peak broadens and thermal hysteresis disappears. As will be shown from the FT-IR data, in samples irradiated with doses near 70 Mrad, the broad dielectric peak actually does not correspond to a phase transition, but the polymer remains in a nonpolar phase even at temperatures far below the dielectric peak, reminiscent of the relaxor ferroelectric behavior in ceramics.

Interestingly, using the dielectric data, we found that the Vogel–Fulcher law can, in fact, be used to fit the change of the dielectric peak temperature with frequency, even for the unirradiated copolymer, which is

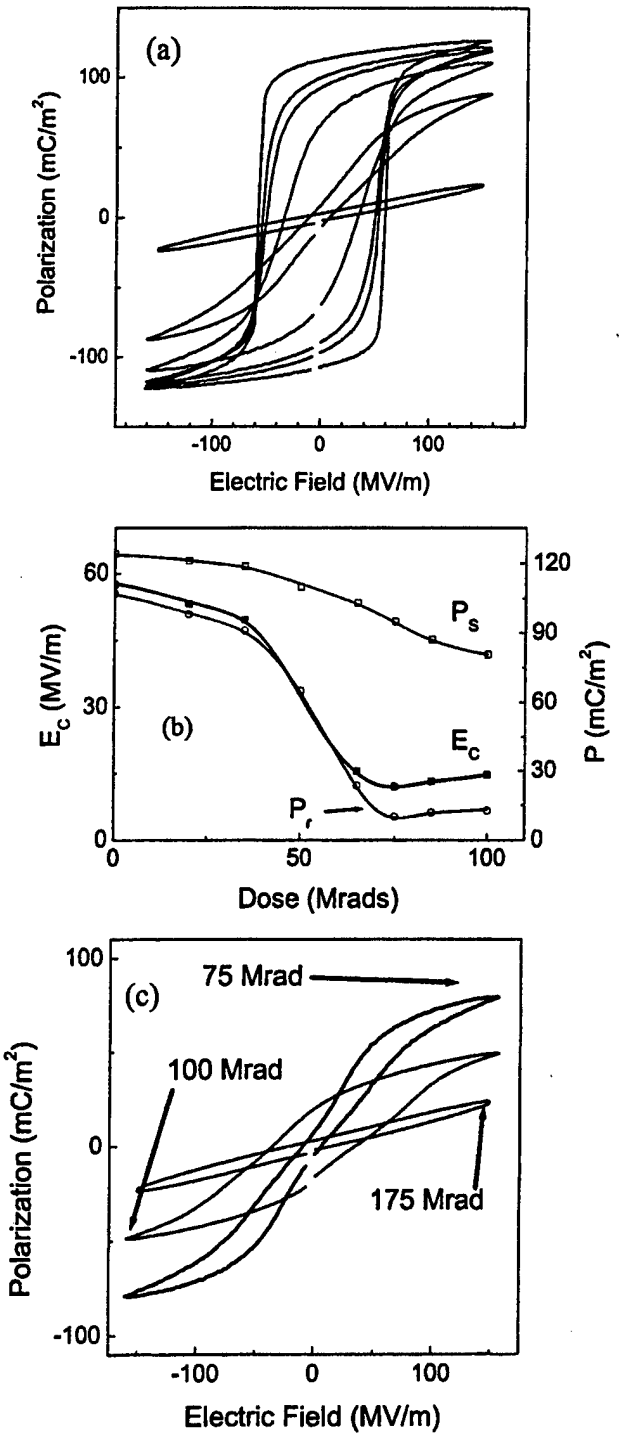


**Figure 2.** (a) Polarization hysteresis loops measured at room temperature and 1 Hz for copolymer films irradiated with different doses. For the polarization level from high to low, the corresponding dose is 0, 20, 35, 50, 75, and 175 Mrad, respectively. (b) Spontaneous polarization $P_s$, permanent polarization $P_r$, and coercive field $E_c$ vs irradiation dose, where $P_s$, $P_r$, and $E_c$ were measured at room temperature and 1 Hz using an electric field with an amplitude of 150 MV/m. (c) Polarization hysteresis loops for films irradiated with 75, 100, and 175 Mrad.

a typical normal ferroelectric. This observation supports an early theoretical result by Tagantsev that the Vogel–Fulcher dielectric behavior can also be observed in a dielectric system with a broad dielectric relaxation distribution that broadens gradually with decreasing

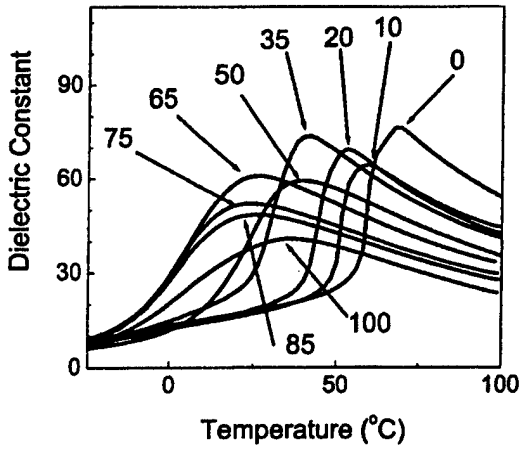


**Figure 3.** Temperature dependence of dielectric constant at 1 kHz measured during cooling of irradiated copolymers. The irradiation doses in Mrad are indicated in the figure.

temperature.[16] The gradual freezing of a dipolar system with temperature is not a necessary condition for the presence of Vogel–Fulcher dielectric behavior.

DSC data for the irradiated copolymers are summarized in Figure 4 (acquired during heating of the samples). The data show that in general both the peak temperature and the enthalpy of the melt decrease with dose, due to the decrease in crystallinity and reduced crystalline ordering in the polymer, except for the samples irradiated at 10 Mrad. The melt enthalpy of the copolymer irradiated with the 10 Mrad dose is actually higher than that without irradiation, implying an increase in the crystallinity. Such an increase in crystallinity with irradiation had been observed earlier and is probably caused by chain scission in the copolymer allowing for an increase in the chain mobility and hence the crystallinity.[17] At higher doses, the cross-linking becomes dominant with a reduction in crystallinity.[13–15]

The peak associated with the original F–P transition of the unirradiated sample changes with dose quite remarkably, which is in sharp contrast with the behavior of the melt transition. For samples irradiated with doses above 50 Mrad, the F–P transition peak almost disappears, and the temperature of the very weak F–P transition changes only to a minor extent with dose (Figure 4b,c). In addition, the peak temperature from DSC data (~45 °C) for the copolymers irradiated in this dose range is higher than the temperature of the broad dielectric maximum (~20 °C), suggesting that the two are associated with different phenomena. It is likely that the weak DSC peak observed here originates from the small residual polar regions in the copolymer, while the dielectric maximum results from the collective dipole responses and thus involves relatively long-range dipolar motions.

**3.2. Structure Changes on the Micro- and Mesoscales. 3.2.1. Evolution of Crystal with Dose As Revealed by Room Temperature X-ray Data.** X-ray data were obtained for copolymers irradiated with different doses, including diffraction peaks perpendicular and parallel to the polymer chains, to follow structural changes in both directions. The data from the (110, 200) diffraction peak, which are due to changes in polymer interchain spacing and ordering perpendicular to the chains in the crystalline regions, are presented in Figure 5. The corresponding data for the (00*l*)

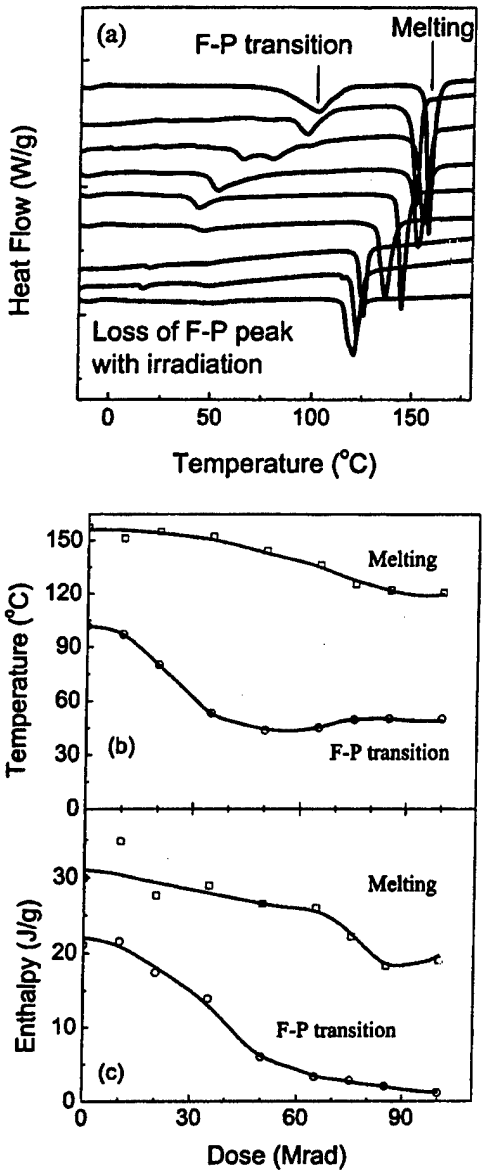


**Figure 4.** (a) DSC data collected by heating irradiated copolymer from −40 to 200 °C. From top curve to bottom curve, the corresponding doses are 0, 10, 20, 35, 50, 65, 75, 85, and 100 Mrad, respectively. (b) Melt temperature and F–P transition temperature. (c) Melting enthalpy and phase transition enthalpy for copolymer irradiated with different doses.

diffraction peak, which arise from the dimensional changes of unit cell along the polymer chain, are presented in Figure 6. Both data sets were acquired at room temperature.

The crystalline phase of P(VDF–TrFE) copolymers has an orthorhombic unit cell in which the *c*-axis is parallel to the polymer chain.[18] Because the ratio of the lattice constants of the unit cell along the "*a*" and "*b*" axes (perpendicular to the chains) is close to $\sqrt{3}$, the lattice has a quasi-hexagonal structure, resulting in the overlap of the (110) and (200) reflections.

We first discuss the X-ray data from the (00*l*) reflection. Clearly, there are two peaks at $2\theta = 28.29°$ and $2\theta = 31.53°$. The peak at $2\theta = 28.29°$ (corresponding to a lattice space of 0.2537 nm) originates from the (001) reflection in the ferroelectric (F) phase, while the peak at $2\theta = 31.53°$ (corresponding to a lattice space of 0.4564

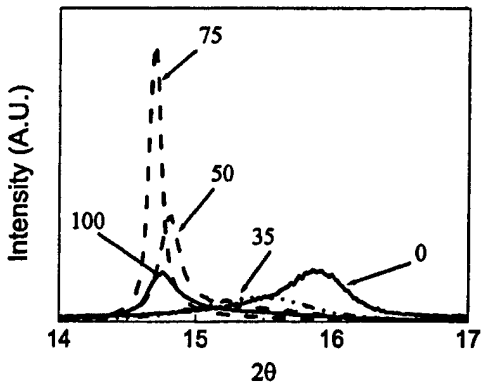


**Figure 5.** The (200, 110) diffraction peak observed at room temperature using the reflection scan for copolymer films irradiated with different dose. The number in the figure expresses the dose in Mrad.

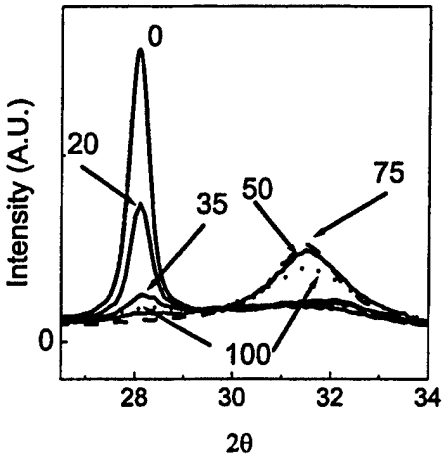


**Figure 6.** The (001) diffraction peak observed at room temperature using the transmission scan for copolymer films irradiated with 0, 20, 35, 75, and 100 Mrad.

nm) originates from the (002) reflection in the nonpolar (NP) phase, i.e., the paraelectric α-phase or δ-phase.[18,29] The data from the (00*l*) reflection (Figure 6) demonstrate quite clearly that the polymorphic transformation caused by irradiation is a first-order process between the F and NP phases. That is, the intensity of the (001) peak in the F phase decreases while the intensity of the (002) peak in NP phase increases with dose. There are two features that should be noted here: (i) Although there is a large variation in the peak intensity for the F and NP phases as the dose changes, the peak position remains nearly the same for all the doses. (ii) The evolution of the F phase peak with dose also displays a reentrant behavior. Initially, as the dose increases, the peak intensity decreases until a dose of 75 Mrad is reached, at which point the sample shows very little sign of the presence of a F phase peak. Beyond 75 Mrad, there is a gradual increase in the peak intensity for the F phase. This reentrant behavior is consistent with observations from polarization loops and dielectric data for the same doses.

By employing the Scherrer equation, the size of the coherent X-ray reflection region $D_{hkl}$ can be estimated,[19]

$$D_{hkl} = \frac{0.9\lambda}{B\cos(\theta)}$$

where $\lambda$ is the X-ray wavelength, $B$ is the full width at

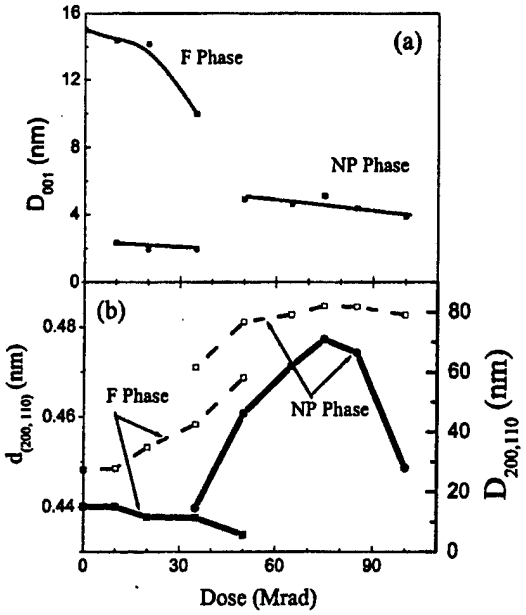


**Figure 7.** (a) Irradiation dose dependence of crystallite size $D_{001}$ parallel to the molecular chain at room temperature. (b) Dose dependence of crystalline size $D_{200,110}$ (solid line) and interchain spacing $d_{(200\,110)}$ (dotted line) measured at room temperature. The data indicate a lattice expansion perpendicular to the chain and contraction along the chain, respectively, in the dose range from 0 to 50 Mrad.

half-maximum (fwhm) of the reflection peak (*hkl*), and $\theta$ is the peak position. In the F phase, the coherent X-ray reflection region is determined by the polarization domain size; in the NP phase, it corresponds to the crystallite size. In Figure 7a, we plot $D_{001}$ for the F phase and NP phase measured for samples treated with different doses. Before irradiation, the polar domain size of the F phase along the *c*-axis is about 15 nm. This value decreases with dose, due to the defects introduced by the irradiation, which break up the polarization coherence. In samples irradiated with a dose of 35 Mrad, $D_{001}$ for the F phase is reduced to 10 nm; for samples treated with doses beyond that, the peak intensity of the F phase drops precipitously. The NP phase peak is visible even in samples irradiated with very low doses, a result that can be attributed to the domain boundary region and can account for its broad appearance. In samples treated with doses higher than 50 Mrad, the NP phase peak dominates; the coherent crystallite size along the polymer chain for this phase is about 5 nm, which is much smaller than that in the F phase.

In contrast, the X-ray data from the (110, 200) reflection, which results from changes of the lattice parameters with doses perpendicular to the polymer chains, show a markedly different evolution behavior. First, the data do not display a clearly defined two-peak pattern. Furthermore, the X-ray peak position changes continuously with the irradiation dose. For instance, from 0 to 35 Mrad, the peak at the original F phase moves to a lower angle, indicating a continuous expansion in the interchain dimension as shown in Figure 7b. Concomitantly, there is a reduction of the ferroelectric domain size from 15 to 7.5 nm. The expansion in the interchain dimension and the reduction of the ferroelectric domain size with the dose in this range indicate that the surface of ferroelectric domain changes to a NP phase. At 35 Mrad, the existence of the NP phase can be observed in the X-ray data as shown in Figures 5

and 7b. As the dose increases from 35 to 50 Mrad, the peak position moves to that of the NP phase, indicating that the crystal now is predominantly nonpolar. Consistent with this shift in the peak position, the (110, 200) peak width also shows a large reduction, because of the disappearance of the ferroelectric domains. In any case, at 50 Mrad, there are still some ferroelectric domains with very small sizes as shown in Figure 7b. For doses beyond 50 Mrad, there is only a negligible variation in the peak position. Meanwhile, in the same dose range, the peak width of the (110, 200) reflection decreases continuously until near 75 Mrad, where $D_{110,200}$ reaches 70 nm, which is close to the crystallite size measured in the paraelectric phase, as will be shown in the next section. Increasing the dose to 100 Mrad causes a further reduction of $D_{110,200}$ to about 26 nm, caused by the reduction of the crystallite size due to increased cross-linking density.

The results show unequivocably that the ferroelectric domain size in unirradiated samples is nearly isotropic (~15 nm). In P(VDF–TrFE) copolymers, the lattice symmetry dictates the polarization direction between neighboring domains in angles of 60°, 120°, and 180°.[20] For a ferroelectric material in equilibrium, the domain size is determined by the domain wall energy, coupling between domain walls, and crystallite size.[21,22] In the polymers investigated here, because of the high nucleation barriers and the high defect concentrations, we believe that the domain size is controlled mainly by defects in the crystallites and the crystallite–amorphous boundary conditions, which can also be regarded as defects. Therefore, with increased doses, the concentration of defects (such as chain ends and pendant groups generated by chain scission) in the crystallites also increases, resulting in the observed reduction of the polarization domain size. Eventually, as the domain size is reduced to a value below a certain critical size, the macroscopic polarization state becomes unstable with respect to the nonpolar phase, leading to the disappearance of the macroscopic polarization. From the data here, it is not clear that the domain size, whether along or perpendicular to the polymer chain, or both, determines this critical size. From the strong intrachain coupling as well as the recent experimental results on the presence of a two-dimensional ferroelectric state in P(VDF–TrFE) films of a few molecular layers thick,[23] it seems reasonable to assume that the polar domain size along the polymer chain may play a more important role.

**3.2.2. Temperature Dependence of X-ray Data for Copolymers with Different Doses.** Presented in Figure 8 are typical X-ray data taken from the (110, 200) reflections as a function of temperature for copolymers irradiated with different doses (0, 35, 50, and 75 Mrad). The data from samples irradiated with a 0–35 Mrad dose show a first-order F–P transition with temperature (two-phase coexistence region). In the nonpolar phase, the X-ray peak width, which becomes quite narrow, is determined by the coherent X-ray scattering region or approximately by the crystallite size along the ⟨110, 200⟩ direction. It is interesting to note that the peak width of the paraelectric phase (nonpolar phase) is nearly the same as that measured at room temperature in copolymers irradiated with 65–85 Mrad doses. This is consistent with the fact that the NP phase is dominant in polymers in that dose range. In samples

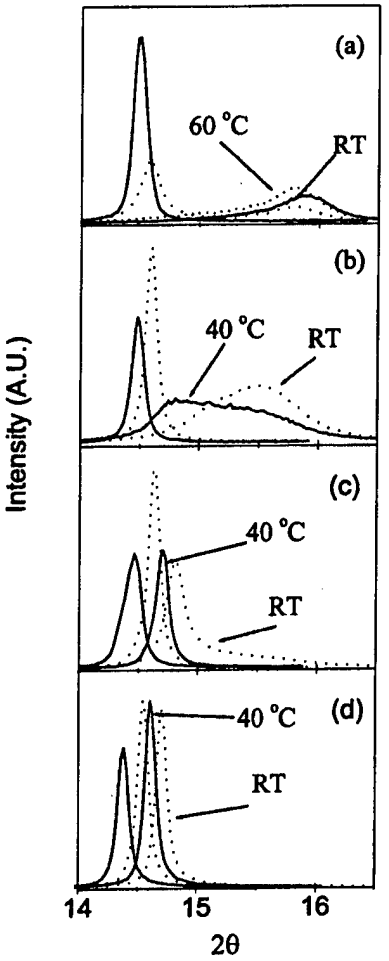


**Figure 8.** The (200, 110) diffraction peak observed at different temperatures using the reflection scan for unirradiated film (a) (solid line, 110 °C; dotted line, 90 °C; 60 °C and RT data are indicated) and irradiated films with different doses (solid line, 90 °C; dotted line, 60 °C; RT and 40 °C data are indicated in the figure): (b) 35 Mrad dose, (c) 50 Mrad dose, and (d) 75 Mrad dose. "RT" is room temperature.

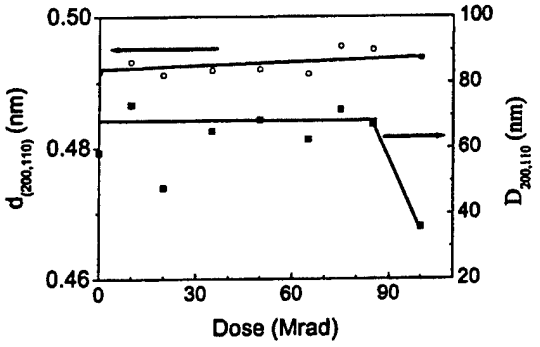


**Figure 9.** Dose dependence of crystalline size $D_{200,110}$ and interchain spacing $d_{(200,110)}$ measured at high temperature (nonpolar phase).

irradiated at 50 Mrad or higher doses, a transition is not observed, and the lattice constant exhibits a typical thermal expansion curve of the nonpolar phase.

The data also show that the crystallite size perpendicular to the polymer chain is not affected by the irradiation until above 85 Mrad (Figure 9). On the other hand, the crystallite size parallel to the chain is reduced by the irradiation even at doses far below. For example,

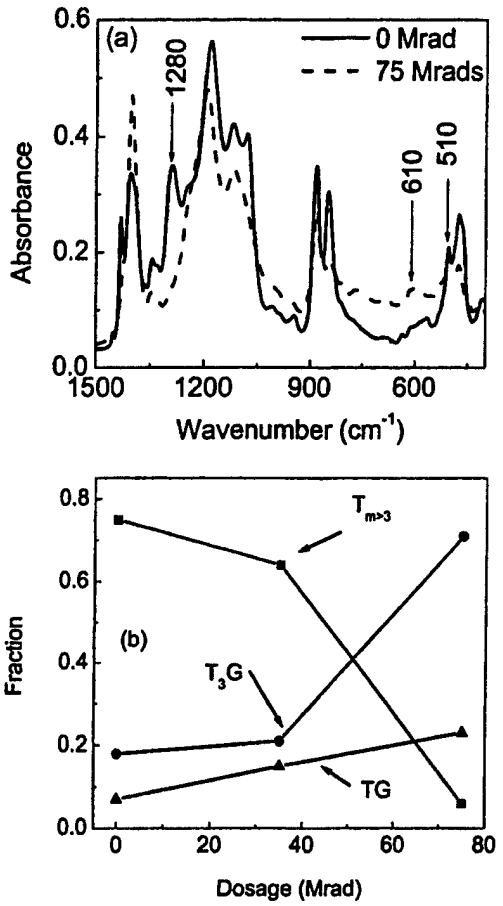


**Figure 10.** FTIR data of P(VDF–TrFE) 68/32 copolymer film at room temperature. (a) Spectrum for stretched film before irradiation and stretched film irradiated at 100 °C with 75 Mrad using 1.2 MeV electrons. (b) Fraction of different conformations in film vs irradiation dose.

above 75 Mrad and at room temperature, the copolymer is in the nonpolar phase; therefore, the X-ray peak width should be that defined by the crystallite size. This is exemplified in Figure 7 where $D_{001}$, which is the crystallite size along the ⟨001⟩ direction, is about 5 nm. This is much smaller than that of the ferroelectric domain size in the copolymer before irradiation.

**3.2.3. Conformational Changes with Dose and Temperature.** The FT-IR spectra obtained on copolymers irradiated at different doses measured at room temperature are shown in Figure 10a (dose = 0, 35, and 75 Mrad). To quantify the conformational change with dose, we focus on three absorbance peaks at 1288 $cm^{-1}$ for the long trans sequence ($T_{m>3}$), 614 $cm^{-1}$ for the trans–gauche (TG), and 510 $cm^{-1}$ for the $T_3G$ conformations, which are due to the vibration of the $CF_2$ group.[24] Before irradiation, the spectrum is characterized by a strong absorbance peak at 1288 $cm^{-1}$, which diminishes with irradiation dose. In Figure 10b, we present a summary of the change of the three conformations with dose, extracted from the data in Figure 10a. In the extraction process, each absorbance peak was fitted to a Lorentzian shape. To account for possible variations in the sample thickness and therefore the absorbance, an internal standard (at 3022 $cm^{-1}$, which is the asymmetric stretching vibration of C–H bond) was used to calibrate those absorbance peaks of interest.[25] The fraction of each conformation can be calculated (data in Figure 10b) following the method of Osaki et al.,[26]

$$F_i = \frac{A_i}{A_{\mathrm{I}} + A_{\mathrm{II}} + A_{\mathrm{III}}}$$

where $i$ = I, II, III, and $A_{\mathrm{I}}$, $A_{\mathrm{II}}$, and $A_{\mathrm{III}}$ are the absorbances of crystal forms I, II, and III, i.e., with all-trans ($T_{m>3}$), $T_3GT_3G'$, and TGTG′ sequences, respectively. $F_i$ is the fraction of chain conformation $i$. Prior to irradiation, the conformation of the samples is predominantly all-trans because of the ferroelectric nature of the material. The absorption bands are due to small concentrations of TG and $T_3G$ conformations in the domain boundary regions and as well as in the interphase regions between the crystallite and amorphous phases, as has been observed in the X-ray data. The trends in the conformational changes with dose are very similar to those observed in the X-ray data. All three conformations exhibit slow changes with doses below 35 Mrad, but at higher doses, large changes occur. For example, at 75 Mrad, the all-trans conformation disappears and is replaced by $T_3G$ conformations randomly mixed with TG conformations, consistent with the X-ray results that demonstrate that the crystallite is in the NP phase.

Prior to irradiation, there is a large and relatively sharp change in the chain conformation in P(VDF–TrFE) copolymer due to the phase transition from a nonpolar phase to a polar phase as the temperature is lowered through the F–P transition. However, for relaxor ferroelectrics, extensive investigations such as Raman scattering experiments carried out on inorganic materials have shown that there is a gradual increase of the population of micropolar regions as the temperature is reduced.[27] In other words, there is a local symmetry breaking from the nonpolar to polar ordering even though macroscopically the sample remains nonpolar.[28] Now the question is whether a similar explanation applies to the irradiated copolymer. To examine this question, we consider the data showing the conformational changes as the temperature is varied for the three samples under different dose treatments (Figure 11). In the unirradiated samples, the absorbance peak intensity remains nearly constant at temperatures below 70 °C. The data point at 100 °C suggests a transition to the nonpolar phase, as indicated by the drop of the peak intensity due to the all-trans conformation and the increase in peak intensities attributed to the $T_3G$ and TG conformations.[29] In samples irradiated with a 35 Mrad dose at 100 °C, the chain conformation is mainly $T_3G$, and there is very little indication of the all-trans conformation (the polar conformation). As the temperature is reduced, the all-trans conformation increases nearly linearly until 30 °C. This can be compared with the dielectric data where a weakly first-order transition was observed to begin at about 30 °C.

In contrast, in the sample irradiated with 75 Mrad at temperatures above 30 °C, there is no suggestion of the all-trans conformation, although a small increase of the all-trans chain conformation is seen at lower temperatures, coinciding with the Vogel–Fulcher temperature, $T_f$. This behavior contrasts sharply with that observed in samples not exposed to irradiation as well as samples irradiated with 35 Mrad, demonstrating that the broad dielectric peak does not correspond to a broad phase transition between a polar and nonpolar phase.

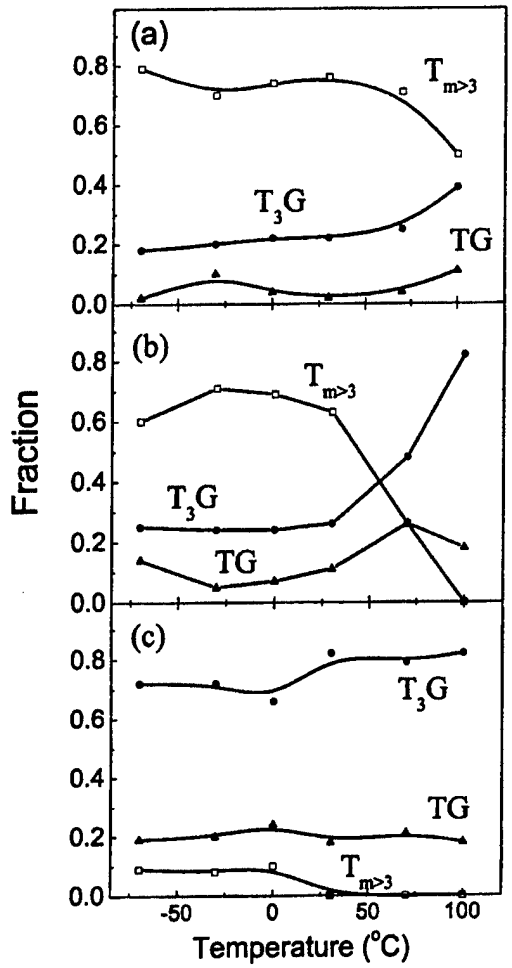


**Figure 11.** Temperature dependence of fractions of different conformations in stretched 68/32 copolymer films: (a) unirradiated, (b) irradiated with 35 Mrad dose, (c) irradiated with 75 Mrad dose.

Furthermore, the absence of the all-trans conformation and only minor changes in chain conformations at temperatures above the broad dielectric peak are indicative of behavior that differs from that observed in relaxor ferroelectrics in inorganic relaxor ferroelectrics, in which there is a large increase in the population of local polar regions with reduced temperature, even at temperatures far above the broad dielectric constant peak.[28]

## IV. Summary

High-energy electron irradiation was carried out at 100 °C on previously solution cast and subsequently stretched P(VDF–TrFE) 68/32 mol % copolymer films, with doses from 0 to 175 Mrad using 1.2 MeV electrons. The polarization behavior of the irradiated copolymer indicates that there is an optimized dose (i.e., 75 Mrad) required to generate a slim P–E loop with relatively high polarization levels at room temperature, which describes a copolymer exhibiting the best electromechanical performance. The structural causes of this phenomenon were explored by means of X-ray diffraction, FT-IR, and DSC measurements. It was found that irradiation lowers the ferroelectric-to-paraelectric phase transition temperature and leads to the disappearance of this transition. More importantly, the irradiation transforms the structure of the crystalline regions from polar, characterized by an all-trans configuration in the molecular chains, to a nonpolar state, represented by the trans–gauche conformations in the molecular chains. However, in copolymers irradiated with higher doses (exceeding 75 Mrad), a reentrant polarization hysteresis is observed in the material, and at very high doses (~150 Mrad), the copolymer is completely transformed into an amorphous phase, as characterized by a linear dielectric response.

The X-ray data indicate that as the dose increases, there is a gradual increase of the interchain spacing with doses from 0 to 50 Mrad, and on the other hand, the lattice constant along the chain exhibits a first-order transition process with dose (a discontinuous change between two phases), a reflection of strong intrachain coupling between the polar and nonpolar regions, and weak interchain coupling between them. Concomitant with this process, the ferroelectric domain size decreases with dose, and as the polar domain size is reduced to below a critical size (a few nanometers), the ferroelectric state becomes unstable and the crystalline region transforms into a nonpolar state (at doses above 50 Mrad). For the irradiated copolymers exhibiting slim polarization loops at room temperature (dose > 50 Mrad), the FT-IR data reveal that there is no significant change in the polymer chain conformations as the temperature passes through the dielectric maximum, consistent with the DSC data showing the disappearance of the regular F–P transition. Interestingly, the Vogel–Fulcher relationship was observed for the dielectric data even for the copolymers without much irradiation, indicating that Vogel–Fulcher dielectric behavior is not necessarily associated with the gradual freezing of a polar system.

**Acknowledgment.** This work was supported by DARPA and ONR.

## References and Notes

(1) Charlesby, A. *Radiat. Phys. Chem.* **1991**, *37*, 5.
(2) Lovinger, A. In *Radiation Effects on Polymers*; Clough, R. L., Shalaby, S. W., Eds.; ACS Symposium Series 475; American Chemical Society: Washington, DC, 1991; Chapter 6.
(3) Lovinger, A. *Macromolecules* **1985**, *18*, 910.
(4) Daudin, B.; Dubus, M.; Legrand, J. F. *J. Appl. Phys.* **1987**, *62*, 994.
(5) Macchi, F.; Daudin, B.; Legrand, J. F. *Ferroelectrics* **1990**, *109*, 303.
(6) Odajima, A.; Takase, Y.; Ishibashi, T.; Yuasa, K. *Jpn. J. Appl. Phys.* **1985**, *24*, 881.
(7) Zhang, Q. M.; Bharti, V.; Zhao, X. *Science* **1998**, *280*, 2101.
(8) Cheng, Z.-Y.; Bharti, V.; Xu, T. B.; Xu, H. S.; Mai, T.; Zhang, Q. M. *Sens. Actuators, A* **2001**, *90*, 138.
(9) Bharti, V.; Xu, T.-B.; Cheng, Z.-Y.; Mai, T.; Zhang, Q. M.; Ramotowski, T.; Wright, K. A. *Jpn. J. Appl. Phys.* **2001**, *40*, 672.
(10) Zhang, Q. M.; Cheng, Z.-Y.; Bharti, V. *Appl. Phys. A: Mater. Sci. Process.* **2000**, *70*, 307.
(11) Bharti, V.; Zhang, Q. M. *Phys. Rev. B* **2001**, *63*, 184103.
(12) Zhang, Q. M.; Scheinbeim, J. Electric Polymers. In *Electroactive Polymer Actuators as Artificial Muscles*; Bar-Cohen, Y., Ed.; SPIE Optical Engineering Press: Bellingham, WA, 2001; Chapter 4.
(13) Bharti, V.; Xu, H. S.; Shanthi, G.; Zhang, Q. M.; Liang, K. *J. Appl. Phys.* **2000**, *87*, 452.
(14) Forsythe, J. S.; Hill, D. J. T. *Prog. Polym. Sci.* **2000**, *25*, 101.
(15) Lyons, B. J. *Radiant. Phys. Chem.* **1995**, *45*, 159.
(16) Tagantsev, A. K. *Phys. Rev. Lett.* **1994**, *72*, 1100.

(17) Pae, K. D.; Bhateja, S. K.; Gilbert, J. R. *J. Polym. Sci., Polym. Phys.* **1987**, *25*, 717.
(18) Hasegawa, R.; Takahashi, Y.; Chatani, Y.; Tadokoro, H. *Polym. J.* **1972**, *3*, 600. Toshiro, K. In *Ferroelectric Polymers*; Nalwa, H. S., Ed.; Marcel Dekker: New York, 1995; Chapter 2.
(19) Warren, B. E. *X-ray Diffraction*; Dover Publications: New York, 1990.
(20) Kepler, R. G.; Anderson, R. A. *J. Appl. Phys.* **1978**, *49*, 1232. Naegele, D.; Yoon, D. Y. *Appl. Phys. Lett.* **1978**, *33*, 132. Tashiro, K.; Kobayashi, M. *Polymer* **1986**, *27*, 667.
(21) Arlt, G. *J. Mater. Sci.* **1990**, *25*, 2655.
(22) Lines, M. E.; Glass, A. M. *Principles and Applications of Ferroelectrics and Related Materials*; Clarendon Press: Oxford, 1977.
(23) Bune, A. V.; Fridkin, V. M.; Ducharms, S.; Blinov, L. M.; Palto, S. P.; Sorokin, A. V.; Yudin, S. G.; Zlatkin, A. *Nature* **1998**, *391*, 874.
(24) Reynolds, N. M.; Kim, K. J.; Chang, C.; Hsu, S. *Macromolecules* **1989**, *22*, 1092.
(25) Kobayashi, K.; Tashiro, K.; Tadokoro, H. *Macromolecules* **1975**, *8*, 158.
(26) Osaki, S.; Ishida, Y. *J. Polym. Sci., Polym. Phys.* **1975**, *13*, 1071.
(27) Burns, G.; Dacol, F. H. *Ferroelectrics* **1990**, *104*, 25.
(28) Cross, L. E. *Ferroelectrics* **1987**, *76*, 241.
(29) Tashiro, K.; Kobayashi, M. *Phase Transitions* **1989**, *18*, 213.

MA0112265

# APPENDIX 20

# High-performance micromachined unimorph actuators based on electrostrictive poly(vinylidene fluoride–trifluoroethylene) copolymer

T.-B. Xu, Z.-Y. Cheng, and Q. M. Zhang[a)]
*Materials Research Institute and Electrical Engineering Department, The Pennsylvania State University, University Park, Pennsylvania 16802*

(Received 17 September 2001; accepted for publication 30 November 2001)

We report on the performance of micromachined unimorph actuators [(polymer micromachined actuator PMAT)] based on the electrostrictive poly(vinylidene fluoride–trifluoroethylene) [P(VDF–TrFE)] copolymer. Because of the high electrostrictive strain and high elastic energy density ($\sim 1$ J/cm$^3$) of the active polymer [the electrostrictive P(VDF–TrFE)], the PMAT exhibits a very high stroke level with high load capability and high displacement voltage ratio. In addition, the experimental data also demonstrate that the PMAT is capable of operating over a broad frequency range ($>100$ kHz). The PMAT performance was modeled and the agreement between the modeling results and experimental data confirms that the response of the PMAT indeed follows the design parameters. © *2002 American Institute of Physics.* [DOI: 10.1063/1.1448661]

Microelectromechanical systems (MEMS) have shown great potential and impact on a broad range of modern technologies such as biotechnology, optical communications, automobiles, and many other domestic and military applications.[1–3] Microactuators are a key component in MEMS. However, in spite of more than a decade of efforts, it is still a challenge to realize microactuators capable of operating over a broad frequency range with high force level and large displacement output.[4–7] The fundamental reason behind this is the lack in the present active material or actuation mechanism which possesses high elastic energy density with high strain capability over a broad frequency range. Recently, we reported that in modified poly(vinylidene fluoride–trifluoroethylene) [P(VDF–TrFE)] polymers, a massive electrostriction with high elastic energy density can be achieved.[8,9] Especially in uniaxially stretched polymer samples, an electrostrictive strain larger than 3.5% with high load capability ($\sim 40$ MPa) along the film stretching direction has been demonstrated, which makes the polymer attractive for microactuators.[9] It is the purpose of this letter to investigate the microactuator device performance of new class of active polymer [polymer microactuator (PMAT)].

The PMAT configuration adopted for this investigation is shown schematically in Fig. 1. The active polymer, which is a film ($\sim 10$ $\mu$m thickness) of uniaxially stretched and high energy electron irradiated P(VDF–TrFE) copolymer, is bonded to an inactive polymer film using Spurr epoxy to form a unimorph actuator. In the current design, the inactive polymer is of the same material as the active polymer except there are no electrodes on the film. The active polymers were characterized for their electromechanical response. Under a field of 100 MV/m, a transverse strain ($S_1$) of 3% was observed along the uniaxial stretching direction and the transverse strain perpendicular to the stretching direction ($S_2$) was about 1/3 of $S_1$ and negative. The elastic modulus along the uniaxial stretching direction is 1 GPa and is about three times larger than that in the perpendicular direction. In the current PMAT, the actuation is generated by the strain along the stretching direction (the $x$ direction in Fig. 1) and the unimorph actuator is bonded to the silicon wafer with Spurr epoxy at the two ends ($x=\pm L_0/2$). Under an electric field, the expansion of the active polymer generates an upward motion of the PMAT (the $z$ direction in Fig. 1). The two ends of the PMAT along the $y$ direction are mechanically free to maximize the actuation. Sputtered Au electrodes are used and a 0.5 mm unelectroded margin is provided to prevent

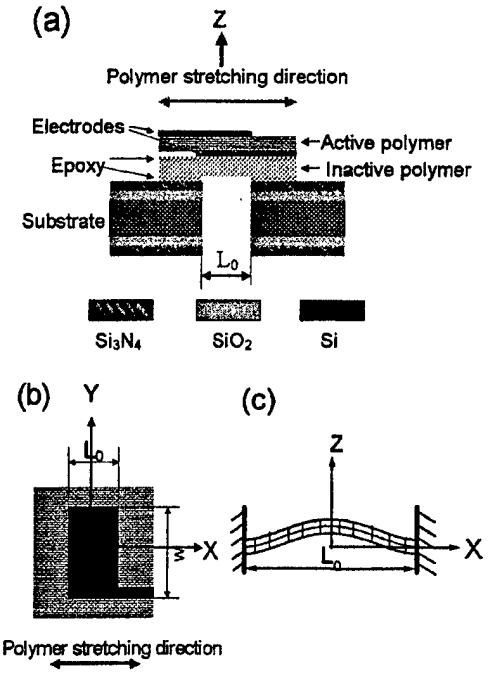


FIG. 1. (a) Schematic of the PMAT investigated. (b) The electrode pattern of the PMAT active polymer (black area) where the electrode width along the $x$ direction is the same as the device actuation length $L_0$ in the same direction and along the $y$ direction, the unelectroded margin width is 0.5 mm to prevent the breakdown at the edges. (c) Schematic of the actuation response of the current PMAT under external fields: because of $S_1>0$, the actuator moves upward from the neutral position ($z=0$).

a)Electronic mail: qxz1@psu.edu

 

electric breakdown [Fig. 1(b)]. It is expected that this unelectroded margin along the $y$ direction will cause some reduction of the actuator strain $S_1$ of the active polymer.

Two groups of actuators were fabricated with different lengths of $L_0$ (the actuation length along the $x$-direction): $L_0=1$ mm (PMAT1) and $L_0=0.5$ mm (PMAT0.5). The width $w$ (along the $y$ direction, Fig. 1) of PMAT1 is 4.5 mm and for PMAT0.5, $w=3$ mm. The inactive polymer film thickness $t_n$ for the PMAT1 group is about the same as that ($t_a$) of the active film and for PMAT0.5, $t_n$ is about half of $t_a$. The actuator pattern on the silicon wafer was fabricated using the standard bulk silicon micromachining technique (KOH anisotropic wetetching) as described in Refs. 10–12. The displacement response was measured by a laser vibrometer (Polytec PI, Inc., model OFV-511) which has a beam size of 5 $\mu$m and upper measuring frequency of 100 kHz. An HP 4192 impedance analyzer was used for electric impedance characterization. To provide high dc bias voltages in the impedance measurement, a special blocking circuit was designed.

For the PMAT investigated here, the actuation displacement along the $z$ direction as a function of the coordinate $x$ can be expressed as[13]

$$z=a\left[\left(\frac{L_0}{2}\right)^2-x^2\right]^2, \tag{1}$$

where the two ends of the actuator are fixed at $x=\pm L_0/2$, as shown in Fig. 1(c). The constant $a$ in the equation is determined by effective strain $S_e$ of the polymer films in the $x$ direction, i.e.,

$$\int_{-L_0/2}^{L_0/2}\left[\left(\frac{dz}{dx}\right)^2+1\right]^{1/2}dx=(1+S_e)L_0, \tag{2}$$

which is based on the geometric constraint that the total length of the actuator after the actuation should be equal to the polymer film length after strain $S_e$. Because of the inactive polymer layer, $S_e$ is different from strain $S_1$ of the active polymer measured in the free condition. From the force balance condition in the $x$ direction, $S_e$ is related to $S_1$ as

$$E_a t_a(S_1-S_e)=E_n t_n S_n, \tag{3}$$

which leads to $S_e=S_1/(1+k)$, where $k=(E_n t_n)/(E_a t_a)$ is a measure of the clamping effect due to the inactive layer (clamping ratio). To include the contribution from the metal electrodes and Spurr epoxy bonding layer, $k$ should be modified to $k=(\Sigma E_{ni}t_{ni})/(E_a t_a)$, where $E_{ni}$ and $t_{ni}$ are the elastic modulus and thickness of $i$th inactive layer, respectively. It should be noted that in the derivation, we omitted the mechanical clamping effect at the two fixed ends ($x=\pm L_0/2$), which will reduce $S_1$ even if $k=0$. All of the analysis is based on the assumption that $L_0 \gg t$, where $t$ is the total thickness of the actuator.

To evaluate the performance of the PMAT, we first present in Fig. 2(a) the displacement profiles measured on PMAT1 and PMAT0.5 as a function of $x$ and along the line of $y=0$ [see Fig. 1(b)]. The solid lines are the fitting from Eq. (1), which match the experimental results (dots) quite well, indicating that the unimorphs function properly. In addition, the displacement profile as a function of $y$ along the $x=0$ line for the PMAT1 was also characterized and the results are shown in Fig. 2(b). The electrode width along the $y$ direction is $w=4.5$ mm for PAMT1 and the width at 90% of the actuation level is about 3.5 mm, indicating the clamping effect due to the unelectroded margins.

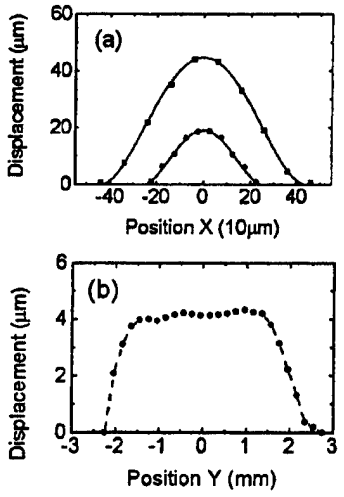


FIG. 2. (a) Displacement profile for PMAT1 (measured at 100 Hz under 100 MV/m field) and PMAT0.5 (measured at 50 Hz under 65 MV/m field) along the $x$ direction where the dots are measured data and solid curves are fitting from Eq. (1). (b) Displacement profile for PMAT1 along the $y$ direction [measured under 52 MV/m dc bias field and 100 V (rms value) ac field at 100 Hz].

The displacement versus applied electric field was measured for PMA1 and the result is presented in Fig. 3(a). The results derived from the Eqs. (1)–(3) based on $S_1$ acquired from an active film in free condition are also presented in Fig. 3(a) for comparison. The experimental data points follow the curve with clamping ratio $k=3$ very well, which seems to be reasonable considering the fact that besides the inactive layer ($k=1$), there are Spurr epoxy layers (the elastic modulus $G=5$ GPa and thickness$\sim 1$ $\mu$m), Au electrodes (200 nm total thickness and elastic modulus $\sim 100$ GPa),

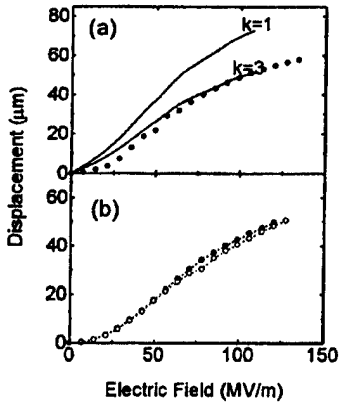


FIG. 3. (a) Displacement at the center of PMAT1 as a function of the applied electric ac field (10 Hz) where dots are the experiment data and solid curves are the calculation based on the Eqs. (1)–(3) and the data on $S_1$ measured at the free condition of the active polymer at 10 Hz. In the figure, the calculated curves with the clamping ratios of $k=1$ and $k=3$ are shown. The model curve is in good accord with the experimental data. (b) Comparison of the displacement at the center of a PMAT measured in air (solid dots) and in silicon oil (open circles) as a function of applied electric field amplitude (100 Hz). There is very little reduction of the displacement due to the fluid loading.

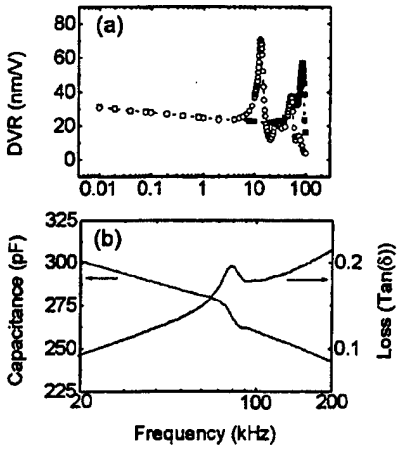


FIG. 4. (a) Displacement voltage ratio (DVR) of a dc field biased (55 MV/m) PMAT1 as a function of ac field frequency (the ac field is 0.64 MV/m). The measurement was carried out both in air (solid dots) and in silicon oil (open circles). Due to the fluid loading, the resonance frequency is shifted to lower frequency. In the data taken from silicon oil, higher harmonics were also observed. (b) Electric impedance data of the same PMAT1 measured in air under the same applied dc and ac electric field. Strong electromechanical resonance was observed.

unelectroded margins, as well as the clamping effect from the two fixed ends. The maximum displacement of the unimorph actuator reaches 60 $\mu$m, corresponding to $S_e = 0.85\%$ in the films. Such a high displacement output of the PMAT is due to the high strain level $S_1$ in the active polymer. By reducing $k$ to equal 1, the displacement output can be increased. It should be pointed out that in the current PMAT design, only the top polymer film is active, resulting in an upward motion of the actuator. If needed, one can alternatively drive the two polymer layers, which will result in the motion of the actuator in both upward and downward directions to double the displacement output.

The frequency dependence of PMAT1 was also characterized. Presented in Fig. 4(a) is the normalized displacement output measured in the frequency range from 10 Hz to 100 kHz (the upper limit of the optic probe). In this measurement, a dc bias field of 55 MV/m was applied so that an effective piezoelectric state was induced. As can be seen, over four frequency decades, the displacement voltage ratio (DVR) decreases from 31 to 18 nm/V. The results demonstrate two main features of the PMAT investigated: (a) it possesses a high DVR, and (b) it is capable of operating over a broad frequency range. At 86 kHz, resonance was observed. Interestingly, when the same PMAT was operated in a liquid (silicon oil), the DVR remains nearly the same in the same frequency range. This result demonstrates the high load capability of the PMAT, which is due to the high elastic energy density of the active material utilized. In the fluid medium, the resonance is shifted to lower frequency (13.2 kHz) due to the fluid loading, which should follow (if the fluid loading does not change the mode shape of the actuator)[14]

$$\frac{f_i|_{\text{in fluid}}}{f_i|_{\text{vacuum}}} = 1/(1+2A_p/M_p)^{1/2}, \tag{4}$$

where $M_p$ is the mass of the resonator plate and $A_p$ accounts for the fluid loading effect. For the fundamental resonance of the PMAT, it can be derived that $(f_i|_{\text{in fluid}})/(f_i|_{\text{in vacuum}}) = 1/6.12$,[14] which is very close to the measured ratio of $13.2/86 = 1/6.5$. For comparison, the electric impedance data measured under the same dc bias field for PMAT1 in air is presented in Fig. 4(b), where a strong electric resonance was also observed in the same frequency range, indicating the strong electromechanical coupling of the device.

The displacement outputs measured under high electric field in air and in silicon oil are compared in Fig. 3(b) and again, there is very little reduction of the displacement in the silicon oil compared with that in air. The acoustic load (stress $T$) of the fluid medium on the device can be derived as $T = 2\ Zv = 2Z\omega z$, where $Z$ is the acoustic impedance of the fluid medium (1.48 Mrayls here), $v$ is the particle velocity, $\omega$ is the angular frequency (200 Hz), and $z$ is the particle displacement. From the data in Fig. 3(b) ($z = 50\ \mu$m), $T$ is about 0.2 MPa. For comparison, to generate such a high stress level using the electrostatic force ($T_e = 0.5\varepsilon_0 E^2$, $\varepsilon_0 = 8.85\times10^{-12}$ F/m is the vacuum permittivity, and $E$ is the applied electric field) would require a field of about 200 MV/m. Meanwhile, to generate a displacement output of 50 $\mu$m in such a device would require 10 000 V. Furthermore, the stress level for the PMAT here is still far below that which can be delivered by the active material used.[9]

The authors wish to thank Professor L. E. Cross for discussions concerning this work. This work was supported by NIH and DARPA.

[1] W. E. Newell, Science **161**, 1320 (1968).
[2] D. L. Polla and L. F. Francis, Annu. Rev. Mater. Sci. **28**, 563 (1998).
[3] H. G. Craighead, Science **290**, 1532 (2000).
[4] J. Joung, J. Shen, and P. Grodzinski, IEEE Trans. Magn. **36**, 2012 (2000).
[5] W. L. Benard, H. Kahn, A. H. Heuer, and M. A. Huff, J. Microelectromech. Syst. **7**, 245 (1998).
[6] E. W. H. Jager, E. Smela, and O. Inganas, Science **290**, 1540 (2000).
[7] I. Ladabaum, B. T. Khuri-Yakub, and D. Spoliansky, Appl. Phys. Lett. **68**, 7 (1996).
[8] Q. M. Zhang, V. Bharti, and X. Zhao, Science **280**, 2101 (1998).
[9] Z. Y. Cheng, V. Bharti, T.-B. Xu, H. S. Xu, T. Mai, and Q. M. Zhang, Sens. Actuators A **90**, 138 (2001).
[10] B. Rashidian and M. G. Allen, Proc. ASME DSC **32**, 171 (1991).
[11] J.-H. Mo, A. L. Robinson, D. E. Fitting, F. L. Terry, and P. L. Carson, IEEE Trans. Electron Devices **37**, 134 (1990).
[12] M. Madou, *Fundamentals of Microfabrication* (CRC, New York, 1997), p. 145.
[13] R. A. Walsh, *Electromechanical Design Handbook* (McGraw-Hill, New York, 2000), p. 5.34.
[14] R. D. Blevins, *Formulas for Natural Frequency and mode Shape* (Krieger, Malabar, FL, 1995), p. 413.

# APPENDIX 21

# Design, Fabrication, and Performance of a Flextensional Transducer Based on Electrostrictive Polyvinylidene Fluoride-Trifluoroethylene Copolymer

ZhongYang Cheng, Tian-Bing Xu, *Member, IEEE*, Qiming Zhang, *Senior Member, IEEE*, Richard Meyer, Jr., David Van Tol, and Jack Hughes

***Abstract*—Taking advantage of the high electrostrictive strain and high elastic energy density of a newly developed electrostrictive polymer, modified poly(vinylidene fluoride-trifluoroethylene) [P(VDF-TrFE)] based polymers, a flextensional transducer was designed, and its performance was investigated. The flextensional transducer consists of a multilayer stack made of electrostrictive P(VDF-TrFE) polymer films and two flextensional shells fixed at the ends to the multilayer stack. Because of the large transverse strain level achievable in the electrostrictive polymer and the displacement amplification of the flextensional shells, a device of a few millimeters thick and lateral dimension about 30 mm × 25 mm can generate an axial displacement output of more than 1 mm. The unique flextensional configuration and the high elastic energy density of the active polymer also enable the device to offer high-load capability. As an underwater transducer, the device can be operated at frequencies below 1 kHz and still exhibit relatively high transmitting voltage response (TVR), very high source level (SL), and low mechanical quality factor ($Q_m$).**

## I. Introduction

Solid state electromechanical actuators and transducers have been widely used in many civilian and military applications, including active vibration control, underwater navigation and surveillance, microphones, etc. [1]–[3]. In many of those applications, transducers and actuators with high power and high displacement output are required. In the past several decades, a great deal of effort has been devoted to the development of electromechanical materials with those desired features [4]–[10]. In parallel, different device configurations also have been exploited to achieve an amplification of the relatively small strain levels in most commonly used piezoelectric, electrostrictive, and ferroelectric materials [11]–[15]. Recently, it was reported that a massive electrostrictive response could be obtained by modifying polyvinylidene (PVDF)-based ferroelectric copolymers with high-energy electron irradiation or by adding another bulkier termonomer to form a terpolymer [16]–[19].

In this paper, we investigate a flextensional transducer that takes advantage of the large strain and high elastic energy of this new class of electrostrictive polymer, especially the actuation along stretching direction for the stretched polymeric film that is of high electromechanical coupling factor [20]. It will be shown that, for a flextensional transducer of a few millimeter thick and 30 mm × 25 mm lateral dimension, a displacement output of more than 1 mm can be generated with a relatively high-loading capability (>10 N). One of the unique factors of this device is that, because of low acoustic velocity of the active polymer (~1400 m/s) and the flextensional configuration, such a small-sized device can be operated at frequencies below 2 kHz. This small device was capable of generating a high-source level and a transmitting-voltage response (TVR) of 123 dB re 1 $\mu$Pa/V@1m.

This paper is organized as follows. The recent results on the electromechanical properties of the electrostrictive poly(vinylidene fluoride-trifluoroethylene) [P(VDF-TrFE)]-based polymers will be summarized briefly to provide background of this newly developed material. The results on the fabrication and characterizations of these multilayer stacks used as the active element in flextensional transducer will be presented. The actuator performance of flextentional transducer will be analyzed, and the experimental results are presented. The results of underwater performance of the flextentional transducer also will be discussed.

In this investigation, the field-induced transverse strain of the multilayer stacks was characterized by a set-up described in [21]. The displacement generated by the flextensional actuator was evaluated by a differential variable reluctance transducer (DVRT, MicroStrain, Inc, Burlington, VT). The electric impedance as a function of frequency of multilayer stacks and flextensional transducers under different direct current (DC) biased field was measured by an HP 4192 (Hewlett-Packard, Santa Clara, CA) impedance analyzer equipped with a blocking circuit. The blocking circuit is used to protect the impedance analyzer from the high DC voltage applied to the multilayer stack. For the underwater performance of the flextensional transducer, the transducer was placed at a depth of 2.78 m in an anechoic water tank measuring 5.3 m wide, 7.9 m long, and 5.5 m deep. The transmitting voltage response (TVR), the free-field voltage sensitivity (FFVR), the directivity pat-

Manuscript received January 10, 2002; accepted April 5, 2002. This work was supported by DARPA and ONR.

The authors are with The Pennsylvania State University, University Park, PA 16802 (e-mail: ZXC7@psu.edu).

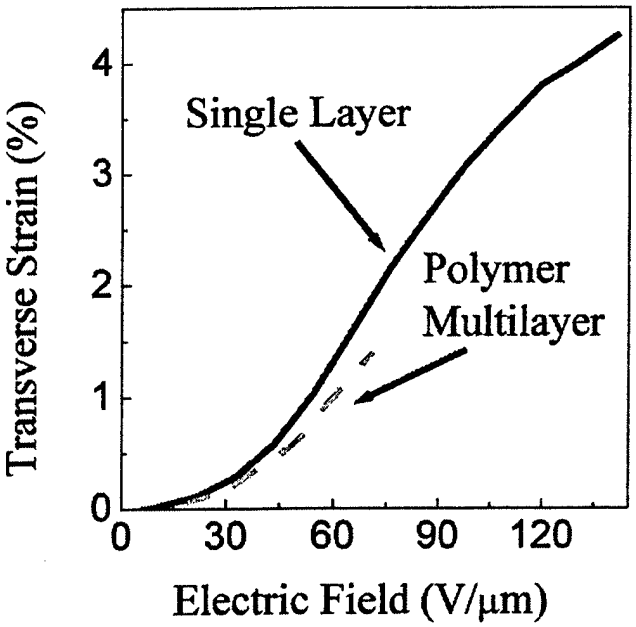


Fig. 1. Transverse strain response along the stretching direction in both irradiated P(VDF-TrFE) 68/32 mol% copolymer film and multilayer of irradiated P(VDF-TrFE) 68/32 mol% copolymer film bonded with an epoxy, Spurr epoxy.

tern, and the electric impedance of the transducer were characterized in the frequency range from 1 kHz to 5 kHz.

## II. Electromechanical Properties of Electrostrictive P(VDF-TrFE)-Based Polymers and Multilayer Actuators

### *A. Electromechanical Properties of Electrostrictive P(VDF-TrFE)-Based Polymers*

P(VDF-TrFE) is a well-known ferroelectric polymer, and in most cases it is used as piezoelectric materials [22]. Compared with piezoelectric ceramics, the electromechanical responses of P(VDF-TrFE) piezopolymers are relatively low. For instance, the piezoelectric $d_{33} = -39$ pm/V and the electromechanical coupling factor $k_{33} = 0.2$ [23] are much below the level of the piezoceramics. In addition, the maximum piezoelectric strain level is about 0.1%. However, by a proper modification, P(VDF-TrFE)-based polymers can be converted to an electrostrictive polymer with a high electric field induced strain and high elastic energy density. For example, in high-energy electron irradiated P(VDF-TrFE) copolymers, a thickness strain (longitudinal strain $S_3$) of $-5\%$ can be induced under a field of 150 V/$\mu$m [24]. In uniaxially stretched and irradiated copolymer films, a transverse strain along the stretching direction of more than 4.0% (see Fig. 1) and an electromechanical coupling factor $k_{31}$ of 0.45 can be obtained [20]. More interestingly, a high electrostrictive response also can be obtained by a nonirradiation approach. In poly(vinylidene fluoride-trifluoroethylene-chlorofluoroethylene) [P(VDF-TrFE-CFE)] terpolymer, an electrostrictive strain $S_3$ of more than $-4.5\%$ has been observed. Table I summarizes those results.

For electromechanical applications, in addition to the maximum induced strain, the elastic energy density, which is a product of stress and strain generated, is another important parameter. In Table I, both gravimetric elastic energy density ($YS_m^2/2\rho$) that is related to device weight and volumetric energy density ($YS_m^2/2$) related to the device size, are included, where $Y$, $S_m$, and $\rho$ are the Young's modulus, maximum induced strain, and density of the material. The data for the piezoceramic and piezopolymer P(VDF-TrFE) also are listed for comparison.

### *B. Fabrication and Characterization of Multilayer Stacks*

Most of the piezoceramic-based actuators are in the multilayer form as shown in Fig. 2(a) [3]. The main purpose of the multilayer approach is to reduce the applied voltage. In the current design of the flextensional transducer [see Fig. 2(b)], using the electrostrictive P(VDF-TrFE)-based polymer as the active element, multilayer stacks also were used to reduce the driving voltage. In the current design, uniaxially stretched high-energy electron irradiated copolymer films were chosen because they deliver high transverse electrostrictive strain that is used to drive the flextensional element (shell) and high electromechanical coupling factor.

The preparation and irradiation of the copolymer films have been described in earlier publications [16], [20]. After irradiation, the films have an average thickness of 15 $\mu$m. The multilayer stacks were fabricated in three steps. The two irradiated films were bonded together to form a bilayer, which improves the dielectric strength. Then, those bilayers were electroded by Au sputtering to the required electrode pattern as defined by a shadow mask (see Fig. 3). The electroded bilayers were laminated together to form a multilayer stack, an electroactive polymer (EAP) stack. One of the key factors in fabricating multilayer stacks is the selection of epoxy to be used to bond the polymer layers together. To ensure an effective stress and strain coupling between the electroactive polymer layers while maintaining high electromechanical performance, the epoxy glue should meet two requirements: provide strong bonding between polymer films, and the glue layer thickness should be thin. A series of epoxy materials were examined in this investigation, including Spurr epoxy (Polysciences, Inc., Warrington, PA), Strain gauge glue, 30-minute epoxy, and different Cyanoacrylate adhesives. It was found that, among them, Spurr epoxy yields the thinnest bonding layer thickness (1 $\mu$m or below). This epoxy also offers relatively strong bonding strength that was tested by the peeling method. After curing, the Spurr epoxy has an elastic modulus of 5 GPa.

For the EAP stacks thus prepared, it is expected that the inactive glue layers would clamp the electric field-induced strain response and raise the elastic modulus of

TABLE I
ELASTIC ENERGY OF SOME ELECTROACTIVE MATERIALS AT ROOM TEMPERATURE.

| Materials | Direction | Y (GPa) | $S_m$ (%) | $YS_m^2/2$ (J/cm$^3$) | $YS_m^2/2\rho$ (J/kg) | Stress (MPa) | Relative speed |
|---|---|---|---|---|---|---|---|
| Piezo-ceramic (PZT-5H) | Longitudinal | 64 | <0.2 | 0.13 | 17 | 128 | >1 MHz |
| | Transverse | 64 | <0.1 | 0.03 | 4 | 64 | |
| Piezo P(VDF/TrFE) | Longitudinal | 4 | <0.15 | 0.0045 | 2.5 | 6 | >1 MHz |
| Irradiated P(VDF/TrFE) | Longitudinal | $Y_{33} = 0.5$ | 5.0 | 0.63 | 313 | 25 | >100 kHz |
| | Transverse | $Y_{11} = 1.0$ | 4.0 | 0.8 | 400 | 40 | |
| P(VDF/TrFE) based terpolymer | Longitudinal | $Y_{33} > 1.1$ | 4.5 | 1.1 | 557 | 45 | >100 kHz |

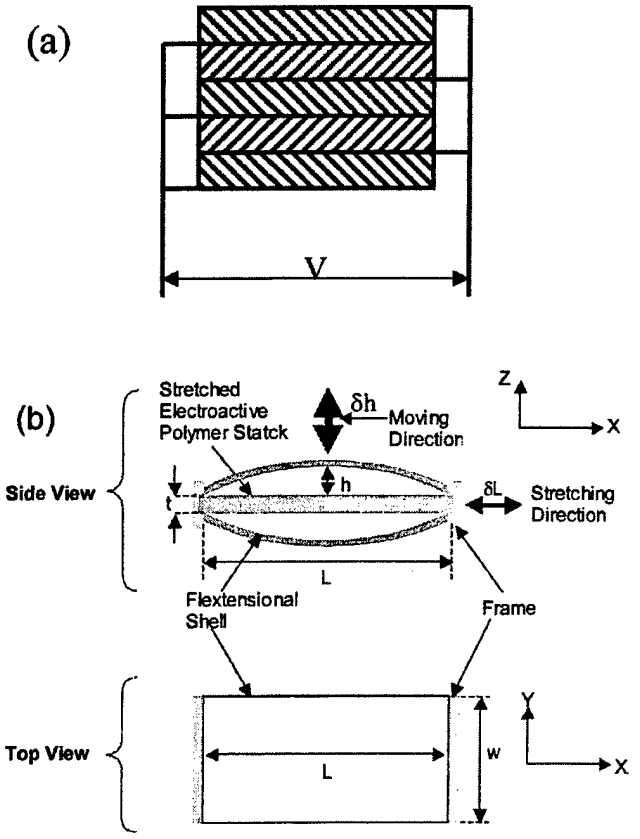


Fig. 2. Diagram of multilayer devices. (a) Multilayer piezoceramic actuators. (b) Flextensional transducer based on stretched electroactive polymers, where $t$ is the thickness of EAP stack.

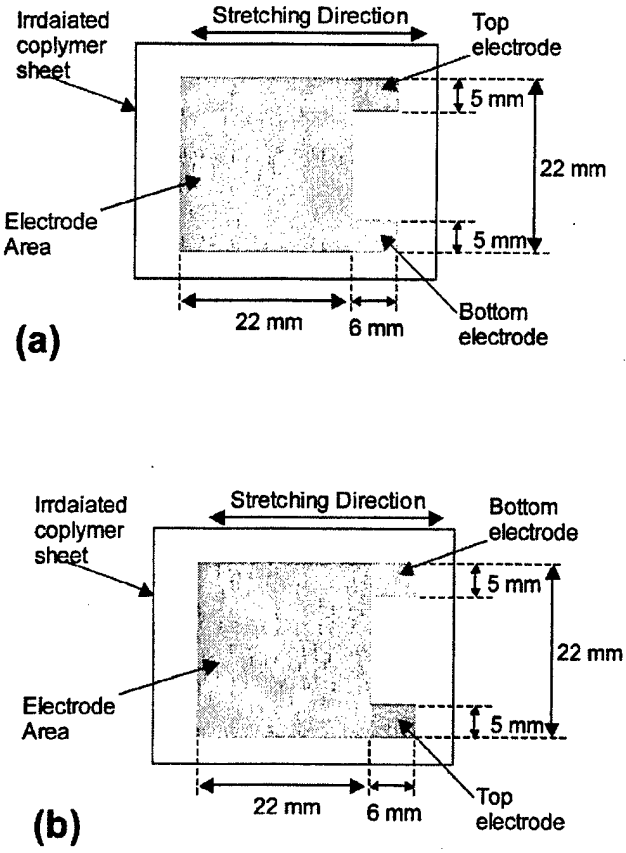


Fig. 3. Pattern of gold electrode on irradiated polymer sheet. In order to make the multilayer, there are two types of electrode as shown in (a) and (b), respectively.

the stack compared to a single layer of active polymer. Indeed, as observed in Fig. 1, the field-induced strain of the multilayer stack is 77% of the single layer strain. In addition, the elastic modulus of the multilayer stack at 22°C is 1.3 GPa, which is higher than the elastic modulus, 1.0 GPa, of polymer layer at the same temperature.

For the flextensional transducers to be investigated, EAP stacks of 1-mm thickness, consisting of 30 layers of irradiated copolymer bilayer films (the thickness of each bilayer is 31 $\mu$m), were used. The electroded area was $22 \times 22$ mm$^2$; the sample width and length (parallel to the stretching direction) were 25 mm and 31 mm, respectively (see Fig. 3). The unelectroded areas provided electric insulation to prevent breakdown at the edges of the films and also were used for the electric connection to the leads to external power supply.

The performance of the stacks was examined in terms of their electromechanical resonance. As shown in Fig. 4, an electromechanical resonance at 17 kHz, which corresponds to the resonance along the stretching direction of the EAP

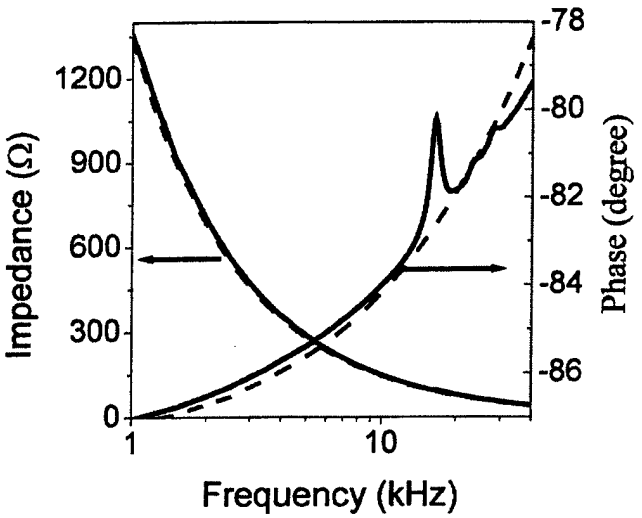


Fig. 4. Frequency dependence of both impedance ($|Z|$) and phase in degree in a multilayer of irradiated P(VDF-TrFE) 68/32 mol% copolymer film bonded with Spurr epoxy under a DC bias of 500 V (solid line) and 0 V (dashed line). The AC single used here is 1 Vrms. The electromechanical resonance occurs at 17 kHz. See text for detailed information of multilayer.

stack, was observed when the EAP stack was under a DC bias field of 16 V/$\mu$m (for an electrostrictive material, a DC bias is required to induce an effective piezoelectric state). The resonance was very similar to that observed in single-layer films. Because of relatively low electromechanical response for the active polymer films in perpendicular to the polymer film stretching direction, no strong resonance was detected along the width direction of the multilayer stack.

## III. Actuator Performance of the Flextensional Transducer

As has been demonstrated in earlier investigations [11]–[14], a flextensional actuator with a structure as shown in Fig. 2 can generate relatively large displacement and force output. Because of the much higher strain level in the electrostrictive PVDF-based polymers, it was expected that a device based on those electroactive polymers will produce large displacement with relatively high generative force.

To build the flextensional actuator, two plastic blocks (frame, made of plexiglass) are attached (glued using 30-minute epoxy and mechanical screws) to the two ends of the multilayer stack as shown in Fig. 2(b). The blocks were used to hold the flextensional elements made of spring steel sheet. The spring-steel sheets (Blue Tempered & Polished Spring Steel, Precision Brand Products, Inc., Downers Grove, IL) are forced to fit into the plastic blocks to form an arc shape [Fig. 2(b)]. Three flextensional transducers with different spring-steel sheet thickness are evaluated here (thickness = 0.125, 0.254, and 0.381 mm, respectively). In this design, the pair of spring-steel arcs is

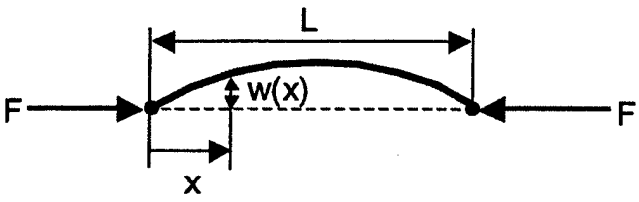


Fig. 5. Deformation of flextensional shell under an uniaxial force ($F$).

under compressive force from the EAP stack; in return, the flextensional element exerts tensile force to the EAP stack. This tensile force serves two functions. One is to maintain the EAP stack under tension, which is needed for the EAP stack to function properly; the second is to transmit the strain generated in the EAP stack, to the amplified displacement output.

For a two-ends supported elastic beam shown in Fig. 2(b) with the two ends free in rotation, based on potential energy criterion for stability, the displacement $w(x)$ as a function of $x$ was derived as Fig. 5 [25]:

$$w(x) = h \sin \frac{\pi}{L} x, \tag{1}$$

where $h$ and $L$ are defined in Fig. 2(b). For the current device $L = 27$ mm. From (1), the total length of the flextensional element can be found:

$$A = L + \frac{\pi^2 h^2}{4L}. \tag{2}$$

In (2), it was assumed that $h^2/L^2 \ll 1$ so that higher order terms could be omitted. Under external electric fields, $L$ will be extended to $L + \delta L$, and $h$ to $h + \delta h$. The ratio $\delta h/\delta L$ can be regarded as a displacement amplification factor of the device and can be found from (2) by assuming that the total length, $A$, of the flextensional element does not change:

$$\frac{\delta h}{\delta L} = -\left[1 - \frac{\pi^2}{4}\frac{h^2}{L^2}\right] \Big/ \left[\frac{\pi^2}{2}\frac{h}{L}\right]. \tag{3}$$

In Fig. 6, the ratio $\delta h/\delta L$ is plotted as a function of $h/L$ based on (3). Clearly, the amplification factor increases with reduced $h/L$. However, the maximum displacement output is constrained such that $\delta h$ cannot exceed $h$. Therefore, for a practical device, there is a balance between the displacement amplification and the maximum displacement.

The displacement output of two flextensional transducers with different $h/L$ ratio was characterized at 1 Hz, and the data are presented in Fig. 7(a). It should be noted that in each flextensional transducer, there were two flextensional elements, generating a total displacement $2\delta h$ [the data in Fig. 6(a) is $2\delta h$]. It also should be noted that the result in (3) is for cases where $\delta h$ is much smaller than $h$. For data in Fig. 7, $\delta h$ became comparable to $h$ when the device was driven under high applied fields. And (3) in those cases could be used only qualitatively. For the

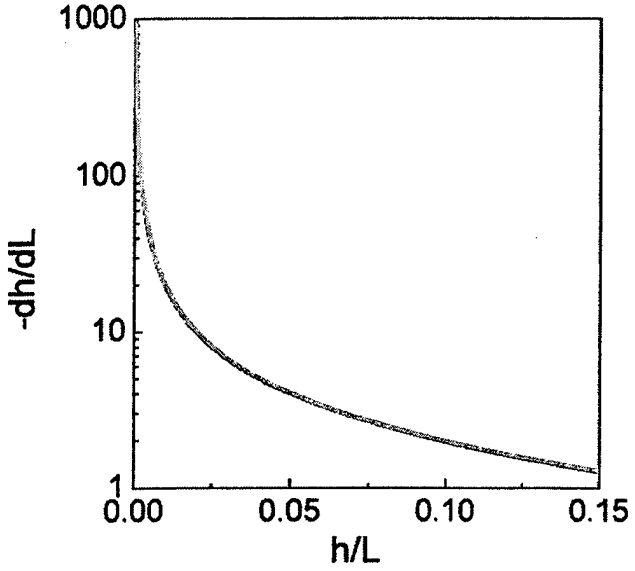


Fig. 6. Displacement amplification versus the ratio of $h/L$ calculated using (3).

flextensional transducers tested here, the thickness of the spring-steel sheet was 0.125 mm, and the initial ratio of $h/L$ is 0.053 and 0.109 ($2\delta h/\delta L = 7.6$ and $2\delta h/\delta L = 3.6$), respectively. It is interesting to note that the displacement output of such a device can be more than 1 mm.

The displacement output under external load also was measured at 1 Hz for the flextensional transducer with the initial ratio of $h/L = 0.109$. In this measurement, a load of given weight was placed on the top of the flextensional transducer, and the displacement output under different applied field was recorded. The data acquired are presented in Fig. 7(b) and showed that, in addition to the high-displacement output, the flextensional transducer with EAP stacks also exhibit relatively high-load capability. In fact, the displacement output of the device increased slightly with increasing load. This is due to the fact that the field-induced strain along the film-stretching direction increases with tensile stress up to 20 MPa. The load applied in the experiment was equivalent to the tensile stress to the EAP stack as produced by the flextensional elements [24].

The displacement profile $w(x)$ of the flextensional element also was measured and is presented in Fig. 7(c) (squares in the figure). The theoretical prediction using (1) (solid line) matches quite well with the experiment data point.

## IV. Transducer Performance of the Device

To assess the resonance behavior of the flextensional transducer, the electric impedance of the device under DC bias was characterized in air. When the two flextensional elements are attached to the EAP stack, the three resonances can be modeled as shown in Fig. 8, in which the

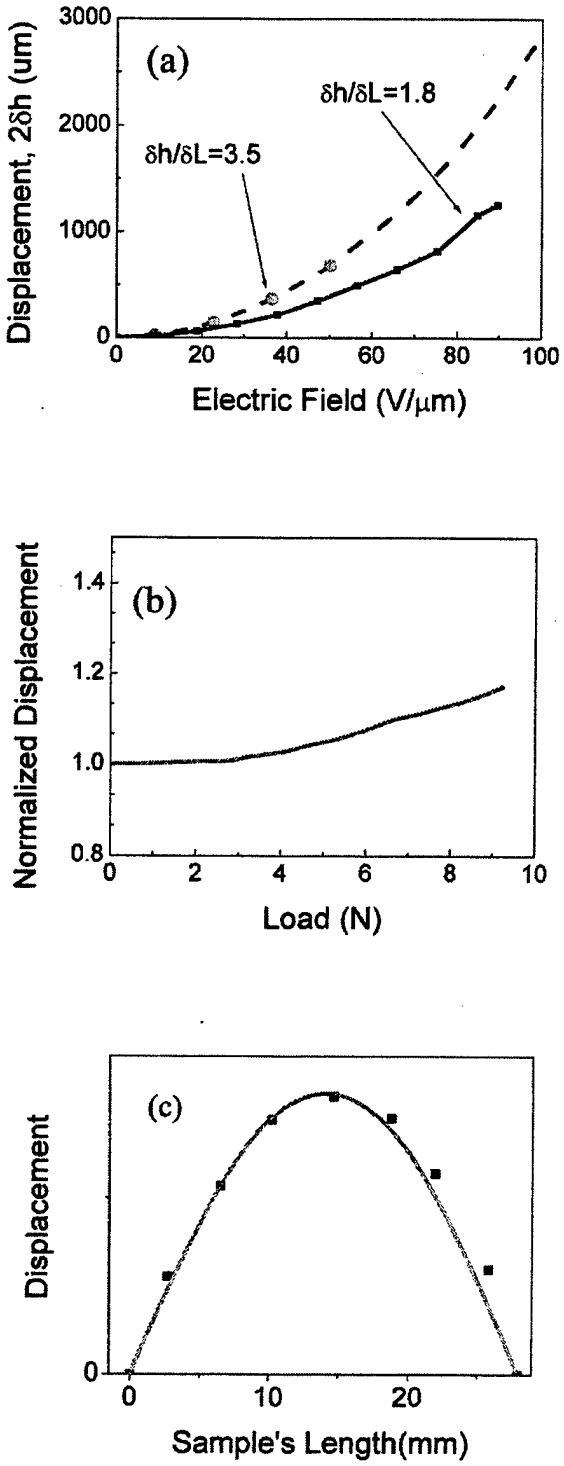


Fig. 7. Displacement response of the flextensional transducer. (a) Displacement at midpoint of flextensional shell versus electric field of 1 Hz in two flextensional transducers. The transducer consists of an EAP stack with a thickness of 1 mm and two flextensional shells with a thickness of 0.125 mm. (b) Displacement at midpoint of flextensional shell versus mechanical load for a flextensional transducer under a constant electric field of 1 Hz. (c) Displacement profile of flextensional transducer under a constant electric field of 1 Hz, where the squares are the measured data and the solid line is calculated using (1).

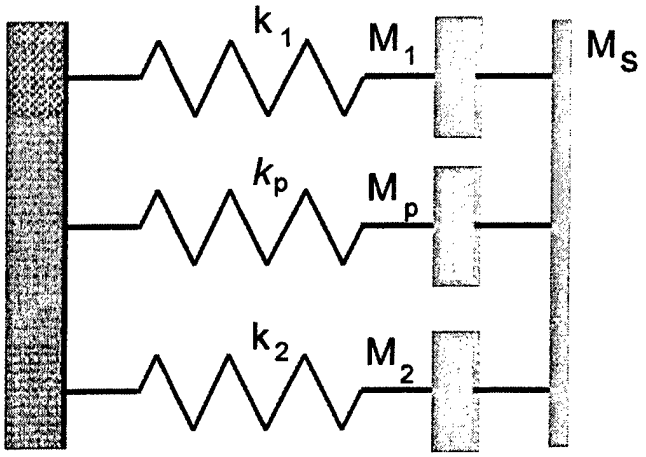


Fig. 8. Equivalent model of flextensional transducer designed in Fig. 5, where, $k_1$, $k_2$, and $k_p$ are the spring constants of flextensional shells and EAP stack; and the mass $M_1$, $M_2$, and $M_p$ are the masses of flextensional shells and electroactive polymer stack. The mass $M_s$ is the total load of the transducer.

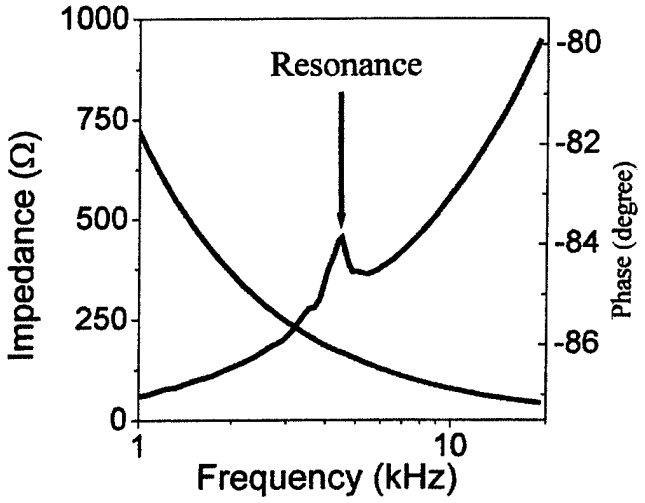


Fig. 9. Frequency dependence of impedance ($|Z|$) and phase in degree for a flextensional transducer in air with a DC bias of 500 V.

branches with the effective elastic constant $k_1$ and $k_2$ represent the two flextensional elements, and the one with the elastic constant $k_p$ denotes the EAP stack. For the devices tested here, it was found that the resonance frequency of the EAP stack was much higher than those from the two flextensional elements and, hence, the lowest frequency resonance was from the flextensional shells. In addition to the elastic modulus and the thickness of the shell, $h$ and $L$ are important parameters in determining the resonance frequency. In other words, the effective elastic constant $k_1$ and $k_2$ in Fig. 8 will vary with $h/L$. In general, a smaller $h/L$ ratio will reduce the resonance frequency of the shell if the length of shell is fixed [25]. Therefore, by adjusting $h$, one also can vary the resonance frequency of the transducer.

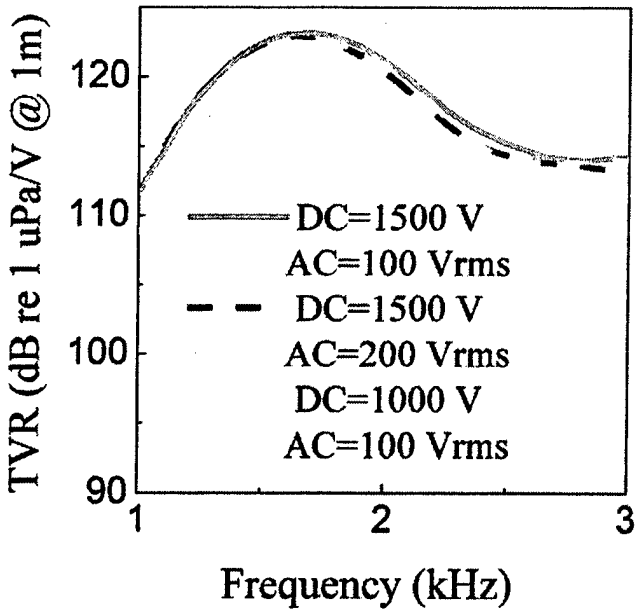


Fig. 10. TVR of flextensional transducer in water with different driving electric fields.

Fig. 9 is the electric impedance measured with a DC bias field of 16 V/$\mu$m for a flextensional transducer in air that has the flextensional shell thickness of 0.375 mm and two EAP stacks. An electromechanical resonance was observed at 4.5 kHz, which was much lower than the resonance frequency from the EAP stack alone (Fig. 4). In this case, the two flextensional elements were nearly the same in terms of $h$ and $L$ and, as a result, there was only one resonance observed. In the case in which two flextensional elements have a small difference in h or other properties that could be introduced in the fabrication process, multiple resonances would be observed, as has been elucidated in Fig. 8. In this flextensional transducer, the flextensional shell thickness of 0.381 mm is chosen so that the in-water resonance frequency of the transducer is near 2 kHz.

For underwater tests, the flextensional transducer was sealed by a polymer (polyurethane, trademark CONATHANE@EN-9, CONAP, Inc., Olean, NY). The polyurethane coating served two purposes: to provide electric insulation between the transducer and the water, and to prevent water leaking into the space between the flextensional shell and EAP stack. The electric impedance of the sealed transducer was tested in water. Due to water loading, the resonance frequency dropped from 4.5 kHz in air to 1.7 kHz in water.

The same transducer also was tested to obtain TVR, directivity pattern, and FFVS. In the TVR measurement, the pressure generated by the transducer as a projector under different DC bias fields and alternating current (AC) fields was measured by a hydrophone placed 1.0 m away from the transducer. One flextensional element face was oriented toward the hydrophone. The data are presented in Fig. 10. A broad resonance was observed centered at

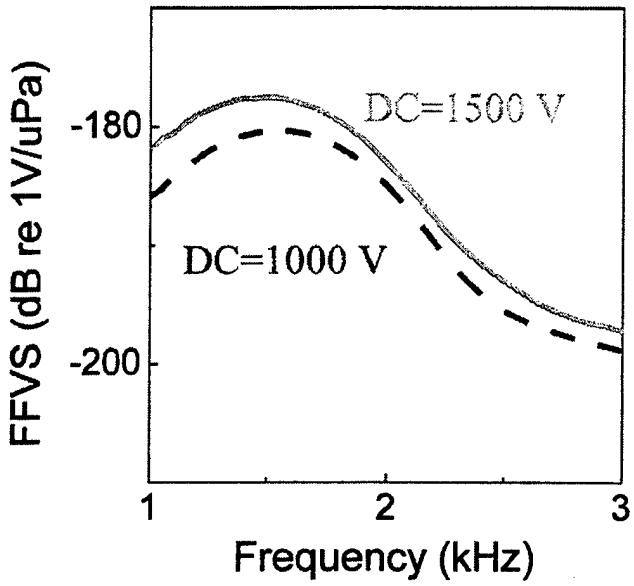


Fig. 11. FFVS of flextensional transducer in water with different driving electric fields.

1.7 kHz. From the resonance peak, the mechanical quality factor, $Q_m$, of the projector operated in water could be calculated by (4) [25]:

$$Q_m = \frac{f_r}{f_h - f_l}, \tag{4}$$

where $f_r$ is the resonance frequency, $f_h$ and $f_l$ are the half-power frequencies, which can be determined from the $-6$ dB points in the TVR curve. For this transducer, the mechanical $Q$ is $Q_m = 1.55$. The TVR near the resonance is 122.5 and 123.2 (dB re 1 $\mu$Pa/V@1m) for the device under DC bias fields of 1000 V and 1500 V, respectively.

The directivity pattern of the transducer was characterized when the transducer was rotated along its x-axis (length), and the distance between transducer and hydrophone was kept the same. In the frequency range from 1 kHz to 5 kHz, it was found that the transducer was an omnidirectional pattern. This was due to the fact that the dimension of the transducer is much smaller that the acoustic wavelength (1.5 m at 1 kHz and 0.3 m at 5 kHz).

For electrostrictive material as the irradiated P(VDF-TrFE) copolymers used here, an effective piezoelectric state can be induced by a DC bias electric field. Thus, the material also can be used to sense acoustic signals. To calculate the receive response of the transducer, the FFVS was obtained and is presented in Fig. 11. For a DC bias of 1500 V, the FFVS was $-177.5$ (dB re 1V/$\mu$Pa) near the resonance frequency.

As an electrostrictive material, the electromechanical response increases with the DC bias field if the DC field is far below the saturation field, which is the case for the DC fields used here, as can be seen from Fig. 1. The observed increase in both TVR and FFVS is consistent with this.

In additional to the relatively high TVR at such a low frequency, the flextensional transducer also was capable of generating high SL because its high electric field limits. The data presented in Fig. 10 were measured under a DC bias of 1000 V and 1500 V using an AC signal of 100 Vrms and 200 Vrms, respectively. That is, the real acoustic pressure reached 169 dB re 1$\mu$Pa@1m. For the flextensional transducer investigated here, a voltage of 1500 V is equal to an electric field of $48 \sim 50$ V/$\mu$m, which is much smaller than the high field limitation in the polymer film as shown in Fig. 1. If a higher DC bias and larger AC signal were applied (for example, a DC bias of 2000 V with an AC signal of 1000 Vrms), a much higher acoustic pressure could be generated.

It should be noted that, because the transducer dimension $b$ (less than 0.03 m) in the current device was much smaller than the acoustic wavelength $\lambda$ which is about 1.5 m at 1 kHz, the acoustic impedance $Z_a$ of the medium (water) as seen by the transducer is nearly imaginary (mass-like load) [26]:

$$Z_a = Z_c \frac{k^2b^2 + jkb}{k^2b^2 + 1}, \tag{5}$$

where $Z_c$ is the characteristic acoustic impedance of water, $k$ is the wave vector ($= 2\pi/\lambda$), $j = \sqrt{-1}$. As a result, the transducer efficiency is low. By working with an array with increased dimension, the efficiency could be improved significantly.

This can be seen from the Mason equivalent circuit shown in Fig. 12(a) for the active polymer operated in the transverse piezoelectric mode. In Fig. 12(a), $C_0$ is the clamped capacitance, $N$ is the transformer ratio, and $Z_T$ is the acoustic impedance of the transducer, including the multilayer stack and the flextensional elements. $Z_T$ is imaginary if mechanical loss is not considered. The acoustic impedance of the medium seen by the transducer $Z_L = R_L + jX_L$, where $R_L = AZ_c \frac{k^2b^2}{1+k^2b^2}$, $X_L = AZ_c \frac{k\,b}{1+k^2b^2}$, $A$ is the transducer area, and $Z_c$ is the characteristic acoustic impedance of eh acoustic medium, respectively. The efficiency is measured by the acoustic energy consumption in the load $R_L$ to the total input electric energy. When $kb \ll 1$, $R_L$ is much smaller than $AZ_c$ and $X_L$.

Now if $M$ such transducers are placed in parallel acoustically to form an array (electrically these transducers are also in parallel), for the sake of simplicity, assuming $kb \ll 1$, the Mason equivalent circuit becomes Fig. 12(b), where $R_L'$ and $X_L'$ are $R_L' = MAZ_c \frac{k^2b^2M}{1+k^2b^2}$ and $X_L' = MAZ_c \frac{k\,b\sqrt{M}}{1+k^2b^2}$. It can be estimated that the efficiency is increased by a factor of $M$ approximately [2].

## V. Summary

A transducer is developed that utilizes the high strain electrostrictive P(VDF-TrFE)-based polymer as the active element and two flextensional caps providing displacement

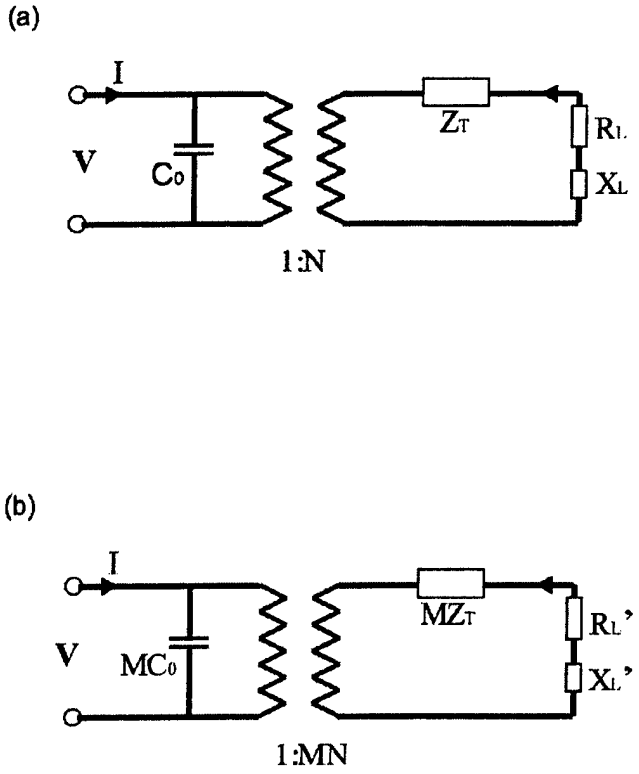


Fig. 12. Mason equivalent circuit for single transducer (a) and transducer array consisting of $M$ transducers (b).

amplification. Analogues to the Moonie and Cymbal transducers previously developed, the flextensional transducer here generates higher displacement compared with the active polymer alone plus higher load capability than the bimorph-type actuators. In the current design, the active polymers are in thin-film form bonded to form a multilayer stack. The actuation of the active polymer is along the film surface direction. The flextensional elements are designed to ensure the active polymers are under tension, which also increases performance.

In this investigation, the displacement amplification and transducer performance were analyzed. It was shown that the device (25 mm × 30 mm lateral dimension and a few millimeters thick) was capable of generating a displacement of more than 1 mm with a load of more than 10 N. As an underwater transducer, the device exhibited a low frequency resonance (<2 kHz) and generated a TVR of 123 (dB re 1 $\mu$Pa/V@1m) and FFVS of approximately −177.5 (dB re 1V/$\mu$Pa). Because of the high saturation field, the device has the potential to achieve a high SL.

## References

[1] P. M. Galletti, D. E. De Rossi, and A. S. De Reggi, Eds. *Medical Applications of Piezoelectric Polymers.* New York: Gordon and Breach, 1988.

[2] G. S. Kino, *Acoustic Waves: Devices, Imaging, and Analog Signal Processing.* Englewood Cliffs, NJ: Prentice-Hall, 1987.

[3] K. Uchino, *Piezoelectric Actuators and Ultrasonic Motors.* Boston: Kluwer, 1997.

[4] L. E. Cross, "Ferroelectric ceramics: Materials and application issues," *Ceram. Trans.*, vol. 68, pp. 15–55, 1996.

[5] R. E. Newnham, "Composite electroceramics," *Ann. Rev. Mater. Sci.*, vol. 16, pp. 47–68, 1986.

[6] S.-E. Park and T. R. Shrout, "Ultrahigh strain and piezoelectric behavior in relaxor based ferroelectric single crystal," *J. Appl. Phys.*, vol. 82, no. 4, pp. 1804–1811, 1997.

[7] Z. Ma, J. I. Scheinbein, and B. A. Newman, "High field electrostrictive response of polymers," *J. Polym. Sci. Part B, Polym. Phys.*, vol. 32, pp. 2721–2731, 1994.

[8] R. E. Pelrine, R. D. Kornbluh, and J. P. Joseph, "Electrostriction of polymer dielectrics with compliant electrodes as a mean of actuation," *Sens. Actuators A*, vol. 64, pp. 77–85, 1998.

[9] J. Su, Q. M. Zhang, and R. Y. Ting, "Space-charge-enhanced electromechanical response in thin-film polyurethane elastomers," *Appl. Phys. Lett.*, vol. 71, no. 3, pp. 386–388, 1997.

[10] Q. M. Zhang, W. Cao, J. Zhao, and L. E. Cross, "Piezoelectric performance of piezoceramic-polymer composites with 2-2 connectivity: A combined theoretical and experimental study," *IEEE Trans. Ultrason., Ferroelect., Freq. Contr.*, vol. 41, pp. 556–564, 1994.

[11] Q. C. Xu, S. Yoshikawa, J. R. Belsick, and R. E. Newnham, "Piezoelectric composites with high sensitivity and high capacitance for use at high pressures," *IEEE Trans. Ultrason., Ferroelect., Freq. Contr.*, vol. 38, no. 6, pp. 634–639, 1991.

[12] R. E. Newnham, A. Dogan, Q. C. Xu, and S. Yoshikawa, "Flextensional 'Moonie' Actuatora," *Proc. IEEE Ultrason. Symp.*, vol. 1, pp. 509–513, 1993.

[13] A. Dogan, K. Uchino, and R. E. Newnham, "Composite piezoelectric transducer with truncated conical edcaps cymbal," *IEEE Trans. Ultrason., Ferroelect., Freq. Contr.*, vol. 44, no. 3, pp. 597–605, 1997.

[14] J. D. Zhang, A. C. Hladky-Hennion, W. J. Hughes, and R. E. Newnham, "Modeling and underwater characterization of cymbal transducer and arrays," *IEEE Trans. Ultrason., Ferroelect., Freq. Contr.*, vol. 48, no. 2, pp. 560–568, 2001.

[15] Q. M. Wang and L. E. Cross, "A piezoelectric pseudoshear multilayer actuator," *Appl. Phys. Lett.*, vol. 72, no. 18, pp. 2238–2240, 1998.

[16] Q. M. Zhang, V. Bharti, and X. Zhao, "Giant electrostriction and relaxor ferroelectric behavior in electron-irradiated poly(vinylidene fluoride-trifluoroethylene) copolymer," *Science*, vol. 280, pp. 2101–2104, 1998.

[17] X. Zhao, V. Bharti, Q. M. Zhang, T. Romotowski, F. Tito, and R. Ting, "Electromechanical properties of electrostrictive poly(vinylidene fluoride-trifluoroethylene) copolymer," *Appl. Phys. Lett.*, vol. 73, pp. 2054–2056, 1998.

[18] Z.-Y. Cheng, T.-B. Xu, V. Bharti, S. Wang, and Q. M. Zhang, "Transverse strain responses in the electrostrictive poly(vinylidene fluoride-trifluoroethylene) copolymer," *Appl. Phys. Lett.*, vol. 74, pp. 1901–1903, 1999.

[19] H. S. Xu, Z.-Y. Cheng, D. Olson, T. Mai, and Q. M. Zhang, "Ferroelectric and electromechanical properties of poly(vinylidenefluoride-trifluoroethylene-chlorotrifluoroethylene) terpolymer," *Appl. Phys. Lett.*, vol. 78, no. 16, pp. 2360–2362, 2001.

[20] Z.-Y. Cheng, V. Bharti, T.-B. Xu, H. S. Xu, T. Mai, and Q. M. Zhang, "Electrostrictive poly(vinylidene fluoride-trifluoroethylene) copolymers," *Sens. Actuators A*, vol. 90, pp. 138–147, 2001.

[21] Z.-Y. Cheng, V. Bharti, T.-B. Xu, S. Wang, Q. M. Zhang, T. Ramotowski, F. Tito, and R. Ting, "Transverse strain response in electrostrictive poly(vinylidene fluoride-trifluoroethylene) films and development of a dilatometer for the measurement," *J. Appl. Phys.*, vol. 86, pp. 2208–2214, 1999.

[22] E. Fukada, "History and recent progress in piezoelectric polymers," *IEEE Trans. Ultrason., Ferroelect., Freq. Contr.*, vol. 47, no. 6, pp. 1277–1290, 2000.

[23] H. Wang, Q. M. Zhang, L. E. Cross, and A. O. Sykes, "Piezoelectric, dielectric, and elastic properties of poly(vinylidene fluoride trifluoroethylene)," *J. Appl. Phys.*, vol. 74, no. 5, pp. 3394–3398, 1993.

[24] Q. M. Zhang, Z.-Y. Cheng, and V. Bharti, "Relaxor ferroelectric behavior in high energy electron irradiated poly(vinylidene

fluoride-trifluoroethylene) copolymers," *Appl. Phys. A*, vol. 70, pp. 307–312, 2000.
[25] W. F. Chen and T. Atsuta, *Theory of Beam-Columns, Volume 1: In-plane Behavior and Design.* New York: McGraw-Hill, 1976, pp. 92–105.
[26] *Procedures for Calibration of Underwater Electroacoustic Transducers,* ANSI-20-1988.
[27] D. E. Hall, *Basic Acoustics.* Malabar, FL: Krieger, 1993.

**Zhong-Yang Cheng** received his B.S. in physics, M.S. and Ph.D degrees in Electronic Materials and Engineering from Xian Jiaotong University, Xi'an, China in 1983, 1988 and 1995 respectively. He is currently a research associate with Materials Research Institute, The Pennsylvania State University. University Park, PA. Before he joined Penn State in 1998, he worked at the Heinrich-Hertz-Institute in Berlin, Germany for one year and in the Department of Physics at the University of Puerto Rico, San Juan, for one and one half years. His research interests are in structure-property studies of various functional materials and the application studies of these materials. He has published more than 50 articles.

**Tian-Bing Xu** (S'98) received his M.S. Degree in Electrical Engineering and Ph.D. degree in Materials from The Pennsylvania State University, University Park, PA, in 1999, and 2002 respectively. Before coming to the United States, he worked for nine years as an Engineer and Associate Director, Ion Beam Laboratory, Institute of Physics, Chinese Academy of Sciences, Beijing, China, following graduation from The Shandong University, Jinan, China. He worked on ion implantation and ion analyses in semiconductors and other materials during that time. From October 1997 to December 2001 he worked, as a graduate research assistant, on electroactive polymer and their application in actuators, transducers, and MEMS. Dr. Xu currently, as a staff scientist, is working on advanced materials and their applications at NASA Langley Research Center, Hampton, VA. He is the author or coauthor of more than 40 papers in peer-reviewed international journals. Dr. Xu is a member of IEEE, SPIE, and Materials Research Society.

**Q. M. Zhang** (M'95–SM'99) is a Professor of Electrical Engineering at the Materials Research Institute and Department of Electrical Engineering at the Pennsylvania State University, University Park, PA. He obtained his Ph.D. degree in solid state physics in 1986 from Penn State University. He spent three years at the Brookhaven National Laboratory, Long Island, NY, as a research scientist working in the area of characterization of solid state thin films. In 1991, he came back to Penn State University as a faculty to conduct research in ferroelectric based materials and devices and electroactive polymer based materials and devices. The research activities in his research group include novel material development, microstructure-property-electroactive response relationships, and device development for transducers and actuators, ferroelectric polymer thin film for memory devices and sensors, micro-electromechanical systems, photonic bandgap crystals, electrooptic and acoustooptic materials and devices, and dielectrics and capacitors. He has more than 185 publications in these areas. He is a senior member of IEEE, and member of Materials Research Society, and American Physical Society.

**Richard J. Meyer, Jr.** joined the Applied Research Laboratory at Penn State University, University Park, PA, in November of 2000 as a Research Associate in the transducer division of Systems Engineering. He studied ceramic science and engineering and graduated with a B.Sc. degree from Penn State in 1993 as the student Marshal for the Materials Science and Engineering department. He received his Masters degree in 1995 in Materials at the Materials Research Laboratory, Penn State University, under the direction of Dr. Thomas Shrout and Ms. Shoko Yoshikawa. He completed his Ph.D. in October 1998 with the development of high frequency 1-3 composite transducers. After graduation he studied one year as a post-doctoral scholar under the supervision of Dr. R. E. Newnham, then was promoted to Research Associate at the Materials Research Laboratory. His research interests include ceramic processing, development of undersea and medical ultrasonic devices and composites materials for actuators and transducers. He currently has more than 30 published papers and 2 patents in the field of ultrasound and actuator material technology.

**David J. Van Toll** works in the Transducer and Arrays Group at the Applied Research Laboratory of The Pennsylvania State University, University Park, PA. He has been involved in a broad range of transducer development projects. Examples of low frequency work (1–10 kHz) include an underwater acoustic intensity probe and a 2 kHz projector/hydrophone pair used in a subsoil imaging system. In the middle frequencies (20–500 kHz), Dave has designed and built transducers for many applications. These include acoustic lens systems, rock locators for a dredging barge, an acoustic intensity probe, and an ocean velocimetry system. He has also been active in the higher frequencies (0.5–5 MHz), having built imaging systems using acoustic lenses as well as building some prototype transducers for other SONAR imaging systems. Dave acquired a B.S. in electrical engineering from Iowa State, Ames, IA (1991), an M.S. in acoustics from Penn State, University Park, PA (1996), and is currently developing a micro-tonpilz transducer material for his Ph.D. degree at Penn State.

**W. Jack Hughes** is in charge of the Transducer and Arrays Group at the Applied Research Laboratory at Penn State University, University Park, PA, and is a Professor of Acoustics and a Fellow in the Acoustical Society of America. He has responsibility for the design, fabrication, and calibration of transducers and arrays used in many navy research and development sonar systems for weapons and mine hunting. Dr. Hughes is also active in medical ultrasonic transducers and is principle investigator of developing a megahertz tonpilz transducer and diver held sonar system. He is active in the areas of linear, two dimensional, planar and cylindrical arrays including theory, fabrication and testing. He has over 30 years experience in the design of tonpilz transducers and arrays, and has developed a very broad bandwidth magnetostrictive/piezoelectric element and array. Also he has developed shaped sensor technology with PVDF and 1-3 composite materials for use in advanced conformal arrays, and continues to be involved in transducer array self-noise reduction. His graduate students have generated thesis in many areas, and encompassing frequencies from ultrasonic arrays down to audio frequencies. Dr. Hughes received his B.S. degree in physics in 1964 from Rensselaer Polytechnic Institute, Troy, NY, his Ph.D. in Acoustics in 1978 from The Pennsylvania State University and has over 22 papers, 3 patents and numerous symposium and workshop presentations in his field.

# APPENDIX 22

ADVANCED MATERIALS

Reflectance spectra were obtained using an integrating sphere (Ø70 mm, 10 mm port openings) versus commercial white and black references (Labsphere). The system response was corrected versus $BaMgAl_{10}O_{17}$:Eu (BAM) generously provided by Philips Research Laboratories.

Received: March 5, 2002
Final version: July 30, 2002

[1] T. Jüstel, D. U. Wiechert, C. Lau, D. Sendor, U. Kynast, *Adv. Funct. Mater.* **2001**, *11*, 105.
[2] M. Pauchard, S. Huber, R. Méallet-Renault, M. Maas, R. Pansu, G. Calzaferri, *Angew. Chem. Int. Ed.* **2001**, *40*, 2839.
[3] G. Ihlein, F. Schüth, O. Krauss, U. Vietze, F. Laeri, *Adv. Mater.* **1998**, *10*, 1117.
[4] I. Braun, G. Ihlein, F. Laeri, J. U. Nöckel, G. Schulz-Ekloff, F. Schüth, U. Vietze, Ö. Weiß, D. Wöhrle, *Appl. Phys. B* **2000**, *70*, 335.
[5] U. Kynast, V. Weiler, *Adv. Mater.* **1994**, *6*, 937.
[6] M. Bredol, U. Kynast, C. R. Ronda, *Adv. Mater.* **1991**, *3*, 361.
[7] I. L. V. Rosa, O. A. Serra, E. J. Nassar, *J. Lumin.* **1997**, *72–74*, 532.
[8] M. Alvaro, V. Fornés, S. Garcia, J. C. Scaiano, *J. Phys. Chem. B* **1998**, *102*, 8744.
[9] J. Dexpert-Ghys, C. Picard, A. Taurines, *J. Inclusion Phenom. Macrocyclic Chem.* **2001**, *39*, 261.
[10] E. O. Malta, H. F. Brito, J. F. S. Menezes, F. R. G. de Silva, C. de Mello Donega, S. Alves, Jr., *Chem. Phys. Lett.* **1998**, *282*, 233.
[11] E. V. Melent'eva, L. L. Kononenko, E. G. Koltunova, N. S. Poluektov, *Zh. Prikl. Spectr.* **1966**, *5*, 245.
[12] J. Kido, H. Nagai, Y. Okamoto, T. Skotheim, *Chem. Lett.* **1991**, 1267.
[13] Q. Xu, L. Li, B. Li, J. Yu, R. Xu, *Microporous Mesoporous Mater.* **2000**, *38*, 351.
[14] A. M. V. de Andrade, N. B. da Costa, Jr., O. L. Malta, R. L. Longo, A. M. Simas, G. F. de Sa, *J. Alloys Compd.* **1997**, *250*, 412.
[15] G. Stein, E. Würzberg, *J. Chem. Phys.* **1975**, *62*, 208.
[16] P. K. Maher, F. D. Hunter, J. Scherzer, *Inorganic Crystal Structure Database*, ref. code 24867, **1971**.
[17] F. J. Berry, M. Carbucicchio, A. Chiari, C. Johnson, E. A. Moore, M. Mortimer, F. F. F. Vetel, *J. Mater. Chem.* **2000**, *10*, 2131.
[18] F. J. Berry, J. Marco, A. T. Steel, *J. Alloys Compd.* **1993**, *194*, 167.
[19] J. Sauer, *Diploma Thesis*, Universität Frankfurt am Main, Frankfurt, Germany **1997**.
[20] M. Bredol, U. Kynast, C. R. Ronda, T. Welker, *German Patent DE 4122009*, **1993**.
[21] B. Yan, H. Zhang, *Mater. Res. Bull.* **1998**, *10*, 1517.
[22] P. A. Tanner, B. Y. H. J. Zhang, *J. Mater. Sci.* **2000**, *35*, 4325.

# High Electromechanical Responses in a Poly(vinylidene fluoride–trifluoroethylene–chlorofluoroethylene) Terpolymer**

By *Feng Xia, Zhongyang Cheng, Haisheng Xu, Hengfeng Li, Qiming Zhang,* George J. Kavarnos, Robert Y. Ting, Gomaa Abdel-Sadek*, and *Kevin D. Belfield*

Electroactive polymers (EAPs) that perform energy conversion between electric and mechanical forms are attractive for a broad range of applications, such as sensors, actuators, artificial muscles, and integrated micro-electromechanical systems.[1–3] Among various EAPs, the poly(vinylidene fluoride–trifluoroethylene), P(VDF-TrFE), piezo-polymer is the one that is most widely used.[2,4] Recently, we reported that after high-energy irradiation treatment P(VDF-TrFE) copolymers (high-energy electron-irradiated P(VDF-TrFE), referred to as HEEIP) can exhibit an electrostriction of 5 % and an elastic energy density higher than 0.5 J cm$^{-3}$, which represents about two orders of magnitude improvement compared with the P(VDF-TrFE) piezo-polymers.[5–7] Subsequent Fourier transform infrared (FTIR) and X-ray studies indicate that such a high electrostrictive response originates mainly from the dimensional change associated with the molecular conformational change.[7–10] In P(VDF-TrFE) copolymers, the molecular conformation changes are associated with electric dipolar change and, hence, external electric fields can be employed to induce electromechanical actuation in those polymers. This actuation mechanism can be utilized to form actuators from the molecular level to macroscopic level.

P(VDF-TrFE) is a ferroelectric polymer in which the ferroelectric phase possesses an all-*trans* conformation.[4] By heating the polymer to above the ferroelectric–paraelectric (F–P) transition temperature, the ferroelectric phase is transformed to a paraelectric (non-polar) phase, which has a mixture of *trans* and *gauche* bonds.[11] This molecular conformational change between the two phases results in strains of more than 7 %.[7,11] However, in P(VDF-TrFE) copolymers this transformation process occurs at temperatures near 100 °C and also involves a very large hysteresis.[7,11] The defects introduced by means of high energy irradiation break the long-range polar regions into microdomains,[8,10,12] thereby stabilizing the non-polar phase at room temperature and significantly reducing or

[*] Prof. Q. M. Zhang, Dr. F. Xia, Dr. Z.-Y. Cheng, Dr. H. S. Xu, Dr. H. F. Li
Materials Research Institute and Department of Electrical Engineering
The Pennsylvania State University
University Park, PA 16802 (USA)
E-mail: qxz1@psu.edu
Prof. G. J. Kavarnos
Department of Chemistry, University of Rhode Island
Kingston, RI 02881 (USA)
Prof. R. Y. Ting, Dr. G. Abdel-Sadek, Prof. K. D. Belfield
Department of Chemistry, University of Central Florida
Orlando, FL 32816 (USA)

[**] This work was supported by DARPA under Contract No. N00173-99-C-2003.

  0935-9648/02/2111-1574 $ 17.50+.50/0 

even eliminating the transformation barrier between the polar and non-polar phases. Consequently, at room temperature an external electric field can induce a continuous transformation from the non-polar to polar phase with very little hysteresis.[5,7,9] The direct link of this process to the conformation change results in a large electrostriction. More recently, it has been shown that a similar modification of the properties of P(VDF-TrFE) copolymer can also be realized by adding a third bulky monomer to form terpolymers that exhibit relatively large electrostriction.[13,14] In addition, the terpolymer approach has the advantage that it eliminates the irradiation process and hence simplifies the processing of the electrostrictive polymer besides removing the undesirable side effects caused by irradiation of the polymer, such as the formation of radicals, chain scission, and crosslinking.[15,16] In this communication, we will show that proper selection of the third monomer effectively reduces the all-*trans* conformation in the polymer; the terpolymer containing 1,1-chlorofluoroethylene (CFE) as the third monomer exhibits significantly improved electromechanical responses compared with other modified P(VDF-TrFE)-based polymers reported.

Figure 1a presents the field-induced strain along the thickness direction ($S_3$) as a function of the applied electric field ($E$). Under a field of 130 MV m$^{-1}$, a thickness strain of –4.5 %

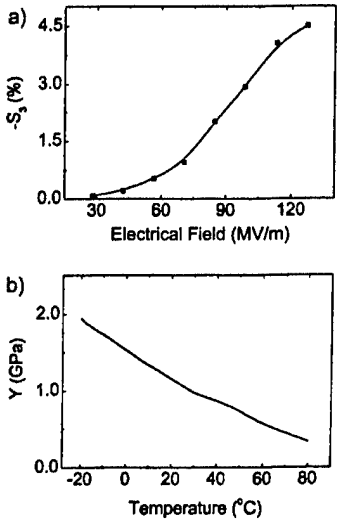


Fig. 1. a) Thickness strain $S_3$ as a function of the applied field amplitude for the terpolymer measured at room temperature at 1 Hz (dots are data points and the solid curve is drawn as a guide to the eye). b) Elastic modulus $Y$ of the terpolymer as a function of temperature measured at 1 Hz.

can be achieved, which is comparable to that observed in HEEIP and higher than those in the other terpolymers.[6,13,14] Because of higher crystallinity in the P(VDF-TrFE-CFE) terpolymer, the elastic modulus $Y$ of the terpolymer here is about three times higher than that of HEEIP and other terpolymers, as shown in Figure 1b, resulting in a higher elastic energy density, $YS^2/2 \approx 1.1$ J cm$^{-3}$. For most practical electromechanical applications, the elastic energy density is a key parameter that measures both the strain- and stress-generating capability of an electroactive material.

In Figure 2, we present the dielectric constant and the polarization measured on the terpolymer. The data reveal that despite a large difference in the electromechanical responses, the polarization response and dielectric behaviors are very

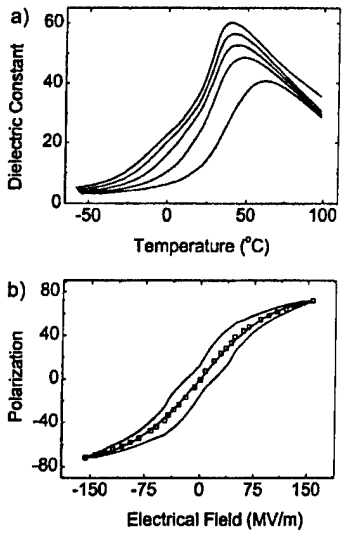


Fig. 2. a) The dielectric constant as a function of temperature measured at different frequencies: curves, from top to bottom, $10^2$, $10^3$, $10^4$, $10^5$, and $10^6$ Hz. b) The polarization response measured at room temperature and 1 Hz. The open squares are the average polarization and the solid line in the middle is the fit to the data using Equation 2.

similar to those observed in HEEIP and other terpolymers.[5,7,14] This can be understood from the fact that the polarization response in a polymeric material can originate from different mechanisms. Some of the polarization responses, such as 180° dipole flipping, generate very little strain response, while other polarization responses, such as the conformational changes discussed earlier, are accompanied by large strain changes.

Combining the electrostrictive strain, the elastic modulus, and the polarization data, the electromechanical coupling factor $k_{33}$ can be determined;[17] its square $k_{33}^2$ measures the energy conversion efficiency from the electric to mechanical form when the thickness strain is used. For an electrostrictive material, Equation 1 has been derived:[18]

$$k_{33}^2 = \frac{kS_3^2}{s_{33}^D\left[P_E \ln\left(\frac{P_s+P_E}{P_s-P_E}\right)+P_s \ln\left(1-\left(\frac{P_E}{P_s}\right)^2\right)\right]} \quad (1)$$

where $s_{33}^D$ is the elastic compliance under constant electric displacement and $P_s$ is the saturation polarization. As has been shown in earlier studies,[19] for ferroelectric-based electrostrictive materials, the polarization response $P_E$ can be approximated as:

$$|P_E| = |P_s| \tanh(kE) \quad (2)$$

Both $k$ and $P_s$ are determined from fits to the polarization data, as shown in Figure 2b; $E$ is the applied field. In the fit,

  0935-9648/02/2111-1575 $ 17.50+.50/0 

the averaged polarization (open squares) is used to remove the small polarization hysteresis in the data. As has been shown for HEEIP, the coupling factor derived in this manner is consistent with that measured using the resonance method based on the IEEE standard.[17] The longitudinal coupling factor thus determined is presented in Figure 3. It is interesting to note that the coupling factor can reach more than 0.55, which is far above coupling factors reported in all known piezoelectric and electrostrictive polymers (the electromechanical conversion efficiency is proportional to the square of the coupling factor).[17] In Table 1, we compare the electromechanical properties of four different types of P(VDF-TrFE)-based polymers, that is, the normal piezoelectric P(VDF-TrFE) copolymer, HEEIP, the P(VDF-TrFE-CFE) terpolymer studied here, and P(VDF-TrFE-CTFE) terpolymer reported earlier[5,7,14,20] (CTFE = chlorotrifluoroethylene). The latter three can be regarded as modified P(VDF-TrFE) polymers with defect structures. The terpolymer with CFE as a modifier shows the highest electromechanical responses among the four different PVDF-based polymers as well as other electroactive polymers reported.[21,22]

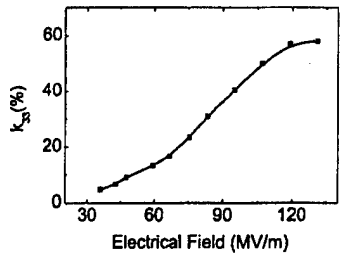


Fig. 3. The room-temperature longitudinal electromechanical coupling factor $k_{33}$ derived using Equation 1 for the P(VDF-TrFE-CFE) terpolymer.

Table 1. Comparison of the electromechanical properties of modified P(VDF-TrFE) polymers. $S_M$ is the maximum strain.

| Polymer | $S_M$ [%] | $Y$ [GPa] | $YS_M^2/2$ [J/cm$^3$] | $k_{33}$ |
|---|---|---|---|---|
| Piezo P(VDF-TrFE) | 0.2 | 3.3 | 0.0066 | 0.27 |
| HEEIP | –5 | 0.4 | 0.5 | 0.30 |
| P(VDF-TrFE-CTFE) | –4 | 0.4 | 0.32 | 0.28 |
| P(VDF-TrFE-CFE) | –4.5 | 1.1 | 1.1 | 0.55 |

Although all three modified P(VDF-TrFE)-based polymers listed in Table 1 possess a macroscopic non-polar phase with similar slim polarization hysteresis and field-induced polarization levels, the high electromechanical response observed in the CFE-based terpolymer indicates the important role played by the molecular microstructure.

P(VDF-TrFE)-based polymers are semicrystalline polymers, in which the polarization, and therefore the electromechanical responses, originates mainly from the crystalline regions.[4,23] In order to achieve a high electromechanical response, a high crystallinity is desirable. For the P(VDF-TrFE) copolymers in the composition range studied here, the crystallinity (the volume fraction of crystalline regions) can reach more than 75 %.[4,7] When a third monomer is added randomly to the polymer chain to form a terpolymer, the crystallinity, in general, will be reduced due to the introduction of defect structures. The crystallinity of a terpolymer depends on the type and the molar fraction of the third monomer. In order to use defects to convert the polymer into an electrostrictor there is a minimum molar fraction required for each type of monomer. Experimental results indicate that CFE is more effective in this regard compared with CTFE. In the terpolymers containing CFE studied here, 4 mol-% of CFE seems to be adequate to nearly eliminate the polarization hysteresis, while in the terpolymers containing CTFE nearly 10 mol-% is required.[13,14] Consequently, a 62:38:4 mol-% P(VDF-TrFE-CFE) terpolymer exhibits a higher elastic modulus in comparison with a 65:35:10 mol-% P(VDF-TrFE-CTFE) terpolymer, resulting in a higher elastic energy density and electromechanical coupling factor in the P(VDF-TrFE-CFE) terpolymer.

Furthermore, even for terpolymers with the same crystallinity, the field-induced strain level can still vary over a large range because of different types of polarization mechanisms responding to an external electric field. For instance, in the normal ferroelectric P(VDF-TrFE) copolymer, the polarization switching is through the dipolar reorientation process in the all-*trans* crystalline region, resulting in an observed relatively low strain change.[4,19] In the modified P(VDF-TrFE) polymers, it is possible that randomly oriented nanopolar regions (small regions with the all-*trans* molecular conformation) exist in the polymer, even though macroscopically the polymer is non-polar. The reorientation of those nanopolar regions under external fields may or may not generate high electrostrictive strains, depending on how these nanopolar regions respond to external electric fields. On the other hand, in the high-energy electron-irradiated copolymers, the FTIR data show that the room-temperature non-polar phase consists of mixture of *trans* and *gauche* (TG) bonds (a mixture of TGTG′ and $T_3GT_3G'$ conformations).[8,10] An externally applied field induces a reversible molecular conformation change from TGTG′ and $T_3GT_3G'$ to an all-*trans* conformation. As a result, a large electrostriction is obtained.[7–9] Analogously, in order to enhance the strain response in the terpolymers, it is highly desirable that the third monomer introduced will favor the formation of TG bonds rather than the all-*trans* conformation.

In order to examine the effectiveness of CFE in influencing the molecular conformations in the terpolymers, we compare the room-temperature FTIR data of 62:38:4 mol-% P(VDF-TrFE-CFE) with that of 65:35 mol-% copolymer and 65:35:10 mol-% P(VDF-TrFE-CTFE) terpolymer. The data are presented in Figure 4, which show that 4 mol-% CFE is as effective as 10 mol-% CTFE in reducing the all-*trans* conformation in the polymer. To quantify the results, the method by Osaki et al. (Eq. 3) was used to calculate the fraction $F_i$ of each chain conformation:[24,25]

$$F_i = \frac{A_i}{A_I + A_{II} + A_{III}} \quad (3)$$

where $i$ = I, II, III, and $A_I$, $A_{II}$, $A_{III}$ are the absorbencies of the chain conformations with all-*trans* ($T_{m>3}$, absorbance peak

  0935-9648/02/2111-1576 $ 17.50+.50/0 *Adv. Mater.* **2002**, *14*, No. 21, November 4

at 1285 $cm^{-1}$), $T_3GT_3G'$ (peak at 510 $cm^{-1}$), and TGTG' (peak at 610 $cm^{-1}$), respectively.[16,26] The results from the data fitting are listed in Table 2, and confirm that CFE is more effective compared with CTFE in reducing the all-*trans* conformation and converting the copolymer into an electrostrictive material.

The results show the importance of the third monomer in influencing the microstructure of the defect-modified P(VDF-TrFE) polymers. By proper molecular design, which enhances the molecular conformation changes accompanying the polarization responses under external electrical fields, the P(VDF-TrFE-CFE) terpolymer exhibits high electromechanical responses (elastic energy density $\approx 1.1\ J\,cm^{-3}$ and electromechanical coupling factor $\approx 0.55$).

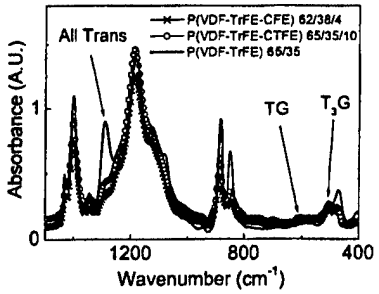


Fig. 4. Comparison of FTIR data among the copolymer (65:35 mol-%; solid curve), the terpolymer P(VDF-TrFE-CTFE) (65:35:10 mol-%; solid curve with open circles), and the terpolymer P(VDF-TrFE-CFE) (62:38:4 mol-%; solid curve with crosses).

Table 2. Comparison of the molecular conformations in three polymers.

| | % $T_{m>3}$ | % $T_3GT_3G'$ | % TGTG' |
|---|---|---|---|
| P(VDF-TrFE) 65:35 | 75 | 18 | 7 |
| P(VDF-TrFE-CTFE) | 34 | 61 | 5 |
| P(VDF-TrFE-CFE) | 36 | 55 | 9 |

## *Experimental*

Terpolymer P(VDF-TrFE-CFE) was synthesized by a bulk polymerization process [13,26]. The VDF/TrFE ratio was evaluated from $^{19}F$ NMR spectra; the CFE mol-% was determined by element analysis. The 62:38:4 mol-% terpolymer was used in this investigation because it exhibits the highest electromechanical response among several compositions synthesized. To facilitate the discussion and comparison with P(VDF-TrFE), the composition of the terpolymer is labeled as $VDF_x$-$TrFE_{1-x}$-$CFE_y$, where the molar ratio of VDF/TrFE is $x$:1–$x$ and $y$ is the mol-% of CFE in the terpolymer. The polymer films were prepared using the solution-cast method with dimethylformamide (DMF) as the solvent. The films were annealed at a temperature near 120 °C to improve the crystallinity. The typical film thickness is about 20 μm, and gold-sputtered electrodes on the two surfaces were used for the electric measurement. The strain along the thickness direction was characterized by means of a piezo-bimorph-based sensor [27]. The dielectric constant was acquired using a HP multifrequency LCR meter (HP 4284A), which was equipped with a temperature chamber. The Sawyer–Tower technique was used to characterize the polarization response in the film [28]. The elastic modulus was measured by a dynamic mechanical analyzer (DMA 2980, TA Instruments). The crystallinity of the polymer films was estimated using a differential scanning calorimeter (DSC 2920, TA Instruments). FTIR spectra were measured at room temperature (Nicolet 510 Spectrometer).

Received: January 14, 2002
Final version: June 12, 2002

[1] *Electroactive Polymer Actuators as Artificial Muscles* (Ed: Y. Bar-Cohen), SPIE, Bellingham, WA **2001**.
[2] T. T. Wang, J. M. Herbert, A. M. Glass, *The Applications of the Ferroelectric Polymers*, Chapman and Hall, New York **1988**.
[3] E. W. H. Jager, E. Smela, O. Inganäs, *Science* **2001**, *290*, 1540.
[4] *Ferroelectric Polymers* (Ed: H. S. Nalwa), Marcel Dekker, New York **1995**.
[5] Q. M. Zhang, V. Bharti, X. Zhao, *Science* **1998**, *280*, 2101.
[6] Z.-Y. Cheng, V. Bharti, T. B. Xu, H. Xu, T. Mai, Q. M. Zhang, *Sens. Actuators, A* **2001**, *90*, 138.
[7] Q. M. Zhang, J. Scheinbeim, in *Electroactive Polymer Actuators as Artificial Muscles* (Ed: Y. Bar-Cohen), SPIE, Bellingham, WA **2001**, Ch. 4.
[8] Z.-Y. Cheng, D. Olson, H. Xu, F. Xia, J. S. Hundal, Q. M. Zhang, F. B. Bateman, G. J. Kavarnos, T. Ramotowski, *Macromolecules* **2002**, *35*, 664.
[9] Q. M. Zhang, Z.-Y. Cheng, V. Bharti, *Appl. Phys. A–Mater. Sci. Process.* **2000**, *70*, 307.
[10] H. Xu, G. Shanthi, V. Bharti, Q. M. Zhang, T. Ramatowski, *Macromolecules* **2000**, *33*, 4125.
[11] K. Tashiro, in *Ferroelectric Polymers* (Ed: H. S. Nalwa), Marcel Dekker, New York **1995**, Ch. 2.
[12] Z.-Y. Cheng, Q. M. Zhang, *J. Appl. Phys*, in press.
[13] A. Petchsuk, T. C. Chung, in *Electroactive Polymers* (Eds: Q. M. Zhang, T. Furukawa, Y. Bar-Cohen, J. Scheinbeim), MRS Proceedings, Vol. 600, Materials Research Society, Warrendale, PA **1999**, p. 53.
[14] H. Xu, Z.-Y. Cheng, D. Olson, T. Mai, Q. M. Zhang, G. Kavarnos, *Appl. Phys. Lett.* **2001**, *78*, 2360.
[15] J. S. Forsythe, D. J. T. Hill, *Prog. Polym. Sci.* **2000**, *25*, 101.
[16] P. Y. Mabboux, K. K. Gleason, *J. Fluorine Chem.* **2002**, *113*, 27.
[17] *IEEE Standard on Piezoelectricity*, ANSI/IEEE Standard 176-1987, **1988**.
[18] C. Hom, S. Pilgrim, N. Shankar, K. Bridger, M. Masuda, S. Winzer, *IEEE Trans. Ultrason. Ferroelect. Freq. Control* **1994**, *41*, 542.
[19] X. D. Zhang, C. A. Rogers, *J. Intell. Mater. Syst. Struct.* **1993**, *4*, 307.
[20] T. Furukawa, *Adv. Colloid Interface Sci.* **1997**, *71*, 183.
[21] W. Lehmann, H. Skupin, C. Tolksdorf, E. Gebhard, R. Zentel, P. Kruger, M. Losche, F. Kremer, *Nature* **2001**, *410*, 447.
[22] J. Su, J. S. Harrison, T. S. Clair, Y. Bar-Cohen, S. Leary, in *Electroactive Polymers* (Eds: Q. M. Zhang, T. Furukawa, Y. Bar-Cohen, J. Scheinbeim), MRS Proceedings, Vol. 600, MRS, Warrendale, PA **1999**, p. 131.
[23] A. Lovinger, *Science* **1983**, *220*, 1115.
[24] S. Osaki, Y. Ishida, *J. Polym. Sci., Part B: Polym. Phys.* **1975**, *13*, 1071.
[25] H. S. Xu, G. Shanthi, V. Bharti, Q. M. Zhang, *Macromolecules* **2000**, *33*, 4125.
[26] T. C. Chung, W. Janvikul, *J. Organomet. Chem.* **1999**, *581*, 176.
[27] J. Su, P. Moses, Q. M. Zhang, *Rev. Sci. Instrum.* **1998**, *69*, 2480.
[28] J. K. Sinha, *J. Sci. Instrum.* **1965**, *42*, 696.

  0935-9648/02/2111-1577 $ 17.50+.50/0 

# APPENDIX 23

Mat. Res. Soc. Symp. Proc. Vol. 698 © 2002 Materials Research Society

# Device Fabrication and Performance of Electrostrictive P(VDF-TrFE) Based Actuators and Transducers

**Z.-Y. Cheng**, T.-B. Xu, J. Hundal, and Q. M. Zhang
Materials Research Institute and Department of Electrical Engineering, The Pennsylvania State University, University Park, PA 16802

Abstract: Taking advantage of the high electrostrictive strain and high elastic energy density of a newly developed electrostrictive P(VDF-TrFE) polymer, a flextensional transducer was designed and its performance was investigated. The flextensional transducer consists of a multilayer stack made of electrostrictive P(VDF-TrFE) polymer films and two flextensional elements which are fixed at their two ends to the multilayer stack, to perform the displacement amplification. Because of the large strain level achievable in the electrostrictive polymer and the displacement amplification of the flextensional elements, the device of a few mm thick and lateral dimension of 1"x1" can generate a displacement output of more than 1 mm along the thickness. The unique flextensional configuration and the high elastic energy density of the active polymer also enable the device to offer high load capability. As an underwater transducer, the device can be operated at frequencies below 2 kHz while still exhibit relatively high transmitting voltage response (TVR), very high source level (SL), and low mechanical quality factor ($Q_m$).

## INTRODUCTION

Solid-state electromechanical actuators and transducers have been widely used in many civilian and military applications including active vibration control, underwater navigation and surveillance, microphones, etc [1]. In many of these applications, transducers and actuators with high power and high displacement output are required. In the past several decades, a great deal of effort has been devoted to the development of electromechanical materials with those desired features [2,3]. In parallel, different device configurations have also been exploited to achieve the "amplification" of the relatively small strain level in most currently used piezoelectric, electrostrictive, and ferroelectric materials [4]. Recently, it was reported that in properly modified PVDF based ferroelectric polymers, i.e., through the high-energy electron irradiation or adding another bulkier ter-monomer to form a terpolymer [5-7], a massive electrostrictive response can be obtained.

In this paper, we investigate a flextensional transducer which takes advantage of the large strain and high elastic energy of this new class of electrostrictive polymer. It will be shown that for a flextensional transducer a few millimeters thick and 1"x1" lateral dimension, a displacement output of more than 1 mm can be generated with a relatively high loading capability (>10 N). One of the uniqueness of the device investigated here is that because of low acoustic velocity of the active polymer (~1400 m/s) and the flextensional configuration, such a small size device can be operated at frequencies below 2 kHz while is capable of generating a high source level (SL) (>185 dB per 1 μPa@1m) and a high transmitting voltage response (TVR) (~ 123 dB per 1 μPa/V@1m).

The recent results on the electromechanical properties of the electrostrictive P(VDF-TrFE) based polymers will first be summarized briefly with the aim of providing background of this newly developed material. In the flextensional transducer, multilayer stacks of the active polymers were used as the active element and the results on the fabrication and characteristics of

these multilayer stacks will be presented. The actuator performance and underwater performance of flextensional transducer will be presented and discussed.

In this investigation, the displacement generated by the flextensional actuator was evaluated by a DVRT (MicroStrain, Inc). For the underwater test, the transducer was placed in an anechoic water tank (5.3 m wide, 7.9 m long, and 5.5 m deep) 2.78 meter under the water.

## ELECTROMECHANICAL PROPERTIES OF ELECTROSTRICTIVE P(VDF-TRFE) POLYMERS AND MULTILAYER ACTUATORS

### Electromechanical properties of electrostrictive P(VDF-TrFE) based polymers

P(VDF-TrFE) is a well known ferroelectric polymer and in most cases, it is used as piezoelectric materials [8]. Compared with piezoceramics, the electromechanical responses of P(VDF-TrFE) piezopolymers are relatively low [9]. For instance, the piezoelectric $d_{33}$=-33 pm/V and the electromechanical coupling factor $k_{33}$=0.2, much below the level of the piezoceramics. In addition, the maximum piezoelectric strain level is about 0.1%. However, by a proper modification, P(VDF-TrFE) can be converted to an electrostrictive polymer with a high strain response and high elastic energy density [5]. For example, in high-energy electron irradiated P(VDF-TrFE), a thickness strain (longitudinal strain $S_3$) of –5% can be induced under a field of 150 V/μm [10]. In uniaxially stretched and irradiated P(VDF-TrFE) films, a transverse strain along the stretching direction of more than 4.5% (see figure 1) and an electromechanical coupling factor $k_{31}$ of 0.45 can be obtained. More interestingly, such kind of high electrostrictive response can also be obtained by non-irradiation approach [7]. In poly(vinylidene fluoride-trifluoroethylene-chlorofluoroethylene) [P(VDF-TrFE-CFE)] terpolymer, an electrostrictive strain $S_3$ of more than –5 % has been observed.

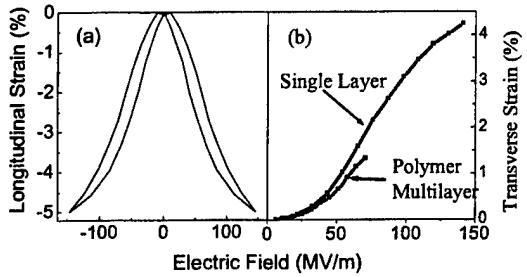


**Figure.1** (a) Longitudinal Strain versus electric field for unstretched and irradiated P(VDF-TrFE) 68/32 copolymer film; (b) Amplitude of transverse strain versus amplitude of electric field for stretched and irradiated P(VDF-TrFE) 68/32 copolymer film.

**Table I.** Elastic energy of some electroactive materials at room temperature

| Materials | Direction | Y (GPa) | $S_m$ (%) | $YS_m^2/2$ ($J/cm^3$) | $YS_m^2/2\rho$ (J/kg) | Stress (MPa) | Relative Speed |
|---|---|---|---|---|---|---|---|
| Piezo-ceramic (PZT-5H) | Longitudinal | 64 | <0.2 | 0.13 | 17 | 128 | >1 MHz |
| | Transverse | 64 | <0.1 | 0.03 | 4 | 64 | |
| Piezo P(VDF/TrFE) | Longitudinal | 4 | <0.15 | 0.0045 | 2.5 | 6 | >1 MHz |
| Irradiated P(VDF/TrFE) | Longitudinal | $Y_{33}$=0.5 | 5.0 | 0.63 | 313 | 25 | >100 kHz |
| | Transverse | $Y_{11}$=1.0 | 4.0 | 0.8 | 400 | 40 | |
| P(VDF/TrFE) based terpolymer | Longitudinal | $Y_{33}$>1.1 | 4.5 | 1.1 | 557 | 45 | >100 kHz |

Table I summarizes those results. For electromechanical applications, in addition to the maximum induced strain, the elastic energy density is another important parameter. In the table, both gravimetric elastic energy density ($YS_m^2/2\rho$) that is related to device weight and volumetric energy density ($YS_m^2/2$) that is related to the device size, are included, where Y, $S_m$ and $\rho$ are the Young's modulus, maximum induced strain, and density of the material. The data for the piezoceramic and piezopolymer P(VDF-TrFE) are also listed for the comparison.

**Fabrication and characterization of multilayer stacks**

Most of the piezoceramic based actuators are in the multilayer form. The main purpose of the multilayer approach is to reduce the applied voltage. In the current design of the flextensional transducer (see figure 2) employing the electrostrictive P(VDF-TrFE) as the active element, multilayer stacks were also used to reduce the driving voltage. The uniaxially stretched high-energy electron irradiated P(VDF-TrFE) films were chosen since it delivers high transverse strain response and high electromechanical coupling factor.

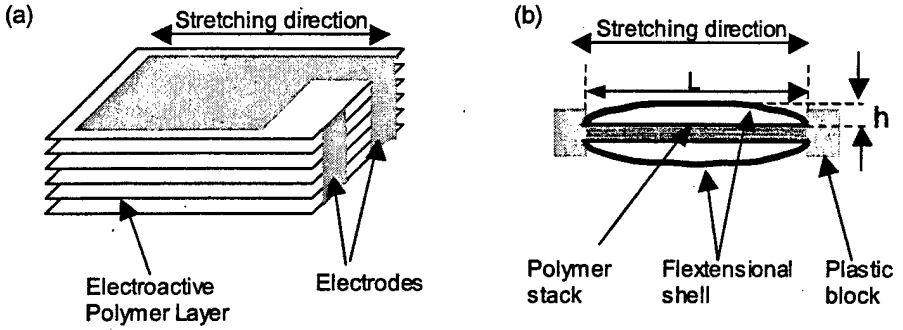


**Figure 2.** (a) Multilayer structure used in this investigation and the electrode pattern. (b) Flextensional transducer configuration.

The preparation and irradiation of the copolymer films have been described in earlier publications [6]. The films after irradiation have an average thickness of 15 μm. The multilayer stacks were fabricated in three steps. First, the two irradiated films were bonded together to form a bilayer to improve the dielectric strength. Those bilayers were electroded by Au sputtering to the required electrode pattern as shown in figure 2(a). The electroded bilayers were finally laminated together to form a multilayer stack. To ensure an effective stress and strain coupling between the electroactive polymer layers while maintaining high electromechanical performance, the epoxy glue should meet two requirements: provide relatively strong bonding between polymer films and the glue layer thickness should be thin. A series of epoxy glue materials were examined in this investigation, including Spurr epoxy (Polysciences, Inc.), Strain glue, 30 minutes epoxy, and different Cyanoacrylate adhesives. It was found that among them, Spurr epoxy yields the thinnest bonding layer thickness (1 μm or below) and also offers relatively strong bonding strength as tested by the peeling method.

For the multilayer stacks thus prepared, as observed in figure 1, the field induced strain of a multilayer stack is 77% of the single layer strain and the elastic modulus of the multilayer stack is higher than that of polymer film.

For the flextensional transducers to be investigated, multilayer stacks of 1 mm thickness, consisting of 30 layers of irradiated copolymer bilayer films (the thickness of each bilayer is 31

μm), were used. The electroded area is 22 mm x 22mm while the sample width and length (parallel to the stretching direction) are 25 mm and 31 mm, respectively.

The high frequency performance of the multilayer stacks was examined in terms of its electromechanical resonance. As shown in figure 3, an electromechanical resonance at about 17 kHz, which corresponds to the resonance along the length direction of the multilayer stack, was observed when the multilayer stack was under a DC bias field of 17 V/μm. The resonance was very similar to that observed in single layer films. Because of relatively low electromechanical response for the active polymer films in perpendicular to the polymer film stretching direction, no strong resonance was detected along the width direction of the multilayer stack.

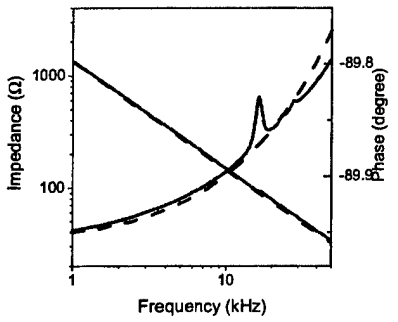


**Figure 3.** The impedance (|Z|) and phase angle of a flextensional transducer under a DC bias of 17 V/μm.

## ACTUATOR PERFORMANCE OF THE FLEXTENSIONAL TRANSDUCER

As has been demonstrated in earlier investigations by Newnham, *et al* [11,12], a flextensional actuator with a structure shown in figure 2(b) can generate relatively large displacement and also force output. Because of the much higher strain level in the electrostrictive P(VDF-TrFE), it is expected that such a device based on those active polymers will produce large displacement with relatively high force output.

The displacement observed at 1 Hz in flextensional transducers with different displacement amplifications is presented in figure 4. In the transducer, two plastic blocks (made of plexiglass) as shown in figure 2(b) to hold the spring steel sheet as the flextensional elements, are attached (glued using 30 minutes epoxy and mechanical screws) to the two ends of the multilayer stack. The spring-steel sheets are forced to fit into the plastic blocks to form an arc shape.

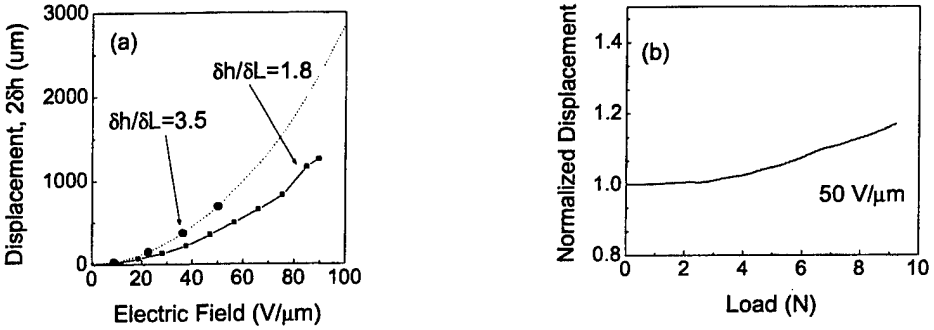


**Figure 4.** (a) Displacement output of two flextensional transducers versus external electric field of 1 Hz. (b). Displacement output of a flextensional transducer, which corresponds to δh/δL=1.8 in (a), versus external mechanical load. Where δh/δL is the displacement amplification ratio, that is, the δh is the displacement at middle point of the transducer corresponding to the length change (δL) of the multilayer.

It should be noted that in each flextensional transducer, there are two flextensional elements, generating total displacement 2δh (the data in figure 4(a) is 2δh). It is interesting to note that the

displacement output of such a device can be more than 1 mm. In addition to the high displacement output, the flextensional transducer with EAP stacks also exhibits relatively high load capability.

## TRANSDUCER PERFORMANCE OF THE DEVICE

For the underwater test, the flextensional transducer was sealed by a polymer of low elastic modulus (polyurethane, trademark CONATHANE@EN-9, CONAP, Inc.). The polyurethane coating serves two purposes: to provide electric insulation of the transducer from the water and to prevent the water from leaking into the space between the flextensional shell and EAP stack.

Both the TVR and FFVS of the transducer were characterized by a hydrophone placed 3.3 meters away from the transducer with one flextensional element directly facing the hydrophone and the other facing in the opposite direction. The directivity pattern was measured by rotating the transducer. In the frequency range from 1 kHz to 5 kHz, it was found that the transducer shows an omnidirectional pattern. This is due to the fact that the dimension of the transducer is much smaller that the acoustic wavelength which is 1.5 m at 1 kHz and 0.3 m at 5 kHz, respectively. The observed TVR and FFVS are presented in figure 5.

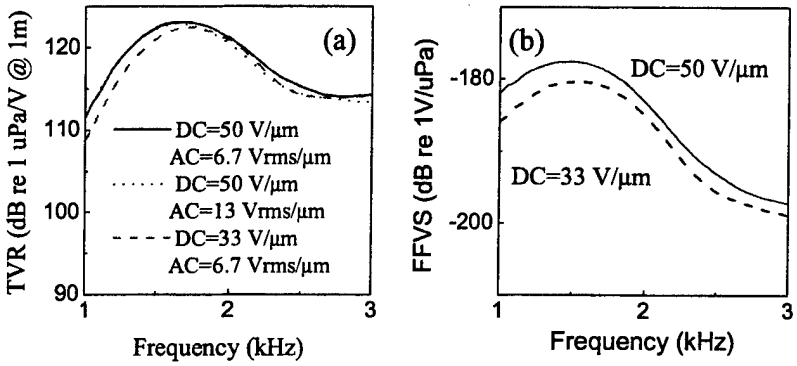


**Figure 5.** (a) TVR versus frequency for a flextensional transducer under different DC bias and with different driving AC filed. (b). FFVS (Free-Field Voltage Sensitivity) versus frequency for the same transducer.

The TVR curve exhibits a broad resonance around 1.7 kHz, which results in a low mechanical quality factor $Q_m$ [$=f_r/(f_h-f_l)$] of the projector, where $f_r$ is the resonance frequency, while $f_h$ and $f_l$ are the half-power frequencies which can be determined from the –6 dB points in the TVR curve. For the transducer examined here, $Q_m$=1.55. The TVR near the resonance is 122.5 and 123.2 dB re 1 μPa/V @1m for the device under DC bias fields of 33 V/μm and 50 V/μm, respectively.

For an electrostrictive material such as the irradiated P(VDF-TrFE) copolymers used here, an effective piezoelectric state can be induced by a DC bias electric field. Thus, the material can also be used in sensing the acoustic signals. For a DC bias field of 50 V/μm, the FFVS of the flextensional transducer can reach –177.5 dB re 1V/μPa near the resonance frequency.

As an electrostrictive material, the electromechanical response increases with DC bias field if the DC field is far below the saturation field, which is the case for the DC fields used here as can be seen from figure 1. The observed increase in both TVR and FFVS is consistent with this.

In addition to the relatively high TVR at such a low frequency, the flextensional transducer is also capable of generating high source level (SL) because of its high saturation field (figure 1). For the flextensional transducer investigated here, a field of 50 V/μm is equal to 1500 volts applied to each bilayer (about 30 μm thickness). If such a field is applied to the transducer, a SL of more than 186 dB re 1 μPa@1m can be achieved. It should be noted that because the

transducer dimension in the current device is much smaller than the acoustic wavelength, the acoustic impedance $Z_a$ of the medium (water) as seen by the transducer is nearly imaginary (mass-like load). As a result, the transducer efficiency is low. By working with an array with increased source dimension, the efficiency can be improved significantly.

## SUMMARY

A flextensional transducer is developed, which employs the high strain electrostrictive P(VDF-TrFE) as the active element and two ends fixed flextensional elements to achieve displacement amplification. In the current design, a multilayer stack was used. Because the actuation of the active polymer is along the film surface direction, the flextensional elements are designed to ensure the active polymers are under tension.

Both actuator and transducer performances of the flextensional transducer are presented. It is shown that the device (1"x1" lateral dimension and a few mm thick) is capable to generate a displacement of more than 1 mm with a load of more than 10 N. As an underwater transducer, the device exhibits a resonance low frequency (<2 kHz) while generating a relatively high TVR (~123.2 dB re 1 μPa/V @1m), FFVS (~–177.5 dB re 1V/μPa). Because of the high saturation field, the device has the capability to achieve a SL of more than 185 dB per 1 μPa@1m

## ACKNOWLEDGEMENT

This work was supported by DARPA and ONR.

## REFERENCE

1. K. Uchino, *Piezoelectric Actuators and Ultrasonic Motors* (Kluwer Academic Publisher, Boston, 1997).
2. L. E. Cross, *Ceramic Trans.* **68**, 15 (1996).
3. E. Fukada, *IEEE UFFC* **47**, 1277 (2000).
4. J. D. Zhang, Ph.D thesis, The Pennsylvania State University (2000).
5. Q. M. Zhang, V. Bharti, and X. Zhao, *Science*, **280**, 2101 (1998).
6. Z. -Y. Cheng, T. -B. Xu, V. Bharti, and Q. M. Zhang, *Appl. Phys. Lett.* **74**, 1901 (1999).
7. H. Xu, Z.-Y. Cheng, D. Olson, T. Mai, and Q.M. Zhang, *Appl. Phys. Lett.* **78**, 2360 (2001).
8. T. T. Wang, J. M. Herbert, and A. M. Glass, *Applications of Ferroelectric Polymers* (Chapman and Hall, New York, 1988).
9. Q.M. Zhang, Z.-Y. Cheng, V. Bharti, T.-B. Xu, in *Electroactive Polymer Actuators and Devices* (EA*PAD)*, edited by Y. Bar-Cohen, *(Proc. SPIE.* **3987**, 2000), p34.
10. Q. M. Zhang, Z.–Y. Cheng and V. Bharti, *Appl. Phys. A* **70**, 307 (2000).
11. Q.C. Xu and R.E. Newnham, *IEEE UFFC* **38**, 634 (1991).
12. J.D. Zhang and R.E. Newnham, *IEEE UFFC* **48**, 560 (2001).

# APPENDIX 24

Mat. Res. Soc. Symp. Proc. Vol. 698 © 2002 Materials Research Society

# Chemical and Physical Changes Associated with High-Strain Electrostriction In Beta-Irradiated PVDF-TrFE

Thomas Ramotowski, O. Richard Hughes, George Kavarnos,* Karen Gleason,** Qiming Zhang,*** and Robert Ting****
Naval Undersea Warfare Center, Newport, RI 02841
*University of Rhode Island, Kingston, RI 02881
**Massachusetts Institute of Technology, Cambridge, MA 02139
***Pennsylvania State University, University Park, PA 16802
****University of Central Florida, Orlando, FL 32816

## ABSTRACT

In 1998, Zhang *et al.* [1] demonstrated that large doses of high-energy beta radiation could transform certain vinylidene fluoride-trifluoroethylene (PVDF-TrFE) copolymers into high-strain electrostrictors. Since that time, U.S. Navy researchers and their colleagues have been analyzing irradiated PVDF-TrFE copolymers to determine what physical and chemical changes are associated with the materials' desirable high-strain electrostictor properties. The most obvious radiation-induced structural change is the introduction and retention of more *gauche*-type linkages in the PVDF-TrFE polymer chains at room temperature as evidenced by FT-IR spectroscopy, and X-ray diffraction data. These additional *gauche* linkages function as defects in the long, all-*trans* sequences normally found in PVDF-TrFE copolymers and, in effect, break up those sequences into the nano-polar domains necessary for high-strain electrostriction. The key role played by the beta radiation in this scenario appears to be the introduction of chemical changes (pendant groups, cross-links and carbon-carbon double bonds) that preserve a higher percentage of *gauche* linkages below the polymer's Curie temperature. TGA, TGA-MS, 19-F NMR, FT-IR, and DMA data supporting the existence of these beta radiation-induced chemical changes will be presented. This research has important implications for synthetic polymer chemists interested in improving the existing materials and/or creating new, high-strain polymeric electrostrictors with or without the use of beta radiation.

## INTRODUCTION

Ferroelectric polyvinylidene fluoride PVDF and vinylidene fluoride-trifluoroethylene copolymers PVDF-TrFE have earned a niche as choice transducer materials for undersea sensors and projectors [2]. This interest is in part due to the lower weight, greater conformability/flexibility, and easier fabrication of these electroactive polymers as compared to lead-based ceramics that have been the traditional materials of choice in Navy sonar applications. Still, piezoelectric polymers such as PVDF and PVDF-TrFE suffer from relatively low energy densities and low coupling. In 1998, researchers at Penn State University demonstrated that PVDF-TrFE copolymer films can be converted into high strain/high energy density materials by electron bombardment [1]. Beta radiation converted normal, ferroelectric copolymer into a relaxor ferroelectric exhibiting electrostrictive strains exceeding 4%. The discovery of so-called "giant" electrostrictive strains in PVDF-TrFE copolymers has renewed

interest for the use of these materials in a variety of applications such as transducers, actuators, and sensors.

To fully achieve the potential of electrostrictive PVDF-TrFE for these applications, it is desirable to understand the effects of irradiation on the chemical and physical structure of the copolymer. The ultimate goals of this research are: (1) to improve certain properties of the high-strain electrotrictive copolymer (e.g., lower the dielectric losses, improve electromechanical coupling, and reduce the required coercive fields), and (2) to eliminate the need for beta irradiation and produce high-strain, electrostrictive PVDF-TrFE copolymers solely via chemical synthesis.

## EXPERIMENT

PVDF-TrFE copolymer powder, 65 mol% VDF and 35 mol% TrFE, was obtained from Solvay and Cie (Brussels, Belgium). The mean molecular weight was about 200,000. Films were fabricated by solvent-casting from methyl ethyl ketone, followed by annealing for one hour at 140°C and cooling to room temperature. The film thicknesses ranged from about 5 μm to over 200 μm. The PVDF-TrFE films were irradiated with 1.2 and 2.55-MeV electrons in a nitrogen atmosphere at selected temperatures. The total absorbed doses were from 20 to 200 Mrads. The electron irradiation experiments were performed at the Massachusetts Institute of Technology's High Voltage Research Laboratory in Cambridge, MA.

Thermogravimetric analysis (TGA) data were collected using a TA Instruments model 2950 TGA. TGA/GC-MS experiments were performed under the direction of Dr. Wei-Ping Pan at Western Kentucky State University using a TA Instruments model 2960 SDT interfaced to a Pegasus II GC-MS system. Dynamic mechanical analysis (DMA) data were collected using a TA Instruments model 2980 DMA. Fourier transform infrared (FTIR) spectra were recorded at room temperature using a Nicolet model 510 Fourier transform infrared spectrometer. Ultraviolet (UV) absorption spectra of the films were obtained with a Perkin-Elmer Lambda 14 ultraviolet-visible spectrometer. X-ray diffraction (XRD) experiments were performed using a Philips model PW-3040 X'Pert X-ray diffractometer. Nuclear magnetic resonance (NMR) experiments were performed under the direction of Professor Karen Gleason at the Massachusetts Institute of Technology using a homebuilt spectrometer tuned to the $^{19}F$ Larmor frequency of 254.0 MHz. A Chemagnetics 3.2 mm variable temperature solids probe capable of a maximum spinning speed of 25 kHz was used to achieve high resolution magic angle spinning (MAS).

## RESULTS

TGA data from irradiated and unirradiated PVDF-TrFE copolymer film samples indicated that irradiation makes the copolymer samples less thermally stable. The 2% TGA conversion temperatures for irradiated samples were lower than the corresponding value for unirradiated films. In addition, as the absorbed dose increased, the 2% conversion temperature decreased. These data were confirmed by TG-GC/MS experiments. Irradiated samples exhibited mass loss events beginning at about 200°C that were caused by the loss of $-CF_3$ and $-CH_2CF_3$ fragments from the polymer chains. These types of fragments were not seen in TG-GC/MS experiments conducted on unirradiated films. Both irradiated and unirradiated films exhibited mass loss events characterized by the loss of $CO_2$, $H_2O$ and HF at temperatures above 250°C.

$^{19}F$ solid state magic angle spinning NMR experiments indicated that the major change in PVDF-TrFE copolymer upon irradiation was the appearance of $-CF_3$-containing pendant and end groups. The most abundant of the new groups was the $>CH-CF_3$ pendant group. Detected in smaller abundances were $-CF_2-CF_3$, $-CHF-CF_3$, and $-CH_2-CF_3$ end groups, as well as an unsaturated end group, $=CH-CF_3$. The abundance of these –CF3-containing groups increased linearly with the absorbed dose. The NMR spectra of irradiated films were not as sharp or as detailed as the spectra of their unirradiated counterparts. This is believed to be a result of crosslink formation in the irradiated samples.

UV-Vis spectroscopy detected the presence of a "shoulder" superimposed on the "normal" (i.e., unirradiated) PVDF-TrFE copolymer UV-Vis spectrum between 200 and 250 nm for all irradiated samples. This intensity of this "shoulder" increased as the absorbed dose increased.

FT-IR spectroscopy indicated that, as the absorbed dose increased, the infrared spectra of the irradiated PVDF-TrFE films at room temperature began to look more and more like the spectra of unirradiated films above their Curie temperature [3,4,5]. Infrared absorptions indicative of all-trans conformations decreased in intensity, while those indicative of *tttg* and *tgtg* conformations increased in intensity (figure 1). At the highest absorbed doses examined during this study, this trend began to reverse. In addition, the infrared spectra of irradiated samples exhibited absorptions between 1700 $cm^{-1}$ and 1800 $cm^{-1}$ indicative of carbon-carbon double bonds.

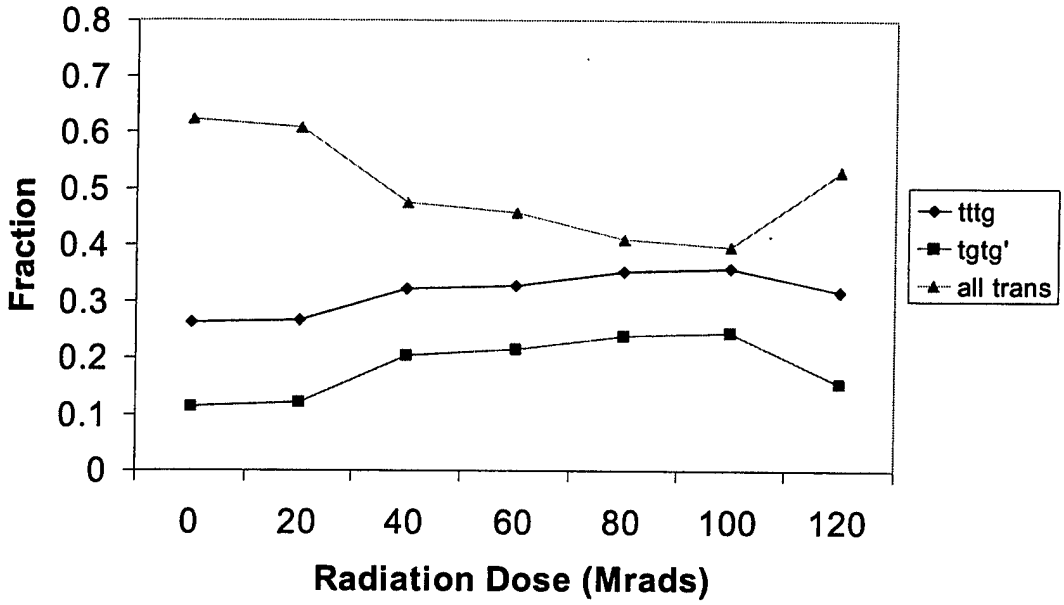


**Figure 1:** Effects of beta radiation on polymer chain conformations in 65/35 PVDF-TrFE

Wide-angle XRD experiments yielded data similar to those provided by FT-IR spectroscopy (figure 2).Unirradiated samples, and samples that had absorbed very low doses of beta radiation, exhibited a (200/110) peak [6] between 19.6° and 20.0° 2θ characteristic of type I (all-trans) crystallites in PVDF-TrFE. At absorbed doses greater than 40 Mrads, the (200/110) peak shifted

to a value between 18.4° and 18.8° 2θ. Those values are characteristic of the type II (*tgtg*) crystallites in PVDF-TrFE. At an absorbed dose of 120 Mrads, the (200/110) peak was located at 18.6° 2θ, but a minor peak was also visible at 19.6° 2θ. This minor peak (also seen in samples with beta radiation doses of 40 and 60 Mrads) is indicative of the all-trans polymer conformation. At 40 and 60 Mrad doses, the minor 19.6 2θ peak represents some of the originally-present all-trans sequences surviving the electron bombardment. The reappearance of this peak in the 120 Mrad dose sample indicates some significant trans sequences are regenerated in higher dose samples.

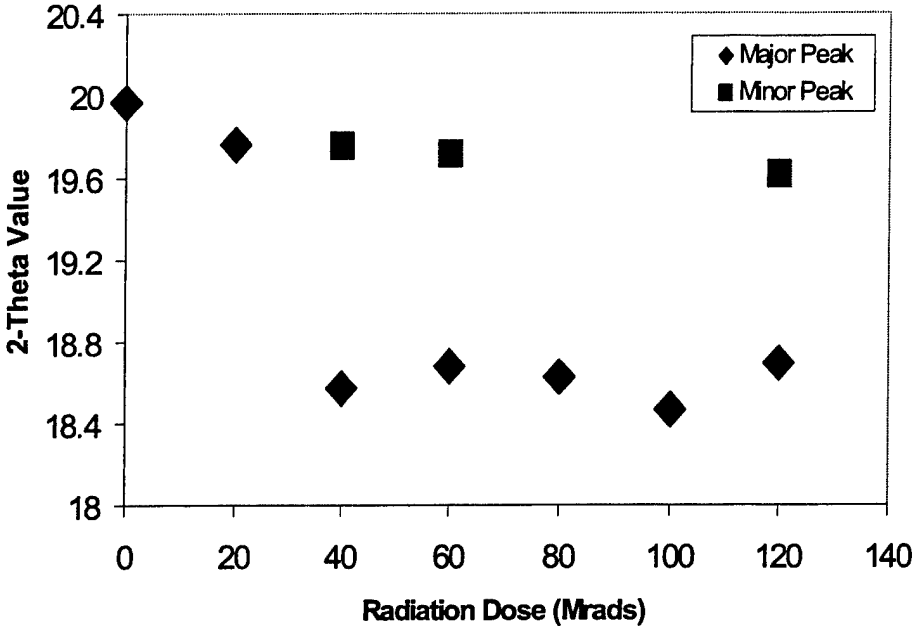


**Figure 2:** Effects of beta radiation on the (200/110) XRD peak for PVDF-TrFE

DMA traces were obtained from unirradiated PVDF-TrFE and from PVDF-TrFE samples that had absorbed up to 120 Mrads of beta radiation. The post-glass transition E' values did not increase with the absorbed radiation dose. Instead, the E' values for all of the irradiated samples were lower than corresponding E' values for unirradiated PVDF-TrFE. DMA data (figure 3) also indicated that the glass transition temperature of the PVDF-TrFE samples initially increased as the absorbed dose increased; however, at an absorbed dose of 80 Mrads, this trend stopped, and thereafter reversed.

## DISCUSSION

From the experimental observations accumulated to date, a clearer picture is emerging of the effects of electron-irradiation on PVDF-TrFE and the consequences of these changes on the ferroelectric and relaxor properties of this material. The available literature on radiation chemistry of fluoropolymers indicated that the dominant change should be chain scission/molecular weight reduction if the irradiation was carried out below the polymer's

melting temperature, and crosslinking/molecular weight increases if it was carried out at temperature above the melting point [7,8,9,10,11]. One study [12] indicated that some carbon-carbon double bonds might be produced. The present study has produced strong evidence for two chemical changes (pendant group and carbon-carbon double bond formation) in addition to the expected chain scissioning events. Evidence was also obtained that crosslinks may form in PVDF-TrFE when it is irradiated below its melting temperature, as has been reported by other researchers [13].

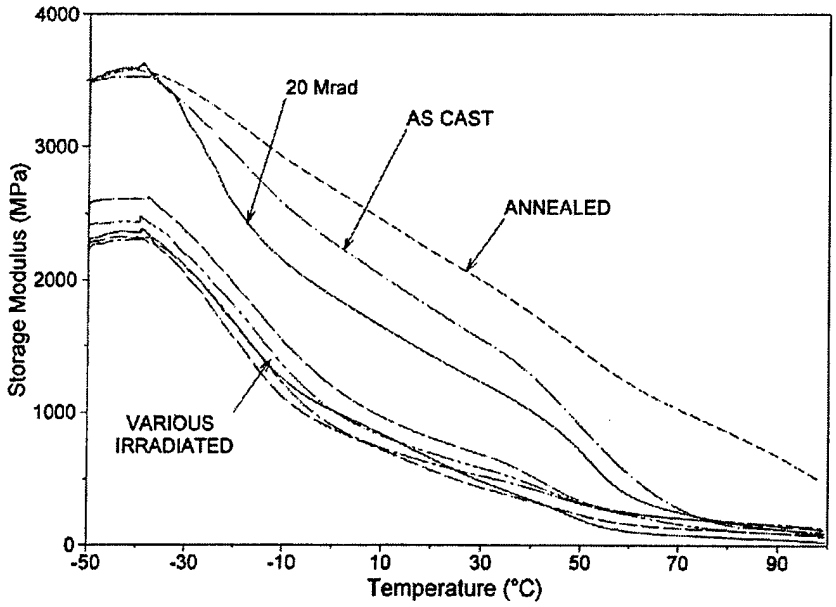


**Figure 3:** DMA E' data from irradiated and unirradiated samples.

The $^{19}F$ NMR, TGA, and TG-GC/MS results are consistent with the formation of pendant groups on the main polymer chains. The majority of these groups appear to be small (one or perhaps two carbon atoms in length). The attachment points for branches to the main polymer chains tend to be the weakest links in such polymers, and the loss of those branches upon heating (as in a TGA experiment) would be expected before evidence was seen of the main chains themselves breaking down.

One might question whether or not a significant amount of chain scission also occurs during the irradiation process. The data collected to date suggest that chain scission is not a major factor until the samples absorb large amounts of beta radiation (> 80 Mrads). The major evidence for this is the DMA data documenting the change in glass transition temperature with absorbed dose. Up until an absorbed dose of ≈ 70 Mrads is reached, the glass transition temperature of the polymer increases, while at the same time (as evidenced by TGA data) its thermal stability is decreases. These two data sets are inconsistent with large amounts of either crosslinking or chain scission, but they are consistent with pendant group formation.

Evidence for the formation of some unsaturated carbon-carbon bonds now exists from at least three sources. The UV-Vis spectra's absorption "shoulder" that increases in intensity with absorbed dose is consistent with the presence of some carbon-carbon double bonds in the

irradiated films, as are the absorptions detected between 1700 $cm^{-1}$ and 1800 $cm^{-1}$ by FT-IR spectroscopy. Direct evidence for the generation of at least some carbon-carbon double bonds was obtained from the $^{19}F$ NMR experiments.

The effects of high doses of beta radiation (>100 Mrads) on PVDF-TrFE copolymers are interesting. Until these high doses are reached, the net result of all the radiation-induced chemical changes is to make PVDF-TrFE copolymers contain more type II (*tgtg*) and type III (*tttg*) conformations at room temperature. Normally, such forms are not favored at such low temperatures, and form I (all trans) is the dominant conformation. At the highest absorbed doses, however, the formation of form I polymer chain conformations appears to be favored within the crystallites. These observations are supported by both FT-IR spectroscopy and wide-angle XRD data. In addition, DMA glass transition data indicate the glass transition of the irradiated copolymer begins to decrease at these high absorbed doses. All of these observations are consistent with an increase in the number of chain scission events at the expense of the other types of changes previously discussed.

## CONCLUSION

The chemical and conformational changes documented during the course of this study have indicated that the electromechanical properties of irradiated PVDF-TrFE films are sensitive to the types of changes the electron bombardment produces within the films. The kinds of changes produced vary with the absorbed dose. To date, the best performing (in an electromechanical sense) irradiated films typically are those that have absorbed between 60 and 80 Mrads of beta radiation. Those doses are at the upper end of the range where pendant groups, crosslinks and carbon-carbon double bonds are generated, but are not high enough for chain scission to be the dominant radiation-induced change in the polymer. Up until a dose of about 100 Mrads, the radiation-induced changes in the PVDF-TrFE samples tend to preserve *gauche*-type conformations at the expense of all-trans conformations. At doses above 100 Mrads, the dominant radiation-induced change in the copolymer samples becomes chain scission, and the trans/*gauche* trend reverses. This suggests that chemical changes that preserve a higher than normal amount of *gauche* character within the copolymer are critical to the "giant" electrostrictive effect in PVDF-TrFE. These observations provide a great deal of insight into the mechanism of "giant" electrostriction in PVDF-TrFE films, and they provide important information for synthetic polymer chemists interested in producing "giant" electrostrictor polymers without the use of radiation.

## ACKNOWLEDGEMENTS

We gratefully acknowledge Kenneth Wright of MIT's High Voltage Research Laboratory for assistance with the irradiation experiments, and Dr. Wei-Ping Pan of Western Kentucky State University for assistance with the TG-GC/MS experiments. This work was funded by the Office of Naval Research and DARPA.

## REFERENCES

1. Q. Zhang, V. Bharti, and X. Zhao, Science **280**, 2, 101 (1998).

2. J. Lindberg, Mat. Res. Soc. Symp. Proc. **459**, 509 (1997).

3. A. B✦chtemann and R. Danz, Vibrational Spec., **11**, 93, (1996).

4. Kaura, T. and V. Bharti, J. Poly. Mat., **11**, 295, (1994).

5. H. Xu, G. Shanthi, V. Bharti, Q. Zhang, and T. Ramotowski, Macromolecules, **33**, 4125, (2000).

6. J. Day, E. Lewis, and G. Davies, Polymer, **33**, 1571, (1992).

7. T. Yoshida, R. Florin, and L. Wall, J. Poly. Sci. Part A, **3**, 1685, (1965).

8. W. Fisher and J. Corelli, J. Poly. Sci. (Poly. Chem.), **19**, 2465, (1981).

9. B. Fuchs and U. Scheler, Macromolecules, **33**, 120, (2000).

10. J. Forsythe and D. Hill, Prog. Polym. Sci., **25**, 101, (2000)

11. Scheler, U., Solid State Nuc. Mag. Reson., **12**, 9, (1998).

12. W. Burger, K. Lunkwitz, G. Pompe, A. Petr, and D. Jehnichen, J. Appl. Poly. Sci., **48**, 1973, (1993)

13. G. Buckley and C. Roland, Appl. Phys. Let., **78**, 622, (2001)

# APPENDIX 25

Mat. Res. Soc. Symp. Proc. Vol. 698 © 2002 Materials Research Society

# Molecular Modeling Studies on High-Strain, Electrostrictive Terpolymers

George J. Kavarnos, Thomas Ramotowski[1], Richard Hughes[1], Qiming Zhang[2] and Dana Olson[2]
Department of Chemistry, University of Rhode Island
Kingston, R. I. 02881, U. S. A.
[1]Submarine Sonar Department, Naval Undersea Warfare Center Division
Newport, R. I. 02841, U. S. A.
[2]Materials Research Laboratory, The Pennsylvania State University
State College, PA 16802, U. S. A.

## ABSTRACT

The finding that irradiation of copolymer films serves to break up the large crystalline regions into polar microregions resulting in a high-strain electrostrictive material has prompted an investigation to identify alternative routes to electrostriction. To determine whether these changes could be reproduced without the need for electron-irradiation, computations on PVDF-TrFE) terpolymer chains containing small levels a third monomer incorporating chlorine have provided a theoretical framework to support the hypothesis that the introduction of chlorine in the polymer chain can produce similar structural defects that disrupt the polar all-*trans* regions into smaller regions. These calculations demonstrate that polar nano-regions can be created since introduction of bulky chlorine atoms into the polymer chains creates conformational defects that provide the mechanism to break up the long-range crystalline regions. The disrupted polar regions can be regarded as distorted defect structures that give rise to random fields and electrostriction. Theoretical predictions as well as experimental support will be presented that show that certain chloro-monomers such as –CFCl-$CH_2$- are indeed quite able to convert P(VDF-TrFE) films into high-strain, electrostrictive films.

## INTRODUCTION

Electrostriction refers to the high strains displayed by certain materials when stressed by electric fields. The magnitude of the electrostrictive strain can be described by the following equation:

$$S = QP^2 \qquad (1)$$

Where Q is the electrostrictive coefficient and P the polarization of the material [1]. Most materials in nature are electrostrictive but only a few have actually been considered for applications requiring large strains. For example, ferroelectric polymers such as poly(vinylidene fluoride-trifluoroethylene) [P(VDF-TrFE)] films, previously annealed, can be converted into an electrostrictive material by exposure to high energy electron-bombardment [2]. It is believed that

electron bombardment of high crystalline P(VDF-TrFE) films breaks up the long-range ferroelectric region into polar microdomains thereby broadening the ferroelectric-to-paraelectric transition and moving the transition to a lower temperature where high strains can be observed when the films are driven by large electric fields. Differential scanning calorimetry, x-ray diffraction, and fourier transform infrared spectroscopy have been used to characterize the changes in the polymer films on electron bombardment and the ensuing effects on polymer structure [3]. These experiments support a theory where the polar all-*trans* form I ($\beta$), long-range ferroelectric regions of annealed P(VDF-TrFE) films are converted by electron-bombardment into nanoregions consisting of coexisting I, II ($\alpha$), and III ($\gamma$) crystallites. The collective polarizations of these crystalline regions give rise to a macroscopic polarization and increase in the dielectric constant. In form II, the packed chains exhibit the *tgtg'* (*t* = trans; *g,g'* = gauche) conformation, resulting in a nonpolar crystallite. In form III crystals, where the chain conformations are *tttgtttg'* the crystal lattice is monoclinic, and the alignment of the form III chains perpendicular to the chain axis is in one direction resulting in a polar cell.

Recently, several groups have discovered that terpolymers of P(VDF-TrFE) with small concentrations of a chloro-monomer also display electrostrictive behavior, without the need for electron bombardment [4-6]. It has been reasoned that substitution of small amounts of a third monomer containing a large atom, i. e., chlorine whose van der Waals radius is 1.8 Å [7], into a P(VDF-TrFE) chain should facilitate the disruption of long *trans* sequences. In an effort to elaborate the mechanism of electrostriction in the terpolymers studied to date, we have been performing molecular dynamical (MD) simulations on model polymer chains and crystal lattices. In this paper, we present the results of these simulations and how they can provide insight into the structure of an electrostrictive polymer.

## APPROACH

The models chosen in this study included 100-monomer long random chains of (1) – $CH_2CF_2$- (PVDF); (2) –$CHFCF_2$- (PTrFE); (3) –$CFClCF_2$- (PClTrFE); (4) -$CHFCH_2$- (PClFE); (5) a random chain of 50 monomers of VDF and 50 monomers of TrFE (50/50 P(VDF-TrFE); (6) a random chain of 40 monomers of VDF, 40 monomers of TrFE, and 20 monomers of ClTrFE (40/40/20 P(VDF-TrFE-ClTrFE); and (7) a random chain of 40 monomers of VDF, 40 monomers of TrFE, and 20 monomers of ClFE (40/40/20 P(VDF-TrFE-ClFE). A multichain model comprised of 8 individual chains of 10-monomer units of P(VDF-TrFE-ClTrFE) packed into a crystal was also studied. Computations were performed on a Silicon Graphics Indigo 2 Workstation utilizing the Accelrys Cerius 4.2 package. To model the molecular dynamics of single chain polymers, the single chains were generated with initial all-*trans* conformations, and then minimized using the PCFF forcefield that was especially designed to handle polymer structures [8]. The PCFF forcefield includes bond, angle, torsion, and short and long-range nonbonded Coulombic and van der Waals interactions. After minimization, the chains were in almost fully extended *trans* conformations. MD simulations on a constant-temperature, constant-volume ensemble of the starting structures proceeded for at least 100 ps in time steps of 0.001 ps. MD simulations were also performed on a multichain superlattices of P(VDF-TrFE) and P(VDF-TrFE-ClTrFE) for 160 ps at 300 K.

## RESULTS AND DISCUSSION

### End-to-end distances

Molecular dynamical simulations were first performed on single chain models PVDF, PTrFE, PClTrFE, and PClFE at 300 K. At 100 ps, the end-to-end distances were calculated (table 1). The PVDF single chain exhibits the largest number of *gauche* linkages, given its smallest end-to-end distance, which implies the presence of *gauche* bonds in the polymer chain.. This conclusion is supported by the experimental fact that PVDF crystallizes from its melt into a mixture of form II crystallites and amorphous regions [9]. The largest end-to-end distance, which is displayed by PTrFE, is consistent with the thermodynamic stability of the all-*trans* conformation of the TrFE monomer compared with its *gauche* form. That the addition of the third fluorine atom in VDF raises the energy of the *gauche* form relative to the *trans* conformation is supported by the experimental observation that with increasing TrFE levels, P(VDF-TrFE) is favored to anneal directly into all-*trans* lamellar crystals [9]. The end-to-end distance of the single chains of PClTrFE indicates the propensity for formation of *trans* bonds of this monomer, given the considerable steric crowding in this monomer. On the other hand, chain folding in PClFE, in which there is less steric crowding, results in intermediate end-to-end distances.

### Dihedral distributions

The dihedral distributions of several chains were calculated after 400 ps, 300 K simulations. A single chain of PVDF yielded an almost equal distribution of *gauche* and *trans* conformations. The dihedral distribution of 50/50 P(VDF-TrFE) is richer in *trans*, however, as predicted from the greater thermodynamically stability of the *trans* conformation of the TrFE unit. Similarly, as shown in figure 1, 40/40/20 PClTrF is shown to favor *trans* while PClFE exhibits a greater percentage of *gauche* bonding. These results provide further support that the steric congestion in PClTrFE favors *trans* bonding. Interestingly, when the dihedral distributions of PClTrFE and PClFE are compared in this fashion, it may be conjectured that annealing of PClFE should favor a greater proportion of mixed *tgtg'*, *tttgttg'*, and all-*trans* forms.

**Table I.** End-to-end distances of single chains following MD simulation

| Polymer | End-to-end distance (Å) |
|---|---|
| PVDF | 23.08 |
| PTrFE | 77.0 |
| PClTrFE | 76.1 |
| PClFE | 49.8 |

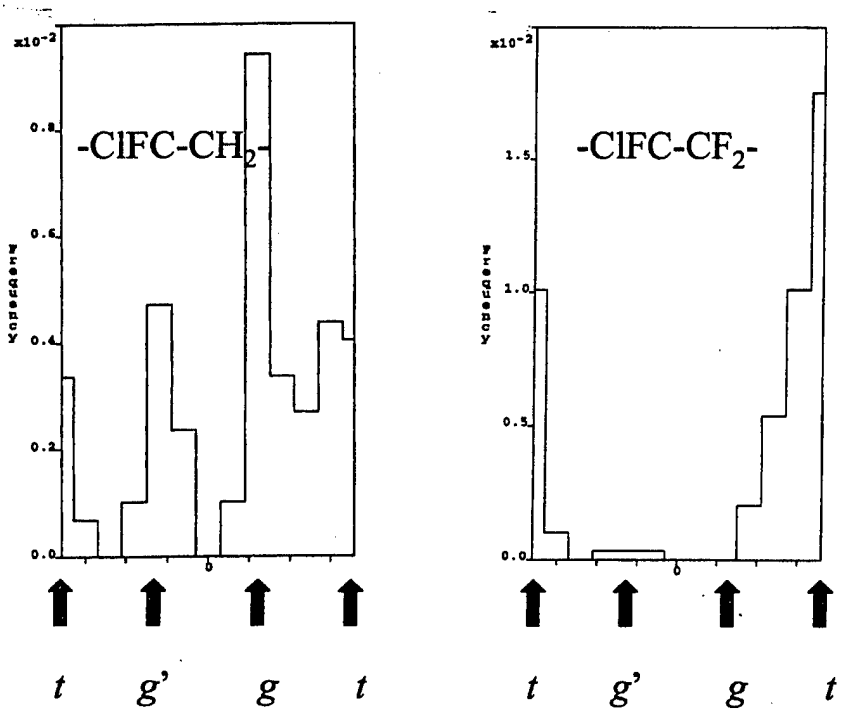


**Figure 1.** Dihedral distributions following an MD simulation at 300 K of 100 monomer chains of PClFE (left) and PCTrFE (right).

## Molecular dynamical simulations of PClTrFE

The question arises concerning the role of the third monomer in electrostriction. As has been postulated in electron-irradiated P(VDF-TrFE), the break-up of the long-range crystal regions into disorted polar structures may be responsible for electrostrictive behavior [6]. This is supported by the almost complete disappearance of the Curie transition, which is, in fact, almost indiscernible after irradiation. This implies a dramatic change in crystallinity. Infrared spectra of the irradiated films provide addition and unequivocal evidence of coexisting forms I, II, and III, suggesting that irradiation induces distortions in the *t* and *g* angles [10]. To examine the effects of chlorine substitution on the degree of torsional distortions in a crystal superlattice, MD simulations were performed at 300 K on 50/50 P(VDF-TrFE) and 40/40/20 P(VDF-TrFE-ClTrFE) superlattices for 160 ps. These models were constructed and initially minimized as form I crystals. The geometries equilibrated after about 10 ps. In both cases, the structures are monoclinic with a slight increase in the lattice dimensions of the terpolymer (table II). The increase in the lattice volume is consistent with the presence of chlorine atoms.

**Table II.** Average lattice dimensions of Form I superlattices during MD simulations

| **Polymer** | **a (Å)**<br>**α (°)** | **b (Å)**<br>**β (°)** | **c (Å)**<br>**γ (°)** | **Superlattice volume (Å$^3$)** |
|---|---|---|---|---|
| 50/50 P(VDF-TrFE) | 18.17<br>90.65 | 9.92<br>72.93 | 26.18<br>89.08 | 4512 |
| 40/40/20 P(VDF-TrFE-ClTrFE). | 18.39<br>91.16 | 10.03<br>72.40 | 26.28<br>89.22 | 4614 |

The torsion energies of these structures and their distributions during the simulation are displayed in figure 2. The higher energy of the terpolymer is a result of increased steric congestion in the polymer chains. However, there is also a clear difference in the distributions of these torsion energies: for the terpolymer, the distribution of frequencies is noticeably broader. This implies that a wider range of torsion angles predominates in the annealed terpolymer. The torsion angles, however, are distributed about 180°, as deduced from figure 1. Again, the widening of the torsion angles can be attributed to the steric crowding in the terpolymer resulting in distorted *trans* dihedral angles.

## CONCLUSIONS

The MD calculations presented in this paper demonstrate that substitution of chlorine atoms in P(VDF-TrFE) copolymers forces the all-*trans* crystallites into distorted structures. This effect is attributed to the large van der Waals radius of the chlorine atom. This is confirmed by the dihedral distributions of the PClTrFE terpolymer as well as the histogram showing a large spread of torsion energies that imply a broad distribution of *trans* angles. Furthermore, given the larger lattice volume calculated for the terpolymer superlattice, distorted structures become more accessible due to enhanced dynamical motion in the expanded lattices. This analysis supports a picture where introduction of ClTrFE into the polymer chain produces defect structures with random fields that prevent long-range ferroelectric coupling. Because the ferroelectric states are destabilized, relaxor behavior possible.

The dihedral distribution of the terpolymer with a $-CClF-CH_2-$ suggests that this terpolymer will exhibit a greater percentage of *gauche* bonding, and a potentially enhanced electrostriction with high mechanical strains. The MD approach described in this paper is currently being applied to multichain superlattices of PClFE, as well as to an evaluation of the dynamical and temperature-dependent behavior of forms II and III of the models presented here.

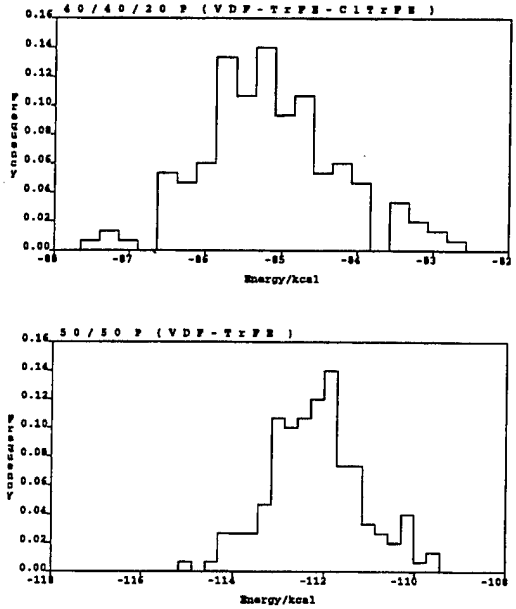


**Figure 2.** Distributions of the torsion energies for the ter- and copolymers

## REFERENCES


1. R. E. Newnham, *Acta Cryst.* **A54**, 729 (1998).
2. Q.M. Zhang, V. Bharti, and X. Zhao, *Science* **280**, 2101 (1998).
3. V. Bharti, H. S. Xu, G. Shanthi, and Q. M. Zhang, *J. Appl. Phys.* **87**, 452 (2000).
4. X. Lu, A. Schirokauer, J. Scheinbeim, *Mat. Res. Soc. Symp. Proc.* **600**, 61 (2000).
5. A. Petchsuk and T. C. Chung *Polymer Preprint,* **41**, 1558 (2000).
6. H. S. Xu, Z.-Y. Cheng, T. Mai, D. Olson, Q. M. Zhang, and G. J. Kavarnos, *Applied Physics Letters* **78**, 2360 (2001).
7. *Lange's Handbook of Chemistry*, 13th Ed., ed. J. A. Dean (McGraw-Hill, 1985), p. 3-121.
8. H. Sun, *Macromolecules* **28**, 701 (1995).
9. K. Koga, N. Nakano, T. Hattori, and H. Ohigashi, *J. Appl. Phys.* **67**, 965 (1990).
10. G. J. Kavarnos, unpublished results.

# APPENDIX 26

Mat. Res. Soc. Symp. Proc. Vol. 698 © 2002 Materials Research Society

# Characterization and Development of P(VDF-TrFE) Based High Performance Electroactive Terpolymers

D. Olson, H.S. Xu, Hengfeng Li, Z.-Y. Cheng, and Q. M. Zhang,
R. Ting[1], G. Abdul-Sedat[1], K.D. Belfield[1], T. Ramotowski[2], R. Hughes[2], G. Kavarnos[2]
Materials Research Institute, The Pennsylvania State University
University Park, PA 16802, U.S.A.
[1]University of Central Florida, Orlando, FL 32816, USA
[2]Naval Undersea Warfare Center, Newport, RI 02841, USA

## ABSTRACT

The structural properties of a class of relaxor ferroelectric polymer, poly(vinylidene fluoride-trifluoroethylene-chlorofluoroethylene) [P(VDF-TrFE-CFE)] terpolymer, were investigated and compared with those of the poly(vinylidene fluoride-trifluoroethylene) [P(VDF-TrFE)] copolymer, the electron-irradiated copolymer, and the chlorotrifluoroethylene (CTFE) based terpolymer. The experimental results suggest that the random incorporation of the bulky chlorofluoroethylene (CFE) monomer into the polymer chain introduces random defect fields, thus randomizing the inter- and intra-chain polar coupling and breaking the large polar domains into smaller domain sizes. Furthermore, CFE also favors intra-chain trans-gauche conformation. As a result, high electrostrictive strain (>5%) was obtained for the terpolymer with a small mol% of CFE.

## INTRODUCTION

Recent work with electron irradiated copolymers has demonstrated that high strain and high dielectric constant polymer systems can be realized through introducing defect structures into the P(VDF-TrFE) copolymer.[1] The electron irradiation introduces random defects into the crystallite regions such as double bonds, bulky pedant groups, and crosslinkings, which stabilize the trans-gauche conformation at room temperature leading to an important change in microstructure and transforming the ferroelectric copolymer system into a relaxor ferroelectric, which exhibits large electrostrictive strain.[2,3] Based on the results on irradiated copolymer systems, it was anticipated that similar systems based on a non-irradiative approach could be realized, which would lead to the development of several new classes of P(VDF-TrFE) based terpolymers. Previous experiments using CTFE and hexafluoropropylene (HFP) ter-monomers have indicated that those terpolymer systems can produce the broad dielectric constant peak observed in irradiated copolymer samples and generate reasonable electrostrictive strain responses.[4] In this paper we investigate the P(VDF-TrFE-CFE) terpolymer, as well as how the ter-monomer affects the field induced strain response.

## EXPERIMENTAL

### Synthesis and sample preparation

P(VDF-TrFE-CFE) terpolymers were systhesized by a bulk polymerization method. The VDF/TrFE ratio was determined from the $^{1}$HNMR and $^{19}$FNMR spectra, while the CFE mol% in

the terpolymers were ascertained by elemental analysis. For easier comparison to the copolymer and irradiated copolymer systems, the composition of the terpolymer is labeled as $VDF_x$-$TrFE_{1-x}$-$CFE_y$ where the ratio of VDF/TrFE is x/1-x and the y is the mole% of the third monomer.

The polymer films were solution cast from a dimethyl formamide (DMF) solution and heated for 6 hours at 70°C under vacuum to form films of 10 to 30 μm thick. Samples were annealed at a temperature 5 °C less than the melting temperature for 2 hrs. Gold electrodes were sputtered onto the films for electric measurement.

## Measurement

The electrostrictive strain was measured using a bi-morph-based cantilever dilatometer,[5] a lock-in amplifier and a high voltage source. The temperature dependence of the dielectric properties were measured on a DEA 2870 Dielectric Analyzer (TA Instruments Co.) with a heating rate of 2°C/min. X-ray data were gathered at room temperature using a Scintag diffractometer with Ni filtered Cu $K\alpha$ radiation ($\lambda$=1.54Å). FT-IR spectra were taken on a Bio-Rad FTS-45 Fourier-transform IR spectrophotometer between 4000 and 400 $cm^{-1}$.

# RESULTS

## Strain and dielectric constant

The strain data for the CFE terpolymer system is presented in figure 1 and compared with the previously measured strain data on the CTFE terpolymer. The CFE and CTFE terpolymer systems exhibit high-field-induced longitudinal strains of –5.3% and –4%, respectively. Because of the difference in the ter-monomer, the two terpolymers show quite different elastic modulus, i.e., the elastic modulus for P(VDF-TrFE-CFE) 62/38/4 is Y=1.0 GPa and for P(VDF-TrFE-CTFE) 65/35/10 is Y=0.4 GPa. Combining the strain data with the elastic modulus of each terpolymer sample leads to elastic energy densities of 1.4 $J/cm^3$ and 0.32 $J/cm^3$, respectively. The unstretched irradiated copolymer system, the Young's modulus is Y=0.4 GPa, with a longitudinal strain of –5% and an elastic energy density of 0.5 $J/cm^3$.[1] It is important to note that the CFE system demonstrates the highest longitudinal strain, despite the CFE ter-monomer being in lower mol% than in the CTFE system.

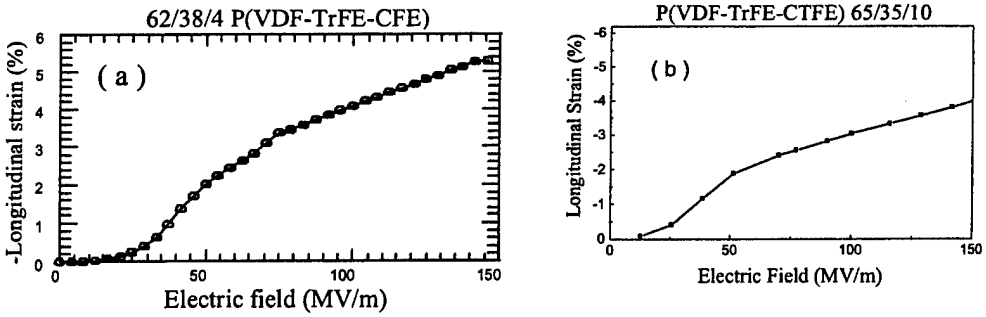


**Figure 1.** (a) P(VDF-TrFE-CFE) 62/38/4 longitudinal strain as a function of driving field, amplitude measured at room temperature and 10 Hz. (b) P(VDF-TrFE-CTFE) 65/35/10 longitudinal strain as a function of field measured at room temperature and 10 Hz.

## Conformation analysis

The introduction of the third monomer into the polymer chain serves to interrupt the ferroelectric domains, thereby reducing their size.[6] Random defect introduction, as in the irradiated copolymer samples, broadens the ferroelectric transition and reduces the ferroelectric-paraelectric transition temperature. The random incorporation of the bulky ter-monomer into the polymer chains forces a conformation change from the all-trans ($T_{m\geq4}$) conformation to the trans-gauche (TG) and $T_3G$ conformations. Figure 2 demonstrates the change in interchain lattice spacing resulting from these changes in conformation. Modeling studies have revealed that the CTFE system favors the all trans conformation along the chain, but due to the increase in the interchain spacing as a result of the larger chlorine atom, the polymer chains fall into the TG conformation. However, in the CFE system, the TG conformation is favored throughout (both inter-chain and intra-chain). It is the change in conformation from the disordered TG and $T_3G$ phase to the all trans β-phase that leads to the observed large electrostrictive strain.

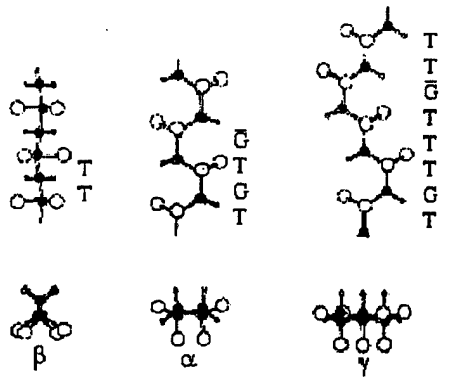


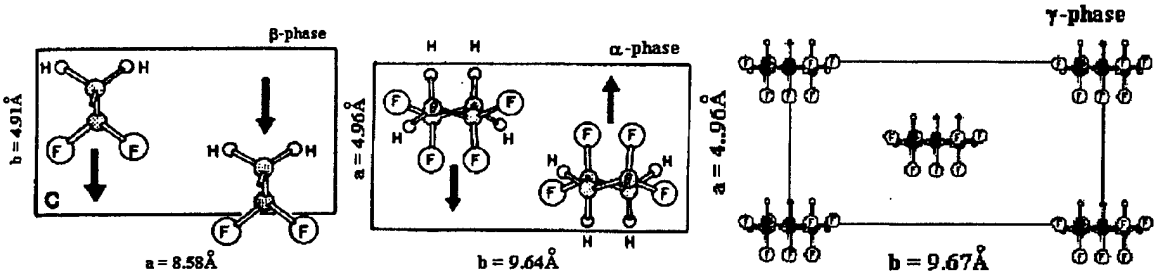


**Figure 1.** The conformations and lattice spacing of the different phases of PVDF.

## FT-IR data: conformational changes

The conformational analysis was undertaken through investigation of the vibrational modes of each of the polymer systems. Thus FT-IR spectra were gathered and analyzed for each of the polymer systems as shown in figure 3. The copolymer spectrum is characterized by a distinct and strong absorption band at 1288 $cm^{-1}$ which belongs to long trans sequences ($T_{m\geq4}$) of the ferroelectric β-phase as well as weak absorbance bands associated with the TG (610 $cm^{-1}$) and $T_3G$ (510 $cm^{-1}$) conformations.[3,7]

Upon the random introduction of the CFE and CTFE monomer units, there is a significant decrease in the ferroelectric β-phase ($T_{m\geq4}$ at 1288 $cm^{-1}$), and the molecular conformation of the terpolymers correspondingly increases in the $T_3G$ (510 $cm^{-1}$) and TG (610 $cm^{-1}$) conformations, resulting in a predominantly paraelectric γ-phase ($T_3G$) in the terpolymer samples unlike the copolymer, which is predominately of the all-trans conformation. The method by Osaki et al. was used to calculate the fraction $F_i$ of the each chain conformation.[8]

$$F_i = \frac{A_i}{A_I + A_{II} + A_{III}} \quad (1)$$

Where i= I, II, III, and $A_I$, $A_{II}$, $A_{III}$ are the absorbencies of the chain conformations with all-trans ($T_{m\geq 4}$, at 1285 $cm^{-1}$), $T_3G$ (peak at 510 $cm^{-1}$), and TG (peak at 610 $cm^{-1}$), respectively. The relative molecular conformation of each polymer sample are presented in Table I. The molecular conformation for the CFE terpolymer results in a higher percentage of $T_3G$ and lower percentage of all trans conformation than does the CTFE terpolymer even though the former possesses less mol% ter-monomer. This results in more conformations switching from $T_3G$ to all-trans and in turn a larger observed induced longitudinal strain. It is interesting to note that the amount of $T_3G$ conformation in the CFE terpolymer is still much less than that for the irradiated copolymer sample though they demonstrate similar longitudinal strains. The reason behind this is the increased crystallinity in the CFE terpolymer compared with the corresponding irradiated copolymer. These data suggest that if the CFE monomer concentration were increased in the composition of the CFE terpolymer, for instance to a 65/35/6 P(VDF-TrFE-CFE), there should be a corresponding increase in the high-field-induced longitudinal strain.

**Table I.** Molecular conformation percentages

| Sample | % $T_{m>3}$ | % $T_3G$ | % TG |
|---|---|---|---|
| 65/35 P(VDF-TrFE) | 82 | 17 | 1 |
| 65/35/10 P(VDF-TrFE-CTFE) | 52 | 44 | 4 |
| 62/38/4 P(VDF-TrFE-CFE) | 43 | 50 | 7 |
| Irradiated 68/32 P(VDF-TrFE) | 0 | 82 | 18 |

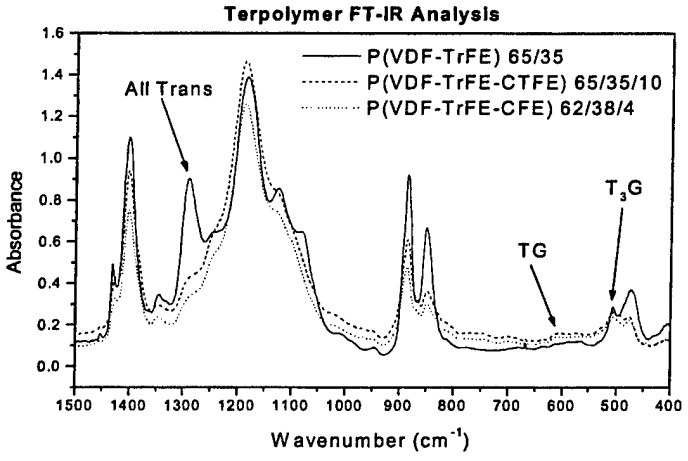


**Figure 2.** Room temperature FT-IR spectra for the P(VDF-TrFE) 65/35, P(VDF-TrFE-CTFE) 65/35/10, P(VDF-TrFE-CFE) 62/38/4 between 1500 and 400 $cm^{-1}$. The spectra demonstrate the conformation change upon introduction of CFE and CTFE monomers to the copolymer system.

## X-ray data: structural changes

The room temperature x-ray diffraction data on (200,110) reflection, which measures the inter-chain distance, for the copolymer, CTFE, and CFE terpolymer systems are presented in figure 4. For 65/35 copolymer, the inter-chain spacing deduced from the (110, 200) reflection is 4.66 Å, while the CTFE terpolymer spacing increases to 4.76 Å, and the CFE terpolymer spacing increases to 4.81 Å, close to the inter-chain spacing of the paraelectric phase of PVDF. After the introduction of the ter-monomer into the polymer chain, the peak shifts to lower angle and therefore indicates the expansion of the lattice with increasing content of the gauche conformation. Again, FT-IR results directly demonstrate the effectiveness of CFE ter-monomer in converting the polymer into a non-polar phase compared with the CTFE ter-monomer.

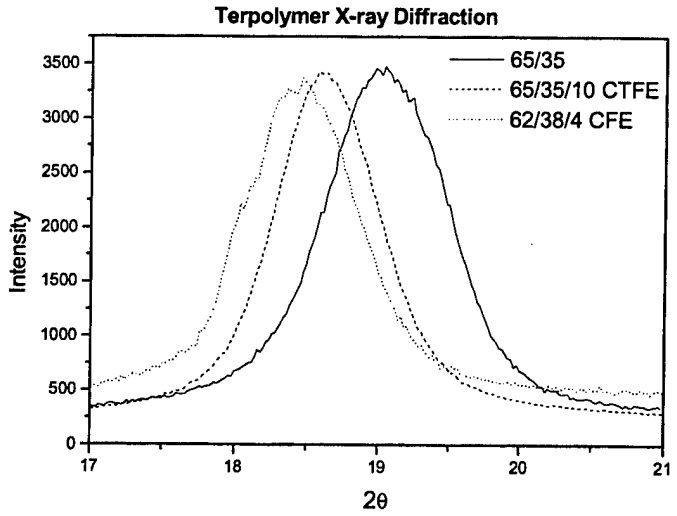


**Figure 3.** X-ray diffraction data (200, 110) taken at room temperature for P(VDF-TrFE) 65/35, P(VDF-TrFE-CTFE) 65/35/10, P(VDF-TrFE-CFE) 62/38/4 (X-ray wavelength is 1.54 Å). Data demonstrate the increase in lattice spacing upon introduction of third monomer into the copolymer system.

## CONCLUSIONS

The random incorporation of the bulky ter-monomer into the P(VDF-TrFE) polymer chain introduces random defect fields into the polymer chain and causes disordering of the ferroelectric phase. The polar domain size is reduced, and the inter- and intra-chain polar coupling are randomized, resulting in the observed ferroelectric relaxor behavior and large electromechanical responses. Because of the steric and electrostatic coupling, the ter-monomer introduced will have different effects on the all trans conformation, and TG and $T_3G$ conformations. The criterion for the proper selection of a ter-monomer to be introduced into the polymer is that it should favor TG and $T_3G$ conformations in the surrounding polymer chains both intra-chain and inter-chain. The X-ray results indicate the expansion of the inter-chain lattice spacing due to the introduction of CFE and CTFE in the crystalline phase. Furthermore, both the X-ray and FT-IR

data show that CFE is more effective in converting the all trans conformation into TG and $T_3G$ conformations, as a result a high electrostrictive strain was obtained.

## ACKNOWLEDGMENTS

This work was supported by DARPA under Contract No. N00173-99-C-2003 and ONR under Grant No. N00014-00-1-0623.

## REFERENCES

1. Q.M. Zhang, V. Bharti and X. Zhao, Scinece **280**, 2101 (1998); Q. M. Zhang and J. Scheinbeim, *Electric Polymers*, Chapter 4 in *Electroactive Polymer Actuators as Artificial Muscles* (Ed. Y. Bar-Cohen, SPIE Optical Engineering Press, WA, 2001).
2. Q.M. Zhang, Z.-Y. Cheng and V. Bharti, Appl. Phys. A **70**, 307 (2000).
3. H. Xu, G. Shanthi, V. Bharti and Q.M. Zhang, Macromolecules **33**, 4125 (2000).
4. H. Xu, Z.-Y. Cheng, D. Olson, T. Mai and Q.M. Zhang, Appl. Pys. Lett. **78**, 2360 (2001).
5. J. Su, P. Moses, and Q. M. Zhang, Rev. Sci. Instruments, **69**, 2480-2484 (1998).
6. Z.-Y. Cheng, D. Olson, H. Xu, F. Xia, J.S. Hundal and Q.M. Zhang, Macromolecules, in press (2001).
7. K. Tashiro, in *Ferroelectric Polymers*, edited by H. S. Nalwa (Dekker, NewYork, 1995).
8. S. Osaki and Y. Ishida, J. Polym. Sci., Polym. Phys. **13**, 1071, 1975.

# APPENDIX 27

# An all-organic composite actuator material with a high dielectric constant

**Q. M. Zhang, Hengfeng Li, Martin Poh, Feng Xia, Z.-Y. Cheng, Haisheng Xu & Cheng Huang**

*Materials Research Institute and Electrical Engineering Department, The Pennsylvania State University, University Park, Pennsylvania 16802, USA*

**Electroactive polymers (EAPs) can behave as actuators, changing their shape in response to electrical stimulation. EAPs that are controlled by external electric fields—referred to here as field-type EAPs—include ferroelectric polymers, electrostrictive polymers, dielectric elastomers and liquid crystal polymers[1–6]. Field-type EAPs can exhibit fast response speeds, low hysteresis[1–8] and strain levels far above those of traditional piezoelectric materials[4–6,9,10], with elastic energy densities even higher than those of piezoceramics[4,5,9–11]. However, these polymers also require a high field (>70 V $\mu m^{-1}$) to generate such high elastic energy densities (>0.1 J $cm^{-3}$; refs 4, 5, 9, 10). Here we report a new class of all-organic field-type EAP composites, which can exhibit high elastic energy densities induced by an electric field of only 13 V $\mu m^{-1}$. The composites are fabricated from an organic filler material possessing very high dielectric constant dispersed in an electrostrictive polymer matrix. The composites can exhibit high net dielectric constants while retaining the flexibility of the matrix. These all-organic actuators could find applications as artificial muscles, 'smart skins' for drag reduction, and in microfluidic systems for drug delivery[1–3,12].**

The elastic energy density is a key parameter, measuring both the stress and strain generation capability of an actuator material. The large operation field required to generate high elastic energy densities in EAPs follows from the principle of energy conservation. To illustrate this point, we take a field-type EAP which is assumed to be a linear dielectric and elastic material. The stored elastic energy density $U_s$ when a polymer is strained is $U_S = 1/2YS^2$, where $Y$ is

the Young's modulus and $S$ is the strain. For a field-type EAP, the total elastic energy density from all the strains generated cannot exceed the input electric energy density because energy must be conserved. As a linear dielectric material, this input electric energy density is $U_E = 1/2K\varepsilon_0 E^2$, where $E$ is the applied field, $\varepsilon_0$ is the vacuum dielectric permittivity ($= 8.85 \times 10^{-12}\,\mathrm{F\,m^{-1}}$), and $K$ is the dielectric constant of the polymer. In most of the polymeric materials, the dielectric constant $K$ is less than ten[13] which is far below those in the inorganic materials, many of which can reach more than 5,000 (ref. 14). So in order to generate a high input electric energy density which can be converted to strain energy, a high electric field is required. For example, to generate a $U_s$ of $0.1\,\mathrm{J\,cm^{-3}}$—which corresponds to the elastic energy density of the best-performance piezoelectric and electrostrictive ceramics[14,15]—in a polymer with a dielectric constant of ten, and assuming a 50% energy conversion efficiency, which is very high for the current field-type EAPs, the field required is $67\,\mathrm{V\,\mu m^{-1}}$. Therefore, in order to reduce the applied field substantially in the field-type EAPs while retaining the high elastic energy density that is required in many practical applications, we need to raise the dielectric constant of this class of polymers substantially.

The composite approach—where high-dielectric-constant particulates were added to a polymer matrix—has previously been used to raise the dielectric constant of polymer-based materials[3,16]. However, because these high-dielectric-constant fillers (frequently ceramics) also possess an elastic modulus that is much higher than that of the polymers, the resulting composite also showed an elastic modulus much higher than that of the polymer matrix and thus a loss of flexibility. In addition, the low dielectric constant of the polymer matrix ($\leq 10$) also resulted in the composite dielectric constant still falling below 100.

Recent investigations[4,9] have shown that the electrostrictive poly(vinylidene fluoride-trifluoroethylene) P(VDF-TrFE), belonging to the class of relaxor ferroelectrics[4], a class of ferroelectric material which in many ways resembles polarglass, exhibits a relatively high room-temperature dielectric constant (>40) and a high electrostriction (strain >4%). Both characteristics are highly desirable in a composite to achieve a high dielectric constant and high field-induced strain, and so we chose the electrostrictive P(VDF-TrFE) as the matrix material for our composite.

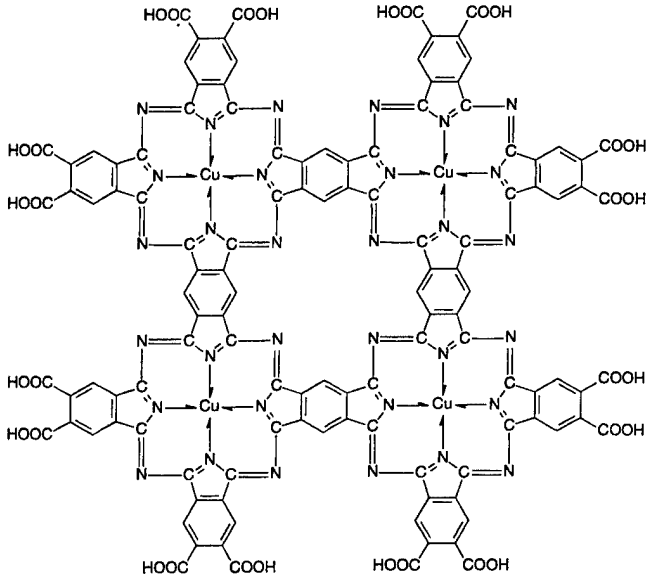


**Figure 1** Schematic of the copper-phthalocyanine (CuPc) oligomer used as the high-dielectric-constant filler.

We selected a metallophthalocyanine (MtPc) oligomer, copper-phthalocyanine (CuPc), as the filler of high dielectric constant (>10,000). Molecular solids formed from MtPc are a class of organic semiconductor materials that are finding applications in organic transistors, chemical sensors, and organic electroluminescent devices[17,18]. A dielectric constant as high as $10^5$ has been observed in CuPc oligomers, whose molecular structure is shown schematically in Fig. 1 (refs 19, 20). The large dielectric constant can be explained in terms of the electron delocalization within MtPc molecules[20,21]. The easy displacement of the electrons under electric fields from the conjugated $\pi$-bonds within the entire molecule results in a high dielectric response. Furthermore, the weak van der Waals intermolecular forces render the molecular solids formed with an elastic modulus not much higher than the polymer matrix. On the other hand, MtPc solids are difficult to process and show a high dielectric loss owing to the long-range intermolecular hopping of electrons[22]. Therefore, the polymer matrix also forms insulation layers to reduce significantly the dielectric loss of the filler.

The resulting composite exhibits almost the same elastic modulus as the polymer matrix and retains its flexibility. For composites containing 40 wt% to 55 wt% of CuPc, which exhibit high dielectric constant while the dielectric loss remains low, the elastic modulus at room temperature is in the range of 0.6 GPa to 1.2 GPa.

The field-induced strain was measured at different applied fields at room temperature and under an a.c. field of 1 Hz. Presented in Fig. 2 is the strain amplitude measured versus the applied-field amplitude for the composite containing 40 wt% of CuPc. A strain near −2% (−1.91%), which is comparable to those in the electrostrictive P(VDF-TrFE)-based polymers, can be induced under a field of $13\,\mathrm{V\,\mu m^{-1}}$. Combining the strain and elastic modulus (0.75 GPa) data yields the elastic energy density of $0.13\,\mathrm{J\,cm^{-3}}$ for the composite under a field of $13\,\mathrm{V\,\mu m^{-1}}$. The results indicate that this all-organic composite approach can result in a more than six times reduction in the applied field compared with the other field-type EAPs with similar strain and elastic energy density[4–6,9,10]. For comparison, the induced strain from the electrostrictive P(VDF-TrFE) copolymer in the same field range is also presented[9]. For the current composite, the applied field of $13\,\mathrm{V\,\mu m^{-1}}$ corresponds to the breakdown field of the material (the highest field that can be applied to the material without electrical shorting), which can be increased by improving the composite quality through further investigation on composite fabrication methods. At fields lower than $10\,\mathrm{V\,\mu m^{-1}}$, the composite can be operated over several hours without changes in the strain response.

The results of the strain measurement indicate that the field-induced strain $S$ is proportional to the square of the applied electric

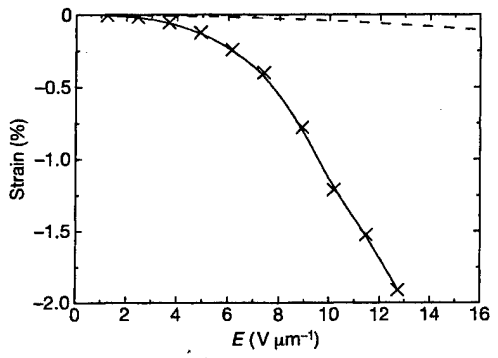


**Figure 2** The strain amplitude as a function of the applied-field amplitude measured at room temperature. The applied-field frequency is 1 Hz. Crosses are the data and the solid curve is a guide to the eye. For comparison, the strain from the electrostrictive P(VDF-TrFE) copolymer at the same field range is also shown (the dashed curve).

field, suggesting that the strain response originates from either Maxwell stress (the electrostatic force), or the electrostriction, or both[4,5,23,24]. When a dielectric material is subject to an electric field $E$, it will experience an electrostatic force (Maxwell stress) that is due to the Coulomb force between charges. The strain induced by the Maxwell stress along the applied-field direction is[23]:

$$S = 1/2K\varepsilon_0 E^2(1+2\sigma)/Y \quad (1)$$

Here we assumed that the dielectric material is isotropic and $\sigma$ is the Poisson's ratio. The electrostriction is strain-generated owing to a change in the polarization in a material under constant stress, which is equal to $S = ME^2$, where $M$ is the electrostrictive coefficient and is proportional to the square of the dielectric constant[24].

Figure 3a presents the dielectric constant as a function of the applied-field amplitude at room temperature and 1 Hz for the composite containing 40 wt% CuPc. At low fields, the composite has a dielectric constant of 225 and a loss factor ($D = K''/K'$) of 0.4. With increased field amplitude, the dielectric constant increases and at 13 V $\mu m^{-1}$, the dielectric constant is about 425 and the loss

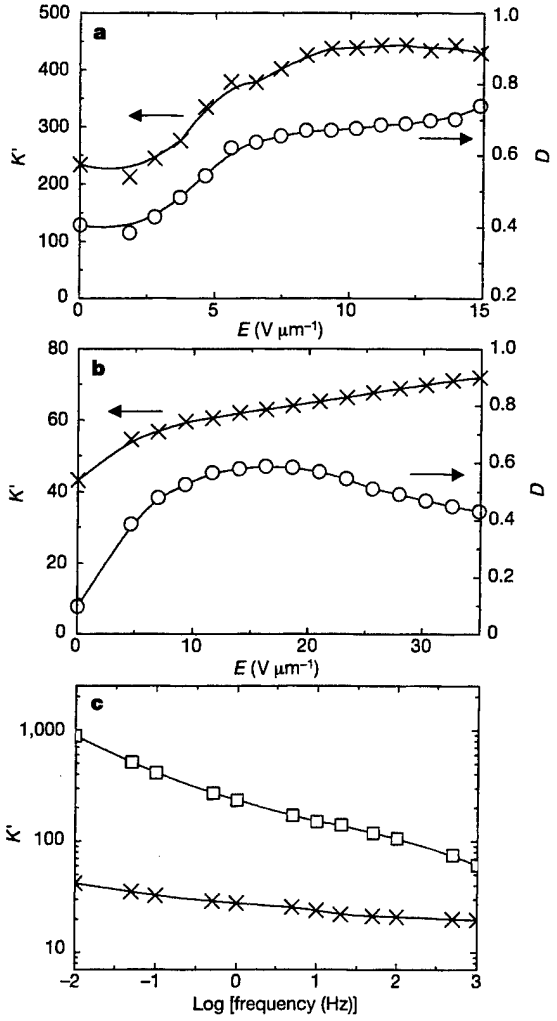


**Figure 3** Dielectric properties of the all-organic composites. **a**, **b**, The real part of the dielectric constant ($K'$) and dielectric loss ($D$) as a function of the applied-field amplitude for the composite with 40 wt% CuPc (**a**) and the polymer matrix (**b**). The field frequency is 1 Hz. **c**, The weak-field (100 V $cm^{-1}$) dielectric constant as a function of frequency for the composite (squares) and the polymer matrix (crosses). Data points are shown and solid curves are a guide to the eye.

remains relatively low (~0.7) compared with that of the polymer matrix (the resistivity of the composite is higher than $10^8\ \Omega$ m). For CuPc, the dielectric constants should not increase with field amplitude[21]. The observed increase of the dielectric constant with the applied-field amplitude is from the P(VDF-TrFE) matrix, which we also measured (Fig. 3b). Such an increase in the dielectric constant with the applied-field amplitude in a ferroelectric material is believed to be caused mainly by the interaction of the polarization with the defect fields in the materials[25].

From the dielectric and elastic data, the contributions to the strain response from the Maxwell stress and electrostriction may be estimated. Assuming that the composite is homogeneous, the strain due to Maxwell stress under a field of 13 V $\mu m^{-1}$ is about −0.1%. For the electrostriction from the polymer matrix, assuming that all the applied field is totally loaded onto the polymer matrix because its dielectric constant is much lower than that of CuPc, the strain is also about −0.1%. The measured strain response, therefore, is about one order of magnitude higher than the combined strain from the two.

In an early study on the field-induced strain in a polyurethane elastomer, it was observed that a nonuniform electric-field distribution can significantly enhance the strain response (more than five times in that case) if the strain is proportional to the square of the local field[26]. The composites investigated here are highly heterogeneous, so that a large variation in the local fields is likely, which will enhance the strain response. In addition, bond length and conformation changes in CuPc due to electron motions, as well as the CuPc molecular reorientation under external fields, may also contribute to the strain response[27].

Figure 3c shows the frequency dependence of the weak-field dielectric constant of the composite. The strong frequency dispersion is due to the space charge polarization (delocalized electrons) in CuPc, which will also result in frequency dependence of the strain response in the composite. For instance, the strain measured at 0.1 Hz is about 1.6 times higher than that measured at 1 Hz.

We note that the approach of using the delocalized charge phenomenon in a composite in which insulation layers block the long-range space charge conduction to realize very high dielectric constant is analogous to that in the ceramic capacitor where semiconductor cores and insulation boundary-layers form the so-called internal boundary layer capacitor, resulting in a material with dielectric constants exceeding 50,000 (refs 14, 28). With further improvement in the composite fabrication process, including using nanoparticulates of CuPc and coating the CuPc particles completely with insulation layers, both the dielectric properties and the breakdown field can be increased substantially. In view of the availability of a large number of organic solids with super-dielectric constant, the results presented here demonstrate the potential of this all-organic composite approach in generating high strain and high elastic energy density under low applied fields in polymer-like materials[21]. □

## Methods

The copper-phthalocyanine (CuPc) oligomer was synthesized by the solution method[29]. Copper sulphate pentahydrate, pyromellitic dianhydride, urea, ammonium chloride, and ammonium molybdate were ground together and then placed in a three-necked flask containing nitrobenzene. The temperature of the flask was maintained at 185 °C for 12 h. The obtained solid material was boiled with hydrochloric acid, and then treated with potassium hydroxide. The final powder was dried at room temperature under vacuum. The typical particle size thus obtained, as measured by scanning electron microscopy, was below 1 μm.

The P(VDF-TrFE) 50/50 mol% copolymer (purchased from Solvay & Cie.) was used as the matrix, which can be easily converted to the electrostrictive material by high energy electron irradiation[4,9]. Composite films were prepared using the solution cast method. P(VDF-TrFE) copolymer was dissolved in dimethylformamide (DMF) and then a proper amount of CuPc powder (determined by the wt% of CuPc in the composite) was added to the solution. The solution was ultrasonically stirred to disperse the CuPc powder. After that, the solution was poured onto a glass plate and dried at 70 °C. The typical film thickness was about 40 μm. The composites were irradiated at 100 °C with electrons of 1.2 MeV energy to convert the copolymer matrix into an electrostrictive polymer with an

improved room-temperature dielectric constant.

The dielectric properties of the composites under different applied-field strength were characterized by directly measuring the magnitude and the phase of the current passing through the composite under a given a.c. voltage. From the complex electric impedance $Z^* = 1/(j\omega C^*)$ and $C^* = (K' - jK'')\varepsilon_0 A/t$, both the real and imaginary parts ($K'$ and $K''$) of the dielectric constant can be determined, where $A$ is the area and $t$ is the thickness of the capacitor, and $\omega$ is the angular frequency. The elastic modulus was determined using a commercial dynamic mechanical analyser (TA Instruments, DMA2980). The electric-field-induced strain along the applied-field direction (longitudinal strain) was measured using a piezobimorph-based sensor[30].

Received 18 April; accepted 25 July 2002; doi:10.1038/nature01021.


1. Bar-Cohen, Y. (ed.) *Electroactive Polymer Actuators as Artificial Muscles* (SPIE, Bellingham, WA, 2001).
2. Zhang, Q. M., Furukawa, T., Bar-Cohen, Y. & Scheinbeim, J. (eds) *Electroactive Polymers* (MRS Symp. Proc. Vol. 600, MRS, Warrendale PA, 1999).
3. Nalwa, H. (ed.) *Ferroelectric Polymers* (Marcel Dekker, New York, 1995).
4. Zhang, Q. M., Bharti, V. & Zhao, X. Giant electrostriction and relaxor ferroelectric behavior in electron-irradiated poly(vinylidene fluoride-trifluofoethylene) copolymer. *Science* **280,** 2101–2104 (1998).
5. Pelrine, R., Kornbluh, R., Pei, Q. & Joseph, J. Highspeed electrically actuated elastomers with strain greater than 100%. *Science* **287,** 836–839 (2000).
6. Lehmann, W. *et al.* Giant lateral electrostriction in ferroelectric liquid-crystalline elastomers. *Nature* **410,** 447–450 (2001).
7. Baughman, R. H. *et al.* Carbon nanotube actuators. *Science* **284,** 1340–1344 (1999).
8. Osada, Y., Okuzaki, H. & Hori, H. A polymer gel with electrically driven motility. *Nature* **355,** 242–244 (1992).
9. Cheng, Z.-Y. *et al.* Electrostrictive poly(vinylidene fluoride-trifluoroethylene) copolymers. *Sens. Actuat. A* **90,** 138–147 (2001).
10. Xu, H. *et al.* Ferroelectric and electromechanical properties of poly(vinylidene-fluoride–trifluoroethylene–cholorotrifluoroethylene) terpolymer. *Appl. Phys. Lett.* **78,** 2360–2362 (2001).
11. Huber, J. E., Fleck, N. A. & Ashby, M. F. The selection of mechanical actuators based on performance indices. *Proc. R. Soc. Lond. A* **453,** 2185–2205 (1997).
12. Dario, P., Carrozza, M., Benvenuto, A. & Menciassi, A. Micro-systems in biomedical applications. *J. Micromech. Microeng.* **10,** 235–244 (2000).
13. McCrum, N., Read, B. E. & Williams, G. *Anelastic and Dielectric Effects in Polymeric Solids* (Dover, New York, 1967).
14. Moulson, A. & Herbert, J. *Electroceramics* (Chapman & Hall, London, 1995).
15. Cross, L. E. Ferroelectric ceramics: materials and application issues. *Ceram. Trans.* **68,** 15–55 (1996).
16. Safari, A., Sa-gong, G., Giniewicz, J. & Newnham, R. Composite piezoelectric sensors. *Proc. 21st Univ. Conf. Ceram. Sci.* **20,** 445–455 (1986).
17. Bao, Z., Lovinger, A. & Dodabalapur, A. Highly ordered vacuum-deposited thin films of metallophthalocyanines and their application in field-effect transistors. *Adv. Mater.* **9,** 42–45 (1997).
18. Tominaga, T., Hayashi, K. & Toshima, N. Accelerated hole transfer by double-layered metallophthalocyanine thin film for effective electroluminescence. *Appl. Phys. Lett.* **70,** 762–763 (1997).
19. Nalwa, H. S., Dalton, L. & Vasudevan, P. Dielectric properties of copper-phthalocyanine polymer. *Eur. Polym. J.* **21,** 943–947 (1985).
20. Phougat, N., Vasudevan, P. & Nalwa, H. *Handbook of Low and High Dielectric Constant of Materials and Their Applications* Ch. 8 (ed. Nalwa, H.)) (Academic, London, 1999).
21. Vijayakumar, P. & Pohl, H. A. Giant polarization in stable polymeric dielectrics. *J. Polym. Sci. Poly. Phys.* **22,** 1439–1451 (1984).
22. Gould, P. D. Structure and electrical conduction properties of phthalocyanine thin films. *Coord. Chem. Rev.* **156,** 237–274 (1996).
23. Landau, L. D. & Lifshitz, E. M. *Electrodynamics of Continuous Media* (Pergamon, Oxford, 1970).
24. Newnham, R., Sundar, V., Yimmirun, R., Su, J. & Zhang, Q. M. Electrostriction in dielectric materials. *Ceram. Trans.* **88,** 15–39 (1998).
25. Damjanovic, D. Logarithmic frequency dependence of the piezoelectric effect due to pinning of ferroelectric-ferroelastic domain walls. *Phys. Rev. B* **55,** R649–R652 (1997).
26. Su, J., Zhang, Q. M. & Ting, R. Y. Space-charge-enhanced electromechanical response in thin-film polyurethane elastomers. *Appl. Phys. Lett.* **71,** 386–388 (1997).
27. Hayashi, K., Kawato, S., Fujii, Y., Horiuchi, T. & Matsushige, K. Effect of applied electric field on the molecular orientation of epitaxially grown organic films. *Appl. Phys. Lett.* **70,** 1384–1386 (1997).
28. Ai-Aliak, H., Illingsworth, J., Brinkman, A., Russell, G. J. & Woods, J. The effects of donor dopant concentration on the grain boundary layer characteristics in *n*-doped $BaTiO_3$ ceramics. *J. Appl. Phys.* **64,** 6477–6482 (1998).
29. Achar, B. N., Fohlen, G. G. & Parker, J. A. Phthalocyanine polymers. II Synthesis and characterization of some metal phthalocyanine sheet oligomers. *J. Polym. Sci. Polym. Chem.* **20,** 1785–1790 (1982).
30. Su, J., Moses, P. & Zhang, Q. M. A piezoelectric bimorph based dilatometer for field induced strain measurement in soft and thin free standing polymer films. *Rev. Sci. Instrum.* **69,** 2480–2484 (1998).



## Acknowledgements

This work was supported by the National Institutes of Health, the Office of Naval Research, and Defense Advanced Research Projects Agency.


## Competing interests statement

The authors declare that they have no competing financial interests.

Correspondence and requests for materials should be addressed to Q.M.Z. (e-mail: qxz1@psu.edu).

# APPENDIX 28

# Influence of the Annealing Conditions on the Polarization and Electromechanical Response of High-Energy-Electron-Irradiated Poly(vinylidene fluoride trifluoroethylene) Copolymer

FENG XIA,[1] Y. K. WANG,[1] HENGFENG LI,[1] CHENG HUANG,[1] Y. MA,[1] Q. M. ZHANG,[1] Z.-Y. CHENG,[2] FRED B. BATEMAN[3]

[1]Electrical Engineering Department and Materials Research Institute, Pennsylvania State University, University Park, Pennsylvania 16802

[2]Materials Engineering, Auburn University, Auburn, Alabama 36849

[3]Radiation Interactions and Dosimetry, National Institute of Standards and Technology, Gaithersburg, Maryland 20899

*Received 15 August 2002; accepted 21 January 2003; revised 19 January 2003*

**ABSTRACT:** In this study, we investigated the influence of annealing conditions before irradiation on the ferroelectric and electromechanical properties of uniaxially stretched high-energy-electron-irradiated poly(vinylidene fluoride trifluoroethylene) (HEEIP) copolymer (68/32 mol %) films. For films annealed at one fixed temperature before the irradiation (one-step annealing), the highest crystallinity, which was highly desirable for enhancing the electromechanical response, was obtained only for films annealed between 132 and 136 °C. In addition, annealing over 10 h in this temperature window resulted in a large increase in the crystal lamellar thickness, which was required for reducing the polarization hysteresis to a minimum in the HEEIP samples. For improvements in the mechanical qualities of the uniaxially stretched films, a two-step annealing procedure was investigated; that is, before the irradiation, the films were first annealed at a lower temperature to release the mechanical stress in the films due to the stretching and then were annealed in the high-temperature window to raise the crystallinity and crystalline size. The experimental results indicated that this approach could produce uniaxially stretched HEEIP films with much improved mechanical qualities. Furthermore, the uniaxially stretched HEEIP films with this two-step annealing exhibited the same electromechanical response as or an even higher one than that from the one-step-annealed HEEIP films. © 2003 Wiley Periodicals, Inc. J Polym Sci Part B: Polym Phys 41: 797–806, 2003

**Keywords:** ferroelectricity; poly(vinylidene fluoride trifluoroethylene); electron beam irradiation; differential scanning calorimetry (DSC); electromechanical response

## INTRODUCTION

Electroactive polymers (EAPs), which perform energy conversion between electric and mechanical forms, are attractive for a broad range of applications.[1–9] In the past several decades, a great deal of effort has been devoted to this class of materials, and this has resulted in marked improvements in the electromechanical properties of EAPs.[1,2,9–11] For instance, the ferroelectric properties of poly(vinylidene fluoride trifluoroethylene) [P(VDF-TrFE)] copolymers can be modified

*Correspondence to:* F. Xia (E-mail: fxx2@psu.edu)

Journal of Polymer Science: Part B: Polymer Physics, Vol. 41, 797–806 (2003)

over a broad range with high-energy irradiation.[12,13] Moreover, in high-energy-electron-irradiated P(VDF-TrFE) (HEEIP) copolymers, an electrostrictive strain of 5% with an elastic energy density near 1 J/cm$^3$ has been obtained, representing a significant improvement in comparison with the electromechanical responses of the piezoelectric P(VDF-TrFE) copolymer.[8,14,15]

In the development of this new EAP material, it has been found that the ferroelectric and electromechanical properties of the copolymers after irradiation are sensitive to processing conditions such as the irradiation dose, the electron energy, the temperature at which the irradiation is performed, and the sample annealing conditions before the irradiation.[15–18] For instance, for improvements in the crystallinity, P(VDF-TrFE) copolymers are normally annealed at a temperature between the Curie transition and the melting transition.[19,20] For HEEIPs, for a high electromechanical response to be achieved, the copolymer can only be annealed over a very narrow temperature window with an annealing time greater than 10 h. In addition, for uniaxially stretched copolymer films, the films after annealing become very brittle along the stretching direction, and even after the irradiation, which causes crosslinking in the polymer, the films are still very prone to mechanical stress, which causes cracking.

To provide an understanding of these phenomena, we investigated, using differential scanning calorimetry (DSC) combined with polarization loop measurements, the influence of the annealing conditions on the transitional behaviors and crystal morphology of a copolymer with a 68/32 mol % composition. Furthermore, we investigated other annealing conditions to improve the mechanical qualities of the uniaxially stretched HEEIP films while maintaining the high electromechanical responses.

## EXPERIMENTAL

The P(VDF-TrFE) (68/32 mol %) copolymer was chosen for this investigation because of its high electromechanical responses among all the HEEIPs investigated.[8,15] The copolymer was purchased from Solvay and Cie of Belgium. The polymer films were fabricated with the solution-cast method with dimethylformamide as the solvent. The films were uniaxially stretched to about 4.5 times at a stretching rate of 2 cm/min. To study the effect of the annealing temperature, we annealed the films at a fixed temperature for 1 h (the thermal cycle of the annealing: the films were heated from room temperature to a selected annealing temperature in 0.4 h, were left at the annealing temperature for 1 h, and were cooled to room temperature in 0.4 h). The films were characterized by DSC and a polarization loop study. The effect of the annealing time was studied at several temperatures, and for the copolymer investigated here, the films annealed at 134 °C yielded the best electromechanical response; therefore, the results obtained at that temperature are reported. A fresh film was used for each annealing temperature and annealing time study.

The irradiation of the copolymer films was carried out at 100 °C with an electron energy of 1.2 MeV and a 70-Mrad dose in a nitrogen atmosphere. For the irradiated copolymer, it was previously observed that the electromechanical, ferroelectric, and dielectric responses, as well as the polymer morphology, depend sensitively on the irradiation dose, the electron energy, and the temperature at which the irradiation is carried out.[15] In addition, the sample processing conditions before the irradiation also affected these responses, as discussed later in this article. For consistency and for comparison, the sample irradiation conditions were kept exactly the same.

To improve the mechanical quality of the HEEIP films, we investigated a two-step annealing process, in which the polymer films were first annealed at a low temperature (115–125 °C) for a certain time period to release the stress stored in the films due to the stretching and then were annealed at a temperature near 134 °C to further improve the crystallinity. The films annealed at 120 °C for 1–2 h and then at 134 °C for 2 h exhibited a much better mechanical quality. Moreover, the films (called the two-step-annealed films) after irradiation maintained the same electromechanical properties as or even better ones than the those from one-step annealing.

The DSC study was carried out at a heating/cooling rate of 10 °C/min with a TA Instrument model 2920 differential scanning calorimeter. The polarization loop was measured at 1 Hz with a Sawyer–Tower circuit. The strain along the stretching direction (transverse strain, or $S_1$) was measured at 1 Hz with a cantilever-based dilatometer.[21] The longitudinal strain (thickness strain, or $S_3$) was measured with a bimorph-based dilatometer.[22] Films 20 $\mu$m thick were used for the electric characterization, and Au films

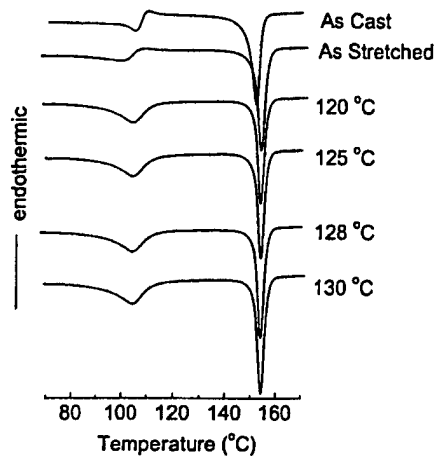


(a)

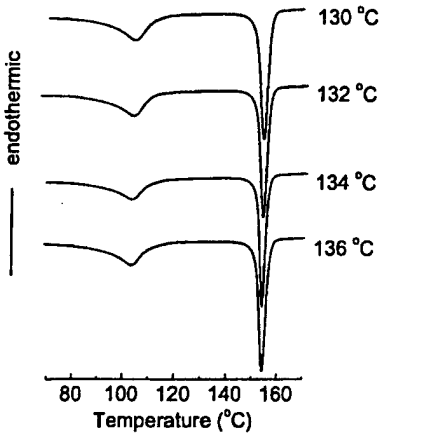


(b)

**Figure 1.** DSC thermograms of uniaxially stretched P(VDF-TrFE) (68/32 mol %) copolymer films annealed at different temperatures for 1 h.

30–50 nm thick were sputtered on the polymer films to serve as the electrodes.

## RESULTS OF ONE-STEP-ANNEALED FILMS

### Effects of the Annealing Temperature

Presented in Figure 1 are selected DSC thermograms measured during heating for stretched films annealed at different temperatures for 1 h (nonirradiated). Two transitions can be observed: the one near 100 °C is the Curie transition temperature ($T_c$) between the low-temperature ferroelectric phase and high-temperature paraelectric phase, and the other near 150 °C is the melting temperature ($T_m$).

In Figure 2(a), we summarize $T_m$ and the melting enthalpy ($\Delta H_m$, or the heat of fusion) of the films as functions of the annealing temperature. For all of the films annealed below the $T_c$ region

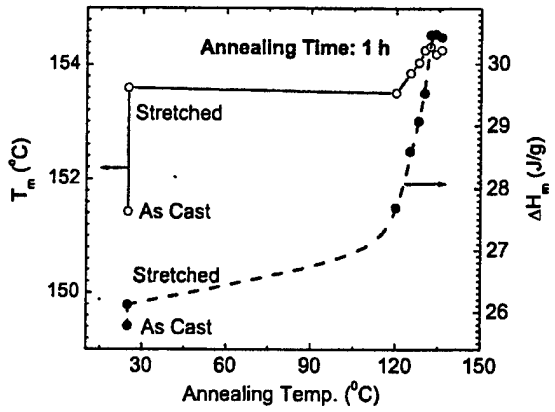


(a)

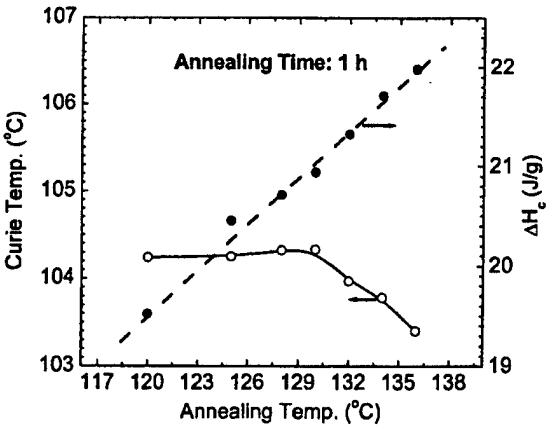


(b)

**Figure 2.** (a) (○) $T_m$ and (●) $\Delta H_m$ as functions of the annealing temperature and (b) (○) $T_c$ and (●) $\Delta H_c$ as functions of the annealing temperature. The solid and dashed curves have been drawn as guides. The films were not irradiated.

(~105 °C), there is no large change in the crystallinity, as revealed by $\Delta H_m$, which does not change much with the annealing temperature.[8] In this temperature region, only local motions of molecular chains are allowed. Therefore, only gauche conformational defects present in the molecular chains of the ferroelectric phase or domain boundaries can be removed,[23] resulting in an increase in $T_c$ and the transition enthalpy as well as a change in the peak shape of the Curie transition.

When the films are annealed in the hexagonal paraelectric phase [above the Curie transition region (>110 °C) and below melting], the molecular chains become relatively mobile along the chain axis, and this improves the chain arrangement and removes various crystal defects (e.g., chain entanglements, stacking faults, dislocations, kink bands, and chain folding) from the hexagonal crystals through the sliding diffusion motion of the molecules. Consequently, the free energy of the hexagonal crystals is lowered, and the molecular chain packing in the crystals becomes more stable. Meanwhile, the crystallites in the mobile hexagonal phase grow, and this results in a prominent increase of $T_m$ and $\Delta H_m$ (related to the crystal lamellar thickness and the crystallinity).

In addition, Figure 2(a) reveals that the annealing temperature above the Curie transition region can further be divided into two regions, a lower temperature region (region I) from 120 to 132 °C, and a higher temperature region (region II) from 132 to 136 °C. In region I, both $T_m$ (related to the crystal lamellar thickness) and $\Delta H_m$ (~crystallinity) increase with the annealing temperature. $T_m$ increases by about 0.8 °C (from 153.5 to 154.3 °C), and this indicates an increase in the crystallite size along the molecular chain direction. Concomitantly, $\Delta H_m$ increases more markedly by about 2.8 J/g (from 27.7 to 30.5 J/g, ca. 10% increase), and this indicates that the crystallinity increases more efficiently with the annealing temperature rising in this region.

In contrast, in region II, neither $T_m$ nor $\Delta H_m$ shows changes with the annealing temperature, and this can be understood by the deorientation of the polymer chains and premelting/recrystallization occurring in this temperature region. Because of the polydispersion of polymers, the melting range of polymer crystals is relatively broad. When the annealing temperature approaches the melting region, the smaller crystallites, which contain a high degree of defects, will experience deorientation and premelting, which will become stronger as the annealing temperature becomes closer to $T_m$ and will reduce the crystallinity. This process counterbalances the increased growth rate of crystallites at higher annealing temperatures.

Figure 2(b) shows $T_c$ and the Curie enthalpy ($\Delta H_c$) for films annealed from 120 to 134 °C. There is an increase in $\Delta H_c$ by about 2.8 J/g (a nearly 15% increase), which is probably a direct result of the increased crystallinity with the increased annealing temperature. As seen in Figure 1, the DSC peak for the Curie transition is very broad (spreading over a temperature range of 70–115 °C) for the uniaxially stretched films, suggesting that there is a rather wide distribution of the Gibbs free energy of the orthorhombic ferroelectric phase because of various defects included in the crystalline regions.[23–25] When the film is annealed in the hexagonal paraelectric phase, the free energies of the hexagonal paraelectric phase will be reduced because of the crystal growth and the formation of more stable molecular chain packing. In parallel, the free energy of the orthorhombic ferroelectric phase will also be reduced because of the reduced number of conformational defects (gauche) in the crystals. Therefore, the observed $T_c$ values for these annealed films will depend on the relative changes of the free energies of the two crystalline phases in the annealing process, which may result in an increase, decrease, or no change in $T_c$.

The polarization hysteresis loops measured on the as-cast films and annealed at 134 °C are presented in Figure 3. As can be seen in Figure 3(a), the polarization level for the as-cast films is quite low (dashed curve). However, there is no large change in the polarization loops for films annealed from 120 to 136 °C. The coercive field ($E_c$) remains nearly constant, whereas the remanent polarization ($P_r$) increases with the annealing temperature and reaches the highest value for films annealed at 132 and 134 °C, at which temperatures $P_r$ is more than 20% higher than for films annealed at 120 °C [Fig. 3(b)]. This increase in $P_r$ is related to the increased crystallinity and improved ferroelectric ordering in the films. The observed drop in $E_c$ and $P_r$ for films annealed at 136 °C might be caused by the chain deorientation and premelting effects, as previously discussed.

For the irradiated copolymers, the ferroelectric and electromechanical responses are mainly from the crystalline region. The results presented indicate that for a high crystallinity to be reached, the annealing should be carried out above 132 °C.

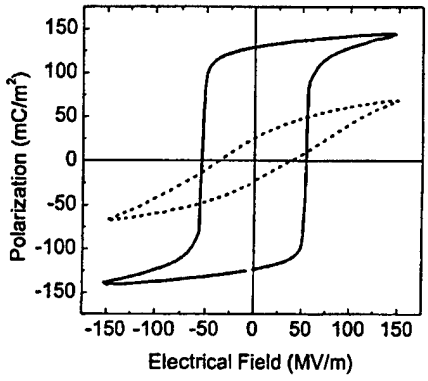


(a)

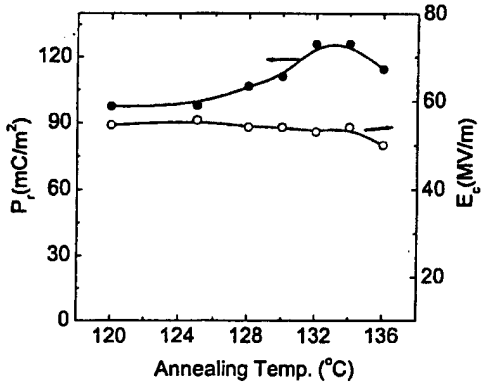


(b)

**Figure 3.** (a) Comparison of the polarization hysteresis loops of (–) the as-cast films and (—) the stretched films annealed at 134 °C for 1 h and (b) (●) $P_r$ and (○) $E_c$ as functions of the annealing temperature. The films were not irradiated.

However, for the deorientation of the polymer chains and premelting to be avoided, it seems that the annealing temperature should also be below 136 °C.

### Effects of the Annealing Time

The effect of the annealing time was studied for films annealed between 132 and 136 °C, and the DSC results obtained at 134 °C annealing are presented in Figure 4 (the results at 132 and 136 °C are similar). One interesting feature revealed by the data is that in contrast to the results in the previous section, the films exhibit a large increase in $T_m$ with the annealing time, whereas there is very little change in $\Delta H_m$. $T_m$ is increased by 3 °C from a 1-h annealing time to a 10-h annealing

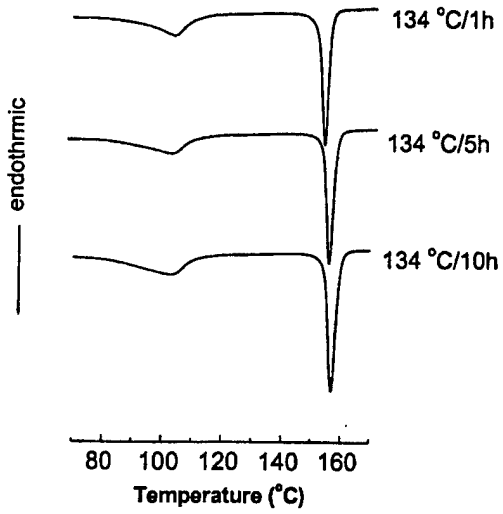


(a)

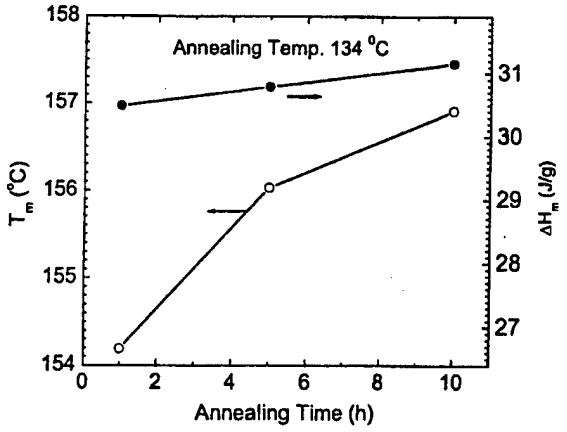


(b)

**Figure 4.** DSC data for uniaxially stretched films annealed at 134 °C with different annealing times: (a) DSC thermograms and (b) summary of (○) $T_m$ and (●) $\Delta H_m$ as functions of the annealing time. The films were not irradiated. The solid curves have been drawn as guides.

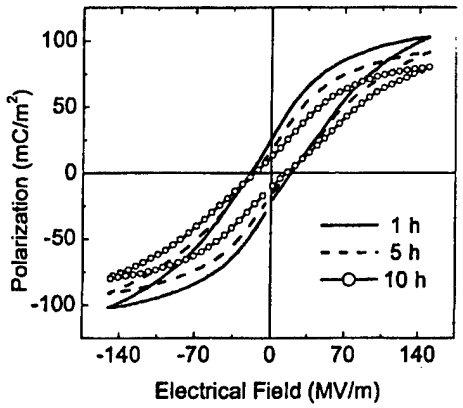


**Figure 5.** Comparison of the polarization hysteresis loops for the irradiated HEEIP films, which were uniaxially stretched and annealed at 134 °C for different times before the irradiation.

time, whereas the corresponding increase in $\Delta H_m$ is relatively small [~0.7 J/g; see Fig. 4(b)]. The results show that in this temperature region, the thickness of lamellae crystals is increased more efficiently by prolonged annealing times than temperature without much of a change in the degree of crystallinity. For the Curie transition, there is very little change in $\Delta H_c$, the transition enthalpy, with the annealing time, which is directly related to the very small change in the crystallinity. However, there is a decrease in $T_c$ with the annealing time (ca. 1.4 °C).

For the films studied here, although there is not much change in the polarization hysteresis loops measured from nonirradiated films, a large reduction of the polarization hysteresis with an increased annealing time is observed for films after the irradiation treatment. Figure 5 presents the polarization hysteresis loops for irradiated films annealed before the irradiation at 134 °C with different annealing times. The data show that the polarization hysteresis (both $E_c$ and $P_r$) decreases with an increased annealing time. For an electrostrictive polymer, it is required that the polarization hysteresis should be as small as possible.[14,15,26] For one-step-annealed (at 134 °C for 10 h) 68/32 HEEIP films, the lowest polarization hysteresis achieved is $P_r = 1\ \mu C/cm^2$ and $E_c = 10$ MV/m. Although in general the polarization hysteresis is reduced with an increased irradiation dose, for films annealed for 1 h, it is difficult to reduce the polarization hysteresis by a further increase in the irradiation dose beyond 70 Mrad.

In the irradiated P(VDF-TrFE) copolymers, there exists a competition between the defects introduced in the irradiation process to destabilize the ferroelectric ordering and the original lattice in forming a ferroelectric phase. For the copolymers containing more than 30 mol % trifluoroethylene, high-energy electron irradiation can be used to convert the copolymer from a normal ferroelectric phase to a relaxor ferroelectric phase (analogues to the polar–glass systems), in which the random defect fields dominate, preventing the formation of the long-range ferroelectric ordering.[8] Therefore, the effectiveness of the random fields for destroying the ferroelectric phase depends on the types of defects and defect concentration. Although the defect concentration will increase with the irradiation dose,[16,18] the types of defects introduced will depend on both the irradiation conditions, such as the electron energy and the temperature at which the irradiation is performed, and the processing conditions before the irradiation. The experimental results here indicate that the crystal lamellar thickness (the annealed films with longer annealing times show a higher $T_m$ and, therefore, larger crystal lamellar thickness) is an important parameter in influencing the type of defects introduced in the irradiation, which could be the conformational changes from the all-trans bonds to the trans–gauche (TGTG′) and $T_3GT_3G'$ introduced in the irradiation process and stabilized in crystallites with large lamellar thickness. These defects may become less stable in crystallites with small lamellar thickness. In addition, even some defects of a chemical type such as crosslinking can also be affected by the crystal lamellar thickness. Thick crystal lamellae may reduce the probability of the formation of crosslinking in the irradiation.

## Discussion

In this section, the Gibbs–Thomson equation and Hoffman–Weeks equation are used to estimate the change in the lamellar thickness of crystallites ($l_c$) in the annealing process.[27,28]

The Gibbs–Thomson equation is based on the thermodynamic argument that $T_m$ of a crystallite with a finite size is depressed below $T_m^0$, the equilibrium melting temperature of an infinitely thickness crystal. For polymer lamellar crystals, in most cases $l_c$ is much smaller than the lateral dimensions.[29] Therefore, the depression of $T_m$ is proportional to the ratio of the free energy ($\sigma_e$) of the folding surface to the equilibrium enthalpy of fusion ($\Delta H_f^0$) of the crystal:[27,30,31]

$$T_m = T_m^0(1 - 2\sigma_e/\Delta H_f^0 l_c) \quad (1)$$

The Hoffman–Weeks equation is a result of a combination of Lauritzen–Hoffman secondary nucleation theory and the Gibbs–Thomson equation.[28,31,32] According to Lauritzen–Hoffman secondary nucleation theory, which relates the initial lamellar thickness ($l_c^*$) to the undercooling ($\Delta T = T_m^0 - T_x$, where $T_x$ is the isothermal crystallization temperature)

$$l_c^* = (2\sigma_{ex}/\Delta G_{fx}) + \delta l_c \cong (2\sigma_{ex}T_m^0/\Delta H_f^0 \Delta T) + \delta l_c \quad (2)$$

In the equation, $\sigma_{ex}$ and $\Delta G_{fx}$ are the basal plane crystal/melt interface free energy and the bulk free energy of fusion at $T_x$, respectively, and $\delta l_c$ is the thickness increment above the critical lamellar thickness. If the difference between the crystallization and observed $T_m$ is solely due to the thickening of the lamellae formed at $T_x$, the Gibbs–Thomson equation yields the observed $T_m$:

$$T_m = T_m^0(1 - 2\sigma_{ex}/\Delta H_f^0 \times \beta \times l_c^*) \quad (3)$$

where the thickening ratio $\beta$ is equal to $l_c/l_c^* \geq 1$. If $\beta$ equals 1 and $\delta l_c$ equals zero (nonthickening), the basal interfacial free energy given in eq 1 ($\sigma_e$) should be equivalent to that in eq 3 ($\sigma_{ex}$), and the crystals growing at $T_x$ will melt simultaneously (i.e., $T_m = T_x$); therefore, eq 3 becomes

$$T_x = T_m^0(1 - 2\sigma_{ex}/\Delta H_f^0 \times l_c^*) \quad (4)$$

Combining eqs 3 and 4 yields the Hoffman–Weeks equation:

$$T_m = T_m^0(1 - 1/2\beta) + (T_x/2\beta) \quad (5)$$

With the Hoffman–Weeks equation, $T_m^0$ can be determined from the plot of a series of $T_m$ as a function of $T_x$. The linear extrapolation of the observed $T_m$ versus $T_x$ to the straight line of $T_m = T_x$ yields $T_m^0$ and $\beta$.

A uniaxially stretched copolymer P(VDF-TrFE) (68/32 mol %) sample was heated in a DSC cell and kept at 200 °C for 5 min before cooling down (at a 35–40 °C/min cooling rate) to a selected $T_x$. The sample was kept at that temperature for 1 h and then cooled down to room temperature in the DSC cell. Afterward, the sample was heated up for the measurement of $T_m$. Figure 6 shows the $T_m$–$T_x$ plot so obtained, which yields $T_m^0$ = 160.7 °C and $\beta$ = 2.26.

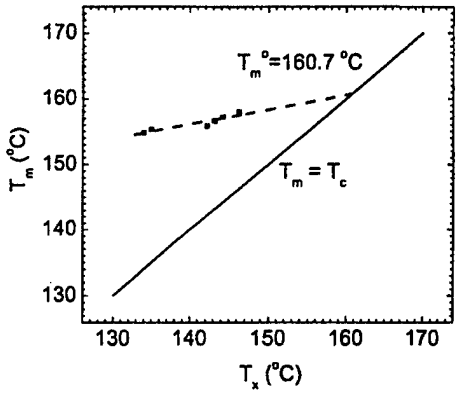


**Figure 6.** Hoffman–Weeks extrapolation ($T_m$–$T_x$ plot).

To estimate the change of the lamellar thickness with the annealing time, eq 1 is rearranged to

$$l_c(1)/l_c(2) = [1 - T_m(2)/T_m^0]/[1 - T_m(1)/T_m^0] \quad (6)$$

where $T_m(1)$ and $T_m(2)$ are the melting temperatures corresponding to crystal lamellae with thicknesses $l_c(1)$ and $l_c(2)$, respectively. From Figure 2, for films annealed at 134 °C, $T_m$ for 1-h annealed films is 154.19 °C [$T_m(1)$ = 427.37 K], and for films annealed for 10 h, it is 156.91 [$T_m(2)$ = 430.06 K]. Substituting these values into eq 6 yields the ratio of $l_c(1)/l_c(2)$ = 0.59. If for a well-annealed P(VDF-TrFE) copolymer film $l_c(2)$ is equal to 15 nm (annealed for 10 h), the lamellar thickness for films annealed for 1 h is $l_c(1)$ = 8.85 nm, which shows a quite large change in the crystal lamellar thickness with the annealing time.[33]

## RESULTS OF TWO-STEP-ANNEALED FILMS

As previously pointed out, although the uniaxially stretched HEEIP films prepared with one-step annealing exhibit a high electromechanical response (a 4% transverse strain and an almost 1 J/cm$^3$ elastic energy density),[8,15] the mechanical quality of the films is not high, and cracks are easily formed when the films are subjected to external stresses. In addition, because of the large shrinkage and increase in the crystallinity of the

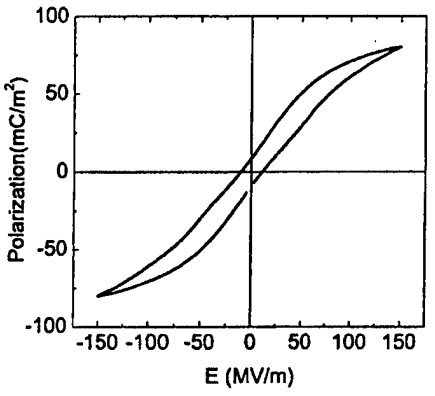


(a)

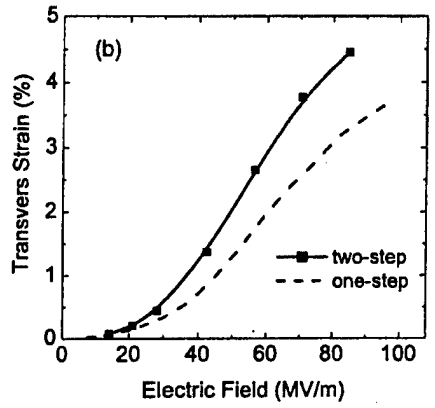


(b)

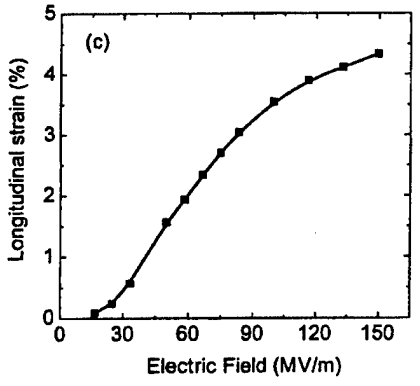


(c)

**Figure 7.** (a) Polarization hysteresis loop, (b) transverse strain, and (c) longitudinal strain of the uniaxially stretched HEEIP films with two-step annealing (120 °C for 2 h and 134 °C for 2 h) before the irradiation. For comparison, the transverse strain of the one-step-annealed samples is also shown in part b as a dashed line. The data points are shown and the solid curves have been drawn as guides.

films occurring simultaneously with annealing at 134 °C, this one-step annealing process is not suitable for large-scale film production. To improve the mechanical quality and also to establish an annealing procedure that can be used for large-quantity film production, we have investigated a two-step annealing process.

The semicrystalline polymers consist of a continuous amorphous phase dispersed with crystalline regions. During uniaxial stretching, the polymer chains in the amorphous part will be reoriented, the molecular axes being aligned parallel to the stretching direction. The crystalline regions will also reorient in the direction of stretching. When the highly oriented films are annealed, the molecular chains in the amorphous part will try to return to their original high entropy state (random coils), and the shrinkage will occur as soon as the molecules can move sufficiently to recoil to their undisturbed state. However, in the semicrystalline polymers, the coiling of the amorphous molecular chains is hindered by the crystalline regions, which tend to maintain their orientation as that at room temperature. Therefore, an internal stress will exist in the polymer and increase with an increased annealing temperature. This internal stress may be partially released by the amorphous polymer chain relaxation in the annealing. In addition, the amorphous part will also be crystallized at elevated annealing temperatures.

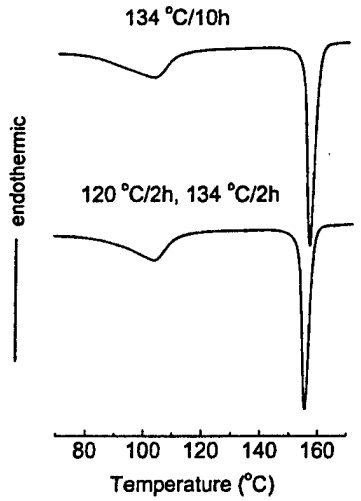


**Figure 8.** Comparison of the DSC thermograms of the uniaxially stretched 68/32 mol % films with one-step annealing (134 °C for 10 h) and two-step annealing (120 °C for 2 h and 134 °C for 2 h).

To optimize the continuously annealing processing for the films, we have investigated a two-step annealing process. In the first step, the film is annealed at 120 °C for more than 0.5 h. After the first step of annealing, the amorphous molecular chains acquire enough energy to relax, and this results in a shrinking of the films along the stretching direction by 10–15%, which helps to reduce substantially the internal stress and to stabilize the film dimensions. Meanwhile, there is not much of an increase in the crystallinity and crystal lamellar size at this annealing temperature. Therefore, the films after the first step of annealing are still quite flexible and can be easily handled. In the second higher temperature annealing, during which the crystallinity and crystallite dimensions increase markedly, the stress level in the films is much lower. Indeed, for films with the second-step-annealing temperature at 134 °C and an annealing time of 2 h, the film mechanical quality is improved quite significantly in comparison with those with one-step annealing for 10 h, and there is not much shrinkage at the second annealing temperature. More interestingly, the polarization loops after irradiation on these films show a very small hysteresis [Fig. 7(a); $E_c$ = 10 MV/m and $P_r$ = 0.7 $\mu$C/cm$^2$], and the films exhibit high transverse and longitudinal strain levels [Fig. 7(b,c)]. In fact, the two-step-annealed HEEIP films (2 h at 120 °C followed by 2 h at 134 °C) exhibit a higher transverse strain (4.4% under 85 MV/m) than those with one-step annealing (3.7% strain under 100 MV/m). whereas the elastic moduli of the two films are the same [see Fig. 7(b)].

Figure 8 shows the DSC thermograms for the copolymer films (nonirradiated) with one-step annealing (134 °C for 10 h) and two-step annealing (120 °C for 2 h and 134 °C for 2 h). The crystallinity (values of $\Delta H_m$) obtained from the two samples are about the same, whereas $T_m$ from the one-step-annealed film is 1.3 °C higher than that of the two-step-annealed film because of the shortened annealing time at 134 °C for the two-step annealing. The fact that the two-step-annealed HEEIP films under these annealing conditions exhibit even smaller polarization hysteresis and higher electromechanical response suggests that the changes in the crystal morphology in the two-step annealing process can compensate for the effect of the reduced crystal lamellar thickness.

## CONCLUSIONS

The influence of the annealing conditions before the irradiation on the electromechanical properties of uniaxially stretched HEEIP films (68/32 mol % composition) has been investigated. For one-step-annealed films, the crystallinity reaches the highest value for films annealed in the temperature range between 132 and 136 °C. Within this temperature window, increasing the annealing time results in an increase in the crystal lamellar thickness, which seems to be required to reduce the polarization hysteresis and to achieve a high electrostrictive strain. With the Gibbs–Thomson equation and Hoffman–Weeks extrapolation, it has been found that when the annealing time is increased from 1 to 10 h, the crystal lamellar thickness is increased by 70% (from about 8.8 to 15 nm), whereas there is very little change in the crystallinity. For the two-step-annealed films, lower temperature annealing is used to release the stress without causing much of an increase in the crystallinity in the films, and higher temperature annealing is used to raise the crystallinity and crystallite size. In this manner, the film mechanical quality can be improved with respect to that of the one-step-annealed films. Furthermore, the two-step-annealed uniaxially stretched HEEIP films with the first annealing at 120 °C for 2 h and with the second annealing at 134 °C for 2 h exhibit better electromechanical responses than the one-step-annealed HEEIP films.

This work was supported by Defense Advance Research Projects Agency (N00173-99-C-2003) and The National Institutes of Health (1 R0 HL65959).

## REFERENCES AND NOTES

1. Wang, T. T.; Herbert, J. M. In The Application of the Ferroelectric Polymers; Glass, A. M., Ed.; Blackie, Chapman & Hall: New York, 1988.
2. Bar-Cohen, Y. Electroactive Polymer Actuators as Artificial Muscles; SPIE: Bellingham, WA, 2001.
3. Smela, E.; Inganas, O.; Lundstrom, I. Science 1955, 268, 1735.
4. Tadokoro, S.; Muramura, T.; Fuji, S.; Kanno, R.; Hattori, M.; Takamori, T. Proceedings of the IEEE International Conference: Robotics and Automation; IEEE: Piscataway, NJ, 1996; p 205.
5. Guo, S.; Nakamura, T.; Fukuda, T.; Oguro, K. Proceedings of the IEEE International Conference: Ro-

botics and Automation; IEEE: Piscataway, NJ, 1997; p 266.
6. Bar-Cohen, Y.; Xue, T.; Joffe, B.; Lih, S. S.; Willis, P.; Simpson, J.; Smith, J.; Shahinpoor, M. Proceedings of the SPIE Symposium: Smart Structure Materials; SPIE: Bellingham, WA, 1997; Vol. 3041, p 697.
7. Wax, S. G.; Sands, R. R. Proceedings of the SPIE Symposium: Smart Structure Materials; SPIE: Bellingham, WA, 1999; Vol. 3669, p 1.
8. Zhang, Q. M.; Scheinbeim, J. In Electroactive Polymer Actuators as Artificial Muscles; Bar-Cohen, Y., Ed.; SPIE: Bellingham, WA, 2001; pp 89–120.
9. Bar-Cohen, Y. Proceedings of the SPIE Symposium: Smart Structure Materials; SPIE: Bellingham, WA, 2001; Vol. 4329.
10. Furukawa, T. Phase Trans 1989, 18, 143.
11. Nalwa, H. Ferroelectric Polymers; Marcel Dekker: New York, 1995.
12. Lovinger, A. In Radiation Effects on Polymers; Clough, R. L.; Shalaby, S. W., Eds.; ACS Symposium Series 475; American Chemical Society: Washington, DC, 1991; Chapter 6.
13. Daudin, B.; Bubus, M.; Legrand, J. F. J Appl Phys 1987, 62, 994.
14. Zhang, Q. M.; Bharti, V.; Zhao, X. Science 1998, 280, 2101.
15. Cheng, Z.-Y.; Bharti, V.; Xu, T. B.; Xu, H. S.; Mai, T.; Zhang, Q. M. Sens Actuators A 2001, 90, 138.
16. Xu, H. S.; Shanthi, G.; Bharti, V.; Zhang, Q. M.; Ramotowski, T. Macromolecules 2000, 33, 4125.
17. Cheng, Z.-Y.; Bharti, V.; Mai, T.; Xu, T. B.; Zhang, Q. M.; Hamilton, K.; Ramotowski, T.; Wright, K. A.; Ting, R. IEEE Trans UFFC 2000, 47, 1296.
18. Bharti, V.; Xu, H. S.; Shanthi, G.; Zhang, Q. M. J Appl Phys 2000, 87, 452.
19. Ohigashi, H.; Koga, K. Jpn J Appl Phys L 1982, 21, 455.
20. Koga, K.; Ohigashi, H. J Appl Phys 1986, 59(6), 15.
21. Cheng, Z.-Y.; Bharti, V.; Xu, T. B.; Wang, S.; Zhang, Q. M.; Ramotowski, T.; Tito, F.; Ting, R. J Appl Phys 1999, 86, 2208.
22. Su, J.; Moses, P.; Zhang, Q. M. Rev Sci Instrum 1998, 69, 2480.
23. Barique, M. A.; Ohigashi, H. Polymer 2001, 42, 4981.
24. Li, G.-R.; Kagami, N.; Ohigashi, H. J Appl Phys 1992, 72(3), 1.
25. Fernandez, M. V.; Suzuki, A.; Chiba, A. Macromolecules 1987, 20, 1806.
26. Bharti, V.; Zhao, X.; Zhang, Q. M. Mater Res Innovat 1998, 2, 57.
27. Marand, H.; Hoffman, J. D. Macromolecules 1990, 23, 3682.
28. Hoffman, J. D.; Weeks, J. J. J Res Natl Bur Stand Sect A 1962, 66, 13.
29. Lauritzen, J. I., Jr.; Hoffman, J. D. J Res Natl Bur Stand Sect A 1960, 64, 73.
30. Hoffman, J. D.; Lauritzen, J. I., Jr. J Res Natl Bur Stand Sect A 1961, 65, 297.
31. Hoffman, J. D.; Davis, G. T.; Lauritzen, J. I., Jr. In Treatise on Solid State Chemistry; Hannay, N. B., Ed.; Plenum: New York, 1976; Vol. 3, Chapter 7.
32. Hoffman, J. D.; Miller, R. L. Polymer 1997, 38, 3151.
33. Tashiro, K. Proceedings of the MRS Symposium; MRS: Warrendale, PA, 1999; Vol. 600, p 35.

# APPENDIX 29

PROCEEDINGS OF SPIE

SPIE—The International Society for Optical Engineering

*Smart Structures and Materials 2003*

# *Electroactive Polymer Actuators and Devices (EAPAD)*

**Yoseph Bar-Cohen**
*Chair/Editor*

**3–6 March 2003**
**San Diego, California, USA**

*Sponsored by*
SPIE—The International Society for Optical Engineering

*Cosponsored by*
ASME—American Society of Mechanical Engineers (USA)
SEM—Society for Experimental Mechanics (USA)
Boeing Company (USA)
Rhombus Consultants Group (USA)
CSA Engineering, Inc. (USA)
ISIS Canada (Canada)


**Volume 5051**

# Poly(vinylidene fluoride-trifluoroethylene) Based High Performance Electroactive Polymers

Feng Xia[a], Hengfeng Li[a], Cheng Huang[a], M. Y. M. Huang[a], H. Xu[a], Francois Bauer[b], Z.-Y. Cheng[c], Q. M. Zhang*[a]

[a]Electrical Engineering Department and Materials Research Institute, The Pennsylvania State University, University Park, PA 16802, USA

[b]Institute Franco-Allemand de Recherches de Saint-louis, France

[c]Materials Engineering, 201 Ross Hall, Auburn University, Auburn, AL 36849-5341, USA

## ABSTRACT

This paper reports two classes of electroactive polymers developed recently which exhibit very high strain and elastic energy density. In the first class of the electroactive polymer, i.e., the defects modified poly(vinylidene fluoride-trifluoroethylene) (P(VDF-TrFE)) polymers, an electrostrictive strain of more than 7% and an elastic energy density above 1 J/cm$^3$ can be induced under a field of 150 MV/m. The large electrostrictive strain in this class of polymers originates from the local molecular conformation change between the trans-gauche bonds and all trans bonds, which accompanies the field induced transformation from the non-polar phase to the polar phase. The second class of the polymer is an all organic composite, which shows a very high dielectric constant (>400) and high strain induced with a low applied field (2% strain under 13 MV/m). The strain is proportional to the applied field and the composite has an elastic modulus near 1 GPa.

**Keywords:** Electroactive polymer, Electrostriction, Actuators, Composites, Dielectric constant.

## 1. INTRODUCTION

Polymer based materials have attracted a great deal of attention and have found many applications for electromechanical devices to perform energy conversion between the electric and mechanical forms such as artificial muscles, smart skins for drag reduction, actuators for active noise and vibration controls, and micro-fluidic systems for drug delivery and micro-reactors[1-4]. Polymers are renowned for their excellent mechanical properties including light weight, flexible, and easy processing, and that polymers can be conformed to complicated shapes. On the other hand, compared with inorganic materials, the electromechanical responses of polymer based materials are quite low. Especially, one of the unique features of the polymers, that is, most polymers can withstand very high strain (>10%) without fatigue, which is not possible in inorganic materials, has not been utilized to develop electroactive polymers with ultra-high electroactive strain responses. Recently, research works from several groups have demonstrated that in several electroactive polymers, strain level far above those from the traditional piezoelectric materials can be achieved[5-8]. Some of these polymers can even display the elastic energy density, a quantity measuring both the strain and stress generation capability of an actuator material, higher than that of piezoelectric ceramics[5,6,8]. This paper will present some of these recent works, including the electrostrictive P(VDF-TrFE) based polymers and all organic composites. In addition, issues related to the development of high performance electroactive polymers will also be discussed.

## 2. ELECTROMECHANICAL PROPERTIES OF DEFECTS MODIFIED P(VDF-TrFE) BASED POLYMERS

Among the all known polymers, piezoelectric P(VDF-TrFE) copolymer is the one that is most widely used and possesses the best performance for electromechanical applications[3]. Its piezoelectric properties are summarized in Table I. As can be seen, the electromechanical responses of the P(VDF-TrFE) copolymer is still much lower than those of piezoelectric ceramics. Furthermore, the maximum piezoelectric strain of the piezo-copolymers is on the order of 0.1%, which is also quite low for most actuator device applications.

Table I. Piezoelectric properties of P(VDF-TrFE) copolymer and its comparison with piezoceramics

| | $d_{33}$ (pm/V) | Y (GPa) | $k_{33}$ | K |
|---|---|---|---|---|
| Piezo-P(VDF-TrFE) | -33 | 3.3 | 0.27 | 8 |
| Piezoceramic (PZT) | 590 | 48 | 0.7 | 3400 |

* $d_{33}$ is the piezoelectric coefficient, Y is the Young's modulus, $k_{33}$ is the longitudinal coupling factor, and K is the dielectric constant.

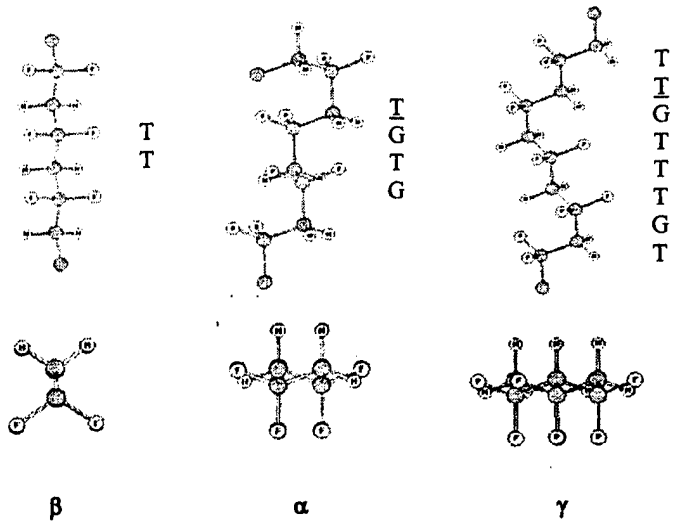


Figure 1. Schematic of the extended chain segments of an all-trans, TGTG' (or TGT$\overline{G}$), and TTTGTTTG' (or TTTGTTT$\overline{G}$) conformations (the filler circles are carbon).

However, in P(VDF-TrFE) copolymers, there are several avenues to raise the electromechanical responses substantially. For example, experimental evidence has shown that there are large strains (~10%) accompanying the phase transformation process between the ferroelectric and paraelectric (F-P) phases[9]. The origin of such a large strain in the F-P transition is due to the molecular conformation change as shown in figure 1. In the ferroelectric phase, the molecules take the all trans conformations, while in the paraelectric phase, the molecular conformation takes the form of a mixture of trans-gauche (TGTG') and $T_3GT_3G'$ conformations. As can be seen from the figure, a large dimensional change occurs when the molecular conformation changes from the all trans to TGTG' and $T_3GT3G'$ conformations. In addition, at temperature regions just above a first order F-P transition, a polar-phase can be electrically induced. It has been shown that in this field induced phase, a very large electro-mechanical coupling factor can be achieved (theoretically ~ 100%)[10].

All these observations indicate that by operating the P(VDF-TrFE) copolymers at near F-P transition region, very high electromechanical response can be realized. To overcome the problems which are common to all the first order phase transformation process in polymers, i.e., large hysteresis, narrow transition temperature region, and that the temperature range of the transition is far above room temperature, all of which are not desirable for practical applications, P(VDF-TrFE) based polymers are modified. In this study, P(VDF-TrFE) based polymers are modified via two approaches: the high energy electron irradiation and copolymerizing the P(VDF-TrFE) with a small amount of third chlorinated monomer to form a terpolymer. Several effects occur when the defects are introduced into the ferroelectric crystalline region of the polymer. First of all, the defect structures weaken the inter- and intra-chain dipolar coupling and hence, lower the F-P transition to near room temperature. In addition, these defect structures also introduce inhomogeneity in the ferroelectric phase which broadens the transition region. Furthermore, they reduce and in some cases eliminate the energy barrier in the transformation between different molecular conformations which in turn reduce or eliminate the hysteresis associated with the transformation. As a result, the normal ferroelectric P(VDF-TrFE) copolymer is transformed into a relaxor ferroelectric polymer with a high electrostriction and improved the electromechanical coupling factor[5,8,11].

As an example, figure 2 compares the dielectric responses between the normal ferroelectric P(VDF-TrFE) copolymer, a high energy electron irradiated copolymer, and a terpolymer. It is evident that the dielectric peak, which is associated with F-P transition in the normal ferroelectric P(VDF-TrFE) copolymer, is broadened markedly and moved to near room temperature for the irradiated copolymer and the terpolymer. In addition, in the defect structure modified polymers (the terpolymer and irradiated copolymer) the broad dielectric peak position shifts with the frequency f as illustrated in figure 2, which can be described quite well by the Vogel-Folcher (V-F) law (figure 2(d)), $f = f_0 \exp[\frac{-U}{k(T_m - T_f)}]$, where U is a constant and k is the Boltzmann constant, $T_f$ can be regarded as the freezing temperature, corresponding to the peak

temperature of the static dielectric constant (~ 0 Hz frequency), and the pre-factor $f_0$ is the upper frequency limit of the system, corresponding to the dipolar response when there is no coupling between the dipolar units in the system. Such a behavior is a typical feature to all the known relaxor ferroelectric materials[12].

### 2.1 Electromechanical properties of the high energy electron irradiated copolymers (HEEIP)

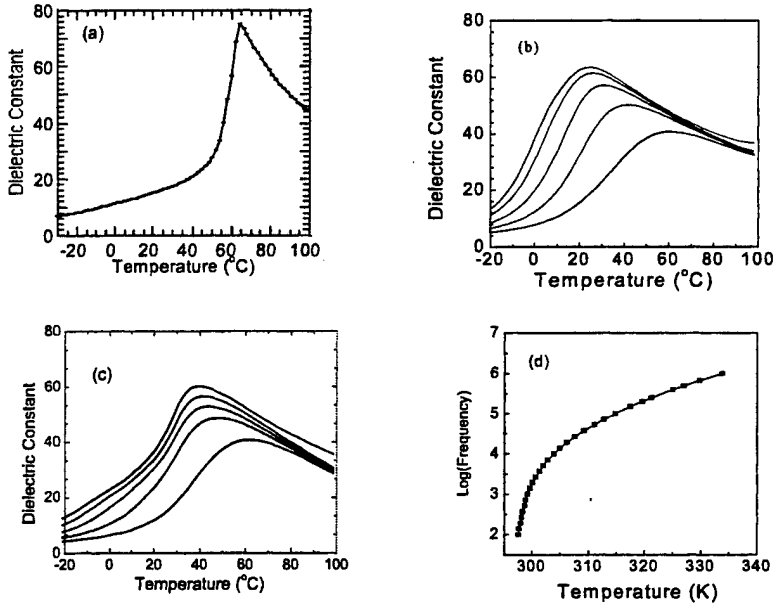


Figure 2. Comparison of the dielectric constant of (a) the P(VDF-TrFE) 65/35 copolymer (at 1 kHz), (b) the irradiated P(VDF-TrFE) 68/32 mol%, and (c) the terpolymer of P(VDF-TrFE-CFE) 62/38/4 mol%. The terpolymer and irradiated copolymer data are measured at frequencies of 100 Hz, 1 kHz, 10 kHz, 100 kHz, and 1 MHz (curves from top to bottom) and the data show that the dielectric peak temperature shifts with frequency. (d) The fitting of the dielectric data (dots) to the V-F law (solid curve).

Presented in figure 3(a) is the field induced strain along the film thickness direction (longitudinal strain $S_3$) for the HEEIP where –5% strain is induced under a field of 150 MV/m. The plot of strain versus the square of the polarization yields a straight line, indicating that the response is electrostrictive in nature ($S_3=Q_{33}P_3^2$, figure 3 (b)). For the irradiated copolymer, $Q_{33}$ is found in the range between –4 to –15 $m^2/C$, depending on the sample processing conditions[8].

Of special interest is the finding that in P(VDF-TrFE) copolymer, large anisotropy in the strain responses exists along and perpendicular to the chain direction, as can be deduced from the change in the lattice parameters between the polar and non-polar phases (see figure 1)[3]. Therefore, the transverse strain (the strain in perpendicular to the applied field direction) can be tuned over a large range by varying the film processing conditions. For unstretched films,

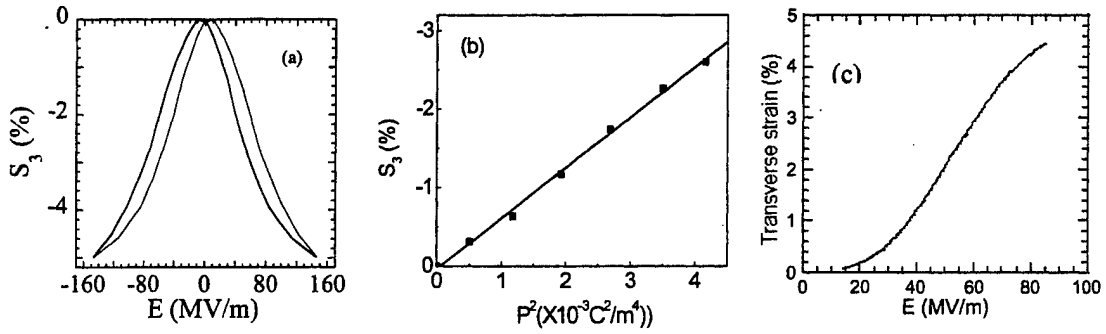


Figure 3. (a) The longitudinal strain as a function of the applied field measured at room temperature for irradiated P(VDF-TrFE) 68/32 mol% copolymer, (b) The longitudinal strain versus the square of the polarization where the data points are shown and the solid line is the fitting of strain versus the square of the polarization, (c) The transverse strain for the irradiated P(VDF-TrFE) 68/32 mol% stretched copolymer film. The strain is measured along the film drawing direction.

the transverse strain is relatively small (~1% level under 100MV/m field) while the amplitude ratio between the transverse strain and longitudinal strain is less than 0.33[13]. This feature is attractive for devices utilizing the longitudinal strain such as ultrasonic transducers in the thickness mode, and actuators and sensors making use of the longitudinal electromechanical responses of the material. On the other hand, for stretched films, a large transverse strain ($S_1$) along the stretching direction can be achieved as shown in figure 3(c), where the transverse strain of more than 4% can be achieved.

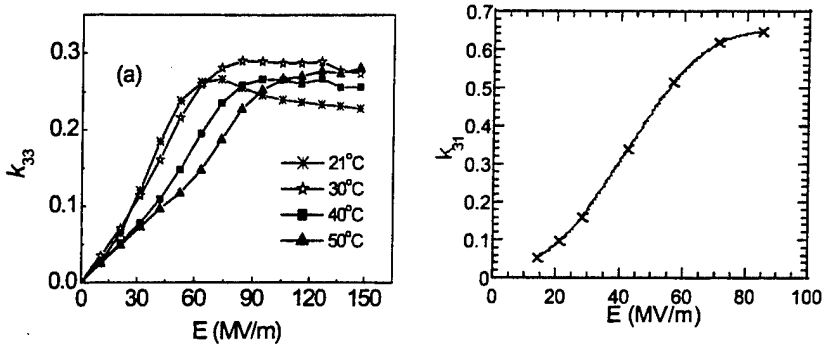


Figure 4. (a) The longitudinal k33 at different temperatures and (b) room temperature transverse k31 electromechanical coupling factors for irradiated 68/32 copolymer films. Data points are shown and solid curves are drawn to guide eyes.

For electrostrictive materials, the electromechanical coupling factor ($k_{ij}$) has been derived by Horn et al. based on the consideration of electrical and mechanical energies generated in the material under external field[14]:

$$k_{3i}^2 = \frac{kS_i^2}{s_{ii}^D\left[P_E \ln\left(\frac{P_S + P_E}{P_S - P_E}\right) + P_S \ln\left(1 - \left(\frac{P_E}{P_S}\right)^2\right)\right]}, \quad (1)$$

where $i$=1 or 3 correspond to the transverse or longitudinal direction (for example, $k_{31}$ is the transverse coupling factor) and $s_{ii}^D$ is the elastic compliance under constant polarization, $S_i$ and $P_E$ are the strain and polarization responses, respectively, for the material under an electric field $E$. The coupling factor depends on $E$, the electric field level. In eq. (1), it is assumed that the polarization-field (P-E) relationship follows approximately:

$$|P_E| = P_S \tanh(k|E|), \quad (2)$$

where $P_S$ is the saturation polarization and $k$ is a constant.

The electromechanical coupling factors for the irradiated copolymers are shown in figure 4. Near room temperature and under an electric field of 80 MV/m, $k_{33}$ can reach more than 0.3, which is comparable to that obtained in a single crystal P(VDF-TrFE) copolymer. More interestingly, $k_{31}$ of 0.65 can be obtained in a stretched copolymer, which is much higher that values measured in unirradiated P(VDF-TrFE) copolymers and, to our knowledge, is the height among all the known ferroelectric, piezoelectric, and electrostrictive polymers. These results are also verified by recent resonance studies in these polymers.

For a polymer, there is always a concern about the electromechanical response under high mechanical load; that is, whether the material can maintain high strain levels when subject to high external stresses. Figure 5 depicts the transverse strain of stretched and irradiated 65/35 copolymer under a tensile stress along the stretching direction. As can be seen from the figure, under a constant electric field, the transverse strain increases initially with the load and reaches a maximum at the tensile stress

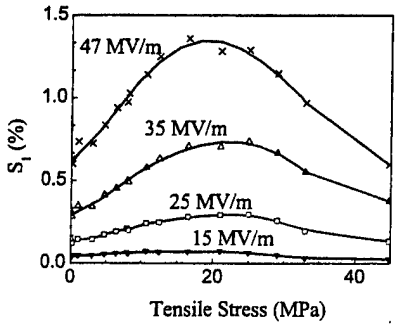


Figure 5. Effect of the tensile stress on the transverse strain (S1) for stretched and irradaied 65/35 copolymer films. Data points are shown and solid curves are drawn to guide eyes.

of about 20 MPa. Upon a further increase of the load, the field-induced strain is reduced. One important feature revealed by the data is that even under a tensile stress of 45 MPa, the strain generated is still nearly the same as that without load, indicating that the material has a very high load capability[15].

**2.2 The electromechanical properties of the terpolymer P(VDF-TrFE-CFE)**

Although high energy irradiations can be used to convert the normal ferroelectric P(VDF-TrFE) into a relaxor ferroelectric with high electrostriction, the irradiations also introduce many damages to the copolymer, for instance, the formation of crosslinkings, radicals, and chain scission[16]. From the basic ferroelectric response consideration, the defect structure modification of the ferroelectric properties can also be realized by introducing randomly in the polymer chain a third monomer, which is bulkier than VDF and TrFE. Furthermore, by a proper molecular design which enhances the degree of molecular level conformational changes in the polymer, the terpolymer can exhibit much higher electromechanical response compared with the high energy electron irradiated copolymer, as will be demonstrated by the terpolymer containing the chlorofluoroethylene (CFE, $-CH_2-CFCl-$) as the termonomer.

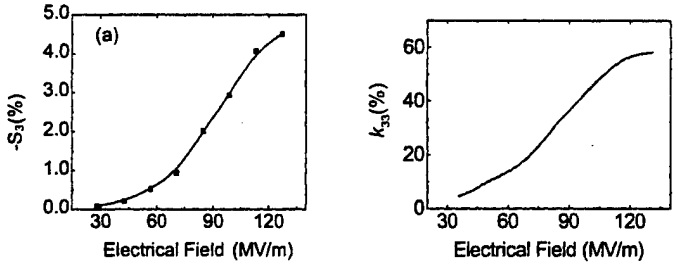


Figure 6. (a) The field induced longitudinal strain (S3) as a function of the applied field and (b) The longitudinal coupling factor k33 for the P(VDF-TrFE-CFE) 62/38/4 mol% terpolymer versus the applied field amplitude.

Presented in figure 6(a) is the field-induced strains along the thickness direction ($S_3$) as a function of the applied electrical field for the terpolymer P(VDF-TrFE-CFE) 62/38/4 mol%. Here the terpolymer composite is labeled as $VDF_{1-x}$-$TrFE_x$-$CFE_y$ where y is the mol% of CFE in the terpolymer. Such a notation makes it easier when comparison is made with the irradiated copolymers. Under a field of 130 MV/m, a thickness strain of – 4.5% can be achieved, which is comparable to that observed in HEEIP. Because of higher crystallinity in the P(VDF-TrFE-CFE) terpolymer, the elastic modulus Y~1.1 GPa of the terpolymer here is much higher than that of HEEIP and other terpolymers, resulting in a high elastic energy density, $YS^2/2$ (~1.1 $J/cm^3$). The longitudinal coupling factor is presented in figure 6(b). It is interesting to note that the coupling factor can reach more than 0.55 which is far above coupling factors reported in all known piezoelectric and electrostrictive polymers.

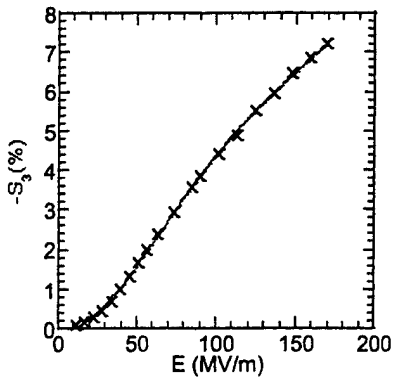


Figure 7. The field induced longitudinal strain (S3) as a function of the applied field for the terpolymer P(VDF-TrFE-CFE) 68/32/9 mol%. Data points are shown and solid curve is drawn to guide eyes.

By increasing the ratio of VDF/TrFE in the terpolymer, the field induced strain level can be raised owing to the fact that the lattice strain between the polar conformation and non-polar conformations increases with the VDF/TrFE ratio[17]. Presented in figure 7 is the thickness strain of the P(VDF-TrFE-CFE) terpolymer at composition of 68/32/9 mol% and a strain of more than 7% can be reached. The results here demonstrate the potential of the terpolymers in achieving very high electromechanical responses by composition optimization.

In table II, we compare the electromechanical properties of four different types of P(VDF-TrFE) based polymers, that is, the normal piezoelectric P(VDF-TrFE) copolymer, HEEIP, P(VDF-TrFE-CFE) terpolymers studied here, and P(VDF-TrFE-CTFE) terpolymer (CTFE: chlorine-trifluoroethylene)[18]. Obviously, the terpolymer with CFE as a modifier shows the highest electromechanical responses.

Although all three modified P(VDF-TrFE) based polymers listed in table II possess macroscopic non-polar phase with similar slim polarization hysteresis and field induced polarization levels, the high electromechanical response observed in the CFE based terpolymer indicates the important role played by the molecular microstructure.

Table II. Comparison of the electromechanical properties of the modified PVDF based polymers and piezoelectric P(VDF-TrFE)

| Polymer | $S_M$ (%) | Y (GPa) | $YS_M^2/2$ (J/cm$^3$) | $k_{33}$ | $k_{31}$ |
|---|---|---|---|---|---|
| PiezoP(VDF-TrFE) | 0.2 | 3.3 | 0.0066 | 0.27 | |
| HEEIP $S_3$ | -5 | 0.4 | 0.5 | 0.30 | |
| $S_1$ | 4.5 | 1.0 | 1.0 | | 0.65 |
| P(VDF-TrFE-CTFE) | -4 | 0.4 | 0.32 | 0.28 | |
| P(VDF-TrFE-CFE) | | | | | |
| 62/38/4 mol% $S_3$ | -4.5 | 1.2 | 1.2 | 0.55 | |
| 68/32/9 mol% $S_3$ | -7 | 0.3 | 0.73 | | |

*$S_M$ is the strain and $YS_M^2/2$ is the volumetric elastic energy density, $k_{31}$ is the transverse coupling factor.

P(VDF-TrFE) based polymers are semi-crystalline polymers, in which the polarization and, therefore, the electromechanical responses originate mainly from the crystalline regions[3]. In order to achieve a high electromechanical response, a high crystallinity is highly desirable. For the P(VDF-TrFE) copolymers in the composition range studied here, the crystallinity (the volume fraction of the crystalline regions) can reach more than 75%. When a ter-monomer is added to the polymer chain to form a terpolymer, the crystallinity, in general, will be reduced due to the introduction of defect structures. The resulting crystallinity in a terpolymer, therefore, will depend on the type as well as the mol% of the ter-monomer added. On the other hand, in order to make use of the defect structures to convert the polymer into an electrostrictor, there is a minimum mol% of each type of ter-monomer required in the terpolymer. Experimental results indicate that CFE is more effective in this regard compared with CTFE. In the terpolymers containing CFE studied here, 4-5 mol% of CFE seems to be adequate to nearly eliminate the polarization hysteresis, while in the terpolymers containing CTFE, nearly 10 mol% is required[11,18].

Furthermore, even for terpolymers with the same crystallinity, the field-induced strain level can still vary over a large range because of different types of polarization mechanisms responding to an external electric field. For instance, in the normal ferroelectric P(VDF-TrFE) copolymer, the polarization switching is through the dipolar re-orientation process in the all trans crystalline region resulting in a strain change that is relatively low as has been observed[19]. Because of the relaxor ferroelectric nature of the modified P(VDF-TrFE) polymers, it is possible that there exist randomly oriented nano-polar regions (small regions with the all-trans molecular conformation) in the polymer even though macroscopically, the polymer is non polar[12]. The re-orientation of those nano-polar regions under external fields may not generate high electrostrictive strains. On the other hand, in the HEEIPs, the room temperature non-polar phase consists of mixture of trans-gauche bonds (mixture of TGTG' and $T_3GT_3G'$ conformations). An externally applied field induces a reversible molecular conformation change between TGTG'/$T_3GT_3G'$ and an all-trans conformation. As a result, a large electrostriction is obtained.[20] Analogously, in the terpolymers, in order to enhance the strain response, it is required that the ter-monomer introduced will favor the formation of TG bonds rather than the all-trans conformation.

The experimental results as well as the analyses all indicate that by further working with terpolymers with different VDF/TrFE ratios and with different types and mol% of the termonomers, a much higher electromechanical response is anticipated in P(VDF-TrFE) based terpolymers.

## 3. AN ALL ORGANIC HIGH DIELECTRIC CONSTANT COMPOSITE

For the polymers presented in the preceding section, although the large strain and large elastic energy density achieved represent a breakthrough in improving the electromechanical response of polymers, the high electric field (> 100 MV/m) required to generate the high strain and high elastic energy density may limit the applications of these polymers. The high operation field required to generate high strain and high elastic energy density in these polymers in fact has its origin from the principle of energy conservation. To illustrate this point, we take, as an example, an electroactive polymer which is assumed to be a linear dielectric and elastic material. The stored elastic energy density when a polymer is strained is $U_S = \frac{1}{2} Y S^2$, where Y is the Young's modulus and S is the strain. For an electroactive polymer, the total elastic energy density from all the strains generated cannot exceed the input electric energy density because of

the energy conservation. As a linear dielectric material, this input electric energy density from the external electric source is $U_E = \frac{1}{2} K\varepsilon_0 E^2$, where E is the applied field, $\varepsilon_0$ is the vacuum dielectric permittivity (=$8.85 \times 10^{-12}$ F/m), and K is the dielectric constant of the polymer. In most of the polymeric materials, the dielectric constant K is less than 10, which is far below those in the inorganic materials, many of which can reach more than 5,000. Hence, in order to generate a high input electric energy density which can be converted to strain energy, a high electric field is required. For example, to generate a strain energy density of 0.1 J/cm$^3$, which is the elastic energy density in piezoceramics[5], in a polymer with a dielectric constant 10, assuming a 50% energy conversion efficiency, which is very high for the current electroactive polymers, the field required is 67 V/μm. Although it was recently reported that a high induced strain (~ 4%) can be generated in a liquid crystal elastomer under a low field (~1.5 V/μm), however, the elastic modulus of the elastomer is quite low (~ 1 MPa) which results in a very low elastic energy density (~0.001 J/cm$^3$)[7]. In order to reduce the applied field substantially in the electroactive polymers while retaining the high elastic energy density, which is required in many practical applications, one has to substantially raise the dielectric constant of this class of polymers.

In the past, the composite approach, in which high dielectric constant particulates are added to a polymer matrix to form a composite, has been employed to raise the dielectric constant of polymer based materials[21]. However, because these high dielectric constant fillers (most often, ceramic materials) also possess an elastic modulus that is much higher than that of polymers, the resulting composite also shows an elastic modulus much higher than that of the polymer matrix and loses its flexibility. In addition, the low dielectric constant of the polymer matrix utilized ($\leq 10$) also results in the composite dielectric constant still below 100.

Recently, we experimented with composites using the high dielectric constant organic solids as the filler and the electrostrictive P(VDF-TrFE) as the matrix. In several semiconductor organic solids, very high dielectric constant has been reported[22-24]. One example is copper-phthalocyanine (CuPc) which exhibits a dielectric constant as high as $10^5$. The large dielectric constant can be explained in terms of the electron delocalization within CuPc molecules. CuPc oligmers are highly conjugated and have a large planar structure. The easy displacement of the electrons under electric fields from the conjugated π-bonds within the entire molecule results in a large displacement of the charges and, hence, a high polarizability and high dielectric response[24,25]. Furthermore, the open molecular structure of the oligmers and the weak van der Waals intermolecular forces render the molecular solids formed with an elastic modulus not much higher than the polymer matrix. On the other hand, CuPc solids are difficult to process and show a high dielectric loss due to the long range intermolecular hopping of electrons. Therefore, in addition to provide a matrix to the CuPc particulates, the polymer matrix also forms insulation layers to significantly reduce the dielectric loss.

The electrostrictive P(VDF-TrFE) polymers are used as the polymer matrix. As has been shown in the preceding section, the electrocstrictive P(VDF-TrFE) polymers exhibit a high room temperature dielectric constant (>50) which is by far the highest among the all known polymers. Moreover, the polymers also exhibit a very high electrostrictive strain. Both features are highly desirable for the composites.

In deeded, the resulting composite exhibits almost the same elastic modulus as the polymer matrix and but still retains the flexibility. For composites containing 40 wt% to 55 wt% of CuPc, which is the composition range of interest, the

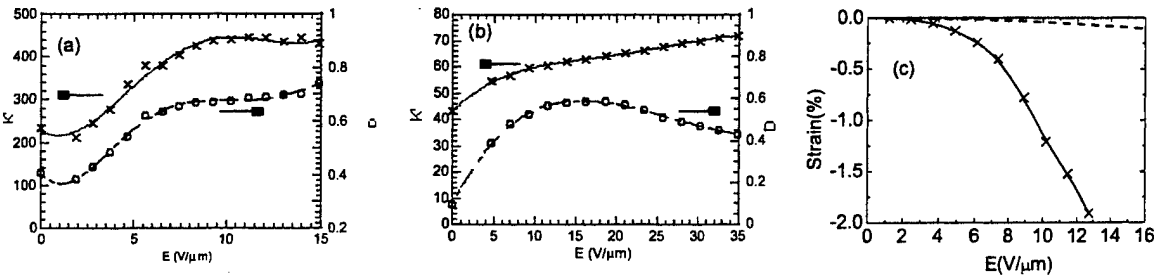


Figure 8. (a) Dielectric properties of the all-organic composites. The real part of the dielectric constant (K') and dielectric loss (D) as a function of the applied field amplitude for the composite with 40wt% CuPc and (b) Dielectric properties the polymer matrix as a function of the applied field amplitude. (c) The strain amplitude as a function of the applied field amplitude measured at room temperature. For the comparison, the strain from the electrostrictive P(VDF-TrFE) copolymer at the same field range is also shown (the dashed curve). The applied field is at 1 Hz. Data points are shown and solid curves are drawn to guide eyes.

elastic modulus at room temperature is in the range of 0.6 GPa to 1.2 GPa, (the density of CuPc is similar to P(VDF-TrFE) and hence the wt% is also similar to the volume %). The composite also exhibits a high dielectric constant as shown in figure 8(a). More importantly, a high strain can be induced with a much reduced applied field. Presented in figure 8(c) is the field induced strain as a function of the applied field amplitude measured on a composite with 40 wt% CuPc in an electrostrictive P(VDF-TrFE) polymer matrix. A strain near 2 % can be induced under a field of 13 V/μm and the strain measured is proportional to the applied electric field. Considering the fact that the composite possesses the same elastic modulus as those of electrotrictive P(VDF-TrFE) polymers, the result demonstrates that this all organic composite approach can result in a near 10 times reduction of the applied field in comparison of the electrostrictive P(VDF-TrFE) polymers. The composite properties such as the breakdown field and dielectric constant can be improved and as a result, much higher strain level with low applied field can be expected in this new class of polymer-like material.

The results of the strain measurement indicate that the field induced strain S is proportional to the square of the applied electric field, suggesting that the strain response originates from either the Maxwell stress (the electrostatic force), or the electrostriction, or both[5,6,26,27]. When a dielectric material is subject to an electric field E, it will experience an electrostatic force (Maxwell stress) due to the Coulomb force between charges. The strain induced by the Maxwell stress along the applied field direction is[26]

$$S = \tfrac{1}{2} K \varepsilon_0 E^2 (1 + 2\sigma)/Y \qquad (3)$$

Here we assumed that the dielectric material is isotropic and $\sigma$ is the Poisson's ratio. The electrostriction is strain generated due to a change in the polarization in a material under constant stress, which is equal to $S = ME^2$, where M is the electrostrictive coefficient and is proportional to the square of the dielectric constant[27].

From the dielectric and elastic data, the contributions to the strain response from the Maxwell stress and electrostriction may be estimated. Assuming that the composite is homogeneous, the strain due to the Maxwell stress under a field of 13 V/μm is about -0.1%. For the electrostriction from the polymer matrix, assuming that all the applied field is totally loaded on the polymer matrix because its dielectric constant is much lower than that of CuPc, it is also about -0.1%. The measured strain response, therefore, is about one order of magnitude higher than the combined strain from the two.

In an early study on the field induced strain in a polyurethane elastomer, it was observed that a non-uniform electric field distribution can significantly enhance the strain response (more than 5 times in that case) if the strain is proportional to the square of the local field[28]. The composites investigated here are highly heterogeneous where a large variation in the local fields is likely, which will enhance the strain response. In addition, bond length and conformation change in CuPc due to electron motions as well as the CuPc molecular reorientation under external fields may also contribute to the strain response[29].

## 4. CONCLUSIONS AND ACKNOWLEDGEMENT

By making use of the large strain associated molecular conformation change and the large ferroelastic coupling in P(VDF-TrFE) based ferroelectric polymers, a very large electrostrictive strain can be obtained in two defects modified P(VDF-TrFE) polymers, i.e., the P(VDF-TrFE) based terpolymers and high energy electron irradiated copolymers. The functions of the defect structures, introduced via the termonomers in the terpolymer or the high energy electron irradiation in the irradiated copolymers, are (1) to broaden the temperature range in which a polar and non-polar phase can reversibly induced by external fields, (2) to eliminate the nucleation barriers in the transformation between the polar and non-polar phases, and (3) to lower the transformation region to room temperature. As a result, a large electrostrictive strain can be achieved at room temperature over a broad temperature range in these modified polymers.

Compared with the high energy irradiation, the terpolymer approach to modify the copolymer is more attractive since it reduces the manufacture cost and simplifies significantly the processing steps. In addition, it reduces greatly the undesirable side effects introduced by the irradiation to the polymers and hence, can produce a modified polymer with much better electromechanical responses compared with the high energy irradiated copolymers, as has indeed been observed.

In order to reduce the high operation fields required in these polymers which originate from the low dielectric constant in the polymers, we investigated an all organic composite approach in which semiconductor organic solids with very high dielectric constant were used as the fillers and the electrostrictive polymers based on modified P(VDF-TrFE) polymers as the matrix. We showed that this approach could produce a composite (with the filler in the 40 – 60 wt% composition range) with high dielectric constant (>400) and a high induced strain under a low applied field.

Furthermore, the new composite exhibits an elastic modulus similar to that of the matrix and is flexible, which are very different from the high dielectric composites developed earlier in which inorganic materials are used as the fillers.

The authors wish to thank Dr. R. Ting and Dr. Belfield for their assistance in the terpolymer synthesis. The authors also wish to thank Dr. J. Runt and Dr. L. E. Cross for comments and discussions. We appreciate greatly the financial support of this work by ONR under grant No. N00014-02-0418, DARPA under contract No. N00173-99-C-2003, and NIH under the grant 1 R0 HL65959.

## REFERENCES

1. Y. Bar-Cohen, (ed.) *Electroactive Polymer Actuators as Artificial Muscles,* SPIE, Bellingham, WA 2001.
2. Q. M. Zhang, T. Furukawa, Y. Bar-Cohen, and J. Scheinbeim, (eds) *Electroactive Polymers,* MRS Symp. Proc. Vol.600, MRS, Warrendale PA 1999.
3. H. Nalwa, (ed.) *Ferroelectric Polymers,* Marcel Dekker, Inc. NY 1995.
4. P. Dario, M. Carrozza, A. Benvenuto, and A. Menciassi, "Micro-systems in biomedical applications". *J. Micromech. Microeng.* Vol.10, pp. 235-244, 2000.
5. Q. M. Zhang, V. Bharti, and X. Zhao. "Giant electrostriction and relaxor ferroelectric behavior in electron-irradiated poly(vinylidene fluoride-trifluoroethylene) copolymer" *Science* Vol.280, pp. 2101-2104, 1998.
6. R. Pelrine, R. Kornbluh, Q. Pei, and J. Joseph, "High-speed electrically actuated elastomers with strain greater than 100%", *Science* Vol.287, pp. 836-839, 2000.
7. W. Lehmann, *et al.* "Giant lateral electrostriction in ferroelectric liquid-crystalline elastomers", *Nature* Vol.410, pp. 447-450, 2001.
8. Z.-Y. Cheng, *et al.* "Electrostrictive poly(vinylidene fluoride-trifluoroethylene) copolymers", *Sensors and Actuators A. Phys.* Vol.90, pp.138-147, 2001.
9. K. Tashiro, K. Takano, M. Kobayashi, Y. Chatani, and H. Tadokoro, "Structure study on ferroelectric phase transition of vinylidene fluoride-trifluoroethylene copolymers (III) dependence of transitional behavior on VDF molar content", *Ferroelectrics* Vol.57, pp. 297-326, 1984.
10. Q. M. Zhang, J. Zhao, T. Shrout, N. Kim, L.E. Cross, A. Amin, and B.M. Kulwicki, "Characteristics of the electromechanical response and polarization of electric-field biased" *J. Appl. Phys.* Vol.77, pp. 2549-2955, 1995.
11. F. Xia, Z.-Y. Cheng, H. Xu, and Q. M. Zhang, G. Kavarnos, R. Ting, G. Abdul-Sedat, K. D. Belfield. "High Electromechanical Responses in Terpolymer of Poly(vinylidene fluoride-trifluoroethylene- chlorofluoroethylene)". *Adv. Maters.* Vol.14, pp. 1574, 2002.
12. L. E. Cross, "Relaxor ferroelectrics: An overview", *Ferroelectrics* Vol.151, pp. 305, 1994.
13. Z.-Y. Cheng, T.-B. Xu, V. Bharti, S. Wang, and Q. M. Zhang. "Transverse Strain
1. Response in the Electrostrictive P(VDF-TrFE) Copolymer". *Appl. Phys. Lett.* Vol.74, pp. 1901-1903, 1999.
14. C. Horn, S. Pilgrim, N. Shankar, K. Bridger, M. Masuda, and S. Winzer, "Calculation of quasi-static electromechanical coupling coefficients for electrostrictive ceramic Materials", *IEEE Trans. Ultrason. Ferro. Freq. Cntr.* Vol.41, pp. 542-551, 1994.
15. V. Bharti, Z.-Y. Cheng, S. Gross, T.-B. Xu, and Q.M. Zhang, "High electrostrictive strain under high mechanical stress in electron-irradiated poly(vinylidene fluoride-trifluoroethylene) copolymer", *Appl. Phys. Lett.* Vol.75, pp. 2653-2655, 1999.
16. P. Mabboux and K. Gleason, "$^{19}$F NMR characterization of electron beam irradiated vinylidene fluoride–trifluoroethylene copolymers", *J. Fluorine Chem.* Vol.113, pp. 27, 2002.
17. Q. M. Zhang and J. Scheinbeim, Chapter 4 in *Electroactive Polymer Actuators as Artificial Muscles* (Ed) Y. Bar-Cohen, SPIE Optical Engineering Press, WA, 2001.
18. H. Xu, Z.Y. Cheng, D. Olson, T. Mai, Q. M. Zhang, and G. Kavarnos. "Ferroelectric and electromechanical properties of poly(vinylidene-fluoride-trifluoroethylene-chlorotrifluoroethylene) terpolymer", *Appl. Phys. Lett.* Vol.78, pp. 2360-2362, 2001.
19. T. Furukawa, "Ferroelectric properties of vinylidene fluoride copolymers", *Phase Trans.* Vol.18, pp. 143, 1989.
20. Q. M. Zhang, Z. Y. Cheng, and V. Bharti. "Relaxor Ferroelectric Behavior in High Energy Electron Irradiated P(VDF-TrFE) copolymers". *Appl. Phys.* Vol. A70, pp. 307-312, 2000.
21. A. Safari, G. Sa-gong, J. Giniewicz, and R. Newnham. *Proc. 21st University Conf. Ceram. Sci.* Vol.20, pp. 445-455, 1986.

22. H.S. Nalwa, L. Dalton, and P. Vasudevan, "Delectric properties of copper-phthalocyanine polymer", *Eur. Polym. J.* Vol.21, pp. 943-947, 1985.
23. N. Phougat, P. Vasudevan, and H. Nalwa, Chapter 8 in *Handbook of Low and High Dielectric Constant of Materials and Their Applications*, H. Nalwa, (Ed.) Academic Press, London, UK 1999.
24. P. Vijayakumar. and H.A. Pohl, "Giant polarization in stable polymeric dielectrics", *J. Polym. Sci. Poly. Phys.* Vol.22, pp. 1439-1451, 1984.
25. P.D. Gould, "Structure and electrical conduction properties of phthalocyanine thin films", *Coordin. Chem. Rev.* Vol.156, pp. 237-274, 1996.
26. L. D. Landau, and E. M. Lifshitz, *Electrodynamics of Continuous Media*, Pergamon, Oxford, 1970.
27. R. Newnham, V. Sundar, R. Yimmirun, J. Su and Q. M. Zhang, "Electrostriction in dielectric materials". *Ceramic Trans.* Vol.88, pp. 15-39, 1998.
28. J. Su, Q. M. Zhang and R. Y. Ting, "Space-charge-enhanced electromechanical response in thin-film polyurethane elastomers". *Appl. Phys. Lett.* Vol.71, pp. 386-388, 1997.
29. K. Hayashi, S. Kawato, Y. Fujii, T. Horiuchi and K. Matsushige, "Effect of applied electric field on the molecular orientation of epitaxially grown organic films". *Appl. Phys. Lett.* Vol.70, pp. 1384-1386, 1997.

# APPENDIX 30

# In-Air and Underwater Performance and Finite Element Analysis of a Flextensional Device Having Electrostrictive Poly(vinylidene fluoride-trifluoroethylene) Polymers As the Active Driving Element

Feng Xia, Zhong-Yang Cheng, and Qiming Zhang, *Senior Member, IEEE*

***Abstract*—A flextensional transducer, in which the electrostrictive poly(vinylidene fluoride-trifluoroethylene) [P(VDF-TrFE)] copolymer was used as the active driving element, was fabricated and characterized. The results show that transducers of several millimeters thick can produce an axial displacement of more than 1 mm in air along the thickness direction, and a transmitting voltage response of 123 dB re 1 μPa/V at 1 m in water at frequencies of several kilohertz. A finite element code (ANSYS, Inc., Canonsburg, PA) was used to model the in-air and underwater responses of the flextensional transducer over a broad frequency range. The calculated resonance frequencies and transmitting voltage response spectra show good agreement with the experimental data. In addition, the performance of both the in-air actuator and underwater transducer was analyzed for different design parameters of the flextensional structure. These results show that the performance of the flextensional transducer could be tailored readily by adjusting the parameters of the flextensional metal shell.**

## I. Introduction

FLEXTENSIONAL devices, including actuator and transducer, act as mechanical transformers that transform and amplify the displacement or force generated in an active element, and thus makes it possible to tune the device performance over a broad range to meet the demands of different applications. Generally speaking, the devices consist of a driving element that is mechanically coupled to a flexible shell, as shown in Fig. 1. Depending on the ratio of height/length (h/L), the flextensional devices can amplify the extensional motion of the active element into a larger extensional motion δh of the shell, or work in the reverse mode that amplifies the force generated in the active element into a larger force of the shell, while the corresponding displacement δh of the shell becomes smaller than that of the active element. In most cases, the shell flexes and the active plate extends, thus deriving the name flextensional. Flextensional transducers have been used widely for underwater transducers [1]–[4], which find applications mainly in the low-frequency range (300–3000 Hz) due to the low resonance frequency in the flextensional shell [3], [5]. According to the shape of the shell, flextensional transducers are divided into seven classes [1], [6], [7]. Among them, classes IV and V have attracted great attention in recent years [2]. The recently developed Moonie and Cymbal by Newnham *et al.* [8] and Zhang *et al.* [9] are essentially miniaturized versions of the class V flextensional transducers. In addition, the Moonie and Cymbal also are investigated for actuator applications because of the displacement amplification function of the flextensional devices. As actuators, the Moonie and Cymbal, which provide a relatively large displacement while maintaining a relatively high-force output, bridge the gap between the monolithic actuators and bimorphs [8], [10].

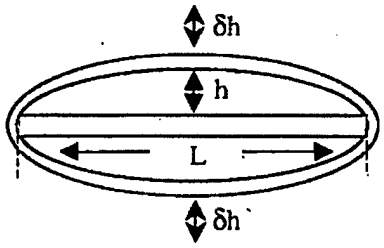


Fig. 1. Schematic of a flextensional device. L is the length of the active driving element, h and δh are the arch height and extensional motion of the flexible shell, respectively.

In the traditional flextensional devices, piezoelectric ceramics are predominately the material of choice for the active driving element [2], [8], [9], which exhibit a strain level of about 0.1% and an elastic energy density of 0.1 J/cm$^3$. Therefore, new materials with higher strain level, higher power density, and lightweight are highly desirable for flextensional devices used for underwater transducers for high power operation, and actuators to generate large displacements and high forces. Recently, a high-energy electron irradiated poly(vinylidene fluoride-trifluoroethylene) [P(VDF-TrFE)] copolymer with electrostrictive strain of

Manuscript received October 9, 2002; accepted March 11, 2003. We gratefully acknowledge the financial support of this work by the Defense Advanced Research Projects Agency and by the Pennsylvania State University.

The authors are with the Department of Electrical Engineering and Materials Research Institute, The Pennsylvania State University, University Park, PA 16802 (e-mail: fxx2@psu.edu).

Z.-Y. Cheng currently is with the Materials Engineering, Auburn University, Auburn, AL 36849.

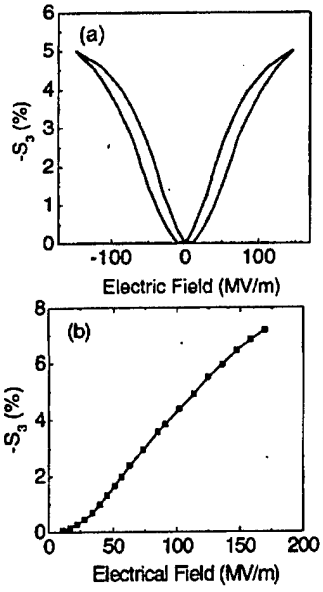


Fig. 2. Electrostrictive strain for (a) high-energy, electron-irradiated P(VDF-TrFE) copolymer and (b) P(VDF-TrFE-CFE) terpolymer without irradiation.

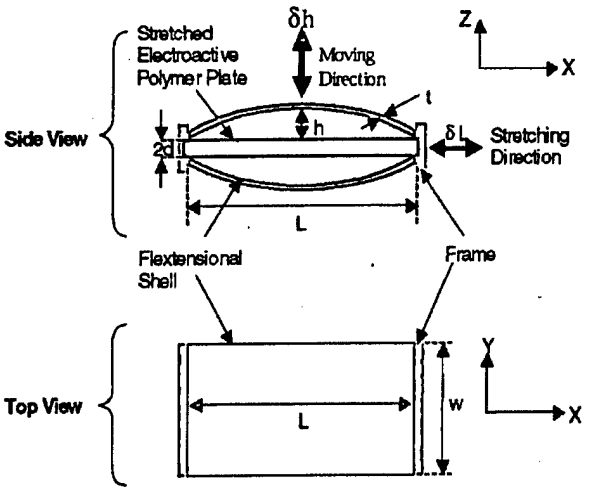


Fig. 3. Sketch of a flextensional transducer based on stretched electroactive polymers, where 2d, L, and w are the thickness, length, and width of the multilayer EAP plate, respectively. t is the thickness of the metal shell, and h is the height of the arch, $\delta$L and $\delta$h are the displacement along X and Z direction.

5% [see Fig. 2(a)] and an elastic energy density of more than 0.5 J/cm$^2$ has been developed [11], [12]. Furthermore, it is shown that the material can be operated to above 100 kHz [11]–[13]. In addition to the high-energy electron irradiated P(VDF-TrFE) copolymers, it has been shown that the large electrostrictive responses also can be achieved in P(VDF-TrFE)-based terpolymers without irradiation [14]. For example, an electrostrictive strain of more than 7% can be induced in the terpolymer of P(VDF-TrFE-CFE) (CFE, chlorofluoroethylene) [Fig. 2(b)]. These features are attractive for the flextensional actuators to generate large displacement and force simultaneously, and for high-power underwater transducers.

Recently, such a flextensional device has been fabricated and tested using the irradiated P(VDF-TrFE) electrostrictive polymers [15]. In this paper, we will review briefly the actuator and underwater transducer performance of the flextensional device. Then, we will present the results of a finite element analysis on the performance of this device that illustrates how the performance depends on the parameters of the flextensional structure.

## II. Experimental Results of Actuator and Underwater Transducer Performance

Fig. 3 is the flextensional device fabricated, which is basically a Class IV flextensional transducer. The electrostrictive P(VDF-TrFE) copolymer was used as the active driving element, which consists of a multilayer plate laminated from the electroactive P(VDF-TrFE) polymer (EAP) films (~30-$\mu$m thick per layer). Two flextensional metal shells were fixed at the two ends of the active polymer plate to amplify the displacement. In this configuration, the transverse strain of the irradiated copolymer is used. The dimensions of the active element are length = 26 mm and width = 31 mm, which is the length and width of the multilayer copolymer plate, respectively. Spring-steel sheets with a modulus of 210GPa (Blue Tempered & Polished Spring Steel, Precision Brand Products, Inc., Downers Grove, IL) were used as the metal shell. As shown in Fig. 3, $\delta$L and $\delta$h denote the displacement along the X- and Z-direction (at the center of the flextensional shell), and hence, $\delta$h/$\delta$L is the amplification ratio of each flextensional shell. The total displacement generated by the device along the Z-direction is 2 $\delta$h.

For the flextensional actuators operated in air (Transducer I), the thickness (t) of the active polymer plate is 2 d = 1 mm and the thickness of the flextensional shell is t = 0.125 mm. Two actuators with two different initial h/L (0.053 and 0.109) were fabricated to demonstrate the displacement amplification effect of the device. The displacement 2 $\delta$h at 1 Hz generated at different driving fields is presented in Fig. 4(a). As can be seen, a displacement of more than 1 mm can be generated along the Z-direction for a flextensional actuator with total thickness of less than 7 mm along the same direction. As shown in Fig. 4(b), the displacement generated does not decrease when a load is applied along the Z-direction, indicating a high-load capability. The slight increase of the displacement with load is due to the increase of the transverse strain response with the tensile stress of the electrostrictive copolymer [16].

To characterize the underwater performance, the thickness 2 d of the active element was increased to 2 mm (to raise the force output) and the flextensional shell thickness

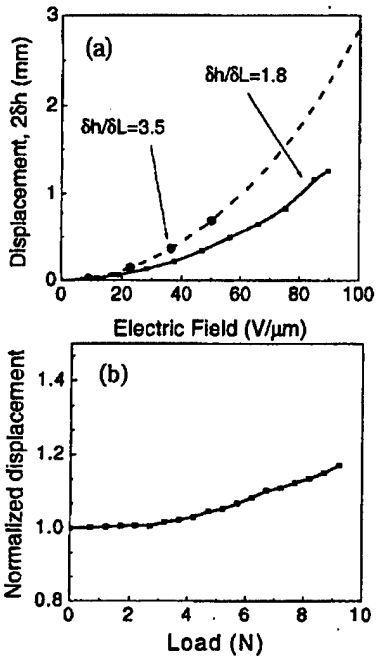


Fig. 4. Displacement responses of the flextensional actuator [15]. (a) Displacement at the midpoint of the flextonsional shell as a function of the electrical field at 1 Hz. (b) Normalized displacement at the midpoint of the shell as a function of the mechanical load at a constant electrical field of 1 Hz.

t was increased to 0.375 mm. The arch height is 3 mm. All the other dimensions of the transducer were kept the same. This transducer is referred to as Transducer II in this paper. The electric impedance of the transducer was first characterized in air, which showed the fundamental resonance due to the flextensional shell occurring at 4.5 kHz. The same transducer then was characterized in water. Due to the mass loading of water, the resonance frequency was reduced to about 1.7 kHz [15]. For the underwater transducer performance, the transmitting voltage response (TVR) was measured,

$$\text{TVR (dB)} = 20\log_{10}(p/p_{ref}) \qquad (1)$$

where $p_{ref} = 1\ \mu$Pa and p is the pressure generated under a 1 V voltage applied across the electrical terminals of the transducer and measured 1 m away from the transducer. The TVR has the unit of decibels to 1 $\mu$Pa per volt at 1 m (dB re $\mu$Pa/V at 1 m). Because the acoustic wavelength is much larger than the size of the transducer, the transducer here can be regarded as a point source, which shows an omnidirectional directivity pattern as measured. Fig. 5 shows the TVR of the transducer under a direct current (DC) bias of 1500 V (for an electrostrictive material, a DC bias is required to generate an equivalent piezoelectric state). A broad resonance centered at 1.7 kHz was observed. The TVR near the resonance is 123 dB re 1 $\mu$Pa/V at 1 m for the device. The mechanical quality factor $Q_m$ is found to be 1.55. Compared with traditional piezoelectric ceramics-based flextensional transducers, the current small size transducer can be operated at low frequency of about 1–2 kHz with relatively high TVR, high source level, and low mechanical quality factor [2], [9], [15].

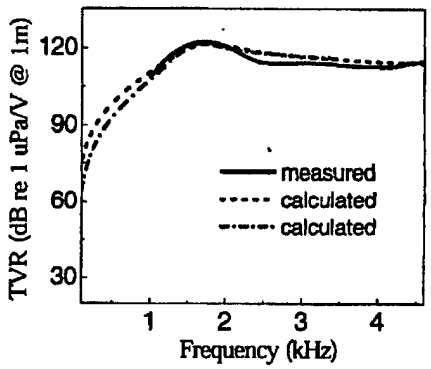


Fig. 5. Measured and calculated TVR of the flextensional underwater transducer. Solid line is the measured values under a DC bias of 1500 V; dashed lines are the calculated values using FEA with two different meshing levels. The calculated data are in accord with the measured data.

## III. Finite Element Modeling of the Flextensional Devices

The finite element analysis (FEA) has been used extensively in modeling complex transducer and actuator structures [9], [17], [18]. The purpose of FEA is to numerically solve complex partial differential equations so as to mathematically describe and predict the physical behaviors of an actual engineering system under various structures and loading conditions. The advantage of FEA is to allow the designer to manipulate and test the effects of all the possible design variables using computer analysis rather than by the more tedious and costly alternative of actually building and testing prototype designs. In this study, ANSYS 5.7 (ANSYS, Inc., Canonsburg, PA) was used to simulate the in-air and underwater performance of the flextensional device. Because no commercial FEA code has been developed to model electrostrictive materials, the electrostrictive polymer was treated as an effective piezoelectric material under DC bias. The effective piezoelectric constants for irradiated copolymer used here are $d_{33} = -226$ pm/V and $d_{31} = 235$ pm/V under DC bias of 50 MV/m. In the FEA modeling, the in-air directly measured data were used to validate the FEA model. As will be shown later, both the modeling results of the transducer in-air and underwater performance are in good agreement with the measured results. Because the modeling of the underwater flextensional transducer involves electrostrictive materials and acoustics, coupled-field and acoustic analysis [19] were used. The modal analysis was carried out to determine the resonance frequencies and mode shapes of a structure, and the harmonic analysis was performed to evaluate the frequency-dependent behaviors [20].

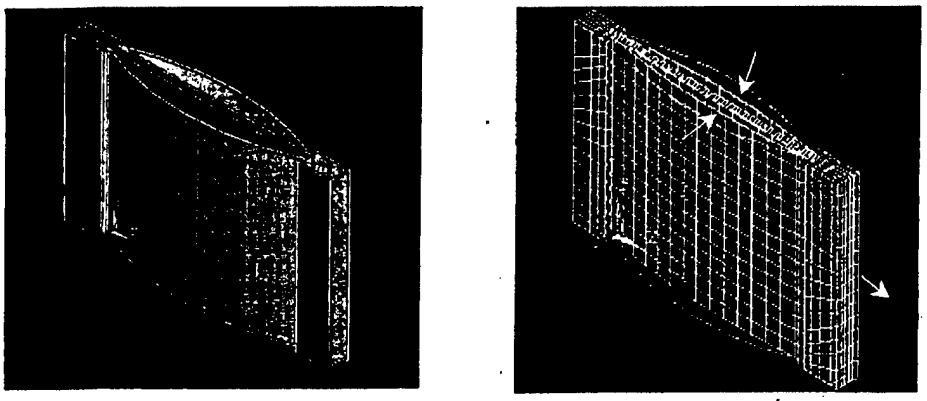


Fig. 6. In-air modeling of the transducer. (a) Geometry of the model, (b) meshing and deformed shape of the transducer in air. Under electrical driving, the electroactive polymer plate extends, and the metal shells flex with the direction shown by the arrows.

### *A. FEA of the In-Air Performance of the Flextensional Transducer*

Figs. 6(a) and (b) present the three-dimensional (3-D) geometry and meshed elements created using ANSYS, in which the coupled-field element SOLID 5 [19] was used to simulate the electroactive polymer. Both 2-D and 3-D models were applied to analyze the in-air performance of the transducer, and the results were consistent with each other. In dealing with the underwater modeling, only the 2-D model was used so that the computing time would be reasonably short for the analysis over different transducer configurations. Such treatment is valid because the acoustic wavelength is much larger than the device size and the directivity pattern is omnidirectional, as has been pointed out earlier. Fig. 6(b) also shows the deformed shell shape when the active element is being electrically driven. As expected, the active polymer plate extends in the X-direction, causing the metal shell to move in the Z-direction to amplify the displacement.

Based on FEA, the displacement $\delta$L, $\delta$h, and amplification ratio $\delta$h/$\delta$L as a function of t (shell thickness) and h (the initial arch height) of the metal shell, as defined in Fig. 3, were obtained. The results are valuable in designing the actuator based on the flextensional device configuration investigated here. The modeling results also were compared with the experimental data to validate the model. In the modeling, the dimensions of the active plate were kept the same; only the dimensions of the metal shell, such as t and h, were varied.

Fig. 7 shows $\delta$L, $\delta$h, and $\delta$h/$\delta$L as a function of metal shell thickness t, and h is 2.8 mm. The applied alternating current (AC) field is 1 Hz with amplitude of 50 MV/m. When t increases from 0.125 mm to 0.8 mm, both $\delta$L and $\delta$h decrease, but their ratio decreases only slightly. For t = 0.125 mm, FEA yields that $\delta$L is 0.115 mm, 2 $\delta$h is 0.405 mm, and $\delta$h/$\delta$L is 1.78, which are consistent with the data shown in Fig. 4(a) with $\delta$h/$\delta$L = 1.8, indicating that

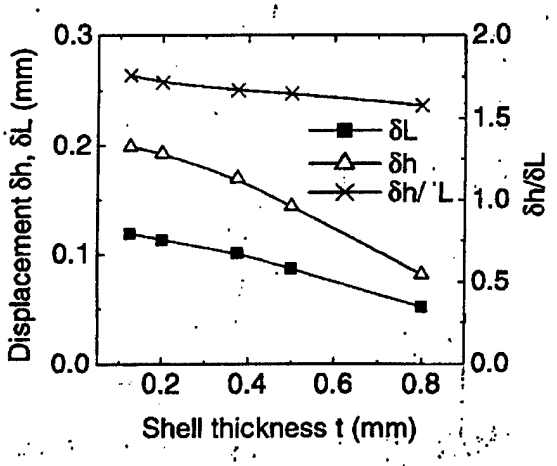


Fig. 7. $\delta$L, $\delta$h, and $\delta$h/$\delta$L at 1 Hz under an AC driving field of 50 MV/m as a function of metal shell thickness t.

the parameters used in the model are valid.

Shown in Fig. 8(a) are $\delta$L and $\delta$h of the transducer as a function of metal shell arch height, h; and t is 0.375 mm, which is the shell thickness. The results are obtained when the device is driven under an AC field of 50 MV/m at 1 Hz. As can be seen, when increasing h, $\delta$L increases and $\delta$h decreases, and $\delta$h/$\delta$L also decrease from more than 4 to less than 1. These results indicate that, as h increases, the force that the metal shell exerts on the active element becomes smaller, resulting in a larger $\delta$L. From an early analytical analysis [15], $\delta$h/$\delta$L is a function of h/L as:

$$\frac{\delta h}{\delta L} = -\frac{1-\frac{\pi^2}{4}\frac{h^2}{L^2}}{\frac{\pi^2}{2}\frac{h}{L}}. \tag{2}$$

As shown in Fig. 8(b), $\delta$h/$\delta$L calculated using (2) is consistent with that obtained from FEA. The small devi-

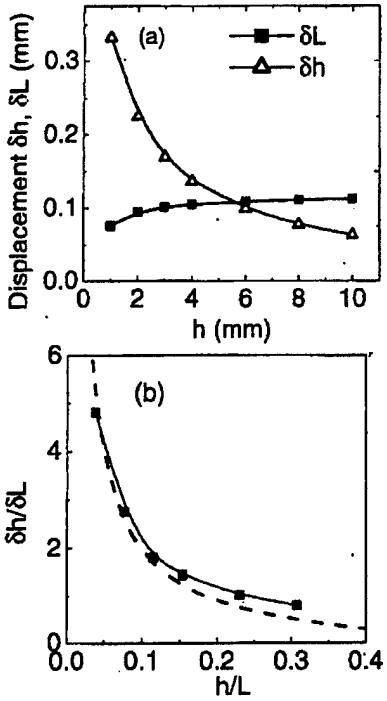


Fig. 8. (a) $\delta L$ and $\delta h$ at 1 Hz under an AC driving field of 50 MV/m as a function of metal shell arch height h; (b) $\delta h/\delta L$ as a function of h/L. The solid line is from FEA modeling, and the dashed line is from analytical modeling.

ation at large h/L values originates from the assumption used in deriving (2), which requires $h^2/L^2 \ll 1$. Also as can be seen in Fig. 8(b), $\delta h/\delta L$ becomes less than 1 when h/L is larger than 0.24, indicating that, at this condition, the flextensional structure will no longer function as a displacement amplifier.

To investigate the frequency dependence behavior of the displacement responses, a harmonic analysis was carried out for the Transducer II. As shown in Fig. 9, a resonance frequency of 4.5 kHz is observed for this transducer. At the resonance frequency, $\delta h$ can reach 0.8 mm in air.

A modal analysis was carried out to find the first 10 vibration modes of this transducer operated in-air. Fig. 10 presents the first two vibration mode shapes of the metal shell, which occur at 4.5 kHz and 11 kHz, respectively. Comparing with the second mode, the first mode shows a large volume change, which is desired for the underwater transducer application. Later, we will show that large volume change and large volume velocity will result in large acoustic power when the transducer is operated in water.

### *B. Modeling of the Underwater Performance of the Flextensional Transducer*

In FEA for underwater modeling, there are basically two approaches, first is to calculate the effective water load and then apply the load on the structure as the water

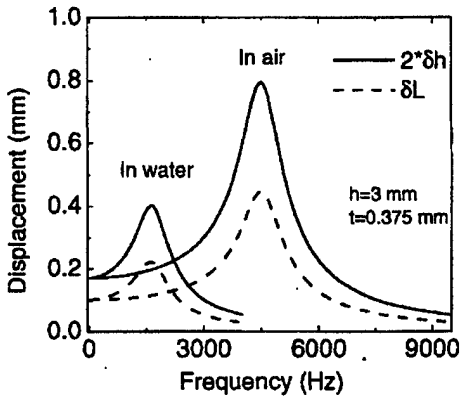


Fig. 9. Displacement under an AC field of 50 MV/m versus frequency for the transducer with t = 0.375 mm and h = 3 mm in air and in water.

media [17]. Second, which is more direct and accurate, is to create an infinite water environment around the transducer. The second approach is used in our study. To create an infinite water environment, two hemispheres of water with a radius of 1 m were first put around the two radiating faces, as shown in Fig. 11(a) (in Fig. 11, the hemisphere of water is not drawn in proportion so that the small transducer can be shown clearly). Then, a structure-fluid interface was defined between the transducer and water hemispheres. The semisphere of water was meshed using a 2-D acoustic element FLUID 29. After that, the outer boundary of the water hemispheres was modeled using the specially designed infinite acoustic element FLUID 129 [19]. These infinite acoustic elements absorb the incident pressure wave, simulating the outgoing effects of a domain that extends to infinity beyond the FLUID 29 elements. As a result, an infinite fluid environment was created around the transducer, as shown in Fig. 11.

In the harmonic analysis [20], an AC signal of 1 V was applied to the two electric terminals of the active polymer plate; and the frequency-dependent parameters, such as pressure in the water and the displacement of the transducers, were determined. Once the pressure was obtained, the TVR could be calculated following (1).

Fig. 11(b) presents the deformed shape of the transducer in water at 1650 Hz, at which the active polymer plate extends and the shell flexes as expected. For comparison with the in-air data, $\delta L$ and $\delta h$ in water as a function of frequency for the transducer with t = 0.375 mm and h = 3 mm also are plotted in Fig. 9. Due to water load, both $\delta L$ and $\delta h$ in water are smaller than those in air, and the resonance frequency is reduced from 4.5 kHz in air to about 1.7 kHz in water. In addition, the water loading also reduces the resonance displacement, indicating the mechanical quality factor $Q_m$ of the transducer becomes smaller in water.

Fig. 12 shows the pressure versus frequency of the water element at the radius of 1 m when the transducer was driven by 1 V (~0.033 MV/m) and 50 MV/m across the

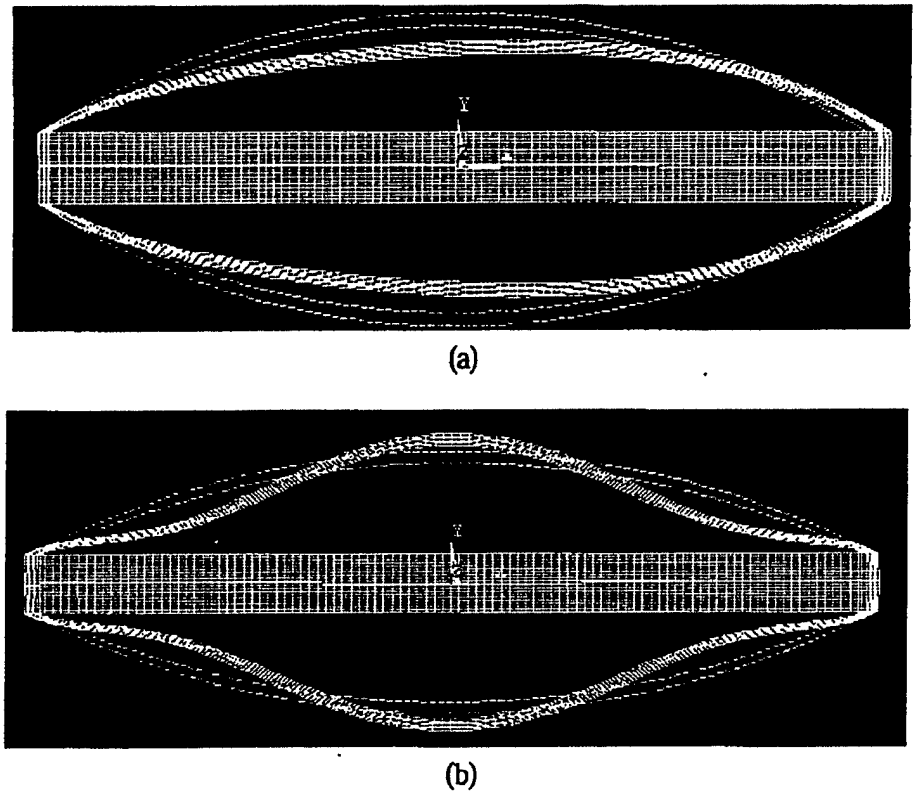


Fig. 10. The first two vibration modes of the metal shell at (a) 4.5 kHz and (b) 11.0 kHz.

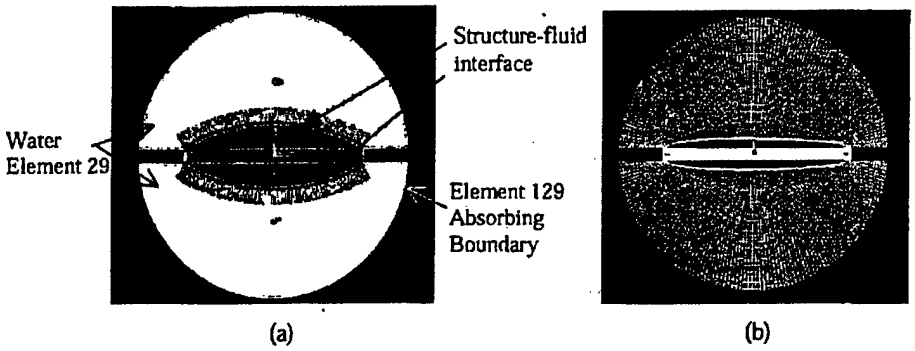


Fig. 11. The underwater modeling of the transducer. (a) The geometry of the underwater model with infinite water media and structure-fluid interface. Element 29 and element 129 are used to model the water and infinite water boundary [19]. (b) The meshing and deformed shape underwater. Comparing with (a), the metal shells flex under electrical driving.

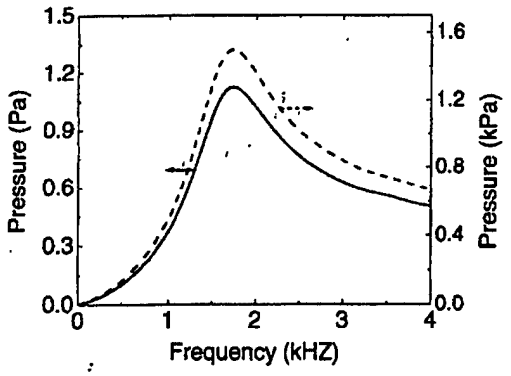


Fig. 12. The pressures as a function of frequency in water 1 m away from the transducer under a driving of 1 V (solid line) and 1500 V (dashed line), respectively.

electrical terminals of the transducer, respectively. Using (1), the TVR is calculated and shown in Fig. 5 to be compared with the experimental data. The calculated TVR curves, which show a resonance frequency about 1750 Hz and a maximum TVR of 122 dB re 1 $\mu$Pa/V at 1 m, are in accord with the experimental data.

Admittance is calculated as $I/V$ where $I$ is the current and $V$ is the applied potential. The current $I$ is related to the accumulated charge on the electrode surface. The nodal charge (nodal reaction force) can be found using POST 26 (the time-history postprocessor) in ANSYS [19], which can be written as:

$$q = q_0 e^{j\omega t}. \tag{3}$$

The current $I$ is equal to:

$$I = \frac{dq}{dt} = j\omega q_0 e^{j\omega t} = j\omega q, \tag{4}$$

and the applied voltage is:

$$V = V_0 e^{j\omega t}. \tag{5}$$

Admittance $Y$ can be determined from:

$$Y = \frac{I}{V} = \frac{q_0 j\omega e^{j\omega t}}{V_0 e^{j\omega t}} = j\omega \frac{q_0}{V_0}. \tag{6}$$

Since $V_0 = 1$ V, Y becomes:

$$Y = j\omega q_0 = j(2\pi f) q_0. \tag{7}$$

Because of the acoustic radiation, $q_0$ obtained from FEA is a complex number, and thus admittance $Y$ is also a complex number. Fig. 13(a) shows the $q_0$ obtained for the transducer operated in air and in water, and Fig. 13(b) presents the $Y$ deduced from $q_0$. Again, due to water load, the fundamental resonance frequency of the transducer is reduced from 4.5 kHz in air to 1.7 kHz in water, which is consistent with the experimental data.

Because the size of this transducer is much smaller than the acoustic wavelength in water, the transducer can be

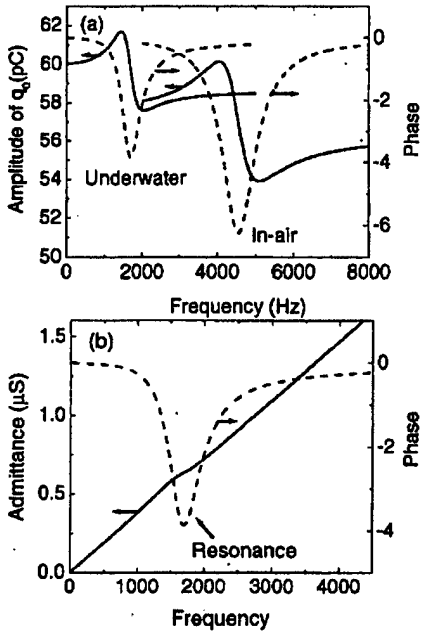


Fig. 13. The underwater modeling results of the flextensional transducer. (a) The induced current versus frequency in air and underwater for the transducer. The solid line is amplitude and the dashed line is phase. (b) Admittance (solid line) versus frequency for the transducer in water. The dashed line is phase.

approximated as a point source. For a point source, it is well-known that the far-field pressure p and acoustic power $P_a$ are related to the volume velocity $Q_0$ as [2]:

$$p = 500 Q_0 f, \tag{8}$$

$$P_a = 1.05 Q_0^2 f^2. \tag{9}$$

Using the pressure data in Fig. 12, the volume velocity $Q_0$ can be obtained, and thus the acoustic power $P_a$ can be deduced. When driven by 1 V, Fig. 14 shows $Q_0$ and $P_a$ as a function of frequency. The maximum $P_a$ is observed at the resonance frequency of 1.7 kHz; and maximum volume velocity $Q_0$ occurs at 1.6 kHz, which is a little lower than the resonance frequency. Under a driving field level of 50 MV/m, $Q_0$ and $P_a$ can reach about 1800 cm$^3$/s and 9.8 W, respectively. As can be seen from (9), for a given frequency and fluid medium, which sets the values of the acoustic wavelength and the specific acoustic impedance of the medium, the power is a function of the volume velocity $Q_0$. Therefore, in order to obtain the largest power output, it is necessary to obtain as large a volume velocity as possible. From the modal analysis, as shown in Fig. 10, lower frequency mode 1 is much better for underwater acoustic devices than mode 2, because mode 1 produces larger volume change. In order to tailor and optimize the transducer performances, the FEA was used to study how the underwater performance of the transducer depends on the parameters of the flextensional structure, such as h and t.

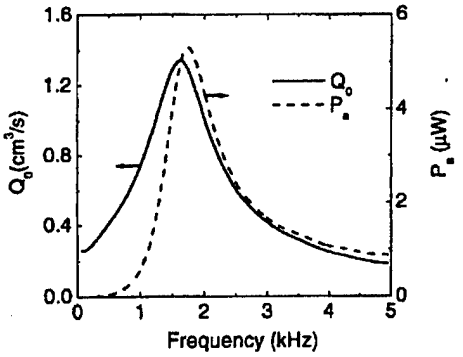


Fig. 14. Volume velocity $Q_0$ and acoustic power $P_a$ versus frequency under a driving of 1 V between the two electric terminals of the multilayer plate.

Again, for the comparison, L, d (d = 1 mm), and w were kept as constants.

Fig. 15 presents the effect of metal shell thickness t on the TVR and fundamental resonance frequency $f_r$ of the device. The resonance frequency increases monotonically with the shell thickness, which is understandable because the vibration mode is mainly due to the shell flexure motion, and its resonance frequency increases with the shell thickness. As seen in Fig. 15(b), the TVR has a maximum at about t = 0.29 mm; and, under this condition, $Q_0$ is about 1.3 cm$^3$/s at the resonance frequency. As presented earlier, the displacement of the transducer decreases with increasing t, resulting in a decreasing volume velocity $Q_0$. However, the increase of resonance frequency will increase the far field p as indicated in (8), thus a maximum value of TVR (pressure) is observed here.

Similarly, the underwater performance of the flextensional transducer with different arch height h also was obtained using FEA. Fig. 16 shows the TVR and resonance frequency in water as a function of h. As h changes from 1 to 8 mm, the resonance frequency increases from 700 Hz to 5.3 kHz, and TVR increases from 116 to 123 dB re 1 μPa/V at 1 m, indicating the operation frequency can be adjusted in a large range. Because the pressure (TVR) is proportional to the volume velocity and frequency as indicated by (8); it is the increase of the resonance frequency with h that results in the observed increase in TVR when h is increased from 1 mm to 6 mm.

These results indicate that this type of transducer can be operated at a frequency range of several hundred hertz to several kilohertz with relatively high TVR (more than 115 dB re 1 μPa/V at 1 m).

## IV. Summary

A flextensional device, using the newly developed high electrostriction electroactive polymers, was fabricated and characterized. The results show that the small device (1 in. × 1 in. in lateral dimension and a few millimeters thick) is capable of generating a displacement at

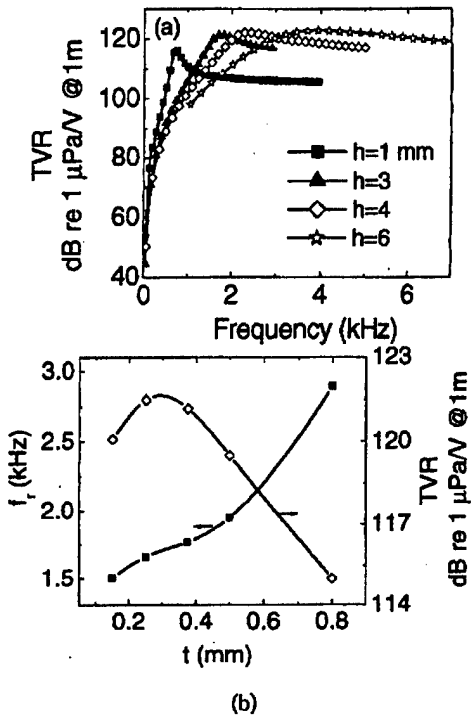


Fig. 15. TVR and resonance frequency $f_r$ of the transducer as a function of metal shell thickness t. (a) TVR versus frequency, (b) $f_r$ (line with squares) and TVR (line with diamonds) at $f_r$ versus t.

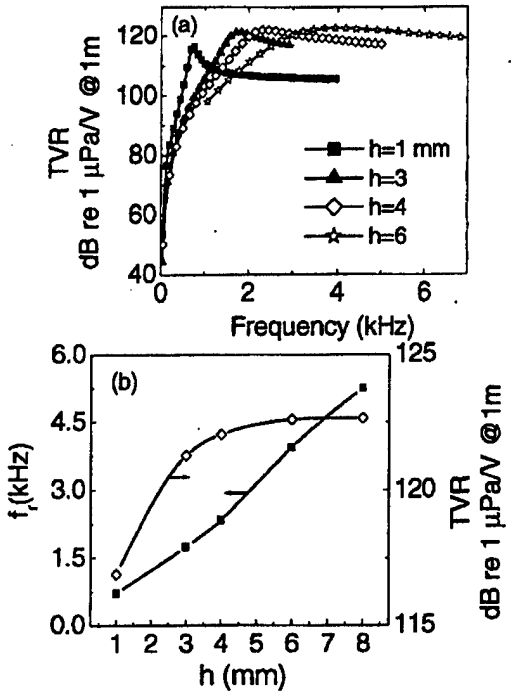


Fig. 16. TVR and resonance frequency $f_r$ of the transducer as a function of arch height h. (a) TVR versus frequency, (b) $f_r$ (line with squares) and TVR (line with diamonds) at $f_r$ versus h.

millimeter-level in air with high load capability. When operated in water, the device exhibits a low frequency resonance (<2 kHz) while generating a relatively high TVR of about 123 dB re 1 $\mu$Pa/V at 1 m. Finite element analysis (ANSYS) was used to simulate the transducer and investigate how the performance depends on the parameters of the flextensional structure. Both in-air and underwater performances of the device were modeled, and the results are in accord with the experimental data. The FEA results indicate that the performance of this flextensional device can be tailored readily by adjusting the parameters of the flextensional metal shell. The results show that this type of transducer can operate at a frequency range of several hundreds hertz to several kilohertz with relatively high TVR.

## REFERENCES


[1] K. D. Rolt, "History of the flextensional electroacoustic transducers," *J. Acoust. Soc. Amer.*, vol. 87, pp. 1340–1349, 1990.

[2] J.-N. Decarpigny, B. Hamonic, and O. B. Wilson, Jr., "The design of low frequency underwater acoustic projectors: Present status and future trends," *IEEE J. Oceanic Eng.*, vol. 16, pp. 107–122, 1991.

[3] J. N. Petzing, J. R. Tyrer, and J. R. Oswin, "Improved interferometric techniques for measuring flextensional transducer vibration patterns underwater," *J. Sound Vib.*, vol. 93, pp. 877–890, 1996.

[4] G. S. Kino, *Acoustic Waves: Device, Imaging, and Analog Signal Processing*. Englewood Cliffs, NJ: Prentice-Hall, 1987.

[5] J. R. Oswin, "Class IV flextensional transducers-modeling, measurement and use," in *Proc. First Eur. Conf. Underwater Acoustics*, 1992, pp. 627–630.

[6] L. H. Royster, "The flextensional concept: A new approach to the design of underwater acoustic transducers," *Appl. Acoust.*, vol. 3, pp. 117–126, 1970.

[7] D. F. Jones, N. N. Abbound, G. L. Wojcik, and D. K. Vaughan, "Performance analysis of a low frequency barrel-stave flextensional projector," presented at 1996 ONR Transducer Mater. Transducers Workshop, State College, PA, Mar. 25–27, 1996.

[8] R. E. Newnham, A. Dogan, Q. C. Xu, and S. Yoshikawa, "Flextensional 'Moonie' Actuator," in *Proc. IEEE Ultrason. Symp.*, 1993, pp. 509–513.

[9] J. D. Zhang, A. C. Hladky-Hennion, W. J. Hughes, and R. E. Newnham, "Modeling and underwater characterization of cymbal transducer and arrays," *IEEE Trans. Ultrason., Ferroelect., Freq. Contr.*, vol. 48, no. 2, pp. 560–568, 2001.

[10] J. M. Herbert, *Ferroelectric Transducers and Sensors*. New York: Gordon and Breach, 1982.

[11] Q. M. Zhang, V. Bharti, and X. Zhao, "Giant electrostriction and relaxor ferroelectric behavior in electron-irradiated poly(vinylidene fluoride-trifluoroethylene) copolymer," *Science*, vol. 280, pp. 2101–2104, 1998.

[12] Z.-Y. Cheng, V. Bharti, T.-B. Xu, H. S. Xu, T. Mai, and Q. M. Zhang, "Electrostrictive poly(vinylidene fluoride-trifluoroethylene) copolymers," *Sens. Actuators A*, vol. 90, pp. 138–147, 2001.

[13] T.-B. Xu, Z.-Y. Cheng, and Q. M. Zhang, "High-performance micromachined unimorph actuators based on electrostrictive poly(vinylidene fluoride-trifluoroethylene) copolymer," *Appl. Phys. Lett.*, vol. 80, pp. 1082–1084, 2002.

[14] F. Xia, Z.-Y. Cheng, H. S. Xu, H. F. Li, Q. M. Zhang, G. J. Kavarnos, R. Y. Ting, G. Abdel-Sadek, and K. D. Belfield, "High electromechanical responses in a poly(vinylidene fluoride-trifluoroethylene-chlorofluoroethylene) terpolymer," *Adv. Mater.*, vol. 14, no. 21, pp. 1574–1577, 2002.

[15] Z.-Y. Cheng, T.-B. Xu, Q. M. Zhang, R. Meyer, J. D. Van Tol, and J. Hughes, "Design, fabrication and performance of a flextensional transducer based on electrostrictive polyvinylidene fluoride-trifluoroethylene copolymer," *IEEE Trans. Ultrason., Ferroelect., Freq. Contr.*, vol. 49, no. 9, pp. 1312–1320, 2002.

[16] V. Bharti, Z.-Y. Cheng, S. Gross, T.-B. Xu, and Q. M. Zhang, "High electrostrictive strain under high mechanical stress in electron-irradiated poly(vinylidene fluoride-trifluoroethylene) copolymer," *Appl. Phys. Lett.*, vol. 75, pp. 2653–2655, 1999.

[17] J. F. Tressler, W. Cao, K. Uchino, and R. E. Newnham, "Finite element analysis of the cymbal-type flextensional transducer," *IEEE Trans. Ultrason., Ferroelect., Freq. Contr.*, vol. 45, no. 5, pp. 1363–1369, 1998.

[18] V. V. Varadan, L. C. Chin, and V. K. Varadan, "Finite element modeling of flextensional electroacoustic transducers," *Smart Mater. Struct.*, vol. 2, pp. 201–207, 1993.

[19] *Coupled-Field Analysis Guide, ANSYS Release 5.7*. Canonsburg, PA: ANSYS, Inc., 2000, ch. 5, pp. 1–19.

[20] *Structural Analysis Guide, ANSYS Release 5.7*. Canonsburg, PA: ANSYS, Inc., 2000, ch. 4, pp. 1–38.


**Feng Xia** received his B.S. degree in materials science and engineering from Tsinghua University, Beijing, China, in 1994, and his Ph.D. degree in electronic materials from Xi'an Jiaotong University, Xi'an, China, in 1999, and his M.S. degree in electrical engineering from Penn State University, University Park, PA.

His research interests include ferroelectric materials and devices, including ferroelectric ceramics, electroactive polymers and all-polymer composites, and their applications as actuators, transducers, artificial muscles and bioMEMs, ferroelectric polymer thin film for memory devices and sensors, and finite element modeling of transducers and actuators. He has published over 30 articles in related fields. He is a member of Materials Research Society and American Ceramic Society.

**Zhong-Yang Cheng** is an assistant professor of Auburn University's Materials Engineering program, Auburn, AL, and a core member of the Auburn University's Detection and Food Safety Center. Prior to joining Auburn University in August 2002, Dr. Cheng was a research associate with the Materials Research Institute at Pennsylvania State University, University Park, PA.

His research emphasis is in preparation and characterization of various functional materials (electroactive polymers, ferroelectrics, piezoelectrics, dielectrics, electrets, nonlinear optical material, and composites) and design, fabrication, and characterization of electromechanical sensors, actuators, and transducers, especially in the application of these functional materials to biosensor development.

**Qiming Zhang** (M'95–SM'99) is a professor of electrical engineering at the Materials Research Institute and Department of Electrical Engineering of Penn State University, University Park, PA. His research activities include novel material development, microstructure-property-electroactive response relationships, and device development for transducers and actuators, ferroelectric polymer thin film for memory devices and sensors, microelectromechanical systems, photonic bandgap crystals, electro-optic and acousto-optic materials and devices, and dielectrics and capacitors. He has more than 185 publications in these areas. He is a senior member of IEEE, and a member of the Materials Research Society and the America Physical Society.

Appendix 12

"Radical telomerization of vinylidene fluoride in the presence of dibromodifluoromethane as telogen", K.D. Belfield, G. G. Abdul-Sadek, Jinyu Huang and R. Y. Ting, presented at the 223rd Amer. Chemical society National meeting, April 7-11, 2002, Orlando, FL. Polymer Preprints, Vol. 43, p. 644 (2002).

# APPENDIX 31

# RADICAL TELOMERIZATION OF VINYLIDENE FLUORIDE IN THE PRESENCE OF DIBROMODIFLUOROMETHANE AS TELOGEN

*Kevin D. Belfield, Gomaa G. Abdel-Sadek, Jinyu Huang, and Robert Y. Ting*

Department of Chemistry, University of Central Florida, P.O. Box 162366, Orlando, FL 32816-2366

## Introduction

Living polymerization techniques have been developed in free-radical and ionic polymerizations to prepare well-defined polymer architectures and block co-polymers. Well-defined block co-polymers have been prepared by living or controlled free-radical polymerizations via formation of telomers. The controlled free-radical polymerizations typically involve polymerization of styrene, acrylate, or methacrylate monomers. Fluoroethylene polymers have been a subject of numerous research and development efforts, resulting in their use in a number of important technological applications. However, there have been fewer reports of controlled free-radical polymerization of fluorinated olefins resulting in the corresponding block co-polymers. Thus, the development of synthetic methodology to prepare well-defined block co-polymers from fluorinated olefins is of significant interest.

Fluorinated telomers are very interesting intermediates involved in a number of applications, including surfactants, membranes, coatings, etc. Such telomers can be prepared either from commercially available fluorinated monomers, from fluorinated telogens, or the combination of the two.[1] Radical telomerization of vinylidene fluoride (VDF), in the presence of various telogens, has been reported,[2-6] thermally, photochemically, or in presence of free radical initiators. Our investigations are centered on the telomerization of VDF using dibromodifluoromethane ($CBr_2F_2$) as a telogen with tri-*n*-butyl boron/$O_2$ or di-*tert*-butyl peroxide as initiators. We wish to report the synthesis and characterization of poly(VDF) telomers, with structural characterization accomplished by multinuclear NMR spectroscopy ($^1H$, $^{13}C$, and $^{19}F$) and elemental analysis.

## Experimental

**Materials:** Vinylidene fluoride (98%) was obtained from SynQuest Labs, Inc. Di-*tert*-butyl peroxide (98%) and dibromodifluoromethane (97%) were purchased from Aldrich and used as received. Tri-*n*-butylboron was used as received from Alfa Aesar.

**Instrumentation:** $^1H$, $^{13}C$, and $^{19}F$ NMR spectra of telomers were obtained on a VARIAN MERCURY 300 MHz instrument, using DMSO-$d_6$ and TMS or $CFCl_3$ as the internal references. Elemental analysis was performed by Atlantic Microlab, Inc. (Atlanta, GA).

**General Procedures:** Telomerization of vinylidiene fluoride was carried out in a 600 mL stainless steel autoclave (Parr) using either tri-*n*-butyl boron or di-*tert*-butyl peroxide initiators at room temperature or 140 °C, respectively for 19 h. In a typical run using tri-*n*-butylboron as the initiator, the autoclave was cooled with liquid $N_2$ and 37 mL of vinylidene fluoride (VDF) was added. The autoclave was charged with dibromodifluoromethane (25 g, 0.12 mol), tri-*n*-butylboron (1.6 g, 9 mmol) and $O_2$ (120 mL, 4.8 mmol) via syringe. The mixture was stirred for 19 h at room temperature, after which time the unreacted monomer and telogen were removed. The telomer was recovered from the autoclave as a yellowish powder, which was then dissolved in acetone and reprecipitated using hexanes. An acetone solution of the telomer was treated with decolorizing charcoal, filtered, and dried under vacuum at 40 °C for 24 h, resulting in a white powder. The preparation of the second telomer, using VDF in the presence of di-*tert*-butyl peroxide initiator at 140 °C, resulted in isolation of a white powder after similar purification conditions.

## Results and Discussion

Bromine-terminated Poly(VDF) was prepared in the presence of dibromodifluoromethane using di-*tert*-butyl peroxide or tri-*n*-butylboron as initiators (Figure 1).

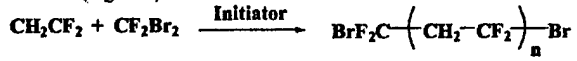


**Figure 1.** Radical telomerization of poly(VDF) with $CF_2Br_2$.

The bromine-terminated poly(VDF) telomer was characterized with by $^1H$, $^{13}C$, and $^{19}F$ NMR. The $^1H$ NMR of poly(VDF) telomer is shown in Figure 2. The peaks observed at 2.8-3.0 ppm are associated with the normal head-to-tail (h-t) structures $-CF_2-CH_2*-CF_2-$, while signals observed at 2.25 ppm correspond to the $-CH_2*-$ resonance in the head-to-head (h-h) or the tail-to-tail (t-t) structures or $-CH_2*-CH_2*-CF_2Br$. Finally, the signals observed at 3.5-3.7 ppm can be attributed to the terminal end group, $-CH_2-CF_2-CH_2*-CF_2Br$.

**Figure 2.** $^1H$ NMR spectrum of a bromine-terminated poly(VDF) telomer.

The composition of the telomers was calculated from NMR data and found to correspond well with the results of elemental analysis (CHBrF), demonstrating the successful preparation of bromine-terminated poly(VDF) telomers. Also shown in Table 1 are molecular weights of the telomers determined by NMR spectroscopy. This and other data, such as thermal analysis (TGA and DSC), will be reported.

**Table 1. Molecular Weight and Element Composition of Bromine-Terminated Poly(VDF) Telomers**

| Telomer | M.W. | Calculation (%) | | | | Elemental analysis (%) | | | |
|---|---|---|---|---|---|---|---|---|---|
| | | Br | C | H | F | Br | C | H | F |
| a | 1362 | 13.8 | 32.0 | 2.58 | 2.35 | 13.51 | 32.29 | 2.52 | 51.35 |
| b | 1490 | 11.7 | 32.6 | 2.60 | 53.0 | 13.41 | 32.29 | 2.62 | 51.35 |
| c | 850 | 18.8 | 29.6 | 2.35 | 49.1 | 17.79 | 30.45 | 2.37 | 48.22 |
| d | 1298 | 12.3 | 32.4 | 2.35 | 52.6 | 11.88 | 30.45 | 2.58 | 48.22 |

**a,b** - using di-*tert*-butyl peroxide as initiator, **c,d** - using tri-*n*-butylboron as initiator.

## Conclusions

Telomers of VDF were successfully prepared in the presence of $CBr_2CF_2$ using di-*tert*-butyl peroxide or tri-*n*-butylboron as initiators. Telomerization using tri-*n*-butyl boron as the initiator can be done at room temperature, resulting in yields higher than that obtained with di-*tert*-butyl peroxide. Preparation of other fluorinated telomers using this methodology is currently under investigation.

**Acknowledgement.** The authors would like to acknowledge DARPA and the State of Florida for support.

## References

(1) Ameduri, B.; Boutevin, B.; Kostov, G. K.; Petrova, P. *J. Fluorine Chem.* **1995**, *74*, 261.
(2) Destarac, M.; Matyjaszewski, K.; Silverman, E. *Macromolecues* **2000**, *33*, 4613.
(3) Zheng, Z.; Ying, S; Shi, Z. *Polymer* **1999**, *40*, 1341.
(4) Chambers, R. D.; Proctor, L. D.; Caporiccio, G. *J. Fluorine Chem.* **1995**, *70*, 241.
(5) Balague, J.; Ameduri, B.; Boutevin, B.; Caporiccio, G. *J. Fluorine Chem.* **1995**, *70*, 215.
(6) Modena, S.; Pianca, M.; Tato, M.; Moggi, G. *J. Fluorine Chem.* **1989**, *43*, 15.

Appendix 13

"Homo and co-fluorinated acrylic ester polymers: Synthesis /characterization and coating onto silicon surfaces", K.D. Belfield and G. G. Abdul-Sadek, presented at the 223rd Amer. Chemical Society National meeting, April 7-11, 2002, Orlando, FL. Polymer Preprints, Vol. 43, p. 588 (2002).

# APPENDIX 32

# *HOMO-* AND *CO-*FLUORINATED ACRYLIC ESTER POLYMERS: SYNTHESIS, CHARACTERIZATION, AND COATING ONTO SILICON SURFACES

*Kevin D. Belfield and Gomaa G. Abdel-Sadek*

Department of Chemistry and School of Optics/CREOL
University of Central Florida, P. O. Box 162366. Orlando, FL 32816-2366

## Introduction

Due to the ability of perfluoroacrylic and perfluoromethacrylic esters to co-polymerize with different fluorine-containing olefins, scuh acrylates are used in the production of various copolymers with specifically tailored properties. Among the currently used polyfluoroacrylates, the polymers and copolymers of fluoroalkyl acrylates and fluoroalkyl methacrylates realized the most practical use. They are employed in the production of plastic light guides, photoresists, water-, oil-, and dirt-repellent coatings, treatment of fibers and textiles, as well as other advanced applications.[1, 2] Due to the ability of some poly(fluoroalkyl methacrylate)s to degrade under the influence of UV, X-ray, and electron beam irradiation, they have found application in microlithiography for the production of integrated circuit boards. They can be used as positive resists, i.e. resists where the irradiated area is easily removed under the action of solvent.[1-3] These materials are among the best resists available with excellent sensitivity and resolution capabilities. Polyacrylates and polymethacrylates having fluoroalkyl groups in the side chains, in particular, are used also as a protective coatings and surface modifiers.[1]

Fluorinated acrylic ester polymers, radically polymerized, are known to be generally amorphous. However, when the ester of the higher normal fluorinated alcohols, typically $F(CF_2)_n(CH_2)_mOH$ with n=7-11 and m=1 or 2, are polymerized, side-chain crystallization occurs in the fluoroalkyl groups and imparts crystalline properties to the polymers.[1] Side-chain crystallization behavior plays an important role in determining the surface properties of the polymer. Moreover, it is to be noted that radically polymerized poly(fluoroalkyl acrylate)s show crystalline properties even if the fluoroalkyl side chains are short (n< 7).[1] Due to their high optical trasmissivity, we have been investigating a number of poly(fluoroacrylates) for advanced optical applications. Herein, we report the synthesis and characterization of several fluorinated homo- and co-polymers along with aspects of their coating on Si substrates.

## Experimental

**General.** 1,1,1,3,3,3-Hexafluoroisopropylacrylate [$CH_2$=CHCOOCH$(CF_3)_2$] was purchase from Oakwood Products, Inc. Zonyl® TA-N [$CH_2$=CHCOO$(CH_2)_2(CF_2)_{4\text{-}14}$F] and HYPALON™ (chlorosulfonated polyethylene) were obtained from DuPont Dow elastomers L.L.C. $CHCl_3$, benzoyl peroxide and THF were obtained from Fisher, Aldrich, and Mallinckrodt AR®, respectively. $^1$H NMR spectra were recorded using a Varian Mercury 300 MHz spectrometer. The spectra were obtained by dissolving 5-6 mg of each sample in $d_7$-DMF. Thermal analyses were performed with a TGA 2050, and DSC 2920 (*TA* Instruments). IR spectra were recorded using a Perkin-Elmer Spectrum 1 spectrometer. Thin films of the polymers were used for IR measurements.

**Polymerization procedure.** The *homo-* and *co-*polymers of 1,1,1,3,3,3-hexafluoroisopropylacrylate [$CH_2$=CHCOOCH$(CF_3)_2$] and Zonyl® TA-N [$CH_2$=CHCOO$(CH_2)_2(CF_2)_{4\text{-}14}$F] were synthesized by radical polymerization as follows: into a screw-capped glass tube containing a small magnetic stir bar, 1,1,1,3,3,3-hexafluoroisopropylacrylate [$CH_2$=CHCOOCH$(CF_3)_2$, dissolved in $CHCl_3$, was introduced. The solution was flushed with $N_2$ while stirring. Benzoyl peroxide was then added as an initiator. The tube was heated in a water bath at 70-75 °C for 1.5-2 h with stirring. Upon completion of the polymerization, the solvent was removed. The polymer was purified by dissolving in ethyl acetate, precipitated in MeOH, and dried at 50-60 °C under vacuum overnight, resulting in a transparent elastomeric polymer. The polymer was soluble in acetone and ethyl acetate, but insoluble in $CHCl_3$ and $CH_2Cl_2$.

Zonyl® TA-N [$CH_2$=CHCOO$(CH_2)_2(CF_2)_{4\text{-}14}$F] was dissolved in ethyl acetate, polymerized, and dried according to the same procedure detailed above for 1,1,1,3,3,3-hexafluoroisopropylacrylate. A white rigid polymer was obtained, which was soluble in DMF and acetone, but insoluble in $CHCl_3$, $CH_2Cl_2$, EtOH, hexanes, and ethyl acetate.

Copolymerization was carried out by using mixtures of 1,1,1,3,3,3-hexafluoroisopropylacrylate and Zonyl® TA-N, in different ratios. The same procedure was followed as in the case of homopolymerization.

## Results and Discussion

Homo- and co-polymers of 1,1,1,3,3,3-hexafluoroisopropylacrylate [$CH_2$=CHCOOCH$(CF_3)_2$] and Zonyl® TA-N [$CH_2$=CHCOO$(CH_2)_2(CF_2)_{4\text{-}14}$F] were synthesized by radical polymerization processes, using benzoyl peroxide as the initiator. The polymerization process was performed under various conditions, using benzoyl peroxide as an initiator, at 70-75 °C. On the other hand, polymerization could be conducted at room temperature using tri-*n*-butylboron/$O_2$ as the initiator. It was observed that the solubility of the synthesized polymers was dependent on their structure. *Homo*-poly(1,1,1,3,3,3-hexafluoroisopropylacrylate) was soluble in acetone and ethyl acetate, but not soluble in $CHCl_3$ and $CH_2Cl_2$. The *homo*-polyZonyl was soluble in DMF and acetone, but insoluble in $CHCl_3$, $CH_2Cl_2$, EtOH, hexanes, and ethyl acetate. The solubility of the copolymer was dependent on the mol% of co-monomers used in the polymerization. As the mol% of the Zonyl co-monomer increased, the solubility of the copolymer decreased, probably due to the increased length of the perfluoroalkyl side chain.

IR spectra of poly(1,1,1,3,3,3-hexafluoroisopropylacrylate) showed a strong absorption at 1741-1782 cm$^{-1}$, corresponding to the ester carbonyl group, and an absorption at 2900-3000 cm$^{-1}$ belonging to the C-H stretching in the polymer backbone. The IR spectrum of polyZonyl had a strong absorption at 1736 cm$^{-1}$, attributable to the carbonyl of the ester group. Although the C-H groups of the two polymer backbones are similar, and the polyZonyl has two $CH_2$ groups in the perfluoroalkyl side chin, the intensity of the absorption at 2900-3000 cm$^{-1}$ was lower than that of poly(1,1,1,3,3,3-hexafluoroisopropylacrylate). The spectra of the copolymers show that as the mol% of the Zonyl co-monomer increases, the intensity of the IR absorption at 2900-3000 cm$^{-1}$ decreases.

Thermal stability and phase transitions were characterized using TGA and DSC, respectively. Thermograms of the polymers were obtained by heating under a nitrogen atmosphere. The degradation temperatures at 5% wt loss of *homo*-poly(1,1,1,3,3,3-hexafluoroisopropylacrylate) was around 250 °C and was 320 °C for the *homo*-polyZonyl. For the copolymers, as the mol% of the Zonyl co-monomer increased, the degradation temperature increased. The DSC thermograms were obtained using a heating rate of 10 °C/min. It was shown that polyZonyl possessed a high degree of crystallinity (large melting endothermic transition at 98.5 °C). Meanwhile, poly(1,1,1,3,3,3-hexafluoroisopropylacrylate) exhibited no melting transition. $^1$H NMR spectra were recorded for all of the polymers.

Disk shaped silicon wafers were coated with some of the synthesized polymers having minimal absorption in the 1860-2900 cm$^{-1}$ (5.6-5.4 μm) for IR optical devices. In the IR spectra, the absorption bands at 3.36 μm were ascribed to C-H stretching.

## Conclusion

Homo- and co-polymers of fluoroalkylacrylates were synthesized. The polymerization process was performed under various conditions, using benzoyl peroxide as an initiator, at 70-75 °C. On the other hand, polymerization could be conducted at room temperature using tri-n-butylboron/$O_2$ as the initiator. The dependence of solubility, thermal stability, and degree of crystallinity of the synthesized copolymers were determined. Controlling the mol% of the Zonyl co-monomer leads to control of the morphology (degree of crystallinity). Successful coating of silicon with low cost polymeric materials, having minimal IR absorption in key spectral regions, facilitates opportunities to coat Si-wafers with different polymeric materials for use in a number of electronic and optical applications.

**Acknowledgements.** The authors would like to acknowledge Lockheed Martin Electronics and Missiles and the State of Florida for support.

## References

(1) Sceirs, J. *Modern Fluoropolymers*; Wiley: New York, **1997.**
(2) Ishikawa, N. *Fluorine Compounds, Modern Technology and Application*; Mir: Moscow, **1984.**
(3) Moreau, W. M. *Microdevices*; Plenum Press: New York, **1988.**